DOMINANTLY INHERITED RETINAL DEGENERATION – EXPLORING THE SPECTRUM OF HUMAN RETINAL DYSFUNCTION AND THE UNDERLYING MOLECULAR PATHOLOGY.

RAJARSHI MUKHERJEE

INSTITUTE OF OPHTHALMOLOGY, UNIVERSITY COLLEGE LONDON

Submitted to the University College London for the Degree of MD(Res)

July 2015

Supervisors: Professor Andrew R Webster

Professor Anthony T Moore

DECLARATION

I, Rajarshi Mukherjee confirm that the work presented in this thesis is my own. Where information has been derived from other sources, I confirm that this has been indicated in the thesis.

Rajarshi Mukherjee

ABSTRACT

The prevalence of retinal dystrophies among people with European ancestry is 1 in 3500-4000. Large majority of these conditions are caused by mutations in single genes inherited in autosomal recessive, autosomal dominant, X-linked recessive or mitochondrial fashion. Identification of the genotype and elucidation of the phenotype of these disorders help in improving the understanding of the pathophysiology and eventually devising novel management strategies. This thesis concentrated on autosomal dominant retinal dystrophies caused by mono-allelic mutations. The overall prevalence of the different genotypes causing autosomal dominant retinitis pigmentosa in the British population was explored. The consequence on the retinal structure (fundus examination, spectral domain optical coherence tomography, fundus autofluorescence imaging) and visual function (visual acuity, perimetry, electrophysiology) of the patients with novel mutations in the *RHO*, *PRPF31*, *PRPH2*, *NR2E3* and *IMPDH1* genes were considered. The genotypes and the phenotypes of retinitis pigmentosa due to *RP1* mutations were explored which provided insight into the understanding of the natural history of the disorder. Intra-familial variability and reduced penetrance are phenomena observed in families with inherited retinal disorders. In families with *PRPF8* mutations, these observations were identified and studied. All dominant alleles appear first in families as a *de novo* mutation. Families with *de novo* mutations within the dominant *GUCY2D* and semi-dominant *CHM* genes were examined which enhanced current knowledge on the counselling of patients with these conditions. In addition, families with mono-allelic mutations in the *RPE65* gene were analysed and unique phenotypes

determined. Overall, results presented in this thesis contribute to an understanding of Mendelian dominant retinal disease that enhances our knowledge of the variability and natural history of the phenotypes.

ACKNOWLEDGEMENTS

This work would have been impossible without the immense help and contribution from the patients who participated in this study and allowed multiple evaluations without hesitation. I am inspired by them and am grateful for their help.

I would like to thank my supervisors Professor Andrew Webster and Professor Anthony Moore for giving me the opportunity to undertake this project. Their enthusiasm and knowledge has contributed to development of a life-long interest in ophthalmic genetics. The other members of the Webster/Moore team especially Dr Donna Mackay and Dr Zheng Li provided practical help and guidance and deserve my special thanks. I am thankful to Dr Naushin Waseem and Professor Shomi Bhattacharya for their encouragement. Professor Graham Holder and Dr Anthony Robson have taught me all I know about electrophysiology and have contributed to all my projects with constructive criticism for which I am grateful. Special thanks to Beverley Scott, Genevieve Wright and Sophie Devery for their help in managing DNA collection and extraction.

I would like to thank the British Retinitis Pigmentosa Society (RP Fighting Blindness), the Special Trustees of Moorfields Eye Hospital and the National Institute for Health Research UK (Moorfields Eye Hospital and UCL Institute of Ophthalmology Biomedical Research Centre) for the financial support.

Finally, I wish to dedicate this thesis to my wife Ruma who has toiled hard with me every step of the way and my children, Tanay and Twisha who make it all worthwhile.

CONTENTS

LIST OF FIGURES:

LIST OF TABLES:

ABBREVIATIONS

aav	Adeno-associated vector
AMP	Adenosine monophosphate
ad	Autosomal dominant
ar	Autosomal recessive
CCD	Charge-coupled device
cDNA	Complementary DNA
cGMP	Cyclic guanosine monophosphate
CMO	Cystoid macular oedema
CNV	Choroidal neovascularisation
CORD	Cone dystrophy and Cone-Rod dystrophy
CSNB	Congenital stationary night blindness
DA	Dark-adapted
dATP	2'-deoxyadenine 5'-triphosphate
dCTP	2'-deoxycytosine 5'-triphosphate
dGTP	2'-deoxyguanosine 5'-triphosphate
dH2O	Distilled water
DMSO	Dimethyl Sulfoxide
DNA	Deoxyribonucleic acid
dNTP	2´-deoxynucleoside 5´-triphosphates
dTTP	2'-deoxythymidine 5'-triphosphate
EDTA	Ethylene diamine tetra acetic acid
EOG	Electro-oculogram
ERG	Full-field electroretinogram
EVS	Exome variant server
ExAC	The Exome Aggregation Consortium browser

FAF	Fundus autofluorescence imaging
GC	Guanylate cyclase
GCAP	Guanylate cyclase assisting proteins
HRR	Hardy-Rand-Rittler test
IRBP	Inter-photoreceptor retinoid-binding protein
IS/OS	Inner segment/ Outer segment of photoreceptors
ISCEV	International Society for Clinical Electrophysiology of Vision
KCl	Potassium chloride
kD	Kilo Dalton
LA	Light-adapted
LCA	Leber's congenital amaurosis
LogMAR	Logarithm of the minimal angle of resolution
LRAT	Lecithin retinol acyltransferase
MEH	Moorfields Eye Hospital, London, UK
MgCl2	Magnesium Chloride
MLPA	Muliplex ligation-dependant probe amplification
mRNA	Messenger RNA
NAD	Nicotinamide Adenine Dinucleotide
OCT	Optical coherence tomography
OD	Oculus dextrus - right eye
OS	Oculus sinister - left eye
PCR	Polymerase chain reaction
PDE	Phosphodiesterase
pERG	Pattern ERG
Pol II	RNA polymerase II
PSC	Posterior subcapsular cataract
RNA	Ribonucleic acid
ROS	Rod outer segment

RP	Retinitis pigmentosa
RPE	Retinal pigment epithelium
TBE	Tris borate EDTA
UV	Ultra-violet

1 INTRODUCTION

1.1 THE RETINA

"In the study of this membrane [the retina], I for the first time felt my faith in Darwinism (hypothesis of natural selection) weakened, being amazed and confounded by the supreme constructive ingenuity revealed not only in the retina and in the dioptric apparatus of the vertebrates but even in the meanest insect eye."

Santiago Ramón y Cajal

The human eye is a highly specialised extension of the brain which acts as a sensory organ enabling the sensation of vision. The eye is comprised of three coats (tunics) from outside inwards, the corneoscleral coat, the uveal coat and the neural layer or the retina.

The retina is the tissue where light from the object of interest forms an image after undergoing refractive changes in the various media of the eyeball. It extends from the optic nerve head posteriorly to the ora serrata, its anterior junction with the pars plana, a part of the ciliary body. Lying in between the temporal vascular arcades of the retina is an oval specialized region called the macula lutea, so called because of the yellow colouration of the region due to presence of macular pigment (Snodderly et al., 1984). Macular pigment is mainly composed of hydroxycarotenoids like lutein and zeaxanthin (Bone et al., 1997). The centre of macular lutea is exclusively formed of cone photoreceptors and is called the fovea

centralis which is responsible for colour vision and provides the highest visual acuity (Provis et al., 2005).

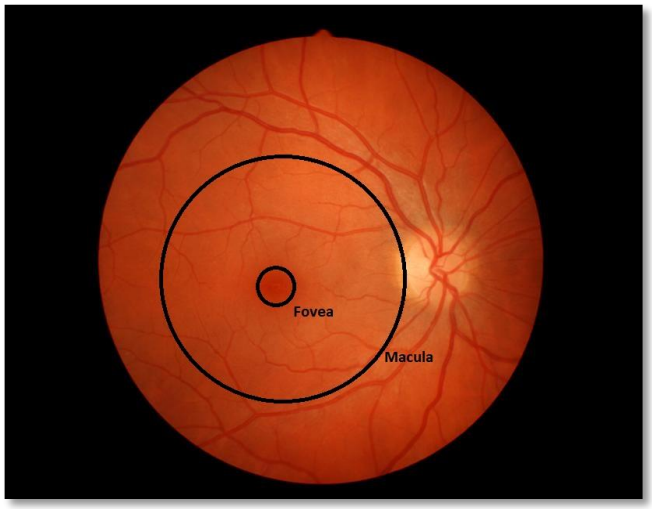

Figure 1-1: Fundus photograph of the human retina showing the fovea and the macula lutea.

Within the fovea centralis, a small central region is devoid of any capillaries called the foveal avascular zone.

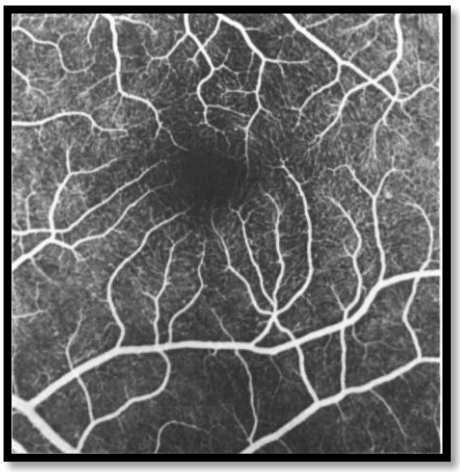

Figure 1-2: Fluorescein angiogram of the macula of a healthy subject demonstrating dark foveal avascular zone. (Laatikainen and Larinkari, 1977)

Embryologically, the retina develops from two closely apposed neuroectodermal cell monolayers. The inner layer develops into a multilayer meshwork of the neurosensory retina while the outer layer stays as a single layer of the retinal pigment epithelium (Galli-Resta et al., 2008). In a cross section, the neurosensory retina has the following histologic layers from outside inwards:

The rod and cone inner and outer segments
External limiting membrane
Outer nuclear layer
Outer plexiform layer
Inner nuclear layer
Inner plexiform layer
Ganglion cell layer
Nerve fibre layer
Internal limiting membrane

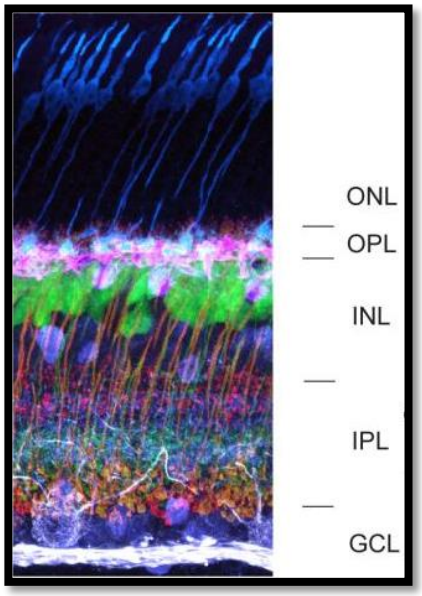

Figure 1-3: Immunostaining of mouse retina. ONL – outer nuclear layer, OPL – Outer plexiform layer, INL – Inner nuclear layer, IPL – Inner plexiform layer, GCL – Ganglion cell layer. Modified from (Hoon et al., 2014)

1.1.1 THE NEUROSENSORY RETINA

The simplistic view of the neurosensory retina is that of an organisation consisting of three levels of neural cells arranged as a series electrical circuit. The light has to pass through all the layers of the retina to reach the outer most layer of the neurosensory retina, the photoreceptors. Stimulated photoreceptors pass the information as an hyperpolarisation event to the next level of neurons, the bipolar cells from where it is passed to the second level of neurons, the ganglion cells. The axons of the ganglion cells form the nerve fibre layer and eventually these neurons carry the information along the optic nerve into the brain. These three cells are the predominant participants in forming of the histological layers of the retina. These layers of the neurosensory retina are actually a meshwork of different specialised cells including photoreceptors, bipolar cells, ganglion cells, horizontal cells, amacrine cells and various glial cells.

The cell bodies of the bipolar, horizontal and amacrine cells contribute to the inner nuclear layer of the retina while the photoreceptor cell bodies form the outer nuclear layer. The plexiform layers are formed by the dendrites, axons and the various ribbon synapses between different neural cells, with contributions from ganglion cells, bipolar cells, horizontal cells, amacrine cells and the photoreceptors. Ganglion cell bodies form the ganglion cell layer while the axons of these cells form the nerve fibre layer.

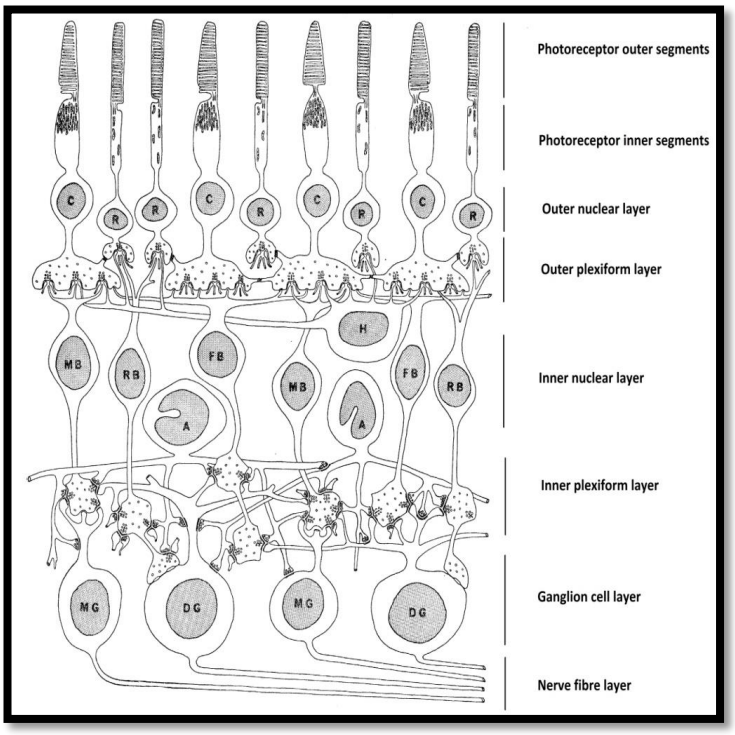

Figure 1-4: Simplified illustration of retinal anatomy. C-Cones, R-Rods, H-Horizontal cell, MB, FB, RB-Different types of bipolar cells, A-Amacrine cell, MG, DG-Different types of ganglion cells. Modified from (Dowling and Boycott, 1966)

1.1.1.1 The photoreceptors – rods and cones

The photoreceptors are highly specialized neuro-epithelial cells which convert the energy from the incident photon into electrical energy. There are two types of photoreceptors, the rods and the cones. There are about 120 million rods in the retina with rods outnumbering the cones by 20:1. Each photoreceptor cell has four distinct parts – the outer segment, the inner segment, the cell body and the synaptic terminal. (Nilsson, 1985) (Figure 1-5)

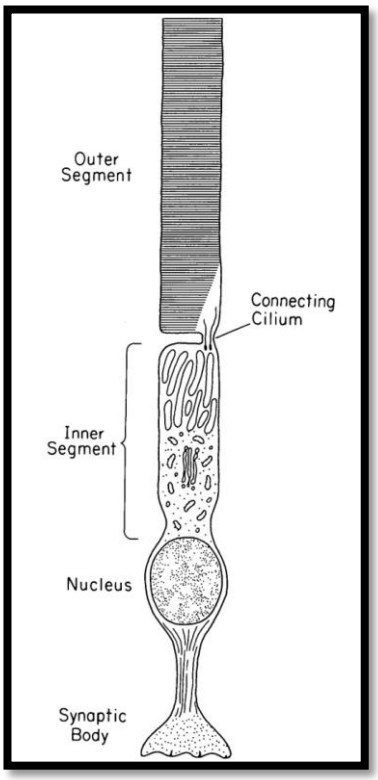

Figure 1-5: Basic organization of a vertebrate photoreceptor. Adapted from (Young, 1976)

The outer segment of the rods contains discrete multiple laminated disks not attached to the cell membrane and a central connecting cilium which has a "9 plus 0" cross-sectional configuration. The cone outer segments are similar except that they are conical ellipsoids and the disks are attached to the cell membrane. Preservation of the structure of photoreceptor outer segments is important for the functioning of the retina as the visual pigments reside in the membranous disks. Disorganization of the outer segment structure can be an indicator of retinal degeneration as observed in patients with retinitis pigmentosa (RP). (Humphries et al., 1997, Yamashita et al., 2009)

As the outer segment of the photoreceptor does not have any significant organelles, it cannot synthesize the proteins and membranes that it

requires for its function, phototransduction. So, the proteins have to be transferred at high flow rates through the connecting cilium which acts as the conduit. The connecting cilium is a specialized structure trafficking protein from the inner segment containing the translational machinery to the outer segment. This non-motile structure is anchored to a basal body in the inner segment and also plays critical role in outer segment disk morphogenesis.(Ramamurthy and Cayouette, 2009)

There are more than 1000 different proteins that have been identified in the connecting cilium making it one of the most complex structures. (Gherman et al., 2006) Mutations in genes encoding these proteins involved in ciliogenesis or protein transport to the outer segment lead to photoreceptor degeneration. This is evidenced in several disorders like RP (Gao et al., 2002, Liu et al., 2004, Connell et al., 1991, Adams et al., 2007, Moore et al., 2006), Usher syndrome (Williams, 2008, Reiners et al., 2006, Weil et al., 1995, Liu et al., 1999) and Bardet Biedl syndrome. (Blacque and Leroux, 2006, Tobin and Beales, 2007, Leroux, 2007, Nachury et al., 2007, Hartong et al., 2006)

Rod photoreceptors saturate at lower intensities of light and are responsible for vision in dim illumination while cones are 25-100 times less sensitive, do not saturate even at high light intensities and are responsible for colour and photopic vision (Rodieck, 1998). There are three varieties of cones – L (Long), M (Medium) and S (Short) classified on the basis of their maximum spectral sensitivity (λ_{max}). Spectral sensitivity is the relative efficiency of detection of light as a function of its wavelength. The λ_{max} for L-cones is 563 nm, M-cones is 532 nm and S-cones is between 417-420 nm (Bowmaker and Hunt, 2006, Stockman et al., 1999). λ_{max} for the more abundant rod opsin, also called rhodopsin is 495 nm.

Rhodopsin is a membrane protein present in the rod outer segment (ROS) discs which is attached to a vitamin A derived chromophore 11-*cis* retinal. Incidence of a single photon on 11-*cis* retinal results in its photoisomerization and generates activated rhodopsin (Metarhodopsin II). Metarhodopsin II activates a G-protein transducin, which in turn stimulates the activity of its effector enzyme phosphodiesterase (PDE). PDE catalyzes hydrolysis of cGMP to 5'-noncyclic GMP and decreases the concentration of cGMP. Low cGMP concentration closes the cGMP gated cationic channel hyperpolarizing the cell membrane. In dark, rhodopsin is inactivated by phosphorylation catalysed by rhodopsin kinase. Intrinsic GTPase inactivates transducin which in turn inactivates PDE. Guanylate cyclase (GC), stimulated by low Ca^{2+} ion concentration due to closure of the cationic channel, synthesizes cGMP from GTP increasing its concentration and opening the channel. Guanylate cyclase is assisted in this reaction by guanylate cyclase assisting proteins (GCAP). Opening of cationic channel depolarizes the membrane and releases neurotransmitter glutamate from rod synaptic terminals. This starts the neural signal for vision.(Arshavsky et al., 2002, Maeda et al., 2003) These series of reactions form the phototransduction cascade. (Figure 1-6)

Qualitatively, cone phototransduction resembles that of rods. It is, however, comparatively insensitive to low intensities of light but is fast and capable of adapting to the ambient levels of illumination to a much higher degree.

Mutations in the rod and cone phototransduction cascade can give rise to retinal disease. Within rod phototransduction pathway, mutations in rhodopsin, *PDE* and *GC* can cause RP while mutations in *GCAP* cause autosomal dominant cone dystrophy. Similarly, mutations in cone opsins

OPN1LW and *OPN1MW* express congenital red-green colour vision defects (Carroll et al., 2012).

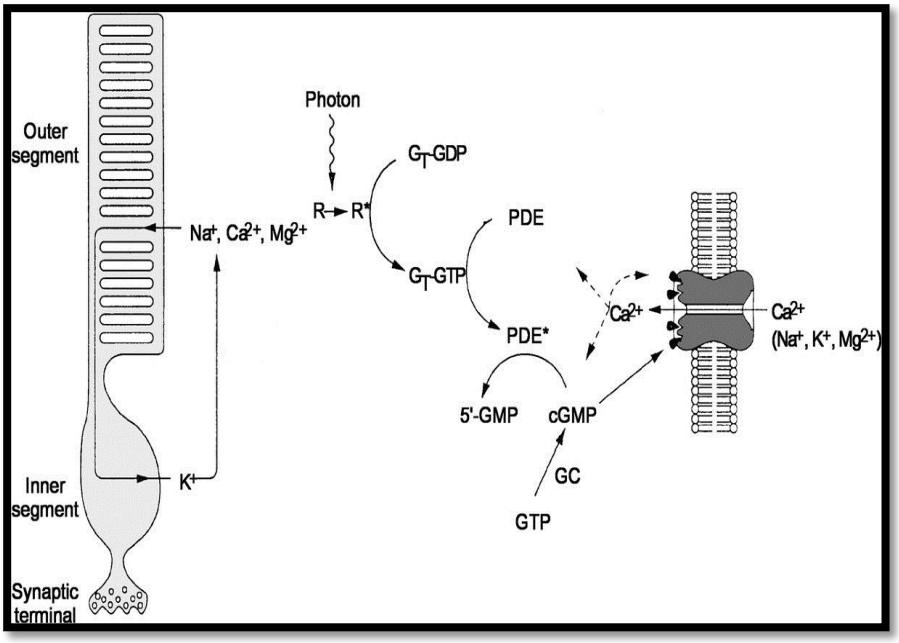

Figure 1-6: The phototransduction cascade. Adapted from (Zimmerman, 1995). R-Rhodopsin, R*-Activated rhodopsin, GT-GDP-Transducin, GT-GTP-Activated transducin, PDE-Phosphodiesterase, PDE*-Activated PDE, GC-Guanylate cyclise

1.1.1.2 The inner nuclear layer

The inner nuclear layer is formed by the cell bodies of three different types of cells – the bipolar cells, the horizontal cells and the amacrine cells.

1.1.1.2.1 The bipolar cell

The photoreceptors make synaptic connections with bipolar cells that in turn form synapses with ganglion cells. Functionally, there are at least two different types of bipolar cells, the ON-bipolar cell and the OFF-bipolar

cells. They are so called because of ON-bipolar cells are inhibited in response to glutamate release by cone synapses while the OFF-bipolars are stimulated. As light hyperpolarizes the cones and hence, inhibits glutamate release, ON-bipolars are stimulated (switched on) by light while the OFF-bipolars are inhibited (switched off). The cones synapse with both ON- and OFF-bipolar cells while the rods synapse only with ON-bipolar cells. In the fovea, a single cone synapses with single bipolar cell but in the periphery one cone can synapse with many different bipolar cells. However, this view might be too simplistic and it is believed that there are at least 9-11 different types of cone-driven bipolar cells in every mammalian retina (Masland, 2001b).

Dysfunction in the bipolar cell function due to mutations in genes like *TRPM1* can cause congenital stationary night blindness (CSNB) (Zeitz et al., 2015).

1.1.1.2.2 The horizontal and the amacrine cells

Horizontal cells receive stimulus from the photoreceptors and also provide inhibitory feedback. Once stimulated by a cone, the horizontal cell suppresses the feeder cone as well as the cones surrounding it. This 'centre-surround' prevents spread of the stimulus as one cone can be connected to multiple ganglion cells through multiple bipolar cells (Masland, 2001a).

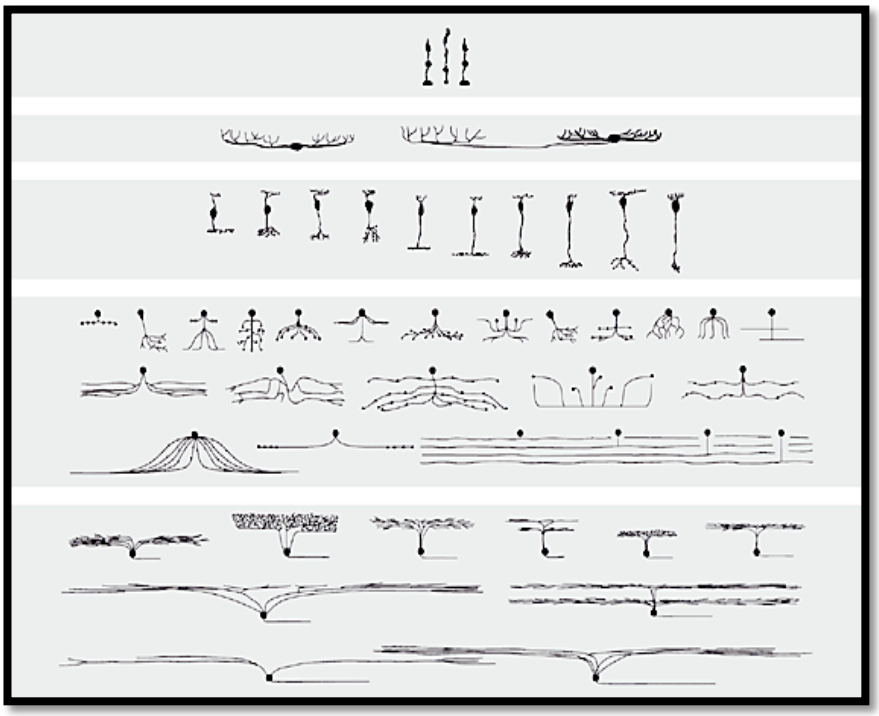

Figure 1-7: Different types of cells in the retina. Adapted from (Masland, 2001b). From the top row to the bottom, photoreceptors, horizontal cells, bipolar cells, amacrine cells and ganglion cells.

There are at least 29 different types of amacrine cells. Although the function of every amacrine cell is not known, they are believed to be performing specific functions like global adjustment of retinal response to bright light (Masland, 2001a).

1.1.1.3 The ganglion cell

The ganglion cell is the final common pathway for the retinal input to reach brain. Traditionally, classified as OFF- and ON-ganglion cells, it is now believed that there are about 10-15 types of ganglion cell types all of which receive input from bipolar cells.(Masland, 2001a) The axons of the

ganglion cells form the optic nerve which terminates in the lateral geniculate nucleus.

1.1.1.4 The glia

Müller cells form the main glial element in the retina. These cells extend from the inner segments of the photoreceptors to the internal limiting membrane, which is formed by their end feet. Besides playing a structural role, they form the external limiting membrane and participate in buffering the ionic concentrations in the extracellular space. The other glial cells observed in the retina are microglia and macroglia (astrocytes, oligodendroglia, Schwann's cells). These cells respond to injury, provide physical support and maintain the ionic composition of extracellular space.

1.1.2 THE RETINAL PIGMENT EPITHELIUM

The retinal pigment epithelium (RPE) consists of single layer of polygonal cells resting on a basement membrane. These epithelial cells have a basal zone which contains the nucleus and an apical zone which is in connection with the photoreceptors' outer segments. In the apical zone, a series of cytoplasmic expansions start from the cell body and partially envelop the outer segment of the photoreceptors for about one-third of their length (Bairati and Orzalesi, 1963). This close interaction between the RPE and photoreceptors is critical for the maintenance of visual function. It facilitates the transfer of retinoids between photoreceptors and the RPE which is required for the visual cycle and the maintenance of photoreceptor excitability.

As discussed earlier, rhodopsin is activated on absorption of a photon. This is achieved by isomerization of 11-*cis* retinal to all-*trans* retinal. Restoration of photoexcitability of rhodopsin is accomplished by converting all-*trans* retinal back to 11-*cis* retinal. The multi-enzyme pathway performing this role is called the visual cycle (Palczewski and Saari, 1997). In photoreceptor outer segments, all-*trans* retinal is converted to all-*trans* retinol by all-*trans* retinal dehydrogenase. All-*trans* retinol is transported out of photoreceptors into the RPE with the help of inter-photoreceptor retinoid-binding protein (IRBP) present abundantly between the photoreceptor outer segments and the RPE apical cytoplasmic extensions (Jin et al., 2009). In the RPE, all-*trans* retinol is esterified by lecithin retinol acyltransferase (LRAT) and then hydrolysed and isomerised to 11-*cis* retinol by Rpe65 Isomerase. Finally, 11-*cis* retinol is oxidized to 11-cis retinal by 11-*cis* retinal dehydrogenase (*RDH5*) which is transported back to the photoreceptors assisted by IRBP. (Figure 1-8)

Mutations in these proteins have been described to cause inherited retinal dystrophies like Leber's congenital amaurosis (LCA) (Thompson et al., 2001, Marlhens et al., 1997, Marlhens et al., 1998), autosomal recessive RP (den Hollander et al., 2009) and fundus albipunctatus (Yamamoto et al., 1999). For example, mutations in the gene *ABCA4* cause Stargardt's macular dystrophy, that in *RDH12*, *LRAT* and *RPE65* cause LCA (Janecke et al., 2004, Thompson et al., 2001, Gu et al., 1997) while *RGR* mutations have been implicated in autosomal recessive RP (Morimura et al., 1999). Mutations in *RLBP1* and *RDH5*, both genes participant in the visual cycle cause fundus albipunctatus phenotype.

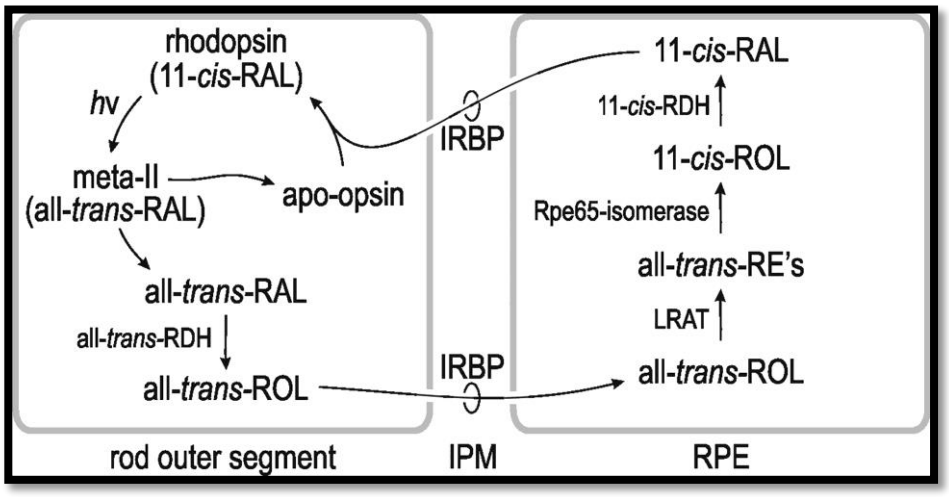

Figure 1-8: The visual cycle. Adapted from (Jin et al., 2009). RAL-Retinal, ROL-Retinol, IRBP-Interphotoreceptor retinoid-binding protein, RE-Retinol ester, IPM-Interphotoreceptor matrix, RDH-Retinal dehydrogenase

Recently, as a therapeutic approach, gene therapy has been attempted to patients with LCA due to mutations in the *RPE65* gene (Bainbridge et al., 2008, Cideciyan et al., 2008, Maguire et al., 2008). The phenotype of the retinal dystrophy consequent upon deficiency of RPE65 protein has unique characteristics like retention of useful visual function and presence of non-functioning photoreceptors early in childhood. Recombinant adeno-associated virus (aav) vector was used to transfect the RPE with human RPE65 coding sequence. The results of these trials demonstrated gene therapy to be a safe procedure showing modest improvement in the visual status of the treated eyes.

The cytoplasmic expansions of the RPE also assist in phagocytosis of the shed tips of the outer segments of photoreceptors, a process essential for photoreceptor survival. These phagocytosed products, once internalized form phagosome and are transported to the basal part of the RPE where they are degraded. (Kevany and Palczewski, 2010) Lipofuscin is formed

from the cellular debris, breakdown of which is difficult for the RPE machinery. In the retina, this autofluorescent material is formed as a result of incomplete digestion of the outer segment (OS) in the RPE (Wolf, 2003). Lipofuscin is converted to A2E, a retinoid toxic to the RPE cells due to its ability to produce free radicals. This mechanism has been hypothesized to be the underlying cause for disorders like macular degeneration. The inherent fluorescence of the lipofuscin can be utilized to document the general health of the RPE using confocal scanning laser ophthalmoscope (von Ruckmann et al., 1995b).

The basal surface of the RPE lays on the Bruch's membrane, which separates the RPE from the choriocapillaris, a layer of fenestrated capillaries. The RPE transports nutrients from the blood to the retina and transports ions, water and waste products from the sub-retinal space to the blood (Futter, 2006)

The RPE is so called due to the presence of pigment granules in its cytoplasm. These granules contain melanin and are predominantly located in the apical and mid-portions of the cell. The exact role of melanin in the RPE is not clear. It plays the role of neutral density filter in scattering light. Melanin is also believed to play a role in retinal development as the albino mammals with disorders of melanin pathways have under-developed retinas. Similarly, in patients with ocular or oculo-cutaneous albinism reduced visual acuity is observed with associated foveal hypoplasia.

1.2 RELEVANT MOLECULAR BIOLOGY OF THE CELL

"And now the announcement of Watson and Crick about DNA. This is for me the real proof of the existence of God."

Salvador Dali

1.2.1 THE CENTRAL DOGMA OF MOLECULAR BIOLOGY

In the year 1953, James D Watson and Francis H Crick elucidated the structure of deoxyribonucleic acid (DNA) which paved the way for significant developments in molecular biology thereafter (Watson and Crick, 1953). Once the structure of DNA was understood, an explanation was needed on its function. Francis Crick in 1958 argued that the sole function of DNA is to carry information for protein synthesis (Crick, 1958). He proposed that information, meaning precise determination of sequence, once passed onto proteins cannot get out. In other words, transfer of information from nucleic acid to nucleic acid or from nucleic acid to protein may be possible but transfer from protein to protein or protein to nucleic acid is not (Crick, 1958). This theory was called the central dogma. The theory was further refined later, on discoveries that DNA can be formed from ribonucleic acid (RNA) and that a single RNA molecule can rarely give rise to more RNA molecules (Crick, 1970). Recent discoveries have shown that this simplistic linear view of the central dogma does not fully explain the complexities of the higher eukaryotic biological systems. Large numbers of RNA molecules can be transcribed from the genomic DNA that does not carry any information for protein formation (Mattick, 2003). These 'non-protein-coding RNAs' derived from the introns

of protein coding genes or from the whole of non-protein-coding genes or from intergenic regions may play important roles regulating or modulating the functional processes undergoing in specific cells. In these cases at least, the information carried by the DNA is not meant solely for protein formation.

1.2.2 TRANSCRIPTION

The unit of heredity responsible for transferring a trait from individuals to their offspring is called a gene (Pearson, 2006). Genes were presumed to be pieces of DNA containing information to form a single protein. Recent advances in RNA biology have completely changed our understanding of a gene and it is proving difficult to impart a physical form to the abstract concept of a gene (Pearson, 2006). Not only that some RNA takes up infrastructural roles (e.g., ribosomal or transfer RNAs) which directly or indirectly facilitate protein coding; large amounts of RNA molecules are manufactured from the DNA template which have roles hitherto unknown (Mattick, 2003).

In the protein coding scheme, the first step in which the double-stranded DNA molecule gives rise to a single-stranded RNA molecule is called the transcription. The catalyst for this reaction in humans is RNA polymerase II (Pol II) which is a globular protein having active sites for DNA template and channels for nucleotide access and RNA exit (Moore and Proudfoot, 2009). This process involves initiation when Pol II binds to a site upstream to desired starting point of the gene. This region is called the promoter. In most eukaryotic genes, the promoter region consists of a TATA box

consisting of a consensus sequence of TATTAA about 25-35 bases upstream from the initiation site (Figure 1-9).

1.2.2.1 Transcription factors

Pol II utilises several co-factors, the transcription factors, during its function. These proteins bind to the cis-regulatory DNA sequences and thus, influence the expression of a gene positively or negatively. Besides promoter regions described above, transcription factors also bind to regions called the enhancers which can lie upstream, downstream or within the introns of a gene (Figure 1-9). The main mode of action of the transcription factors is to bind to specific DNA sequences and alter its own three-dimensional conformation. This change exposes or hides other functional domains within itself which recruits or binds other transcription factors. The function of whole transcription machinery is to modulate gene expression by enhancing or reducing the process of transcription.

There are about 3000 transcription factors in humans (Phillips and Hoopes, 2008). All transcription factors have at least two domains – a DNA-binding domain and a Trans-activating domain (Latchman, 1997). The transcription factors are classified into different families on the basis of the tertiary structure of its DNA-binding domain. The Trans-activating domain interacts with trans-elements like other transcription factors or co-factors.

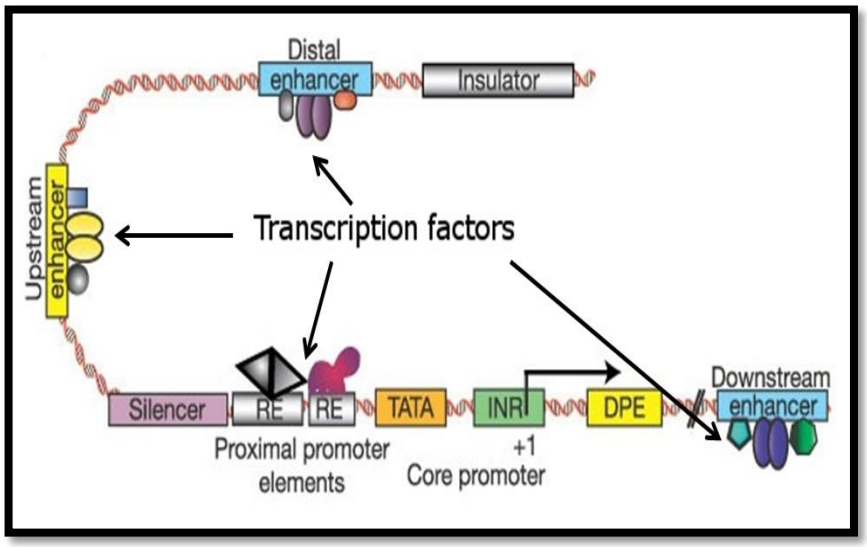

Figure 1-9: Transcription machinery. Modified from (Levine and Tjian, 2003) TATA-TATA box, INR-Initiator, DPE-Downstream promoter elements

Nucleotide sequence and genomic organization of the transcription factors are relatively conserved through evolution (Coolen et al., 2005). Sequence alteration of the transcription factors hamper their functionality and can have profound phenotypic consequences. For example, amino acid substitution S50T in the trans-activating domain of transcription factor *NRL* results in autosomal dominant retinitis pigmentosa (Bessant et al., 1999). So far, at least three transcription factors, *CRX*, *NRL* and *NR2E3* have been implicated in causation of autosomal dominant retinitis pigmentosa (Daiger et al., 1998).

1.2.3 SPLICING

At the end of transcription, the molecule that is generated is called the primary transcript, a faithful copy of the DNA template from which it is

formed. This molecule undergoes a series of processing reactions which result in the formation of the final mature mRNA. In most eukaryotes, the three major RNA processing reactions include splicing, capping and polyadenylation. Capping involves covalent bonding of 7-methylguanosine to the 5′ most nucleotide of the primary transcript by a 5′-5′ phosphodiester bond. Polyadenylation is the process of addition of around 200 adenylate (AMP) residues at the 3′ end of the RNA transcript. However, the process which exerts the most profound influence in changing the primary transcript to the mature mRNA is splicing.

Splicing is a series of reactions where the sections of the transcript carrying the genetic information, called exons are separated from the sequence carrying no coding information, called introns. The exons are identified, clipped out and finally re-joined to form the mature mRNA. The process of splicing involves cleavage of the 5′ end of an intron which usually begins with nucleotides GU. The cut end of the intron then attaches itself to a conserved adenylate (A) of another region called the branch point located between 18-40 nucleotides upstream from the 3′ end of the intron. This forms a loop called the lariat. The final step is cleavage of the 3′ end of the intron usually containing the dinucleotide AG and covalent bonding of the two exons (Clancy, 2008) (Figure 1-10). A protein-RNA complex called the spliceosome mediates the whole splicing machinery.

A defect in the splicing machinery is responsible for several types of retinal dystrophies. For example, monoallelic mutations in *PRPF3, PRPF4*, *PRPF6*, *PRPF8*, *PRPF31* and *SNRNP200*, all of which encode splicing factors are implicated in autosomal dominant retininitis pigmentosa (Chakarova et al., 2002, Tanackovic et al., 2011a, McKie et al., 2001, Vithana et al., 2001, Benaglio et al., 2011, Chen et al., 2014). It is still not clear why defects in a ubiquitous process affect the retina predominantly. There can be few

possible explanations. The retinal protein machinery is high performing leading to high demands on splicing which results in splicing defects causing early dysfunction. Splicing factors may have to fulfil a completely unidentified function in the retina or splicing factors may produce retina specific transcripts which are critical to retinal function. (Faustino and Cooper, 2003)

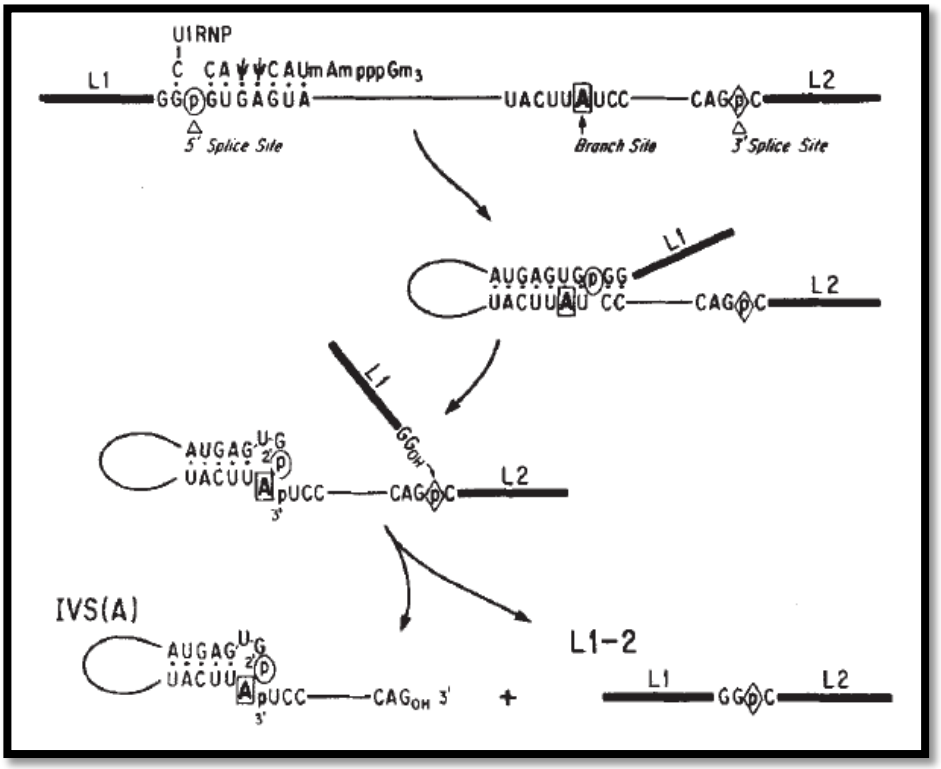

Figure 1-10: Lariat formation in splicing Modified from (Konarska et al., 1985). L1 and L2 represent the exons while IVS (A) represents the spliced intron.

1.3 AUTOSOMAL DOMINANT RETINITIS PIGMENTOSA

1.3.1 HISTORY

"To suppose that the eye with all its inimitable contrivances for adjusting the focus to different distances, for admitting different amounts of light, and for the correction of spherical and chromatic aberration, could have been formed by natural selection, seems, I freely confess, absurd in the highest degree."

Charles Darwin

In 1857, Franciscus Cornelius Donders, a Dutch military doctor coined the term 'Retinitis pigmentosa' (RP) for a condition of progressive loss of visual fields (Donders, 1857). He believed this disorder was due to an inflammatory cause. Two years after the publication of Donders' work, the seminal work of Charles Darwin, 'The Origin of Species' was published which changed the science of heredity and evolution forever. Around the same time (1856-1863), an Augustinian priest, Gregor Johann Mendel was experimenting on plant hybridization on nearly 30,000 pea plants at St. Thomas' Abbey, Brno. Mendel read his paper at the meetings of Natural History Society of Brünn in 1865 where he laid down the two general laws of inheritance, the law of segregation and the law of independent assortment which are the basis of modern genetics (Mendel, 1866). Four years later, in 1869, a German ophthalmologist, Theodor Karl Gustav von Leber made an important observation whilst working at the Ilvesheim Institute for the blind. He reported an 'intrauterine' form of RP where affected children have nystagmus, photophobia and extremely poor visual

function (Leber, 1869). He called it 'amaurosis congenita' which later came to be known as Leber's congenital amaurosis (LCA).

While Mendel's laws elucidated the modes of inheritance, the first description of a human disease with Mendelian inheritance pattern was reported by William Bateson and Sir Archibald Garrod in 1902 when they suggested recessive inheritance for alkaptonuria (Dunwell, 2007, Prasad and Galbraith, 2005, Garrod, 2002). William Bateson, a botanist with no medical qualifications is widely regarded as the person most responsible to spread the ideas of Mendel after they were rediscovered independently and almost simultaneously by three workers, Hugo De Vries, Carl Correns and Eric von Tschermak in the year 1900 (Harper, 2005, De Vries, 1900, Correns, 1900, Tschermak, 1900). Bateson collaborated with renowned ophthalmologist Edward Nettleship and together they described the genetics of many ophthalmic disorders for the first time (Harper, 2005, Rushton, 2000). In his book '*Mendel's principles of heredity*', Bateson describes aniridia, congenital cataract, ectopia lentis and one family of stationary night blindness as autosomal dominant disorders while most families of stationary night blindness and colour blindness were called 'sex-limited' (Bateson, 1909). Nettleship published large pedigrees of families with RP demonstrating Mendelian modes of inheritance in the disorder (Jay and Phil, 1983, Nettleship, 1907).

RP is now believed to be heterogeneous group of progressive retinal disorders which can be transmitted in autosomal dominant (30-40%), autosomal recessive (50-60%) and X-linked (5-15%) fashion (Bunker et al., 1984, Grondahl, 1987). Rare cases of digenic inheritance have been reported (Kajiwara et al., 1994). Similarly, rare instances of mitochondrial DNA mutations causing RP have also been described (Mansergh et al., 1999).

Linkage, a tendency of characters to be co-inherited through generations was first proposed by Morgan following his experiments with *Drosophila* in his famous 'fly room' (Morgan, 1910). In 1911, Wilson pointed out for the first time in humans that colour-blindness could be linked to the X chromosome (Wilson, 1911). In 1972, the complete sequence of a gene from bacteriophage was determined for the first time (Min Jou et al., 1972). Within the next few years, complete nucleotide sequences of several human genes were identified (Kerem et al., 1989, Baralle, 1977, Spritz et al., 1980). Finally, in the year 1990, 133 years after the disease got its name; first disease causing mutation to cause autosomal dominant RP was identified in a large Irish family using linkage and candidate gene analysis (Dryja et al., 1990b). The gene, Rhodopsin is believed to be the commonest cause of autosomal dominant RP (Sullivan et al., 2006a, Hartong et al., 2006).

1.3.2 Molecular genetics

Currently, mutations in 26 genes have been implicated to cause autosomal dominant RP (adRP) (RetNet) (Table 1-1).

Table 1-1: Genes encoding proteins mutation in which causes adRP

Function	Gene
Membrane protein	Rhodopsin (*RHO*)
	Peripherin 2 (retinal degeneration, slow) (*RDS/PRPH2*)
	Retinal outer segment membrane protein 1 (*ROM1*)
	Sema domain, immunoglobulin domain (Ig), transmembrane domain (TM) and short cytoplasmic domain, (semaphorin) 4A (*SEMA4A*)
	Olfactory receptor, family 2, subfamily W, member 3 (*OR2W3*)
Structural protein	Retinitis pigmentosa 1 (oxygen-regulated protein 1) (*RP1*)
	Fascin homolog 2, actin-bundling protein, retinal (Strongylocentrotus purpuratus) (*FSCN2*)
Splicing factors	Pre-mRNA processing factor 3 (*PRPF3*)
	Pre-mRNA processing factor 4 (*PRPF4*)
	Pre-mRNA processing factor 6 (*PRPF6*)
	Pre-mRNA processing factor 8 (*PRPF8*)
	Pre-mRNA processing factor 31 (*PRPF31*)
	Retinitis pigmentosa 9 (Pim-1 kinase associated protein) (*RP9*)
	Small nuclear ribonucleoprotein 200kDa (U5) (*SNRNP200*)
Transcription factors	Cone-rod homeobox (*CRX*)
	Neural retina leucine zipper (*NRL*)
	Nuclear receptor subfamily 2, group E, member 3 (*NR2E3*)
Enzymes	Inosine 5'-monophosphate dehydrogenase 1 (*IMPDH1*)

	Carbonic anhydrase IV (*CA4*)
	Retinol dehydrogenase 12 (all-trans/9-cis/11-cis) (*RDH12*)
	Hexokinase 1 (*HK1*)
Nuclear protein	Retinal pigment epithelium-specific protein 65kDa (*RPE65*)
Ubiquitination	Topoisomerase I binding, arginine/serine-rich (*TOPORS*)
	Kelch-like 7 (Drosophila) (*KLHL7*)
Signalling	Guanylate cyclase activator 1B (retina) (*GUCA1B*)
Voltage gated ion channels	Bestrophin 1 (*BEST1*)

Molecular genetics of the commonest causes of adRP is discussed below.

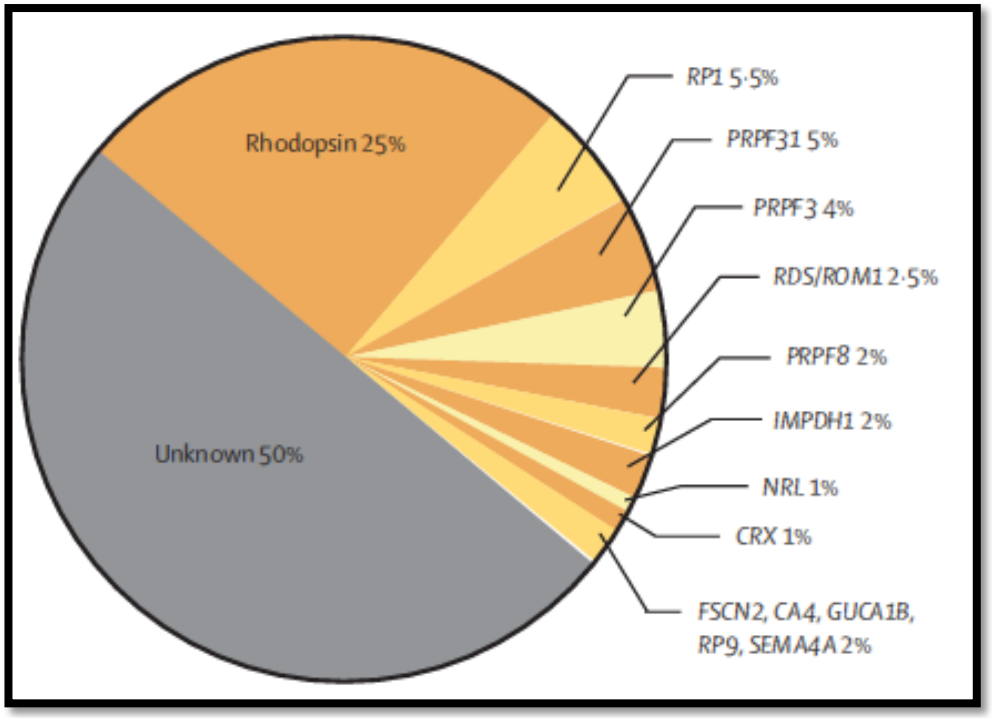

Figure 1-11: Relative contribution of different genes to RP. Adapted from (Hartong et al., 2006)

1.3.2.1 *RHO* (MIM +180380)

Locus – 3q21-q24

This gene encodes Rhodopsin, the visual pigment present in rod outer segments. First cloned in 1984, the main function of Rhodopsin is to absorb light and to instigate the phototransduction cascade which results in the neural signal for vision (Nathans and Hogness, 1984). It is a membrane protein with 7 trans-membrane domains, 3 cytoplasmic and 3 intradiscal loops (Figure 1-12). The chromophore retinal attaches itself to Lysine-296 of the seventh trans-membrane domain (Palczewski et al., 2000). The *RHO* gene is expressed solely in rod photoreceptors.

RHO was the first gene demonstrated to have a missense mutation segregating with adRP (Dryja et al., 1990b). Since then, more than 100 different mutations have been identified in *RHO* contributing to the largest number of adRP patients. A classification of the missense mutations has been proposed on the basis of the behaviour of the mutant protein (Mendes et al., 2005).

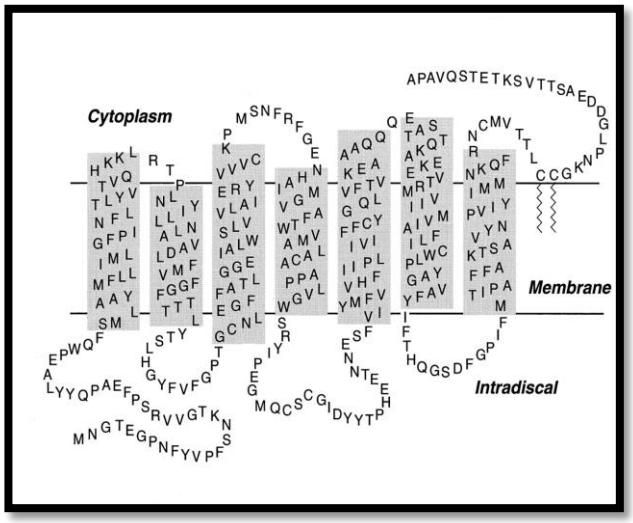

Figure 1-12: Schematic structure of Rhodopsin molecule showing seven trans-membrane domains and intradiscal and cytoplasmic loops.

Table 1-2: Classification of missense mutations in *RHO*. Adapted from (Mendes et al., 2005)

Classification	Behaviour	Site of point mutation	Misfolds
Class I	Fold normally but are not transported to the outer segment	L328, T342, Q344, V345, A346, P347	No
Class II	Are retained in the ER and cannot easily reconstitute with 11-*cis*-retinal	T17, P23, G51, T58, V87, G89, G106, C110, L125, A164, C167, P171, Y178, E181, G182, C187, G188, D190, H211, C222, P267, S270, K296	Yes
Class III	Affect endocytosis	R135	No
Class IV	Do not necessarily affect folding but affect rod-opsin stability and posttranslational modification	T4	No
Class V	Mutations show increased activation rate for transducin	M44, V137	No
Class VI	Show constitutive activation of opsin in the absence of chromophore and in the dark	G90, T94, A292,	No
Unclassified	No observed biochemical or cellular defect or not studied in detail	N15, Q28, L40, F45, L46, P53, G109, G114, S127, L131, Y136, C140, E150, P170, G174, P180, Q184, S186, T193, M207, V209, P215, M216, F220, E249, G284, T289, S297, E341	

The phenotype of the patients with *RHO* mutations can be grouped into three categories within limits of intra-familial and extra-familial variability. Cideciyan and colleagues classified these adRP families into Class A and Class B (Cideciyan et al., 1998).

Patients in Class A present with night blindness and decreasing visual fields in early life. Ophthalmic examination shows progressive generalised retinal dystrophy with intraretinal pigmentation, narrowing of the arterioles and pale optic discs (Jacobson et al., 1991). These patients have severe generalised rod-cone dystrophy on electrophysiology.

Class B patients have sectoral RP. The affected individuals are either asymptomatic or have very mild symptoms of night blindness. The intraretinal pigmentation and narrowing of arterioles are usually limited to inferior part of the retina. In the patients with true sector RP, the dystrophy does not progress to involve the rest of the healthy retina. These patients were classified as Class B1. The Class B2 families show progression and the dystrophy is characterised by generalised dysfunction on electrophysiology. Specific mutations in *RHO*, which may play a role in

glycosylation of the protein, have been implicated to cause true sector RP (Tam and Moritz, 2009).

Recently, a third phenotype was described in a French family (Audo et al., 2010b). The younger members showed focal photoreceptor or RPE abnormality in the posterior pole with patchy chorioretinal atrophy which were of larger size in the older members. Electrophysiological abnormalities consistent with generalised rod dysfunction were noted.

RHO mutations have also been associated with other retinal dystrophies like congenital stationary night blindness (Dryja et al., 1993, Rao et al., 1994, al-Jandal et al., 1999, Zeitz et al., 2008) and autosomal recessive RP (arRP) (Rosenfeld et al., 1992, Kumaramanickavel et al., 1994, Azam et al., 2009, Kartasasmita et al., 2011). Interestingly, all the families with arRP have homozygous mutations in *RHO* while the heterozygous carriers were unaffected.

1.3.2.2 *RP1* (MIM *603937)

Locus – 8q11-q13

In 1999, three groups working independently, identified the *RP1* gene and associated it with adRP (Pierce et al., 1999, Sullivan et al., 1999, Guillonneau et al., 1999). Rp1 protein is expressed exclusively in the photoreceptors and is a microtubule-associated ciliary protein (Liu et al., 2002, Liu et al., 2004). All the mutations causing adRP in this gene are truncating and limited to a hotspot in the terminal exon (Berson et al., 2001). However, in families from China and Japan, stop mutation c.Arg1933Ter near the C-terminal of the RP1 protein causing truncation of

the protein had no deleterious effect (Baum et al., 2001, Kawamura et al., 2004). In other words, haploinsufficiency of the C-terminal 224 amino acids of RP1 does not cause RP (Baum et al., 2001).

Studies exploring the phenotype of families with *RP1* mutations showed that reduction of rod photoreceptor function was much worse than that of cones. There was evidence of apparent non-penetrance within the families but even in these asymptomatic individuals, loss of photoreceptor function could be demonstrated on electrophysiology. Visual acuities remained near normal in most patients until late in life (Bowne et al., 1999, Jacobson et al., 2000, Payne et al., 2000).

Homozygous frameshift mutations as well as biallelic mutations in the *RP1* gene have been shown to cause autosomal recessive (ar) RP in several families (Khaliq et al., 2005, Riazuddin et al., 2005, El Shamieh et al., 2015). Although detailed phenotypic data is not available for these patients, they were night blind and lost central vision before 20 years of age. Electrophysiology showed a severe rod-cone dystrophy with early macular dysfunction (El Shamieh et al., 2015).

1.3.2.3 *PRPF31* (MIM *606419)

Locus – 19q13.4

This gene identified in 1996, encodes a protein with 20% homology with *S. cerevisiae* pre-mRNA splicing gene Prp31 (Weidenhammer et al., 1996). This level of sequence identity to the yeast genes suggested this highly conserved protein to be involved in pre-mRNA splicing. PRPF31 works as a part of the U4 complex of the spliceosome complex.

PRPF31 was associated with RP11 locus in 2001 when mutations were identified in four families and three individuals with adRP (Vithana et al., 2001). The adRP families associated with RP11 locus were known to have incomplete penetrance in an 'all or none' manner, where gene carriers displayed either fully symptomatic phenotype or completely asymptomatic phenotype (McGee et al., 1997). It was demonstrated that the wild type allele can have high or low expressivity and dictate the phenotype in the individual with the mutation. Because most of the missense *PRPF31* mutations described so far are null alleles and wild type high expressing allele is identified in all the nonpenetrant mutation carriers, decreased gene dosage as a consequence of haploinsufficiency is likely to be the explanation for the nonpenetrance (Rivolta et al., 2006, Vithana et al., 2003). Another group showed by linkage analysis that *PRPF31* expression was significantly associated with one expression quantitative trait locus on chromosome 14q21-23 which might offer explanation of non-penetrance in some of these families (Rio Frio et al., 2008).

1.3.2.4 *PRPF8* (MIM *607300)

Locus – 17p13.3

Cloned in 1999, this gene encodes a protein with 86% homology with the nematode protein and 62% with the yeast protein (Luo et al., 1999). It is a component of both the major U2 and minor U12-dependent spliceosome. As with all the splicing factors, this gene is expressed ubiquitously.

Mutations in this gene, the first splicing factor associated with adRP were identified in seven families in 2001 (McKie et al., 2001). Mutations in *PRPF8* have been described as causing a severe form of adRP with most

of the affected subjects having onset of night blindness in the first or second decade of life (Towns et al., 2010). The phenotype caused by Prp8 mutations in yeast correlates with the severity of RP caused by their human equivalent mutations.

1.3.2.5 *PRPF3* (MIM *607301)

Locus – 1q21.2

In 1997, *PRPF3* gene was identified and it was described to be a splicing factor associated with U4/U6-U5 tri-snRNPs and U4/U6 snRNP (Lauber et al., 1997, Wang et al., 1997, Horowitz et al., 1997).

The adRP RP18 locus was associated with the *PRPF3* gene and mutations in the gene were identified in several families (Chakarova et al., 2002). Three mutations described so far (p.Thr494Met, p.Pro493Ser, and p.Ala489Asp) have been localized to a small region in exon 11 of the gene making it a mutational hotspot (Gamundi et al., 2008).

Although variability in the adRP phenotype due to mutations in *PRPF3* have been described (Vaclavik et al., 2010), the majority of the patients have an early onset of night blindness, severe visual field constriction, loss of central vision between the fourth and fifth decade, and a flat electroretinogram after the age of 30 (Wada et al., 2004, Inglehearn et al., 1998, Xu et al., 1996).

1.3.2.6 *PRPF6* (MIM #613983)

Locus – 20q13.33

PRPF6 was identified as a splicing factor in the year 2000 as a protein with 29% identity and 48% similarity at the amino acid level with the yeast equivalent splicing factor Prp6p (Makarov et al., 2000). During the formation of the spliceosome, this protein mediates the assembly of U4/U6.U5 complex (the tri-snRNP). PRPF6 acts as a molecular bridge between the U5 snRNP and U4/U6 snRNP (the di-snRNP) which helps is formation of the tri-snRNP (Tanackovic et al., 2011a).

This splicing factor gene has recently been implicated in causing adRP on the basis of mutation screening (Tanackovic et al., 2011a). In the only family affected by the disorder, two brothers carried the mutation p.Arg729Trp in the *PRPF6* gene. The phenotype described is identical to that of typical retinitis pigmentosa with loss of peripheral vision, night blindness, arteriolar attenuation and optic disc pallor.

1.3.2.7 *RP9* (MIM *607331)

Locus – 7p14.2

In the year 2000, Maita et al cloned the *RP9* gene (Maita et al., 2000). RP9 was observed to localize in nuclear speckles containing the splicing factor SC35 and to interact with another splicing factor, U2AF35. Later, it was observed to be associated with PRPF3 in a tri-SNP spliceosome complex associating it with splicing. (Maita et al., 2004, Maita et al., 2005)

Only two mutations have been identified in this gene so far, both implicated in adRP (Keen et al., 2002). The disease expresses variably within these families with presence of asymptomatic obligate mutation carriers who showed mild phenotype only on electrophysiology (Kim et al., 1995).

1.3.2.8 *SNRNP200* (MIM *601664)

Locus – 2q11.2

A U5-specific 200-kD protein was cloned in 1996 and was later shown to play a central role in pre-mRNA splicing (Lauber et al., 1996, Zhang et al., 2009).

Mutations in this gene were initially demonstrated to cause adRP in the Chinese families (Zhao et al., 2009, Li et al., 2010, Zhang et al., 2013, Liu et al., 2012). Recently, more families of North American descent were identified carrying mutations in the *SNRNP200* gene (Benaglio et al., 2011). The phenotype of the disorder is that of typical retinitis pigmentosa. The onset of disease is in early teen age years with progressive loss of rod and cone function. During the fourth decade, the patients have severe loss of visual function with undetectable cone or rod responses on electrophysiology.

1.3.2.9 *PRPF4* (MIM *607795)

Locus – 9q32

First cloned in the year 1997, this splicing factor gene encodes one of several proteins that associate with U4 and U6 snRNPs (Lauber et al., 1997). As with other splicing factors, this protein is ubiquitously expressed (Chen et al., 2014).

Recently, mutations in *PRPF4* have been implicated in autosomal dominant retinitis pigmentosa (Chen et al., 2014, Linder et al., 2014). The affected patients have shown variable expressivity but all showed intra-retinal pigment migration, pale optic discs and narrow retinal vessels.

1.3.2.10 *RDS/PRPH2* (MIM *179605)

Locus – 6p21.1-cen

In 1991, using a probe derived from the coding region of the mouse Rds cDNA, human *RDS* was cloned (Travis et al., 1991a). The encoded protein is a membrane-associated glycoprotein localized to photoreceptor outer segment discs. It plays a role in stabilization of the outer segment discs (Travis et al., 1991b).

Mutation in *RDS*|*PRPH2* gene was shown to cause adRP in a large Irish family for the first time in 1993 (Farrar et al., 1993). Other groups demonstrated a variety of phenotypes caused by *RDS* mutations like adRP, macular dystrophy, retinitis punctata albescens, pattern dystrophy, central areolar choroidal dystrophy, cone-rod dystrophy and adult-onset vitelliform macular dystrophy (Travis and Hepler, 1993, Nichols et al., 1993a, Nichols et al., 1993b, Wells et al., 1993, Nakazawa et al., 1996). Most mutations are associated with a particular phenotype consistently, for example p.Cys118del causes adRP. However, multiple phenotypes

have also been described within the same family (Weleber et al., 1993, Aleman et al., 2009).

1.3.2.11 *IMPDH1* (MIM +146690)

Locus – 7q31.3-q32

Inosine monophosphate dehydrogenase (IMPDH) was cloned in 1988 using a polyclonal antibody directed against the purified protein (Collart and Huberman, 1988). There are two IMPDH isozymes – I and II. Only IMPDH1 is expressed by the photoreceptors, although most mammalian cells express both the isozymes (Jain et al., 2004, Bowne et al., 2006a). IMPDH catalyses a key step in guanine nucleotide biosynthesis catalyzing the conversion of Insoine monophosphate to xanthosine monophosphate (Hedstrom, 1999).

Several missense mutations have been demonstrated to be associated with the adRP phenotype (Kennan et al., 2002, Bowne et al., 2002). Bowne et al associated the locus LCA11 with *IMPDH1* by demonstrating two families with missense changes (Bowne et al., 2006a). The enzymatic activity of IMPDH in retinal dystrophy patients is within normal range and it is proposed that an additional nucleic acid binding role is being played by the protein. Impairment of this binding may be the cause of photoreceptor degeneration in adRP (Hedstrom, 2008).

1.3.2.12 *TOPORS* (MIM *609507)

Locus – 9p21

Human *TOPORS* was cloned in 2001 when it was designated as *LUN* (Chu et al., 2001). Although the exact function of TOPORS protein is unknown, it binds to DNA topoisomerase I and p53 and plays a role in ubiquitination and sumoylation (Zhou et al., 1999, Rajendra et al., 2004). Recently, it has been demonstrated that TOPORS protein localizes to the basal body of the photoreceptor connecting cilium and may play a role in the regulation of the functioning of the primary cilium (Chakarova et al., 2011).

In 2007, mutations in *TOPORS* were associated with adRP (Chakarova et al., 2007). The phenotype was distinct in that the younger members had perivascular cuff of retinal pigment epithelial atrophy, surrounding the superior and inferior arcades. This progressed to diffuse pigmentary retinopathy in older subjects (Chakarova et al., 2007, Bowne et al., 2008, Selmer et al., 2009).

1.3.2.13 *KLHL7* (MIM *611119)

Locus – 7p15.3

This ubiquitously expressed gene was first cloned in humans in 2006 although subsequently more transcripts have been identified (Bredholt et al., 2006, Friedman et al., 2009). Although the physiological function of the encoded protein Klhl7 is unknown, it is a member of BTB family

proteins that are associated with the ubiquitin-proteasome pathway of protein degradation (Perez-Torrado et al., 2006).

Friedman et al linked *KLHL7* to adRP by discovering four families of European descent with three mutations in the gene (Friedman et al., 2009). The phenotype of one of these families showed progressive generalised rod-cone dystrophy with young members having milder involvement than the older individuals (Hugosson et al., 2010)

1.3.2.14 *CRX* (MIM +602225)

Locus – 19q13.3

Cloned in 1997, *CRX* functions as a transcription factor for several retinal genes (Freund et al., 1997). *CRX* is expressed exclusively in the retina by the photoreceptors and the cells of the inner nuclear layer (Furukawa et al., 1999).

Three different phenotypes have been associated with mutations in *CRX*, autosomal dominant cone-rod dystrophy, Leber's congenital amaurosis and adRP (Sohocki et al., 1998, Sullivan et al., 2006a). After summarising all the mutations in *CRX*, Rivolta et al failed to find an association between the mutation and the phenotype. Interestingly, they observed relatively high proportion of *CRX* mutations being *de novo* (4/18). (Rivolta et al., 2001)

1.3.2.15 *NR2E3* (MIM *604485)

Locus – 15q23

NR2E3 is also a transcription factor mainly expressed in the retina that was cloned in 1999 (Kobayashi et al., 1999, Haider et al., 2000, Cheng et al., 2004). NR2E3 is believed to interact with NRL, another transcription factor, to suppress cone-specific gene expression and to activate a subset of rod-specific genes (Cheng et al., 2004). (Figure 1-13)

Primarily implicated to cause enhanced S-cone syndrome, only one missense change (p.Gly56Arg) in this gene has been described to cause adRP (Haider et al., 2000, Coppieters et al., 2007).

1.3.2.16 *NRL* (MIM +162080)

Locus – 14q11.1-q11.2

Another transcription factor implicated in adRP, *NRL* was first identified in 1992 (Swaroop et al., 1992). The present understanding of the interaction between the transcription factors *NRL* and *NR2E3* is such that *NRL* stimulates *NR2E3* to suppress cone-specific gene expression and stimulate rod-specific gene expression (Figure 1-13).

NRL was associated with adRP in 1999 when a missense change was identified at the highly conserved codon 50 (Bessant et al., 1999). Since then several missense changes have been identified in *NRL* which cause adRP, all limited to affecting three highly conserved codons 50, 51 and 122 (Nishiguchi et al., 2004). Functional analysis of these amino-acids have shown that they lie within minimal transactivation domain (codon 50

and 51) or the hinge domain (codon 122) which interact with TATA-binding protein at the promoter of target genes (Friedman et al., 2004, Kanda et al., 2007).

The patients with these mutations have rod-cone dystrophy with severely reduced scotopic electroretinogram within the first two decades of life. They also have peri-papillary atrophy and may develop bull-eye macular atrophy later in life (Bessant et al., 2003). Interestingly, recessive *NRL* mutations are associated with a phenotype resembling enhanced S-cone syndrome (Nishiguchi et al., 2004).

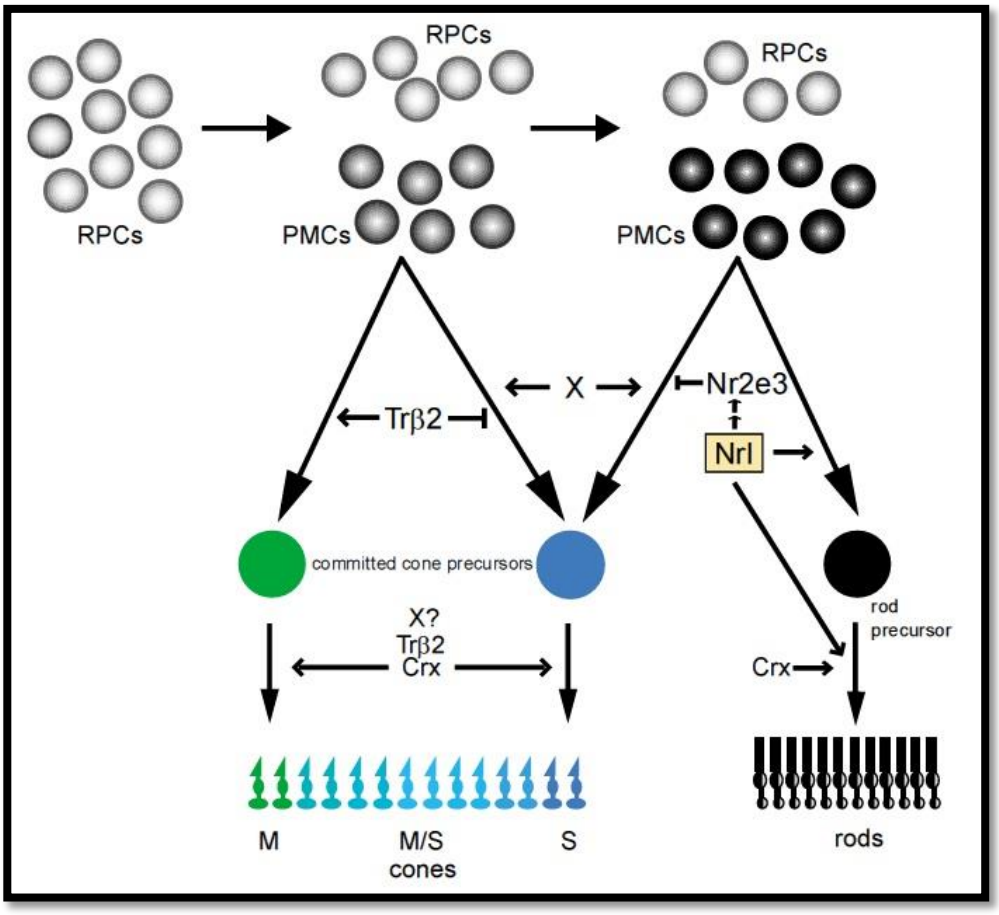

Figure 1-13: Photoreceptor differentiation. Retinal progenitor cells (RPC) develop into post-mitotic cells (PMC) which generate cone precursors or rod precursors. NRL stimulates NR2E3 to suppress cone generation and stimulate rod generation. Adapted from (Mears et al., 2001)

1.3.2.17 *RDH12* (MIM *608830)

Locus – 14q23.3

Cloned in 2002 by Haeseleer at al, the exact role this retinol dehydrogenase plays in photoreceptor cells is not known (Haeseleer et al., 2002). In the mouse retina, Rdh12 detoxifies 4-hydroxynonenal, a toxic product of lipid peroxidation and protects photoreceptors from light-induced apoptosis (Marchette et al., 2010).

Primarily implicated in Leber's congenital amaurosis, the *RDH12* gene has been associated with adRP in only one family (Fingert et al., 2008).

1.3.2.18 *RPE65* (MIM *180069)

Locus – 1p31.3-p31.2

This RPE65 protein was first characterised in 1993 by Hamel et al (Hamel et al., 1993) while the gene *RPE65* was cloned two years later (Nicoletti et al., 1995). This was the first retinal pigment epithelium specific gene to be characterised.

The expressed RPE65 protein acts as a molecular chaperone (Xue et al., 2004). In its membrane-associated form, RPE65 acts as a chaperone for all-trans-retinyl esters and is palmitoylated. In its soluble form, it is not palmitoylated and acts as a chaperone for vitamin A.

The predominant phenotype of patients with biallelic mutations in the *RPE65* gene is that of early onset retinitis pigmentosa or Leber's congenital amaurosis (Marlhens et al., 1997, Gu et al., 1997). Recently, a dominant

phenotype caused by monoallelic mutations in the *RPE65* gene was described (Bowne et al., 2011). These patients had a distinct phenotype of extensive chorioretinal atrophy and variable intraretinal pigmentation.

1.3.2.19 *CA4* (MIM *114760)

Locus – 17q23.1

This gene was first implicated in adRP when the mutation p.R14W was identified in 2 South African families (Rebello et al., 2004). 2 other mutations, p.R69H and p.A12T in the same gene were identified by different groups in a selection of Chinese adRP families (Alvarez et al., 2007, Tian et al., 2010). However, the original sequence variant p.R14W was identified in 6 of 143 normal Swedish controls casting doubt in its validity as a pathogenic variant (Kohn et al., 2008).

1.3.2.20 *ROM1* (MIM *180721)

Locus – 11q12.3

This gene has only been identified to be involved in causation of adRP in a digenic fashion in association with the *PRPH2* gene (Kajiwara et al., 1994). In patients of these families, existence of the sequence variant alone in either of the genes did not cause pathology although some of the patients did have reduction in the electroretinogram amplitudes.

1.3.2.21 *SEMA4A* (MIM *607292)

Locus – 1q22

This gene was implicated in adRP in 1 Pakistani family by direct mutation screening (Abid et al., 2006). In animal studies, it has been shown that point mutations in this gene cause retinal degeneration in homozygous conditions (Nojima et al., 2013).

1.3.2.22 *FSCN2* (MIM *607643)

Locus – 17q25.3

This gene was implicated in causing adRP in 4 unrelated Japanese families each showing presence of c.208delG mutation (Wada et al., 2001). However, in Chinese, Spanish, Italian and North American populations, this change has been identified as benign polymorphism casting doubt on the causation of adRP by the gene *FSCN2* (Gamundi et al., 2005, Ziviello et al., 2005, Sullivan et al., 2006a, Zhang et al., 2007).

1.3.2.23 *GUCA1B* (MIM *602275)

Locus – 6p21.1

This gene has been associated with adRP in 3 unrelated Japanese families all of whom exhibited p.G157R mutation (Sato et al., 2005b). However, in 2 large screenings of retinal dystrophy families with European and North

American ancestry, no pathogenic variants could be identified (Payne et al., 1999, Kitiratschky et al., 2011).

1.3.2.24 *BEST 1* (MIM *607854)

Locus – 11q12.3

This gene has been associated with autosomal dominant infantile vitelliform macular dystrophy since 1998 (Petrukhin et al., 1998). More recently, other phenotypes have been identified with mono or biallelic mutations in the *BEST1* gene (Kramer et al., 2000, Burgess et al., 2008).

Davidson et al reported 5 adRP families, 4 of European descent and 1 of Pakistani origin with mutations in the *BEST1* gene (Davidson et al., 2009). The phenotypes described were highly variable varying from predominantly macular involvement to advanced peripheral intraretinal pigmentation.

1.3.2.25 *HK1* (MIM *142600)

Locus – 10q22.1

Hexokinase (HK) is an enzyme participating in catalysis of the first step of glucose metabolism, phosphorylation of glucose to glucose-6-phosphate using ATP. Of the 4 different types, HK1, HK2, HK3 and HK4, HK1 is most ubiquitously expressed and is the predominant isozyme in brain, erythrocytes and lymphocytes (Bianchi et al., 1997). There is no clear cut explanation of why mutation in a ubiquitous enzyme causes dominant

retinitis pigmentosa. It is postulated that *HK1* may possess unique, yet unidentified functions exclusively in the retina (Sullivan et al., 2014).

Recently, one missense mutation in *HK1*, p.Glu847Lys, has been associated with adRP in six different families with four different ancestries (Wang et al., 2014, Sullivan et al., 2014). The affected individuals had variable phenotypes with some remaining asymptomatic until the fifth decade of life. Most showed signs of typical adRP with attenuated vessels, pale optic discs and intra-retinal pigment migration.

1.3.2.26 *OR2W3* (MIM *616729)

Locus – 1q44

Recently, *OR2W3*, an olfactory receptor gene has been associated with adRP in two independent families of Chinese origin. The single mutation p.Arg142Trp was identified using linkage and whole exome sequencing methods. OR2W3 expresses in retinal pigment epithelial cells and the encoded protein is believed to have multiple functions in addition to its role in olfaction (Ma et al., 2015). Interestingly, *OR2W3* shares exons with a much larger gene *TRIM58* with yet unknown function while the encoded protein shares sequence identity with *JAG1*, a gene associated with Alagille syndrome.

1.4 AIMS OF THE STUDY

Retinal dystrophies are the most heterogeneous of the inherited eye disorders. Although all the modes of Mendelian and non-Mendelian inheritance patterns are observed, this study will mainly concentrate on the patients with autosomal dominant retinal dystrophies. Genotype and phenotype correlations continue to be observed, although accurate clinical data on large cohorts of molecularly characterised patients remains to be collected.

Moorfields eye hospital (MEH) maintains a large inherited eye disorder database which contains molecular data of patients with known mutations. A significant number of families either have novel mutations in the known genes or mutations in genes that have not yet been identified. In the inherited retinal diseases clinic of MEH, new families are being examined regularly. The resource of families with dominantly inherited retinal degeneration is powerful, is growing and will form the basis of this thesis.

The main aims of this project are:

- To identify the families and individuals with known and unknown molecular diagnosis
- To design an extended algorithm for the analysis of mutations in known genes so that changes that would be missed so far in standard clinical testing can be identified
- To evaluate the phenotype of individuals and families with a known molecular diagnosis
- To determine the longitudinal natural history of families for whom retrospective data is available

2 MATERIALS AND METHODS

2.1 STUDY SUBJECTS

2.1.1 ETHICAL APPROVAL AND CONSENT

This study adhered to the tenets of the Declaration of Helsinki and was approved by the Moorfields and Whittington Hospitals Ethics Committee (WEBA1006; 05/Q0504/38).

Fully informed consent was obtained from all the individuals involved in this study.

2.1.2 CONTROL PANEL

The control population screened for this study was 98 apparently normal, randomly selected British Caucasian donors (Human random control DNA panel 2, Health protection agency culture collections, Salisbury, UK)(Crick, 1958). The *RP1* gene was sequenced in the control panel in order to ascertain the pathogenicity of the variations identified.

2.1.3 AFFECTED SUBJECTS

A panel of all families carrying the diagnosis of adRP was collected by using an SQL query in the Inherited Eye Disease database maintained at

Moorfields eye hospital (MEH). Blood samples from one proband of each family were included in the study. Samples were ascertained from other family members for segregation studies, where deemed necessary.

2.2 PHENOTYPING

2.2.1 HISTORY AND CLINICAL EXAMINATION

Patients were examined in the Genetics clinic, Medical retina firm, MEH under the supervision of Prof. Andrew Webster. Clinical information has also been collected retrospectively from MEH electronic databases and clinical and genetic notes.

2.2.1.1 History

A full clinical history was obtained including age of onset, symptoms at presentation like night blindness, difficulty in bright light or reduced peripheral vision, age of diagnosis, if any and progression of the symptoms. Particular visual difficulties in bright or dim illumination, symptoms of visual field impairment, difficulties in recognizing colours and presence of any refractive error were ascertained. Medical history was acquired and any other relevant drug history was noted. A family history was taken including a full pedigree with any history of consanguinity within the family and ethnicity.

2.2.1.2 Visual acuity

The term 'visual acuity' was coined by Donders who defined it as a ratio between a subject's performance and standard performance. In the year 1862, Snellen published his famous letter chart, which was designed using special targets called optotypes. The Snellen visual acuity test is still the most commonly used test of visual acuity.

The test involves a chart with rows of letters of diminishing size. Each row is accorded a number which indicates the distance at which a person with normal visual acuity should correctly identify the letters. The visual acuity is recorded as a fraction in which the numerator denotes the distance at which the subject is able to resolve the letters while the denominator indicates the distance at which a normal person should correctly identify the row. Normal vision is 6/6.

The other chart used in this study was designed by Ian Bailey and Jan Lovie in 1976. The measure of visual acuity provided by this chart is known as LogMAR (Logarithm of the minimal angle of resolution). The range of visual acuity measurements in LogMAR charts is equivalent to Snellen acuities and vary from 0.0 (6/6) to 1.0 (6/60).

In our study, patients underwent full ophthalmic examination including best–corrected visual acuities with Snellen chart which were converted to LogMAR values in some instances for ease of statistical analysis.

2.2.1.3 Colour vision

In this study, colour vision was tested using the Ishihara pseudoisochromatic plates and/or the Hardy-Rand-Rittler plates (American Optical Co., New York, USA).

2.2.1.3.1 Ishihara pseudoisochromatic plates

These plates were designed to test red-green colour deficiency. There are 24 pseudoisochromatic plates containing numerals and 1 test plate for demonstration of the visual task. 20 plates are for red-green screening which include 3 for subjects without numerical skills. The last 4 plates are for classification of red and green cone deficiencies (Figure 2-1).

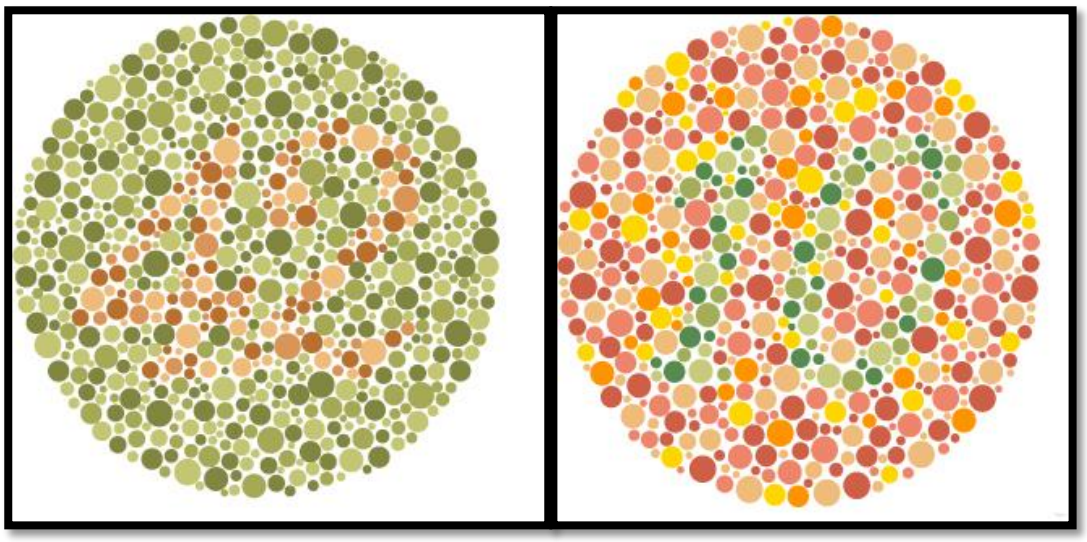

Figure 2-1: Ishihara colour test plates

2.2.1.3.2 Hardy-Rand-Rittler test (HRR)

This test is designed to identify and to grade the severity of red (protan), green (deutan), and blue (tritan) colour vision defects. Its ability to detect tritan defects distinguishes it from the Ishihara test plates. There are 24 plates which contain symbols of neutral colours increasing in saturation with successive plates of the test. There are 4 introductory plates, 6 plates for colour vision screening, and 14 plates for grading the severity of protan, deutan and tritan defects (Figure 2-2).

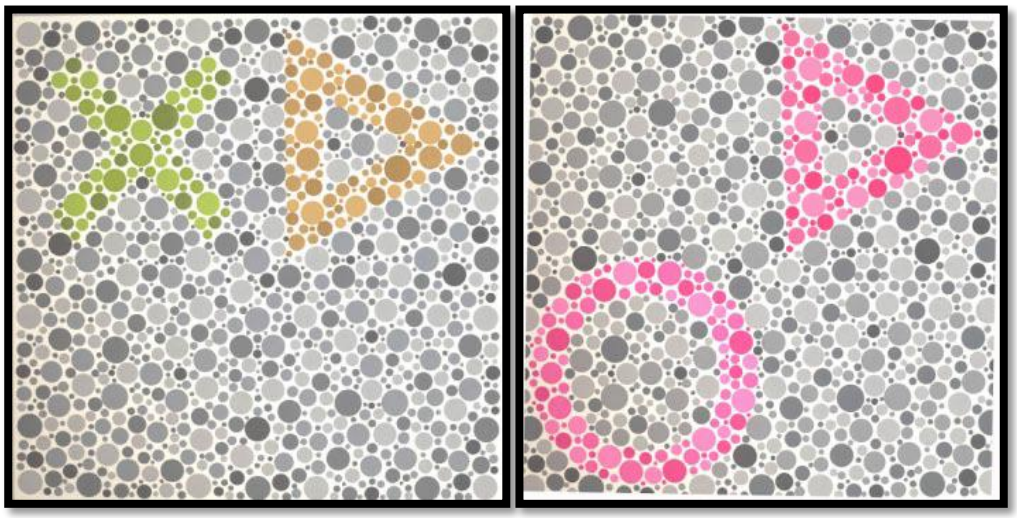

Figure 2-2: HRR colour test plates.

2.2.1.4 Fundoscopy

Purkinje was probably the first to observe the pupillary 'red reflex' and wrote that when light was thrown at the eye "the whole pupil lit up in a beautiful orange colour" (Thau, 1942). Although Charles Babbage, an English mathematician was the first to invent an ophthalmoscope, Hermann von Helmholtz's effort proved to be the more popular instrument (Keeler, 1997, Wade, 2007). Christian Theodor Georg Ruete invented

indirect ophthalmoscopy in 1852 and in 1911, Allvar Gullstrand, one of the few Ophthalmologists to receive a Nobel prize, developed the slit lamp (Simonsz, 2004, Nordenson, 1962).

In all our patients, slit-lamp biomicroscopy and fundoscopy were carried out after dilating the pupils.

2.2.2 VISUAL FIELDS

Visual field data were collected from the patients using Goldmann visual field or Esterman binocular visual field.

2.2.2.1 Kinetic perimetry

Kinetic perimetry is a method of plotting the visual field by moving the target from the non-seeing area towards the seeing area. By varying the size, luminosity and colour of the stimulus, various isopters are drawn to describe the subject's visual field in detail. The kinetic perimeter used in our study was the Goldmann perimeter. Wherever available, Goldmann visual field data was used for subsequent analysis.

Patients underwent Goldmann perimetry only if their best-corrected visual acuity was better than counting fingers and if their measured visual field could be reliably replicated on repeat testing. The testing was performed unilaterally with spectacle correction. The largest and the brightest target, V4e was used for all patients. If the V4e isopter was completed without difficulty then the III4e target was used and the field recorded.

2.2.2.2 Static perimetry

During static perimetry, the target is not mobile. It tests the threshold of individual points in the retina by varying the luminosity of the target at each point. We used Esterman suprathreshold visual field in some patients. This data was used only to assess the progression of the disorder. This visual field testing was performed by visual field technicians of MEH.

The visual field area contained within the V4e isopter was used for subsequent analysis. The field area was scanned electronically. A two dimensional planimetry package 'Retinal area analysis tool' designed by Dr A.S. Halfyard and Prof. H.W. Fitzke (2002) was used to calculate the area in square degrees.

2.2.3 RETINAL IMAGING

In the majority of cases, imaging was performed by medical photographers (Moorfields Eye Hospital Medical Illustration Department).

2.2.3.1 Fundus photography

This principle of fundus photography is the same as that used for indirect ophthalmoscopy. The images from digital fundus CCD cameras are high resolution and are stored as a digital dataset. The photographs are taken with the subject 2-3 cm away from the camera imaging at an angle of 30° creating a photograph about 2.5 times the original life size. Colour fundus

photography was performed using a Topcon TRC 50IA retinal camera (Topcon Corporation, Tokyo, Japan).

2.2.3.2 Fundus autofluorescence imaging (FAF)

FAF was developed at UCL Institute of Ophthalmology, London, UK using a confocal scanning laser ophthalmoscope (von Ruckmann et al., 1995a). The principle of the device is to detect autofluorescence signal from the retinoid fluorophores which mainly reside in the retinal pigment epithelium. Using scanning laser ophthalmoscope, a spatially coherent, low-divergence, narrow beam from a laser is delivered to the retina and the reflectance is detected and is converted to an image. A mean image is constructed superimposing several images together.

FAF was carried out using SPECTRALIS HRA2 (Heidelberg Engineering, Heidelberg, Germany). An excitation filter of wavelength 488 nm and a cut-off filter of 500 nm wavelength are used. Two different fields of view, 35° or 55° are captured using different lenses.

The big advantage of FAF is ease of evaluation of the retinal pigment epithelial health using naturally occurring fluorescence as an indicator. Several studies have indicated a correlation between distinct FAF patterns and types of retinal dystrophy (Robson et al., 2006, Robson et al., 2004).

In a normal FAF image (Figure 2-3), the optic disc appears black due to absence of retinal pigment epithelium. The foveal autofluorescence is reduced due to presence of the macular pigment, lutein and zeaxanthin, increased amount of melanin in the foveal retinal pigment epithelium and presence of foveal "blue light filter" (Subczynski et al., 2010).

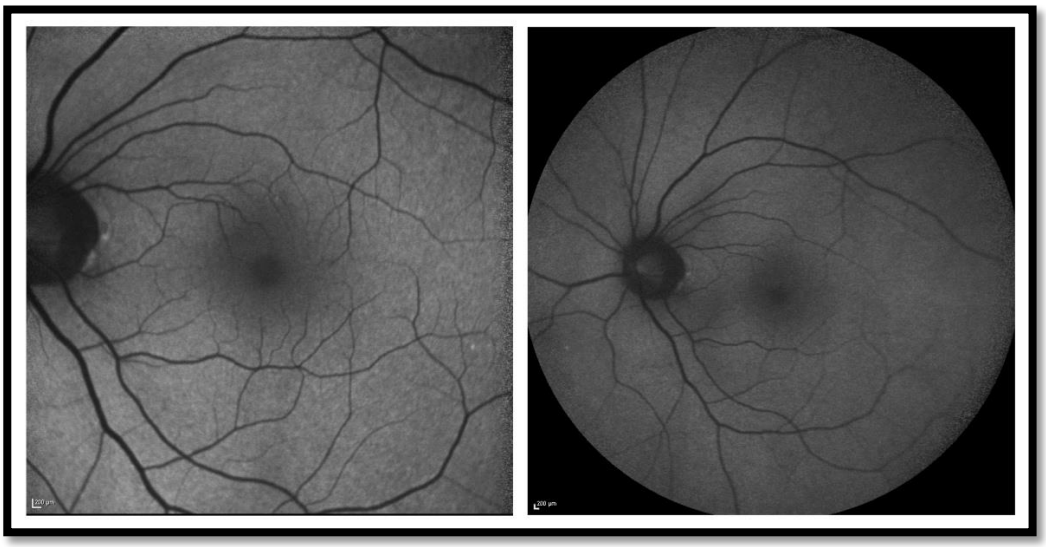

Figure 2-3: Normal fundus autofluorescence images - 30° on the left and 55° on the right.

2.2.3.3 Optical coherence tomography (OCT)

The principle of OCT is to measure time delay and the magnitude of reflected infrared light from the retina resulting in generation of cross-sectional or even three-dimensional images. First *in vivo* study using OCT was published in 1993 (Swanson et al., 1993) and OCT became commercially available soon after. Use of infrared light with a wavelength of around 820 nm improved the resolution of the images and removed the need for tissue contact with the imaging probe. Current OCT models can resolve up to 2µm (axial resolution) and by using Fourier transformation, a mathematical concept, has improved image acquisition speed and resolution significantly. With a significant increase in imaging speed, current OCT models can acquire up to 312,000 A-scans per second, making three-dimensional reconstructions possible. OCT data was obtained using a SPECTRALIS® Spectral-domain OCT (Heidelberg

Engineering, Germany) and/or a STRATUSOCT Model 3000 scanner (Zeiss Humphrey Instruments, Dublin, California, USA).

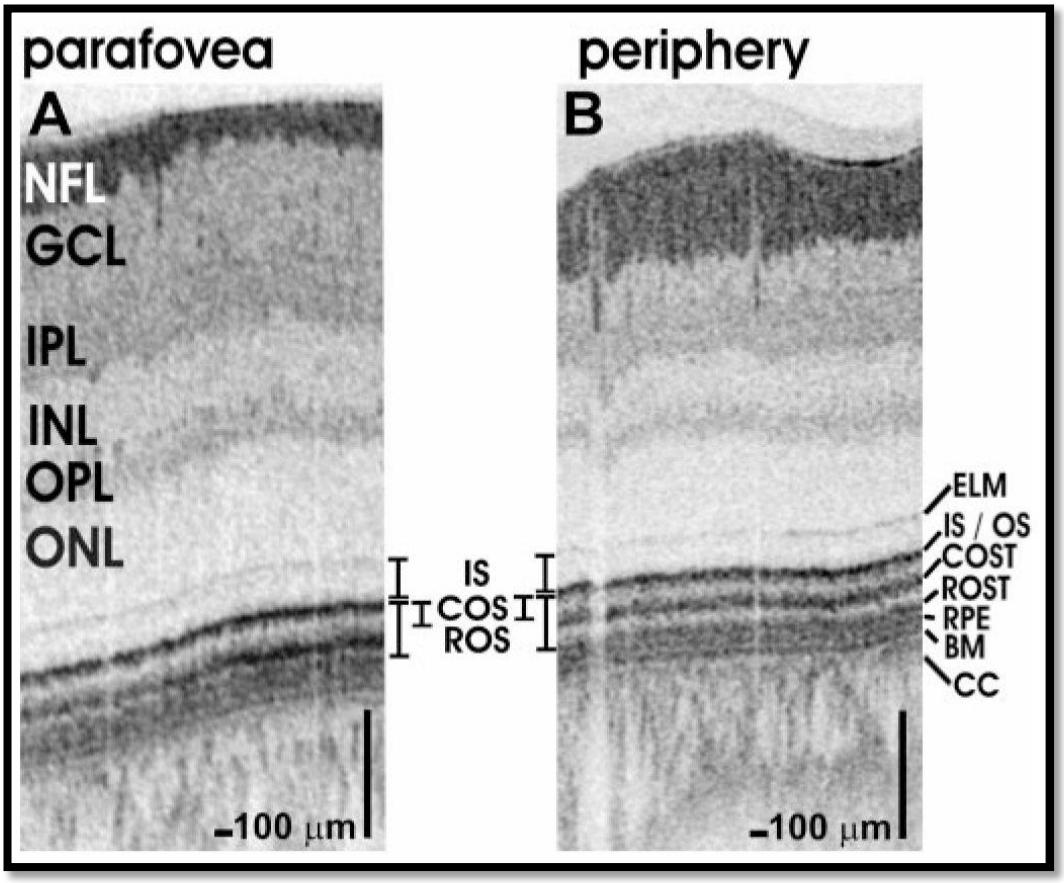

Figure 2-4: OCT layers – adapted from (Srinivasan et al., 2008). NFL – Nerve fibre layer, GCL – Ganglion cell layer, IPL – Inner plexiform layer, INL – Inner nuclear layer, OPL – Outer plexiform layer, ONL – Outer nuclear layer, ELM – External limiting membrane, IS – Inner segment, OS – Outer segment, COS – Cone outer segment, ROS – Rod outer segment, COST – Cone outer segment tip, ROST – Rod outer segment tip, RPE – Retinal pigment epithelium, BM – Bruch's membrane, CC – Choriocapillaris.

The precise interpretation of all the layers of an OCT image of the retina is still being resolved. Improvements in axial resolution and image acquisition speed are still being developed. Similar to FAF, several studies have pointed out specific OCT image patterns and their correlation with

retinal conditions (Huang et al., 2000, Gloesmann et al., 2003). In this study, the OCT layers have been interpreted as Figure 2-4.

2.2.4 ELECTROPHYSIOLOGY

Electrophysiological assessment involved obtaining a full-field electroretinogram (ERG), a pattern ERG (pERG), and an electro-oculogram (EOG). Electrophysiological testing was performed in the MEH Electrophysiology Department and the results were interpreted and reported by Professor Graham E Holder or Dr Anthony G Robson.

Table 2-1: Origins of components of ERG and pERG (Heckenlively and Arden, 2006)

ERG waveform	**Cellular origin**
a – wave	Dark adapted a – wave is primarily driven by rod photoreceptors; Light adapted a – wave in rod saturating background is cone driven
b – wave	Primarily reflects the activity of ON – bipolar cells
d – wave	Partly produced by depolarization of OFF – bipolar cells
Photopic fast flicker	Probably driven by post-receptoral cells of the cone system
pERG	Retinal ganglion cells

All electrophysiological analyses were performed incorporating the published standards of the International Society for Clinical Electrophysiology of Vision (ISCEV) (Marmor et al., 2009, Bach et al., 2013, McCulloch et al., 2015).

After 20 minutes of dark adaptation, full-field Ganzfeld stimulation was provided in order to ensure uniformity, full-field extension and correct luminance of the stimulus. White flashes of increasing intensities between 0.01 and 10.0 cd.s.m^{-2} were used to record dark adapted ERGs. The dimmest flash dark-adapted (DA) 0.01 ERG elicits rod-specific ERG response arising in the rod bipolar cells.

The bright flash or DA 3.0 ERG is a mixed rod-cone response dominated by the rod system under scotopic conditions. The electronegative a-wave is generated by the photoreceptors and the positive b-wave dominated by the post-receptoral ON-bipolar cell activity. On the ascending limb of the b-wave, the small wavelets present are called the oscillatory potentials which are believed to arise from amacrine cells.

A non-ISCEV standard additional red flash ERG was obtained to compare dark adapted cone and rod system function. In healthy individuals, the red flash ERG has an early cone component and later rod component.

To record generalized photopic cone system function, 10 minutes light adaptation to a standard background (25 cd.s.m^{-2}) was followed by recording the flicker ERG to a 30Hz flashing stimulus, the so called the Light adapted (LA) 3.0 flicker ERG. As temporal resolution of the rod system is lower than the cone system, this isolates the cone mediated activity. This response is dominated by the inner retinal cone-system activity.

A stimulus of 3.0 cd.s.m^{-2} flash on a background illumination of 30 cd.m^{-2} is used to elicit the single flash transient photopic ERG which was used to assess generalized light adapted cone function. The a-wave of this waveform partly represents the cone photoreceptor activity while the b-wave reflects post phototransduction activity.

Non ISCEV standard ON–OFF ERGs were obtained using a long duration orange stimulus (560 cd.m^{-2}, duration 200 ms) superimposed on a green light–adapting background (150 cd.m^{-2}). This separates the cone ON-bipolar cell activity from OFF-bipolar cell activity. The onset of the stimulus generates a positive polarity b-wave shaped largely by the cone ON pathway; the stimulus offset generates a positive polarity d-wave mainly arising from the cone OFF pathway (Table 2-1).

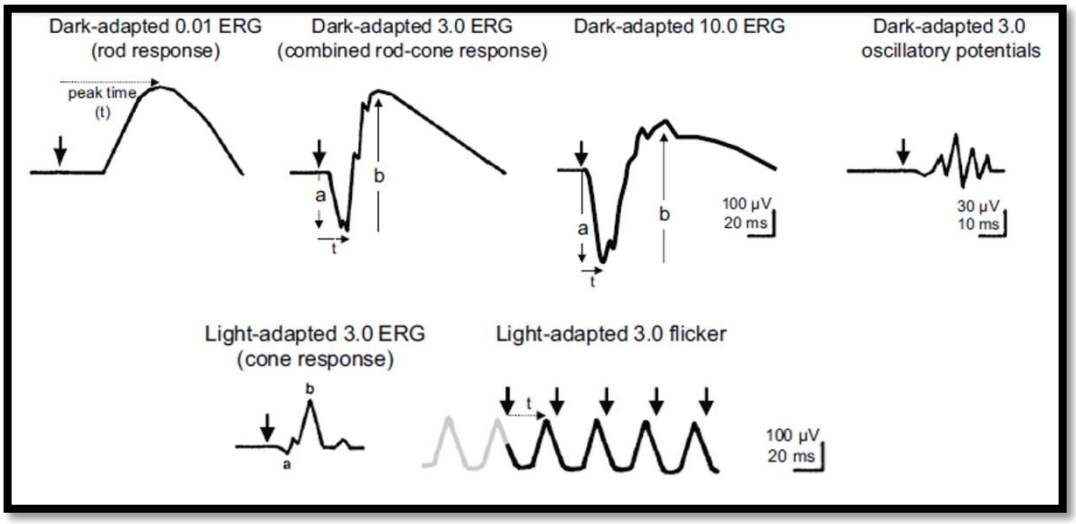

Figure 2-5: ISCEV standard ERG. Adapted from (McCulloch et al., 2015)

The normative data of the full-field ERGs have been published elsewhere (Robson et al., 2010) .

The pERG is the response obtained by presenting an alternating black and white checkerboard of constant mean luminance to the central retina. Driven by the macular photoreceptors and other retinal cells, this response is largely generated at the ganglion cell level. This is a small response, typically about 2-8 µV in amplitude, which is largely influenced by the optics of the eye and also the integrity of photoreceptors, bipolar cells and retinal ganglion cells. It has a small initial negative component which peaks

at about 35 ms (N35) followed by a larger positive component P50 at approximately 45 – 60 ms. This is followed by a large negative component N95 peaking at 90-100 ms.

Table 2-2: Interpretation of the electrophysiological findings. Modified from (Sergouniotis, 2012)

Electrophysiological changes	**Interpretation**
Reduced EOG light rise, normal ERG	RPE dysfunction
Reduced dark-adapted 0.01 ERG b-wave and 11.0 ERG a-wave	Rod photoreceptor dysfunction
Reduced dark-adapted 0.01 ERG b-wave, normal a-wave and markedly subnormal b-wave in dark-adapted 11.0 ERG (electronegative)	Postreceptoral (inner retinal) disease
Normal dark-adapted 11.0 ERG, reduced light-adapted responses	Cone photoreceptor dysfunction
Normal full field ERG, abnormal pERG P50 or multifocal ERG	Macular dysfunction
Normal full field ERG, preserved pERG P50, abnormal pERG N95	Ganglion cell dysfunction

2.3 MOLECULAR GENETIC METHODS

2.3.1 STRATEGY FOR MUTATION DETECTION

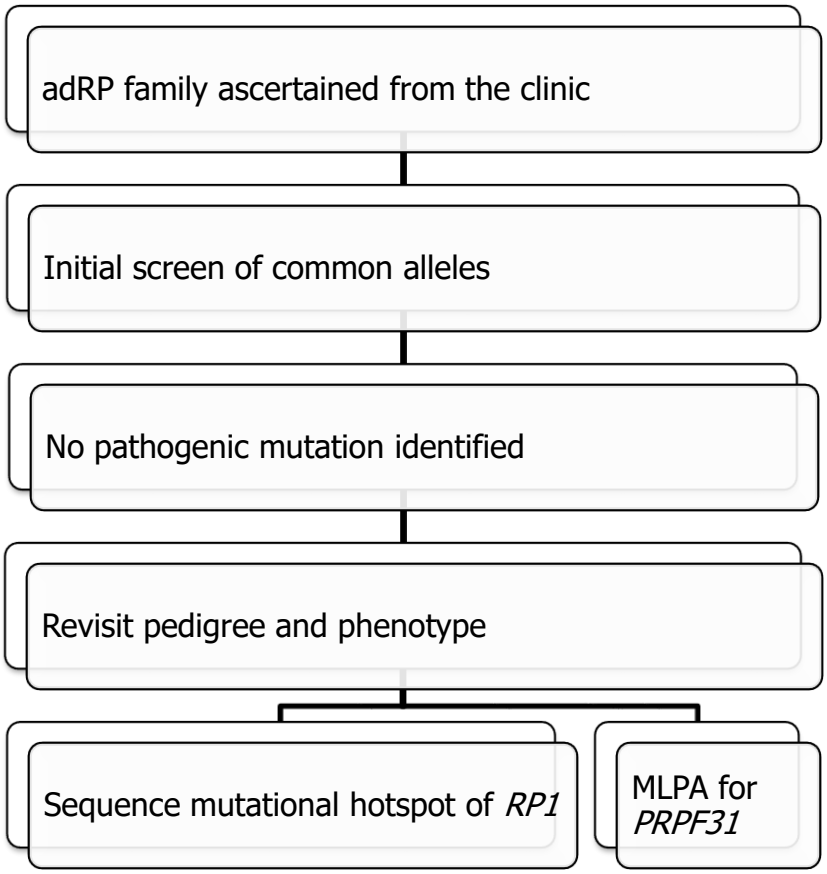

Initial screen for the most frequent alleles responsible for adRP was performed in the St. Mary's Hospital Academic Medicine Department, Manchester Academic Health Sciences Centre, University of Manchester, Manchester, UK as a service. The rest of the steps were performed by me in the laboratory of UCL Institute of Ophthalmology, London, UK.

2.3.2 STRATEGY FOR GENOTYPING

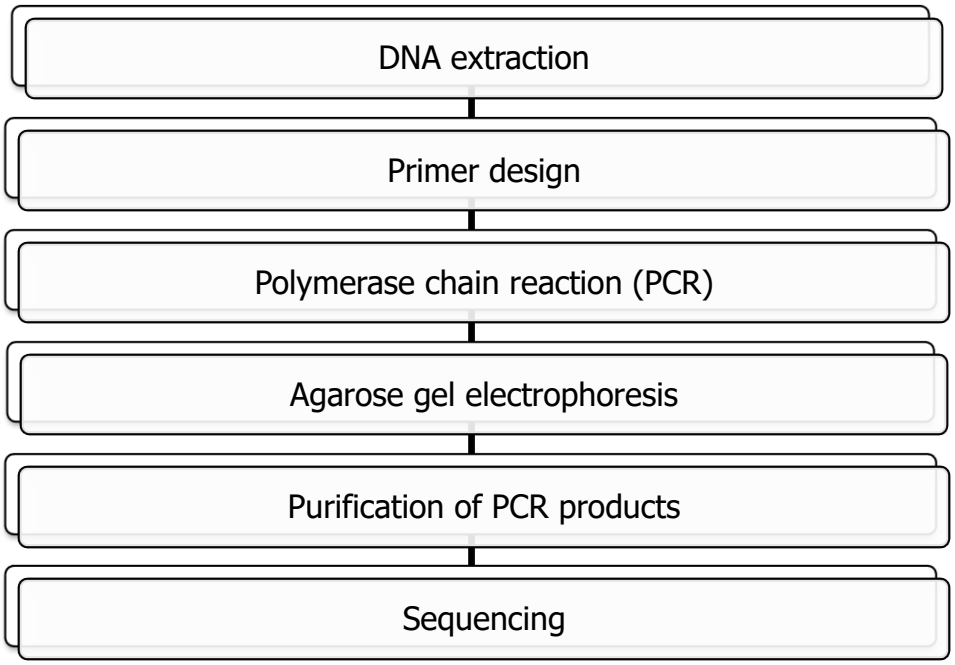

2.3.3 DNA EXTRACTION

Peripheral venous blood samples were collected in two 9ml sodium EDTA (Vacutainer) bottles and appropriately labelled. The samples were logged in the inherited eye disease database and stored at 4°C until DNA was extracted. The majority of blood samples were collected by Ms Genevieve Wright and Mrs Sophie Devery while most of DNA extraction was performed by Ms Bev Scott and Dr Naushin Waseem.

2.3.3.1 Principles of DNA extraction

The cells in the blood sample were lysed with an anionic detergent. After lysis, RNase enzyme was used to digest the RNA in the sample. Proteins were salt precipitated and removed. Finally, the genomic DNA in the sample was recovered by precipitation with alcohol. The genomic DNA thus obtained was stored in -20°C for future use. Two different kits with the following protocols were used.

2.3.3.2 Gentra® Puregene® blood kit (Qiagen, Hilden, Germany)

The leukocyte-enriched buffy coat was prepared from the EDTA whole blood sample by centrifuging the sample at 2500 x g for 10 minutes at room temperature (15 – 25°C). The buffy coat was visible as the middle layer between the superficial clear plasma layer and the bottom layer of erythrocytes. 1 ml of buffy coat was extracted from 10 ml of centrifuged whole blood to harvest 10X enrichment. 3 ml of RBC lysis solution was mixed with 1 ml buffy coat and incubated for 10 minutes in room temperature. The mixture was centrifuged at 2000 x g for 5 minutes to pellet the leukocytes. Vortexing suspended the pellet in 200 µl solution to which 3 ml of cell lysis solution was added to lyse the cells. 15 µl of RNase A solution was added and the mixture was incubated for 15 minutes at 37°C. It was incubated in ice for 3 minutes. 1 ml of protein precipitating solution was added and the mixture was centrifuged at 2000 x g for 5 minutes. This precipitated the protein into a tight brown pellet. 3 ml of isopropanol was added to the supernatant, mixed and centrifuged at 2000 x g for 3 minutes. Supernatant was discarded and 3 ml 70% ethanol was added and centrifuged for 1 min at 2000 x g. The supernatant was

discarded and the DNA pellet was air dried and finally dissolved in 300 µl DNA hydration solution and incubated for 1 hour at 65°C.

2.3.3.3 Nucleon genomic DNA extraction kit (Tepnel Lifesciences, Manchester, UK)

4 ml of Nucleon Reagent A was added to 1 ml of whole blood and vortexed for 4 minutes at room temperature. The mixture was centrifuged at 1300 x g for 5 minutes. The supernatant was discarded and the pellet was suspended in 350 µl of Nucleon Reagent B to ensure that the detergent was fully dissolved. The mixture was incubated at 37°C for 10 minutes. 2.5 µl of RNase A solution was added and the mixture was incubated at 37°C for 30 minutes. To deproteinise the mixture, 100 µl of sodium perchlorate, 600 µl of chloroform and 150 µl of Nucleon resin was added. The mixture was centrifuged at 350 x g for 1 minute. 900 µl of absolute ethanol was added to 450 µl of the supernatant and centrifuged at 4000 x g for 5 minutes. 1 ml of 70% alcohol was added to the DNA pellet and centrifuged. Finally, the DNA pellet was air dried and dissolved in TE buffer.

2.3.4 PRIMER DESIGN

The reference sequences were obtained from Ensembl genome database (Flicek et al., 2010). Primers were designed to anneal to the genomic sequence such that the coding region and the intron-exon boundaries are amplified within the DNA fragment. The primers had minimal secondary structure and no primer-dimer formation. The primers were limited to be

18-30 nucleotides length and the melting temperatures of the pair were matched as closely as possible. The properties of the primers were checked with OligoCalc (Kibbe, 2007) and the sequences were submitted to NCBI BLAST database (Altschul et al., 1997) to check specificity. The amplimer size was limited to 800 bp.

2.3.5 Polymerase Chain Reaction

Polymerase chain reaction (PCR) is method of amplifying small segments of DNA that has revolutionised molecular genetics (Kleppe et al., 1971, Mullis, 1990b, Mullis, 1990a). To permit such selective amplification, primers are designed complementary to specific regions either side of the area that requires amplification (amplimer). In the presence of a DNA polymerase, an enzyme that synthesizes DNA, and the four deoxynucleoside triphosphates, dATP, dCTP, dGTP and dTTP, the primers anneal to the denatured DNA and initiate the synthesis of new DNA strands complementary to the target sequence. This starts a chain reaction with newly synthesized DNA strands acting as templates for further DNA synthesis in subsequent cycles. The products of the PCR will include about 10^5 copies of the desired amplimer after about 35 cycles of PCR. PCR was performed using MolTaq (Molzym, Bremen, Germany) DNA polymerase. The standard PCR cycling parameters used are described in Table 2-3.

Table 2-3: PCR cycling parameters

Stage	Temperature (°C)	Time	Cycle(s)
Initial denaturation	94-95	3-5 minutes	1
Denaturation	94-95	30-45seconds	35
Annealing	50-70	30 seconds	
Extension	72	1 minute	
Final extension	72	5-7 minutes	1
Hold	4	For ever	1

The protocol used is elaborated in the manufacturer's instructions (Table 2-4).

Occasionally, extra $MgCl_2$ or DMSO up to 10% v/v was added to PCR reactions to enhance efficiency. For difficult or problematic PCR applications, different polymerases were used including BioTaq (Bioline) DNA polymerase, Platinum Taq DNA Polymerase High Fidelity (Invitrogen) or Platinum Pfx DNA Polymerase (Invitrogen), all according to the manufacturers' instructions.

Table 2-4: Molzym PCR protocol

Component	Volume	Final concentration
Buffer (1.5mM MgSO4)	3 µl	1X

Enhancer	0.3 µl (Molzym)	1.5 mM
dNTP mixture	0.24 µl (Promega)	0.2 mM of dATP, dGTP, dCTP and dTTP
Forward primer	1 µl	0.33 mM
Reverse primer	1 µl	0.33 mM
MolTaq polymerase	0.2 µl (5U/µl)	0.03 U/µl
dH_2O	23.26 µl	
DNA template	1 µl	10-50 ng/µl
Total	30 µl	

2.3.6 AGAROSE GEL ELECTROPHORESIS

Although it had been used to separate proteins earlier (Hammarlund and Rising, 1953), agarose gel electrophoresis was first used to separate, purify and isolate fragments of DNA in 1966 (Thorne, 1966). 2% w/v agarose gel was prepared by dissolving 2 gm of molecular grade agarose (Bio-Rad Laboratories, Berkeley, California, USA) in 100ml of 1X TBE buffer (Eppendorf, Hamburg, Germany). 5 µg of Ethidium bromide (Final concentration 0.5 µg/ml) (Flint and Harrington, 1972) was added to the mixture and the gel was set. To validate the amplified fragments of DNA following PCR, 3 µl of DNA was mixed with 2 µl of 1X loading dye (Bioline, London, UK) and placed in the wells of the agar gel along with standard size marker (Bioline, London, UK). The electrophoresis was performed at 150mV for 30 minutes in 1X TBE buffer till the fragments were separate.

The separated fragments were visualized on a transilluminator (UV light of wavelength 210nm) and photographs were taken in a camera with orange filter (BioDoc-It 210, UVP, Upland, California, USA).

2.3.7 Purification of PCR products

Once the correct size of the amplified PCR product was verified by agarose gel electrophoresis, the product was purified using vacuum-based Montage PCR_{96} cleanup kit (Millipore, Watford, UK). This used size exclusion separation method. 100 µl of PCR products were loaded into the wells of the $MultiScreen_{96}$ PCR plate. Vacuum was applied at 24 inches Hg for 5-10 minutes till the wells had emptied. The samples were reconstituted with 100 µl of nuclease free water and vacuum was applied again. The samples were reconstituted with 100 µl of nuclease free water for the second time and mixed vigorously on a plate shaker for 5 minutes. The purified PCR products were pipetted out from each well and stored for future use.

2.3.8 Automated DNA sequencing

Frederich Sanger's method of dideoxy mediated chain-termination sequencing (Sanger et al., 1977a, Sanger et al., 1977b) was used to ascertain the nucleotide sequence of the PCR amplimer with BigDye® Terminator v3.1 (>500 bp) cycle sequencing kit (Applied Biosystems. Foster City, California, USA) bi-directionally. The protocol used for the sequencing reaction is described in Table 2-5.

Products following sequencing reaction were purified using Montage SEQ_{96} Sequencing Reaction cleanup kit (Millipore, Watford, UK). 5 µl of the sequence reaction samples was diluted with 20 µl of Injection solution. The mixture was transferred into the wells of SEQ_{96} plate and vacuum of 25 inches Hg was applied for 3-5 minutes until the solution was completely removed. 20 µl of Injection solution was added to each well again and the process was repeated. For the third time, 20 µl of Injection solution was used to suspend the sequence reaction samples by shaking them on a microplate shaker for 10 minutes. The purified products were transferred on to an injection plate.

Table 2-5: PCR product sequencing reaction protocol

Component	**Volume**	**Concentration**
PCR product	1 µl	10-50 ng
Primer	1 µl	1 µM
Buffer (BigDye sequencing buffer)	2.5 µl	1X
BigDye terminator	0.5 µl	
dH2O	5 µl	
Total	10 µl	

Table 2-6: Sequencing reaction cycle

Temperature	**Time**	**Cycles**
96°C	1 minute	1
96°C	10 seconds	25
50°C	5 seconds	
60°C	4 seconds	
4°C	Hold	For ever

The sequencing reaction cycle used is shown in Table 2-6. 48-capillary 3730 DNA analyser (Applied Biosystems, Foster city, California, USA) was used to perform automated capillary electrophoresis.

Seqman Pro software (Lasergene version 8.02 sequencing analysis software suite, DNAStar Inc., Madison, Wisconsin, USA) was used to compare electropherograms with those with the disease from control samples. Other softwares, Sequence Scanner Software v1.0 (Applied Biosystems, Foster city, California, USA) and Sequencher 4.10.1 (Gene Codes Corporation, Ann Arbor, USA) were also used for sequence analysis.

2.3.9 MULTIPLEX LIGATION-DEPENDANT PROBE AMPLIFICATION (MLPA)

Mainly used to detect copy number variations, this technique utilizes multiple probes of unique length that are hybridized to the target sequence. Each probe pair contains the same primer sequence at 3' and 5' ends permitting their amplification in a single PCR reaction using a single primer pair. In MLPA, each probe pair hybridizes to the target close to one another permitting ligation. The ligated probe is then amplified. Amount of PCR product generated is dependent on successful ligation and reflects the number of target sequences (Schouten et al., 2002) (Figure 2-6) (http://www.applied-maths.com/applications/multiplex-ligation-dependent-probe-amplification-mlpa-analysis)

This technique was used to discover large deletions or insertions in the *PRPF31* gene in families of adRP with incomplete penetrance where Sanger sequencing failed to find a mutation. The procedure was performed using the SALSA MLPA P235 Retinitis kit (MRC-Holland, Amsterdam, Netherlands).

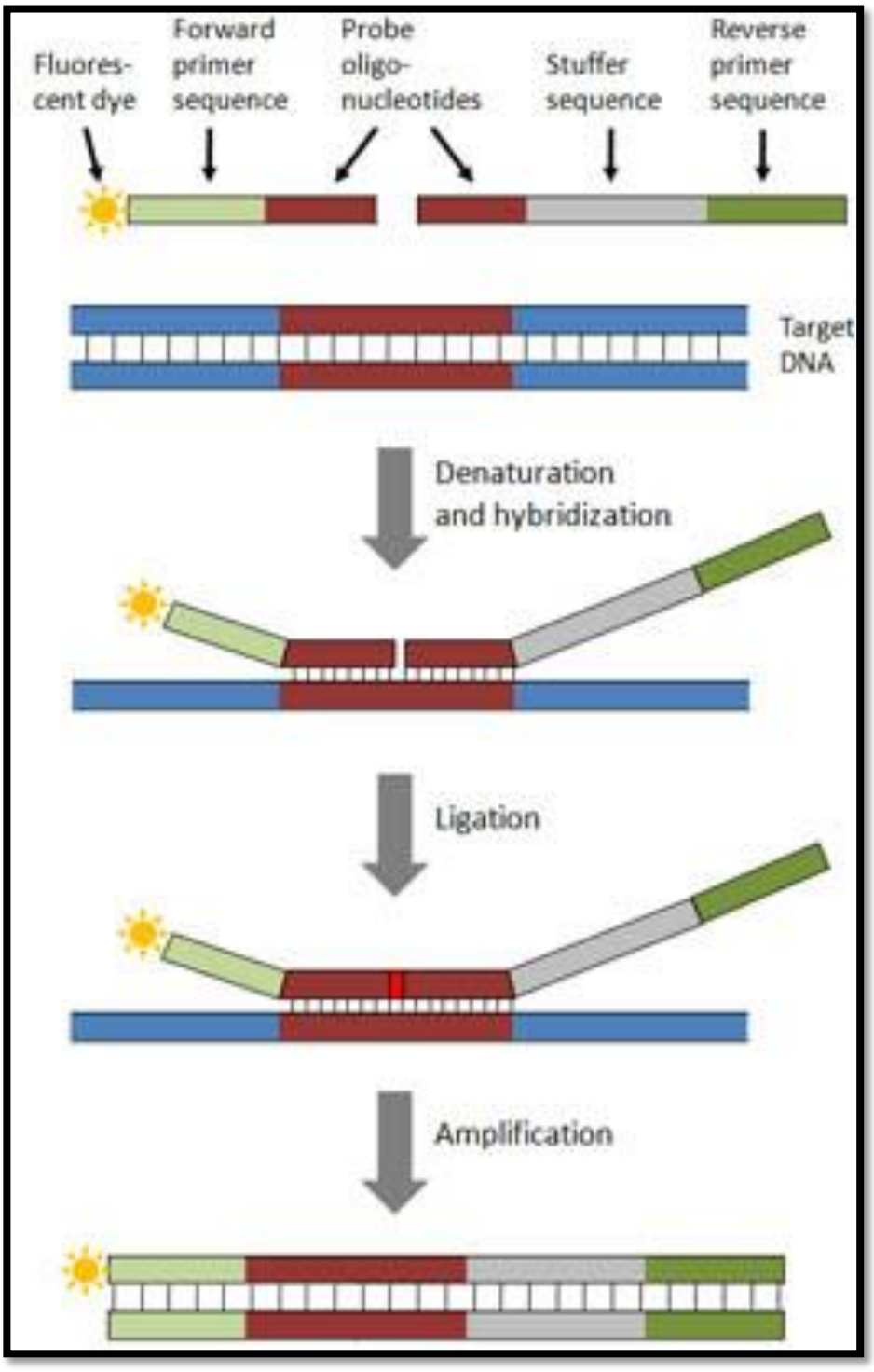

Figure 2-6: Principles of MLPA

Table 2-7: Components in the SALSA MLPA Retinitis kit

Component	Ingredients
SALSA MLPA Buffer	KCl, Tris-HCl, EDTA, PEG-6000, oligonucleotides
SALSA Ligase-65	Glycerol, BRIJ (0.05 %), EDTA, Beta-Mercaptoethanol (0.1 %), KCl, Tris-HCl, Ligase-65 enzyme (bacterial origin)
Ligase Buffer A	Nicotinamide Adenine Dinucleotide (NAD) (bacterial origin).
Ligase Buffer B	Tris-HCl, non-ionic detergents, $MgCl_2$
SALSA PCR Primer Mix	Synthetic oligonucleotides with fluorescent dye (FAM, Cy5, IRD800, ROX or unlabeled), dNTPs, Tris-HCl, KCl, EDTA, BRIJ.
SALSA Polymerase	Glycerol, non-ionic detergents, EDTA, DTT (0.1 %), KCl, Tris-HCl, Polymerase enzyme (bacterial origin).

Table 2-8: Steps of MLPA and its protocol

Reactions	Temperature	Time	Steps
DNA denaturation	98°C	5 minutes	5 µl of DNA sample for denaturation
	25°C	pause	
Hybridisation	95°C	1 minute	Mix 1.5 µl of MLPA buffer and 1.5 µl of probemix with 3 µl of denatured DNA for hybridisation
	60°C	16-20 hours	

Ligation	54°C	pause	Mix 25 µl of dH_2O, 3 µl of Ligase Buffer A, 3 µl of Ligase Buffer B and 1 µl of Ligase-65 enzyme to the hybridised DNA.
	54°C	15 minutes	
	98°C	5 minutes	
	20°C	pause	
PCR	95°C	30 seconds	Add 4 µl of SALSA PCR buffer and 26 µl of dH_2O to 10 µl of ligation product. To it add 7.5 µl of dH_2O, 2 µl of SALSA PCR primer mix and 0.5 µl of SALSA polymerase. Run the PCR for 35 cycles.
	60°C	30 seconds	
	72°C	60 seconds	
	72°C	20 minutes	
	15°C	pause	
Capillary Electrophoresis	86°C	3 minutes	0.7 µl of PCR product, 0.3 µl of ROX or LIZ size standard and 9 µl of HiDi formamide is used in 3730 DNA analyser (ABI, California, USA).
	4°C	2 minutes	

2.3.10 *MICROSATELLITE MARKERS*

Microsatellites are di-, tri- or tetra-nucleotide repeats showing allelic polymorphisms that can be used to follow a chromosomal segment through a pedigree (Strachan and Read, 2004). First used in 1989, the commonest ones used are $(CA)_n$ repeats. They are highly informative and are distributed throughout the genome (Litt and Luty, 1989).

Microsatellite markers for chromosome 17p (D17S799, D17S1876, D17S1791, D17S1828) were identified from Marshfield map (Broman et al., 1998) and the primers were obtained from ABI Prism Linkage Mapping Set version 2.5 (Applied Biosystems, Foster city, California, USA). PCR reactions were performed as follows (Table 2-9).

Table 2-9: PCR reaction mix for microsatellites

Component	**Volume**
Buffer (1.5mM MgSO4)	1.5 µl
Enhancer (1.5 mM)	0.75 µl
dNTP mixture (0.2 mM of dATP, dGTP, dCTP and dTTP)	0.3 µl (Promega)
Primer mix (5 µM of each primer)	0.6 µl
Taq polymerase (5U/µl)	0.15 µl
dH2O	10.7 µl
DNA template (10-50 ng/µl)	1 µl
Total	15 µl

All four markers were multiplexed into a single reaction. The microsatellite markers labelled with dye FAM or VIC (D17S799, D17S1876 and

D17S1791) were diluted 1:20 while the marker labelled with dye NED (D17S1828) was diluted 1:10. 5 µl of diluted D17S799, D17S1791 and D17S1876 PCR products and 10 µl of diluted D17S1828 PCR product were pooled. 0.5 µl of pooled PCR products was mixed with 0.5 µl of LIZ as size standard and 9 µl of HiDi formamide. The mixture was incubated at 95°C for 5 minutes and then rapidly cooled in ice before loading for genotyping. 3730 DNA analyser (Applied Biosystems, Foster city, California, USA) was used to genotype the region. Genotyping analysis was performed using GeneMapper software (version 4.1; Applied Biosystems, Foster city, California, USA).

Table 2-10: PCR conditions for the microsatellite markers

Stage	Temperature	Time	Cycle(s)
Initial denaturation	94°C	2 minutes	1
Denaturation	95°C	1 minute	30
Annealing	55°C	45 seconds	
Extension	72°C	45 seconds	
Final extension	72°C	10 minutes	1
Hold	4°C	For ever	1

2.3.11 BIOINFORMATICS

In order to ascertain the pathogenicity of the single nucleotide variations identified by genetic analysis, an *in-silico* approach was adopted. An online tool CONDEL (Gonzalez-Perez and Lopez-Bigas, 2011) was utilised which combines the results of SIFT (Kumar et al., 2009), Polyphen-2 (PPH2) (Adzhubei et al., 2010), Mutation assessor (MA) (Reva et al., 2011) and Functional analysis of hidden Markov models (FATHMM)

(Shihab et al., 2015). SIFT algorithm estimates the conservation of an amino acid through evolution using sequence alignment. A SIFT value of <0.05 indicates changes damaging to the protein function. In addition to sequence alignment methods, PPH2 evaluates the effect of the mutation on protein structure and estimates the evolutionary role. A PPH2 value of ≥1 indicates pathogenicity. MA uses a different algorithm to assess the evolutionary conservation of amino acids in a protein. FATHMM uses the mathematical concept of 'Hidden Markov Model' to add pathogenicity weights to protein sequences and domains. To further analyse the variations identified, presence of these missense changes were searched in two large databases – Exome Variant Server (EVS) and Exome Aggregation Consortium browser (ExAC). EVS contains whole exome analysis data from 2203 African-American and 4300 European American individuals (EVS, 2015). Similarly ExAC contained data obtained from large scale exome sequencing of 60706 individuals (ExAC, 2015). Absence of the missense changes in these databases decreased the changes of them being polymorphisms.

Table 2-11: Experiments conducted and data collected by author

Phenotyping	
History and clinical examination	Author
Goldmann visual fields	Author
Statistical analysis	Author
Genotyping	
Primer design for *RP1*, *RPE65* and *GUCY2D*	Author
DNA extraction (3 patients)	Author

PCR for *RP1*, *RPE65*, *GUCY2D* and *CHM*	Author
Gel electrophoresis	Author
DNA Sequencing	Author
MLPA for *PRPF31*	Author
Microsatellite marker analysis	Author
Bioinformatics	Author

3 RESULTS

3.1 A SURVEY OF THE MOLECULAR PATHOLOGY OF 287 FAMILIES WITH AUTOSOMAL DOMINANT RETINITIS PIGMENTOSA

3.1.1 INTRODUCTION

Retinitis Pigmentosa is a spectrum of inherited eye disorders with varied genotypes and phenotypes. It transmits within families in autosomal dominant, autosomal recessive, X-linked recessive or digenic fashion (Bunker et al., 1984, Grondahl, 1987, Kajiwara et al., 1994). Mutations in at least 26 different genes have been implicated in autosomal dominant retinitis pigmentosa (adRP) (RetNet) (Table 1-1). Although in some instances careful assessment of the phenotype may suggest which gene is likely to be causative and should be screened first, such cases are a minority. The gold standard strategy to ascertain the molecular diagnosis is to Sanger sequence all the genes implicated in adRP in their entirety. This is prohibitively time consuming and expensive. In this study, we propose an algorithm for screening the most common alleles in the genes causing adRP followed by phenotype-directed gene sequencing. This strategy can be quick and a relatively inexpensive method of identifying the underlying molecular basis of disease in a large proportion of families and help finding potentially valuable families to identify novel disease-causing genes.

We describe the result of genetic analysis of families with adRP presenting to a single UK tertiary referral hospital. The results provide

valuable insight into the predominant genetic causes of adRP in the British population.

3.1.2 METHODS

We ascertained families with the clinical diagnosis of adRP, based upon the phenotype and family history, from the inherited eye disease clinics at Moorfields Eye Hospital (MEH). After informed consent was obtained, one affected member from each family was screened for mutations in the known genes causing adRP.

3.1.2.1 Genotyping

An algorithm was constructed based on the observation that pathogenic alleles in the adRP genes are confined to specific regions of the gene (Bowne et al., 1999, Gamundi et al., 2008, DeAngelis et al., 2002, Towns et al., 2010, Wada et al., 2005b, Coppieters et al., 2007, Keen et al., 2002) (Table 3-1). Notable exceptions to this rule are the genes *RHO*, *PRPH2* and *PRPF31*.

This part of the study was conducted at St. Mary's Hospital Academic Medicine Department, Manchester Academic Health Sciences Centre, University of Manchester, Manchester, UK as a part of the National Health Service.

Table 3-1: The algorithm for screening the most common alleles and the mutational hotspots of genes causing adRP

Gene	Exon / Mutation	Technique
RHO	Exons 1-5	Bi-directional Sanger sequencing
PRPH2/RDS	Exons 1-3	
PRPF3	Exon 11	
PRPF8	Exon 42	
NR2E3	Exon 2-3	
IMPDH1	Exon 8-10	
NRL	Exon 2	
RP9	c.410A>T, p.H137L	Pyrosequencing
PRPF31	c.527+3A>G and c.1115_1125del11, p.Arg372GlnfsX99	
RP1	c.2029C>T, p.R677X	

If no positive result was obtained following the above-described algorithm, the mutational hotspot (codon 617-1081) of exon 4 of the *RP1* gene was sequenced bi-directionally in two overlapping polymerase chain reactions (PCR). I performed this part of the genotyping at UCL Institute of Ophthalmology.

Finally, in families where the pedigree structure / clinical findings indicated non-penetrance, all the exons and the intron-exon boundaries of *PRPF31* were sequenced. In families with non-penetrance, which still did not yield a positive result, Multiplex Ligation-dependent Probe Amplification (MLPA) was performed to detect large copy-number variations in *PRPF31* not detectable by PCR and sequencing. I performed the MLPA in the genetics laboratories of the UCL Institute of Ophthalmology.

After identifying a mutation in an individual, the segregation of the allele within the affected members of the family was verified by PCR and direct Sanger sequencing or MLPA.

The pathogenicity of the novel missense changes identified were tested *in-silico* using the tool CONDEL (Gonzalez-Perez and Lopez-Bigas, 2011) which combines the results of SIFT (Kumar et al., 2009), Polyphen (PPH2) (Adzhubei et al., 2010), Mutation assessor (MA) (Reva et al., 2011) and Functional analysis of hidden Markov models (FATHMM) (Shihab et al., 2015). The novel splice-site mutations were analysed using online tools like Human Splicing Finder (Desmet et al., 2009) and Spliceman web server (Lim et al., 2011).

3.1.2.2 Phenotyping

Phenotypic analysis of patients was limited to those with novel mutations. The aim of this strategy was to identify unique features in these patients that have not been described before to expand the current phenotype.

Identification of a true autosomal dominant inheritance can sometimes be difficult based on phenotypic characteristics and family history. In some cases, notably in families with X-linked RPGR mutations, female carriers may present with variable phenotype including severe disease making identification of carriers difficult (Rozet et al., 2002). This, in absence of a male-to-male transmission, makes the pedigree structure similar to that of autosomal dominant inheritance. In order to identify presence of such families, we compared the number of affected females in our families with known and unknown molecular diagnosis.

3.1.3 RESULTS

Two hundred and eighty-seven families with adRP were included in this survey. One family harboured two mutations – one branch carrying *RHO* p.G106R while the other branch had the *PRPF31* variant p.E183_M193dup. This family has been included as both *RHO* and *PRPF31* mutation carrier for calculations. All the mutations identified in this study are listed in Table 5-1 in Appendix.

The initial screen of the common alleles was performed in 265 families at the St. Mary's Hospital Academic Medicine Department, Manchester Academic Health Sciences Centre, University of Manchester, Manchester, UK. This identified mutations in 143/265 (53.9%) families. Among the rest 122 families with no molecular diagnosis, mutational hotspot of the *RP1* gene was screened. In addition, another group of 22 families who did not undergo Manchester screening were sequenced for the *RP1* hotspot. This identified mutations in the *RP1* gene in 38 additional families. 10 families with no molecular diagnosis from the screening described above but clear evidence of non-penetrance had further sequencing and MLPA of the whole of the *PRPF31* gene. This identified 3 more families with *PRPF31* mutations.

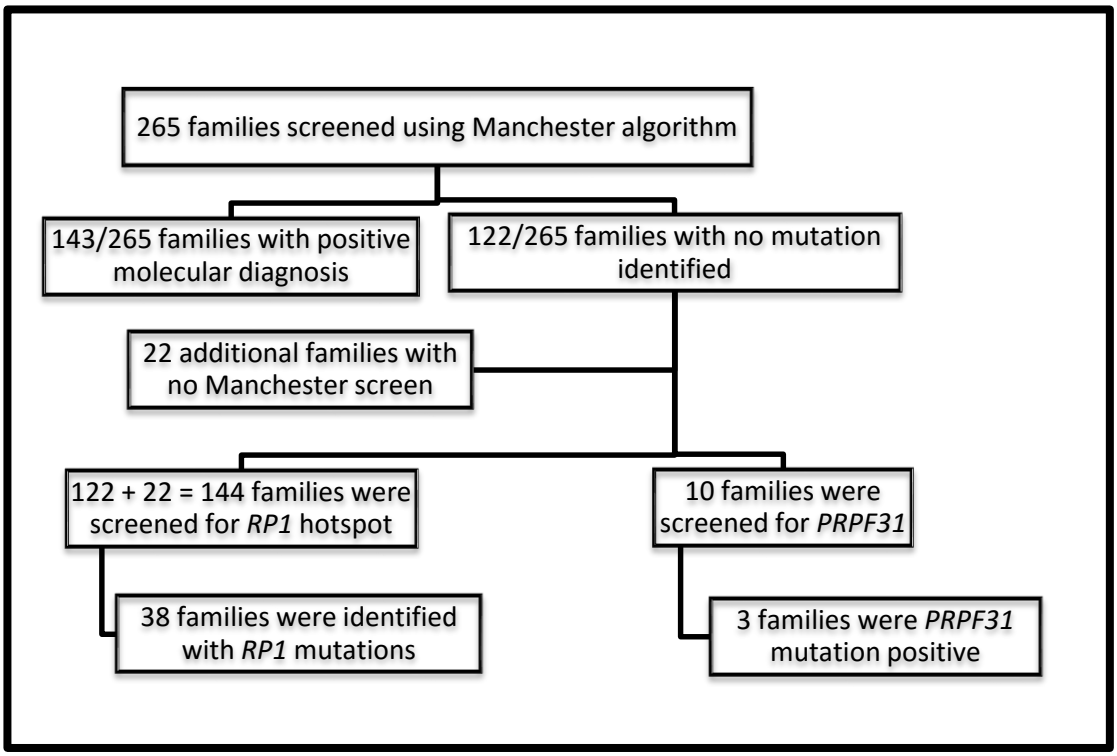

Figure 3-1: The strategy of mutation screening adopted in this

In total, our strategy identified mutations in 183 (63.1%) adRP families. The relative contribution of each gene towards adRP in our cohort is depicted in Figure 3-2. Variants in RHO, RP1 and PRPF31 together accounted for 51.6% of our families. No pathogenic mutation was found in 36.9% (106/287) of adRP families.

3.1.3.1 Rhodopsin

A mutation in *RHO* was the most common (22.6%) molecular diagnosis in our cohort (Figure 3-2). The initial screening of the whole of the *RHO* gene identified 25 different mutations in *RHO*, 2 of which were novel

(Table 5-1). The mutations in our cohort were distributed throughout all the exons of the gene. Specifically, 22/25 (88%) of the mutations were missenses, while two mutations produced in-frame deletions. One mutation was identified as a splice site mutation. Except for the mutation c.937-1G>T (splice site mutation) which may produce a null allele, in all other cases the protein was predicted to be expressed.

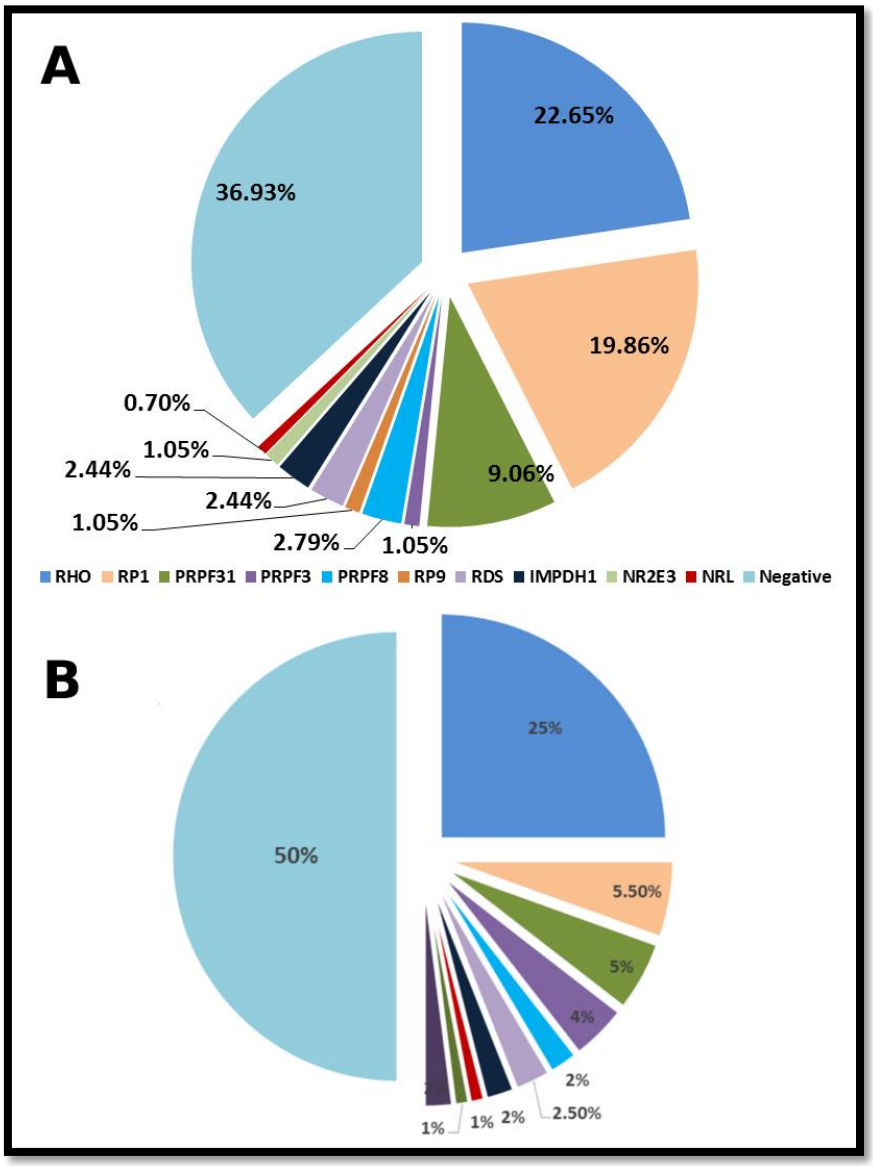

Figure 3-2: A – The pie chart showing the relative contributions of different genes in the causation of adRP in our cohort B – The adRP genotypes as described by previous authors (Hartong et al., 2006)

2 families were identified with novel *RHO* mutations –family GC16058 with *c.511C>A, p.P171T* and family GC19225 with *c.512C>G, p.171R*. In order to identify the impact of these missense changes on the protein structure and function, in-silico analysis of the mutations were performed (Table 3-2). Both the substitutions were absent from EVS or ExAC databases (ExAC, 2015, EVS, 2015).

Table 3-2: Analysis of the novel *RHO* mutations

Mutation	SIFT	PPH2	MA	FATHMM	CONDEL	Conclusion
c.511C>A, p.P171T	0	1	4.72	1.06	0.7441108	Likely deleterious
c.512C>G, p.P171R	0	1	4.72	1.02	0.7471266	Likely deleterious

Both the novel mutations affect Prolene 171 in the fourth transmembrane region of rhodopsin. Other substitutions of this amino acid have been described in different families with adRP suggesting that P171 is vital for the function of the protein (Dryja et al., 1991, Antinolo et al., 1994, Vaithinathan et al., 1994). It has been proposed that substitutions in this amino acid is likely to cause misfolding of the rhodopsin protein causing retention of the mutant protein in the endoplasmic reticulum and impairing reconstitution with 11-cis-retinal (Mendes et al., 2005).

3.1.3.1.1 Phenotype of the patients with novel mutations in RHO

Phenotyping was performed on 3 affected members of the families GC16058 and GC19225 who harboured novel *RHO* mutations

The proband of the family GC16058 is of Indian origin, who presented at the age of 50 years with dimness of vision, night blindness and reduced peripheral vision. She experienced difficulty in peripheral vision in her early teens and night vision problems when she was 16 years of age. The central vision deteriorated since. The visual acuities were 6/24 in both eyes.

She was identified to have intra-retinal pigmentation in the mid-peripheral retina, attenuated arterioles, optic disc pallor and atrophic changes in the posterior pole (Figure 3-3). In addition, there were bilateral posterior sub-capsular cataracts which were operated. She demonstrated steady decline of her visual function since and at the age of 61 years, she had visual acuities of 6/24 in both eyes and severely restricted visual fields of less than 5 degrees. Serial OCT evaluation failed to identify any macular oedema although there was photoreceptor drop-out in the foveal region.

The other affected individual was the son of the proband of family GC16058. He presented at 23-years of age with mild symptoms of night blindness. His visual acuities were 6/9 both eyes and his visual fields to confrontation was full. On examination at 27-years of age, his visual acuities were 6/6 both eyes with correction. Ophthalmic evaluation showed mid-peripheral intraretinal pigment migration, constricted visual fields but no evidence of macular oedema or cataracts (Figure 3-4). A ring of hyperautofluorescence in the posterior pole was evident on autofluorescence imaging surrounding the fovea. On OCT evaluation of the retina, the perifoveal zone was healthy although there was disturbance in the photoreceptor- retinal pigment epithelium layers in the retinal periphery.

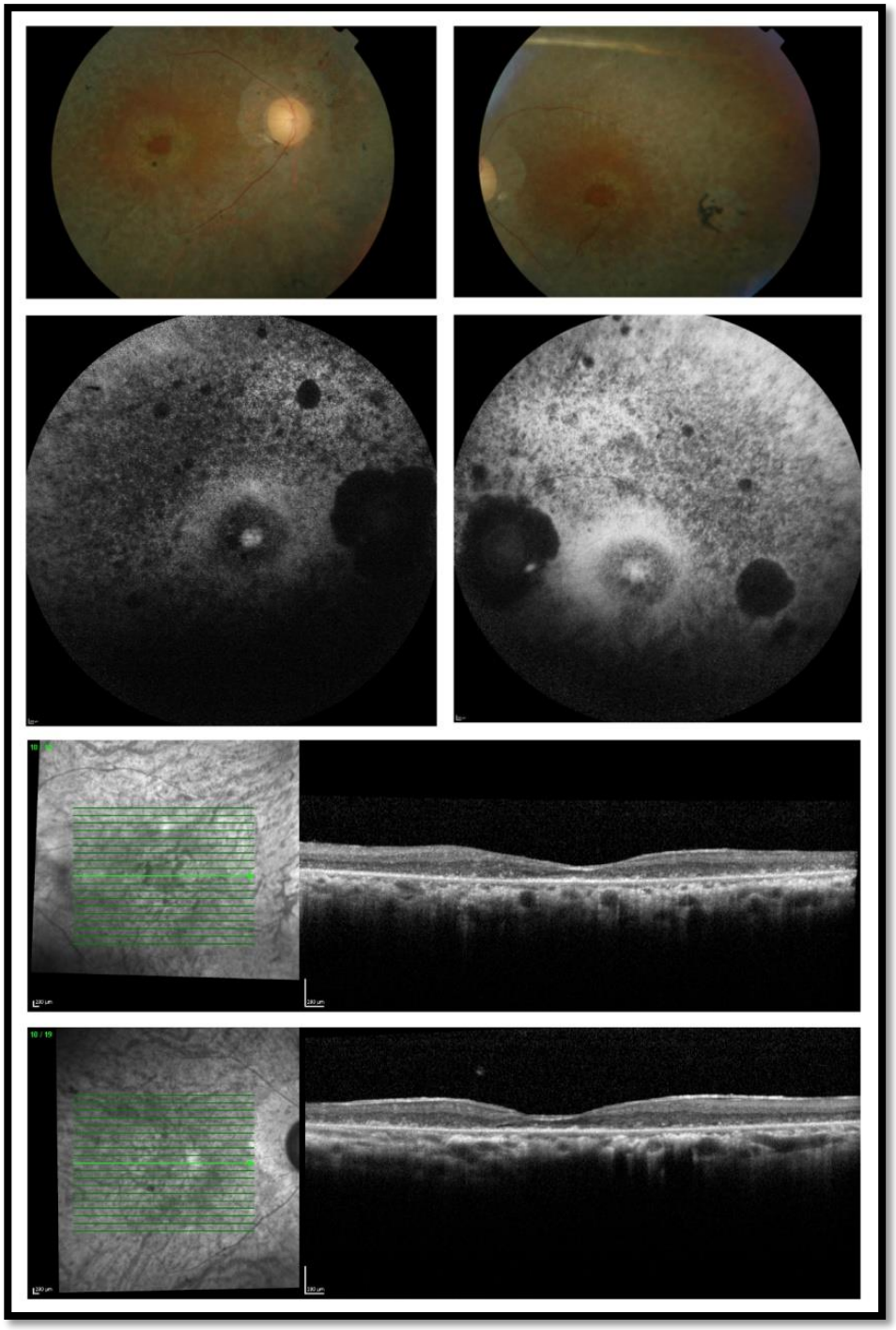

Figure 3-3: Phenotype of 61-year-old female with p.P171T mutation in *RHO*

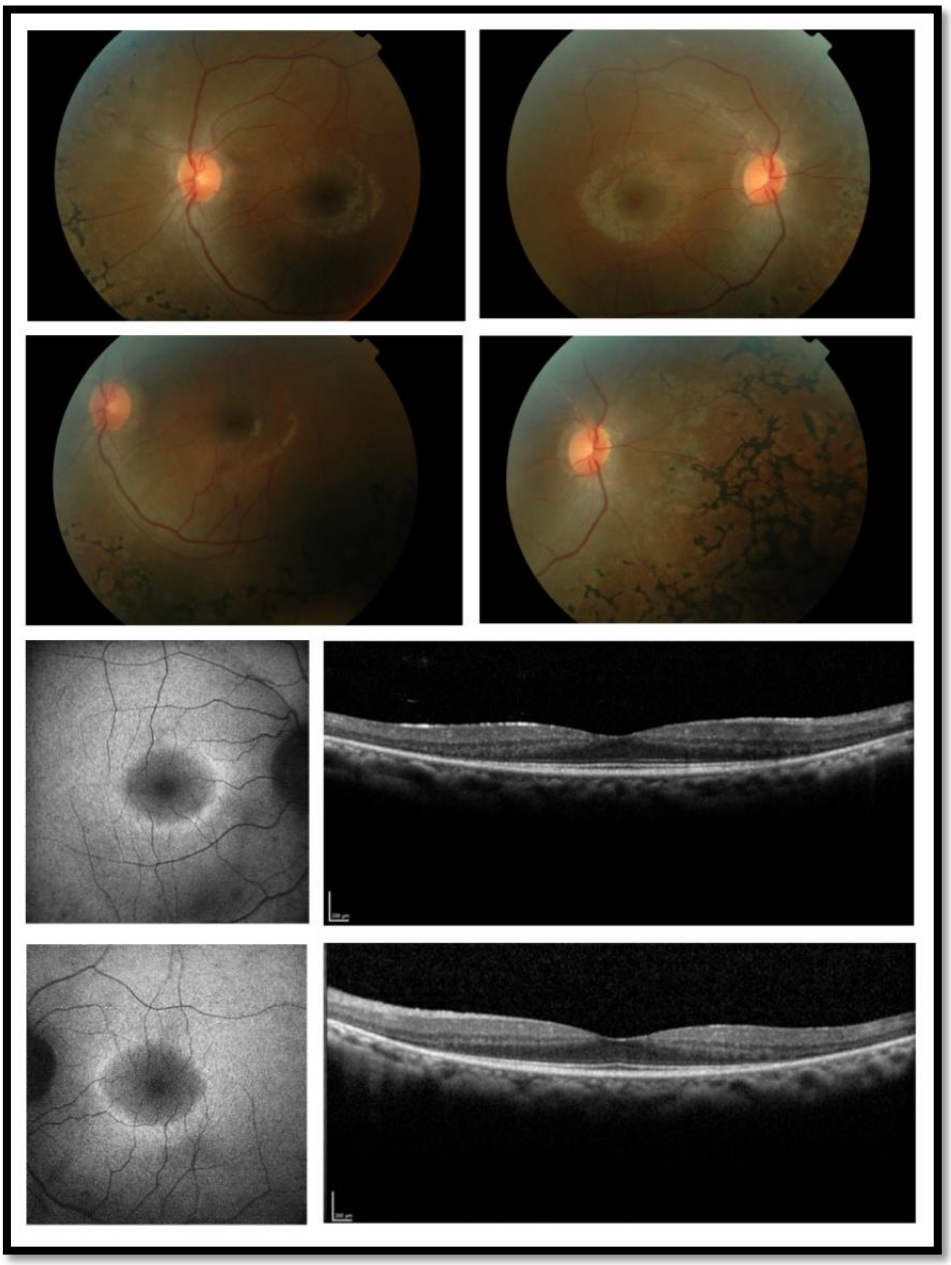

Figure 3-4: Phenotype of 27-year-old male with p.P171T mutation in *RHO*

The proband of family GC19225 presented with night vision problems at the age of 15. He was diagnosed with retinitis pigmentosa at the age of 33. When examined at the age of 39, his visual acuities were 6/9 in each eye.

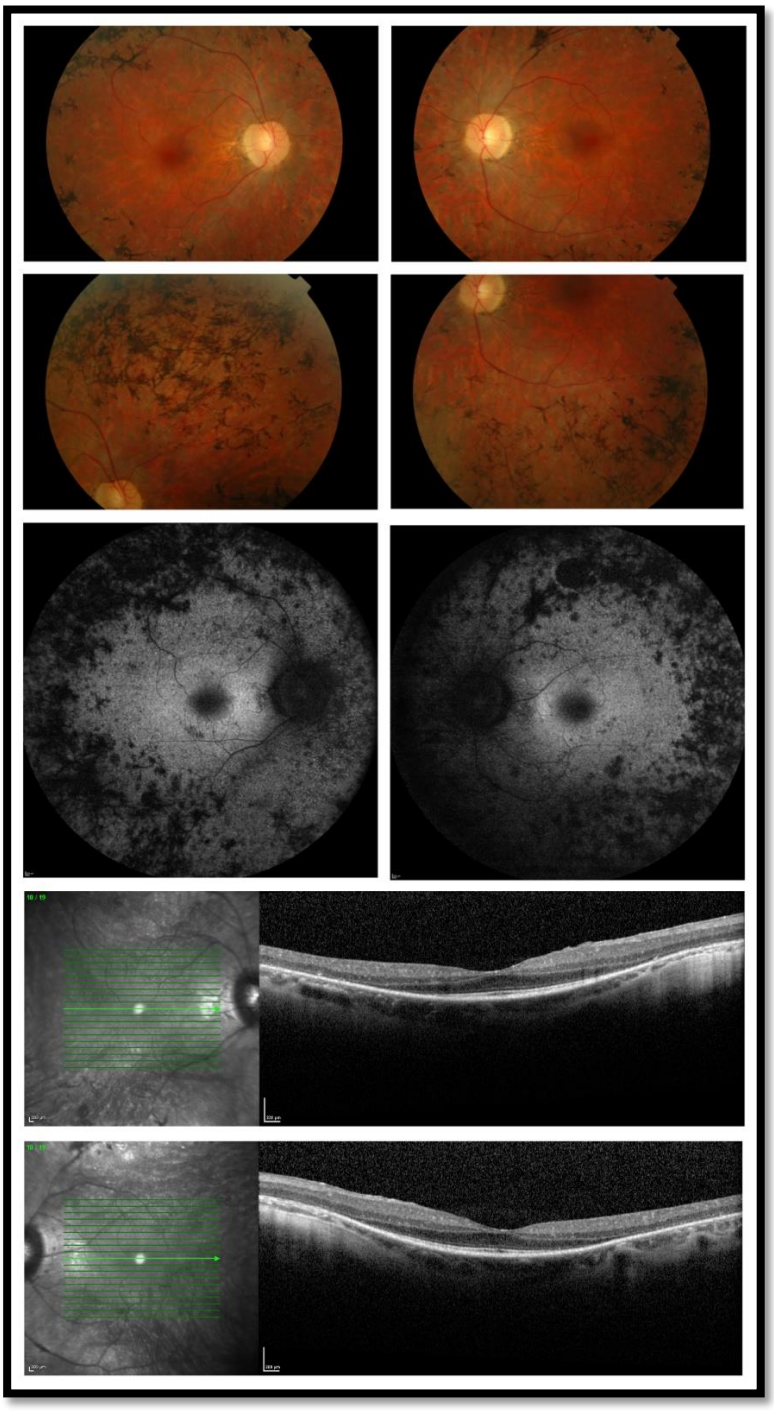

Figure 3-5: Phenotype of 39-year old male with p.P171R mutation in *RHO*

He had constricted visual fields, mid-peripheral intraretinal pigment, attenuated arterioles and pale optic discs. No cataract or macular oedema could be identified (Figure 3-5). Although there was no evidence of OCT abnormality of the central posterior pole, autofluorescence could not identify a well-demarcated high-density ring. The peripheral retina on OCT showed disruption and discontinuity of the outer retinal layers.

These three individuals with novel *RHO* mutations noticed night vision problems between 15-23 years age and were diagnosed as RP between 23-50 years of age. Patients had visual acuity better than 6/9 until 39 years of age but at age 50-years, it deteriorated to 6/24. All three showed intraretinal pigment migration, dystrophic retinal architecture, attenuated retinal arterioles and optic disc pallor. Hyperautofluorescent ring in the perifoveal region could only be identified in the FAF region in the youngest at age 27 years. None of these three showed any macular oedema.

It is well-known that the *RHO* mutations cause a variable phenotype which has been variously classified (Cideciyan et al., 1998). In general, the three major phenotypes are diffuse retinal involement from early age, mild retinal disease at early age which may remain sectoral or may become diffuse. The phenotypic data from a mutation in P171 has shown a phenotype of diffuse retinal pathology (Antinolo et al., 1994). In one Spanish family, affected members showed onset of the disease by the middle of the second decade resulting in severe loss of visual field by the age of 40. This is similar to the phenotype described in our study.

3.1.3.2 *RP1*

RP1 was the second most common gene (19.9%) in our cohort (Figure 3-2). 19 families were identified by the initial screen of the allele c.2029C>T. 38 additional families were identified during the second *RP1* screen. Five of the thirteen mutations identified were novel (Table 5-1). All the mutations were predicted to cause a frameshift or were nonsense. However, as all the mutations were downstream to the terminal intron, the alleles would be predicted to be expressed resulting in a faulty protein, and not undergo nonsense-mediated decay (Holbrook et al., 2004). The phenotype of the patients with mutations in the *RP1* gene has been described in the next section.

3.1.3.3 Splicing factors

The splicing factors *PRPF31*, *PRPF8*, *PRPF3* and *RP9* formed the next most common group of genes with 40/287 (13.9%) families harbouring mutations in one of these genes (Figure 3-2). 37/40 mutations in these genes were identified by the initial screen at Manchester. Subsequent *PRPF31* screen with sequencing and MLPA found mutations in 3 additional families. All the mutations identified in *PRPF3* or *PRPF8* were missense changes. There was only one missense mutation in the *RP9* gene.

8 novel mutations were identified in this group, all in the *PRPF31* gene (Table 5-1). Sixteen out of twenty (80%) mutations found in *PRPF31* were either nonsense or splice site mutations, all of which would be predicted to produce a null allele as none of them reside in the terminal

exon. We also identified 3 missense mutations and 1 in-frame insertion. The mutations in *PRPF31* were not limited to one particular domain of the protein.

Of the novel mutations identified in the *PRPF31*, 2 were splice-site mutations, 1 was a missense change while the rest were stop mutations or frameshifts. In-silico analysis of the missense mutation c.584T>A, p.L195P in *PRPF31* is shown in the Table 3-3. This mutation was not present in EVS or ExAC databases (EVS, 2015)

The novel mutation likely to affect the splice site, c.238+2T>C was analysed in-silico using tools like Human Splicing Finder (Desmet et al., 2009) and Spliceman web server (Lim et al., 2011). Both the tools concluded that this change is likely to disrupt the splice donor site which might result in interruption of splicing of *PRPF31* mRNA. Similar analysis was performed on the second novel intronic substitution, c.1146+2T>C. Using the same analysis tools Human Splicing Finder and Spliceman web server, this missense change was also predicted to disrupt the donor splice site affecting correct splicing of the *PRPF31* mRNA.

Table 3-3: In-silico analysis of novel *PRPF31* substitution

Mutation	**SIFT**	**PPH2**	**MA**	**FATHMM**	**CONDEL**	**Conclusion**
c.584T>A, p.L195P	0.08	0.522	2.395	-1.19	0.616788	Likely deleterious

3.1.3.3.1 Phenotype of the patients with novel mutations in PRPF31

11 affected individuals from 8 families were phenotyped for the study. The phenotypic characteristics are described in the Table 3-4 and

Figure 3-7, Figure 3-8, Figure 3-9, Figure 3-10, Figure 3-11, Figure 3-12, Figure 3-13, Figure 3-14, Figure 3-15, Figure 3-16 and Figure 3-17.

These patients were divided into three groups on the basis of their mutations – stops or frameshifts, splice-site mutations and substitutions. No clear differentiation could be made on the phenotypes of each group. There was wide variation among different affected members in each group and even within the same family.

Table 3-4: Phenotypic characteristics of patients with novel *PRPF31* mutations. Pt – Patient, PSC – Posterior sub-capsular cataract, CMO – Cystoid macular oedema, IOL – Pseudophakia, HM – Hand movements, CNV – Choroidal neovascularisation, CVS - Confrontation visual field, A/S - Asymptomatic

Family (Mutation)		**Pt**	**Onset**	**Age at exam**	**BCVA in better eye**	**Visual field in better eye**	**Comment**
Frameshift or stop mutations	GC16468 (p.Glu68*)	01	19 years	30 years	6/24	20°	CMO
		02	48 years	59 years	6/24	15°	CMO
		03	17 years	32 years	6/36	5°	PSC, CMO
	GC3031 (p.Gln177*)	01	Mid-teens	45 years	6/24	5°	IOL

	GC19105 (p.His270Thrfs *51)	01	Early teens	36 years	6/18		CMO, Myopia
	GC107 (p.Arg293Glyfs *28)	01		68 years	HM		CMO, IOL, Glaucoma
	GC19272 (p.Lys363*)	01	9 years	17 years	6/6	Full CVS	CMO
Splice site mutations	GC21373 (c.238+2 T>C)	01	<10 years	36 years	6/6	10°	
	GC16220 (c.1146+2 T>C)	01	12 years	23 years	6/5	20°	CMO
Missense mutation	GC1485 (p.Leu195Pro)	01	Early teens	71 years	HM		CMO, CNV
		02	A/S	48 years	6/6	Full	

The symptomatic individuals began to experience night blindness with/without peripheral vision problems in late first decade or early second decade of life. One individual was asymptomatic (GC1485-02) and one started experiencing night vision problems (GC16468-02) in late forties. The pedigrees of two of the families showed non-penetrance from history (Figure 3-6) although we could examine only one unaffected mutation carrier (GC1485-02). Visual acuities were affected variably and were influenced by cataract, cystoid macular oedema (CMO) and foveal involvement by the disease process.

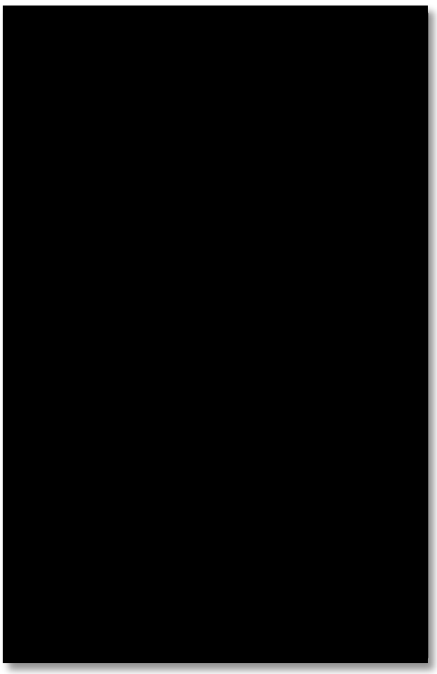

Figure 3-6: Pedigree of family GC107 showing non-penetrant individual in a red square.

Figure 3-7: GC16468-01 at 27-years of age

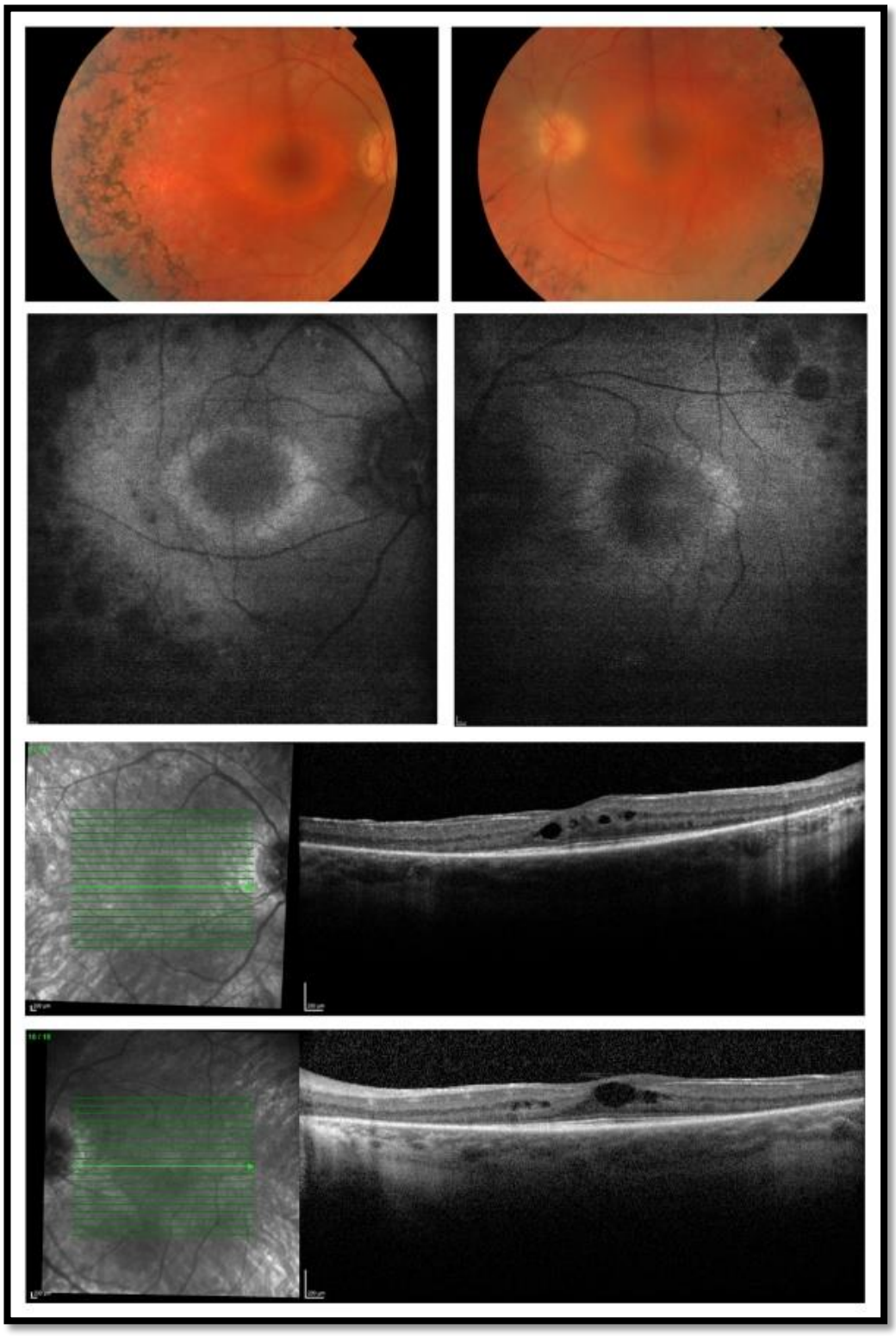

Figure 3-8: GC16468-02 at 55-years-age

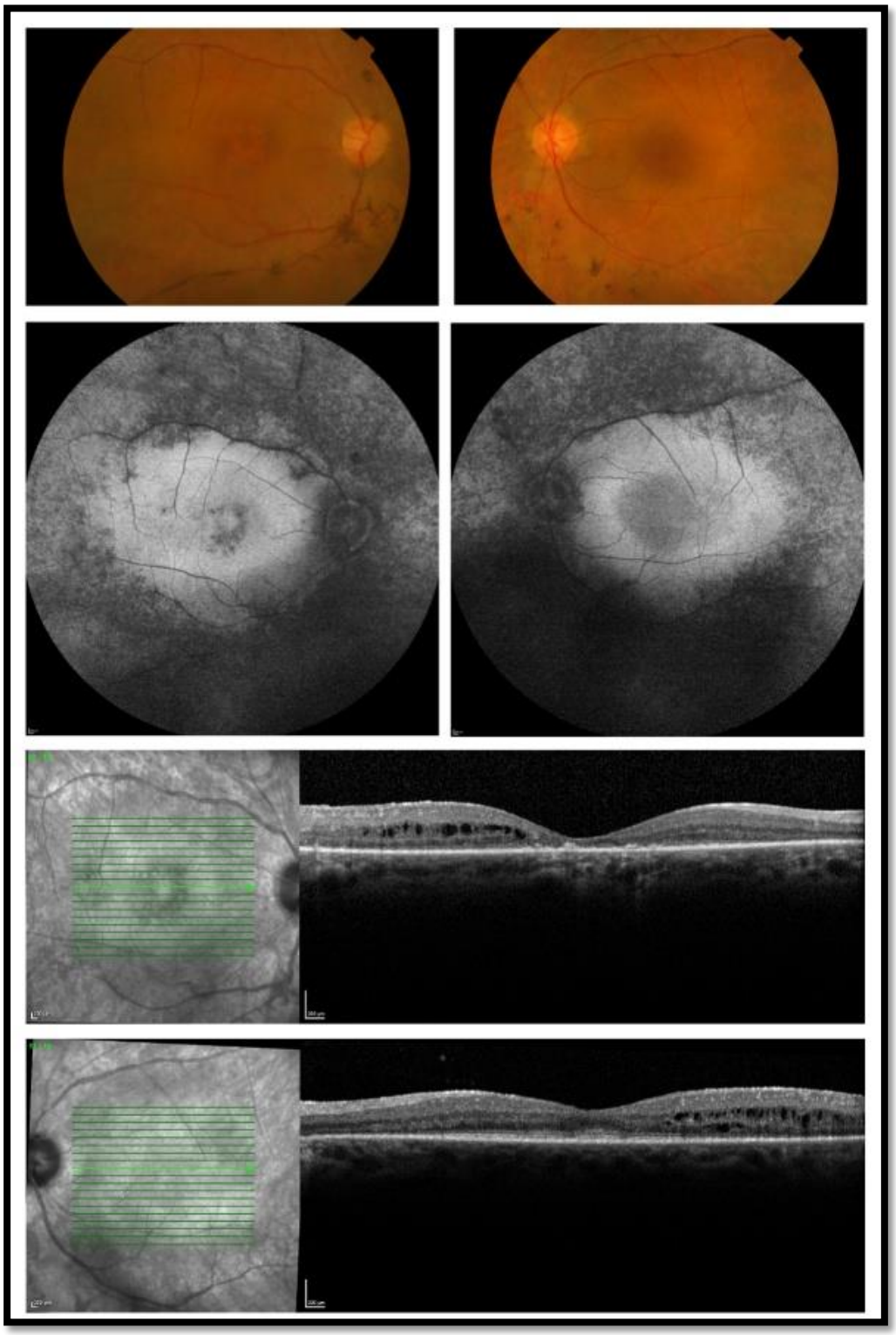

Figure 3-9: GC16468-03 at 30 years of age

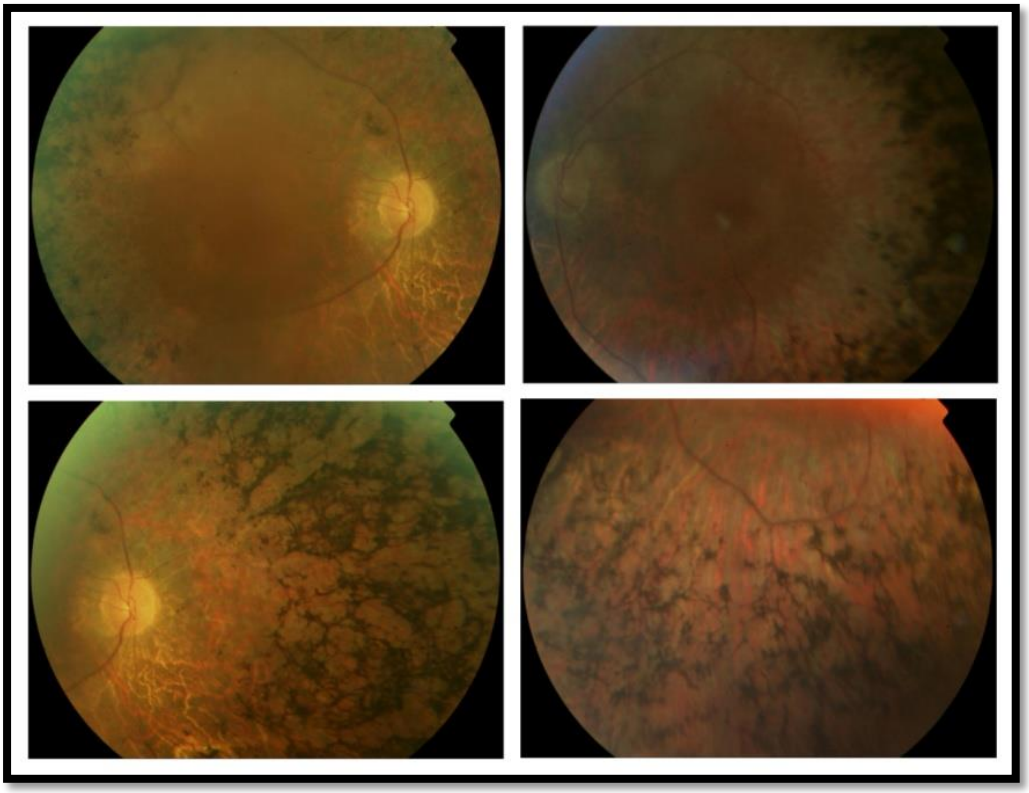

Figure 3-10: GC3031-01 at 43-years-age

Visual fields were reduced to less than 20° in all individuals over 23 years of age although a 17-year-old female (GC19272-01) had full field to confrontation. Fundus examination of the affected individuals showed typical features of attenuated arterioles, pale atrophic optic discs and bone spicule intraretinal pigment migration in the mid-peripheral retina. 8/11 (72.72%) individuals had documented CMO, one of whom went on to develop choroidal neovascularisation (CNV) in the left eye (GC1485-01) (Figure 3-16).

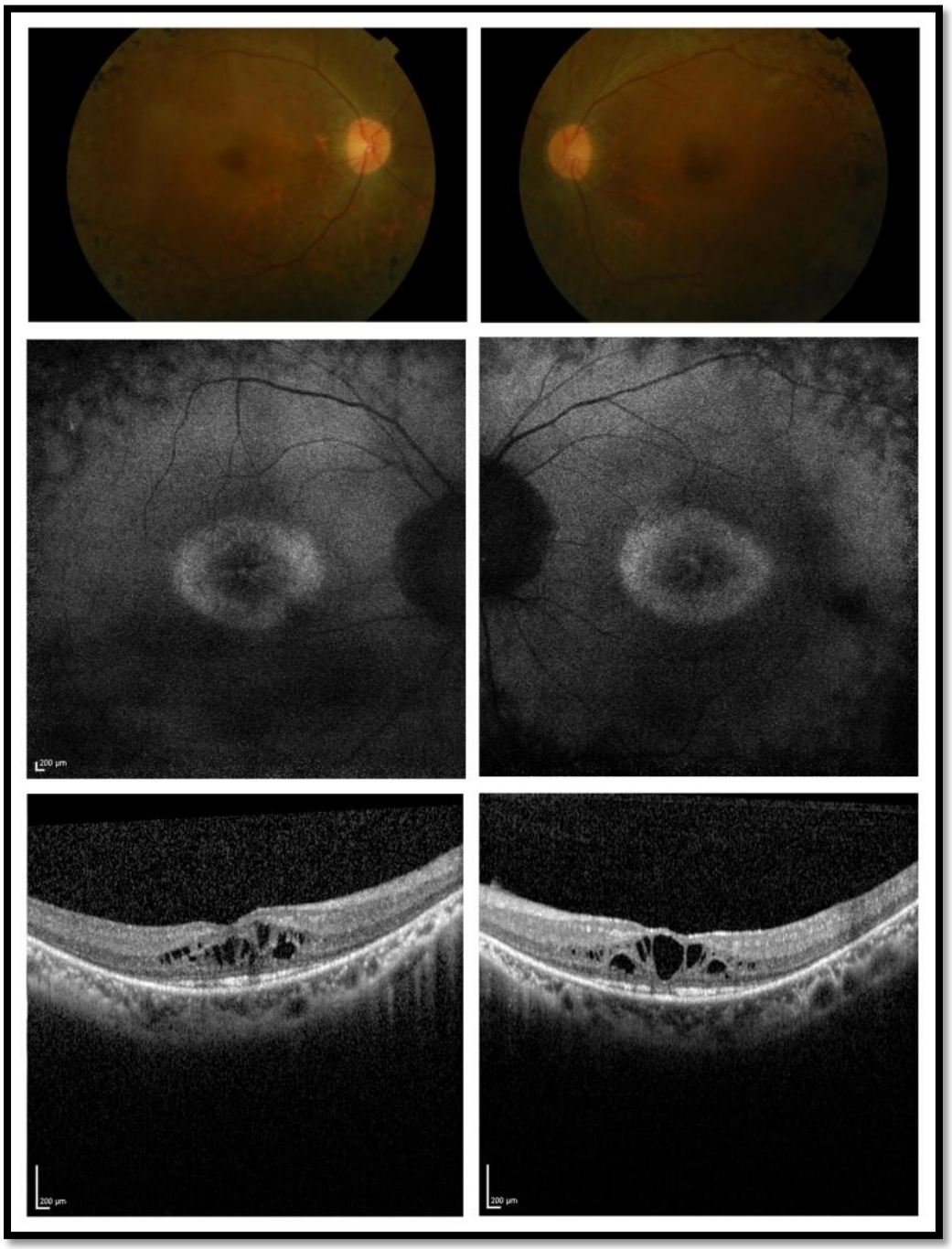

Figure 3-11: GC19105-01 at 34-years-age

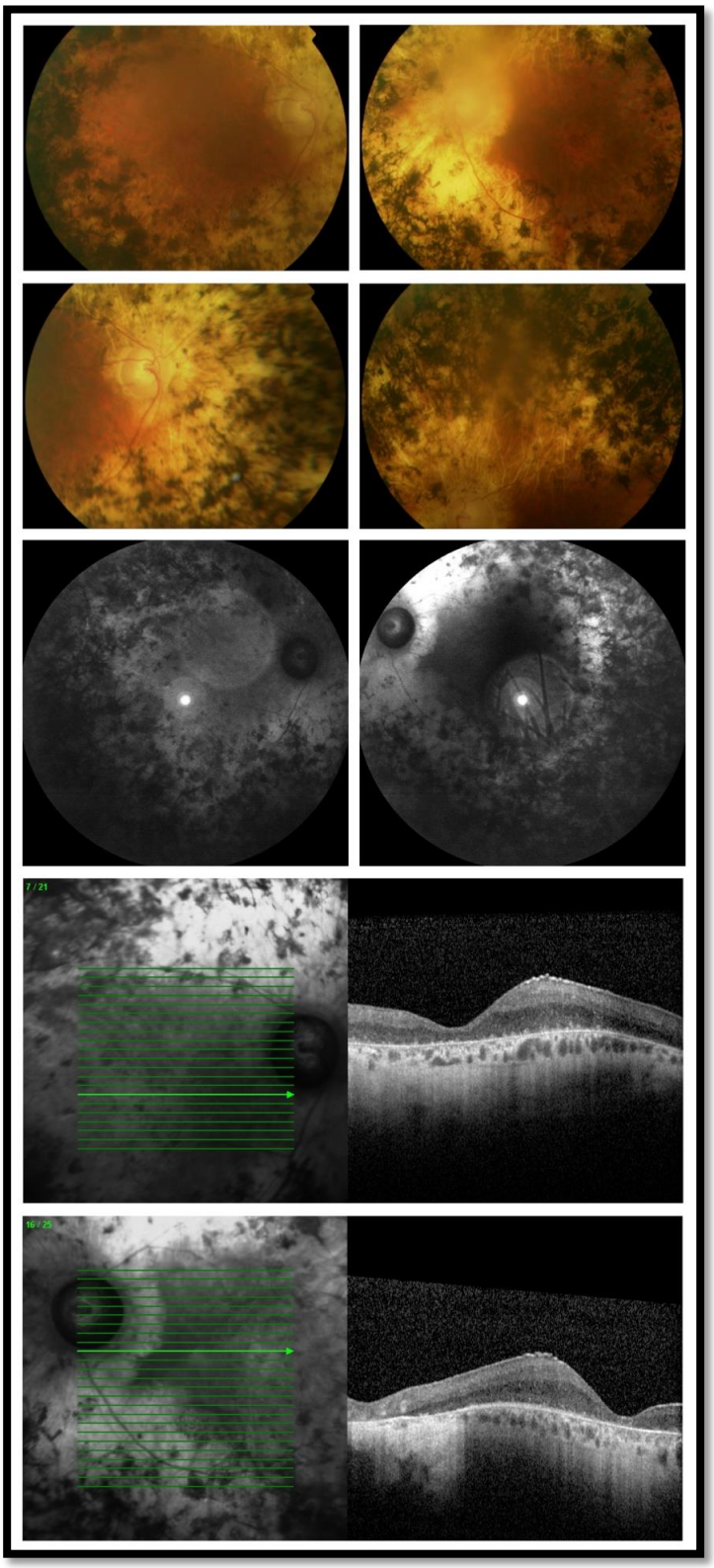

Figure 3-12: GC107-01 at 69 years of age

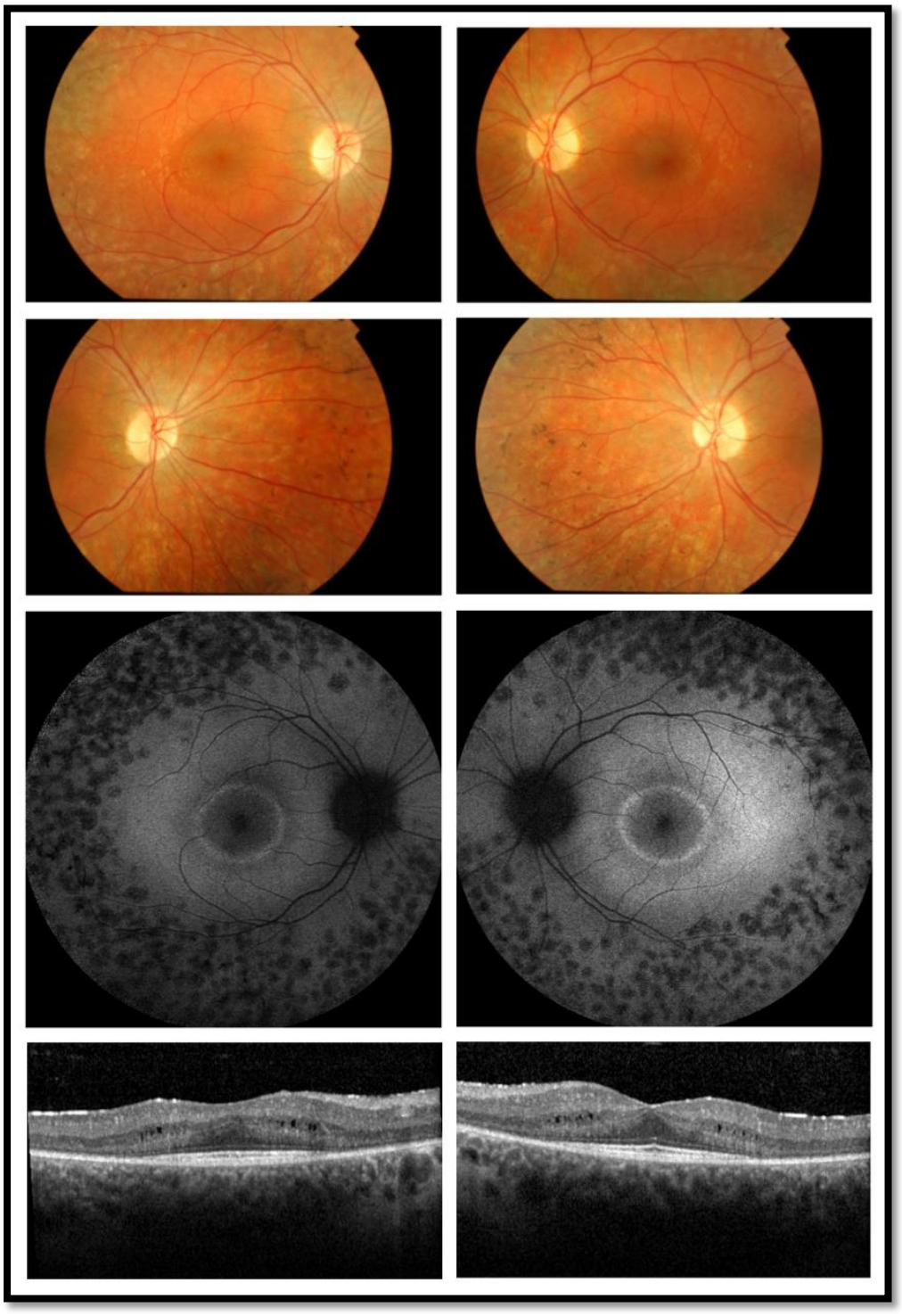

Figure 3-13: GC19272-01 at 18 years of age

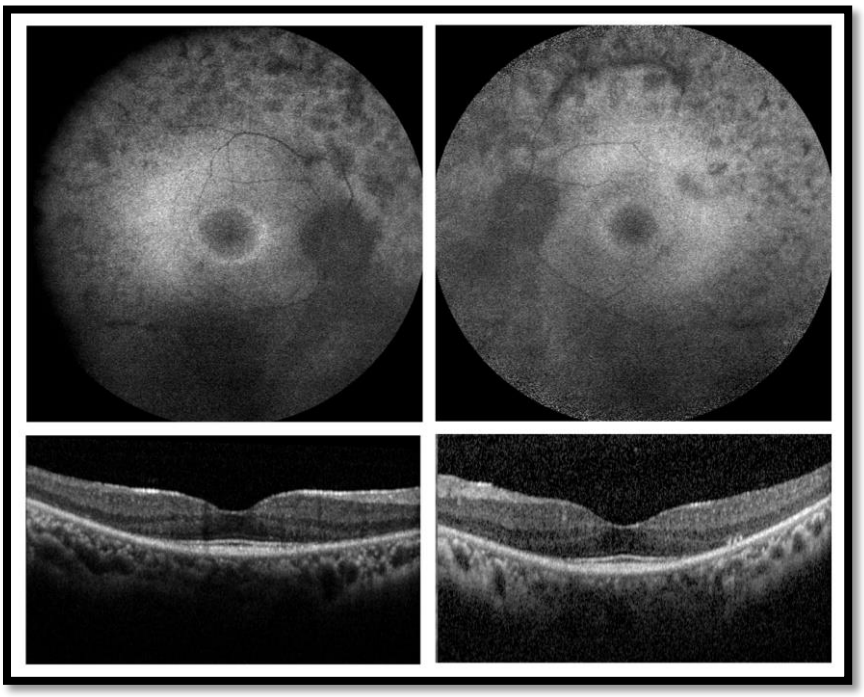

Figure 3-14:GC21373-01 at 36-years-age

Similar to the observations in this study, the literature describes the variable nature of the phenotype in patients with *PRPF31* mutations (Audo et al., 2010a). Incidence of non-penetrance have been observed in several families and it has been suggested that high penetrance is an exception rather than rule (Audo et al., 2010a). In patients who show the disease phenotype, disease onset is within the first two decades of life in the majority (Pan et al., 2014, Xu et al., 2012, Sato et al., 2005a, Audo et al., 2010a), similar to that observed in our novel mutation families. Variable involvement of the macula later in the disease have been observed by other groups as well (Audo et al., 2010a). We observed a relatively high percentage of patients with cystoid macular oedema (72.72%). This might be due to ages of the patients in our cohort as 9/11 patients were above 30-years-age.

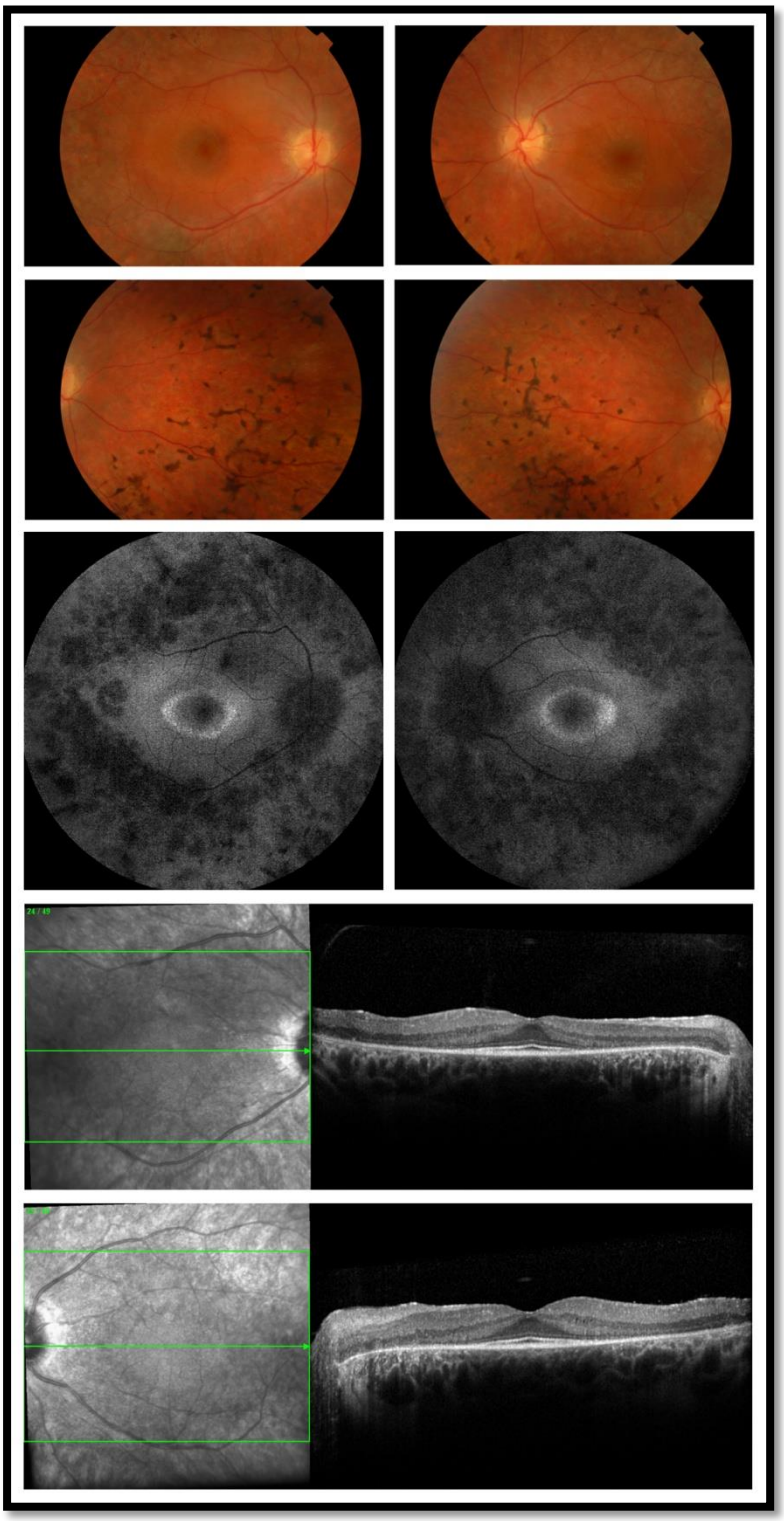

Figure 3-15: GC16220-01 at age 23 years

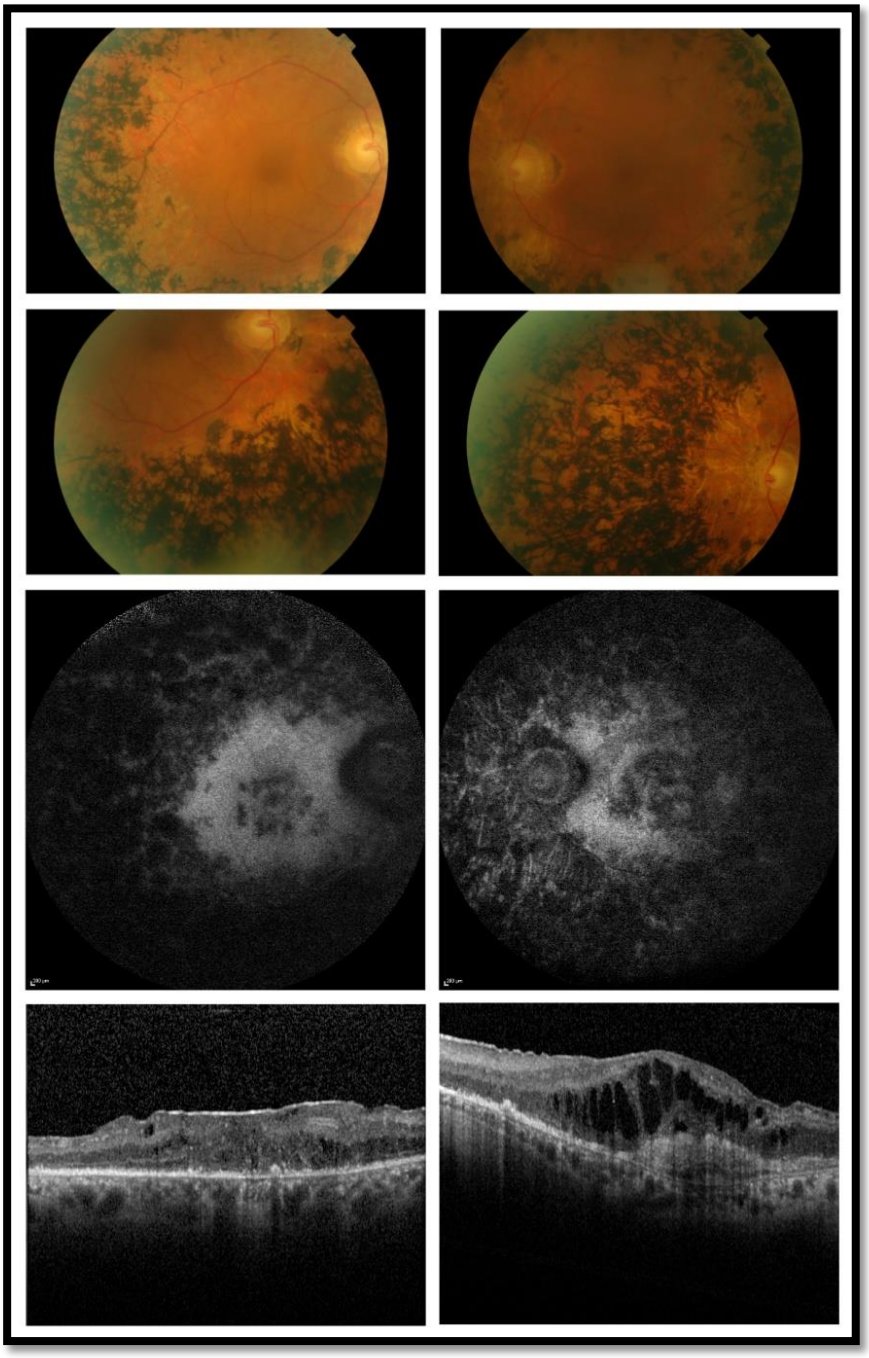

Figure 3-16: GC1485-01 – OCT and FAF showing CNV in the left eye

Choroidal neovascularisation following RP is not common (1.7%) (Triolo et al., 2013) and has not been described in any patients who have been molecularly diagnosed. Our patient refused any treatment due to his advanced RP.

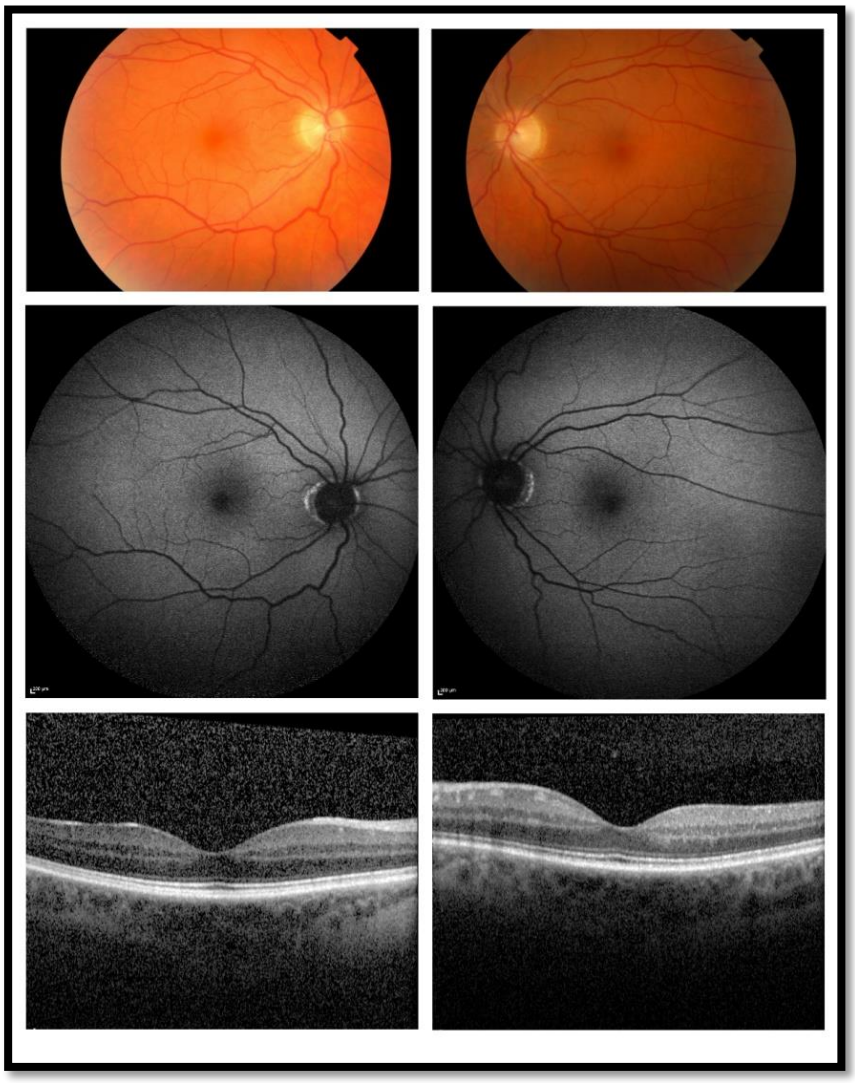

Figure 3-17: GC1485-02 at 46 years of age – an unaffected mutation carrier of *PRPF31*

3.1.3.4 *RDS/PRPH2*

Seven mutations were identified in *PRPH2*, with two being in-frame deletions and the rest substitutions. These mutations were not limited to one particular region of the gene. We identified one novel mutation c.653C>T, p.S218L which was analysed in-silico and was found likely to have deleterious effect on the functions of the protein (Table 3-5).

This substitution was also absent from the ExAC and EVS servers (EVS, 2015, ExAC, 2015).

Table 3-5: In-silico analysis of novel *PRPH2* mutation

Mutation	SIFT	PPH2	MA	FATHMM	CONDEL	Conclusion
c.653C>T, p.S218L	0.08	0.983	2.45	-2.34	0.604356	Likely deleterious

3.1.3.4.1 Phenotype of the family with novel PRPH2 mutation

One member of this family GC18899 could be phenotyped for this study (Figure 3-18). This affected female started noticing dimness of vision in dim lighting conditions at early teen age years and was diagnosed to have adRP at the age of 16 years. At 34-years-age, she had corrected visual acuities of 6/12 OD and 6/18 OS. She had reduced inferior visual fields to confrontation. Colour vision was affected as she could not identify the universal plate on Ishihara pseudo-isochromatic testing. Ocular examination showed symmetrical wide-spread degenerative changes of both the retina with foveal involvement. There were optic disc pallor, retinal pigment epithelial atrophic changes, attenuated arterioles and intra-retinal pigment migration in both eyes.

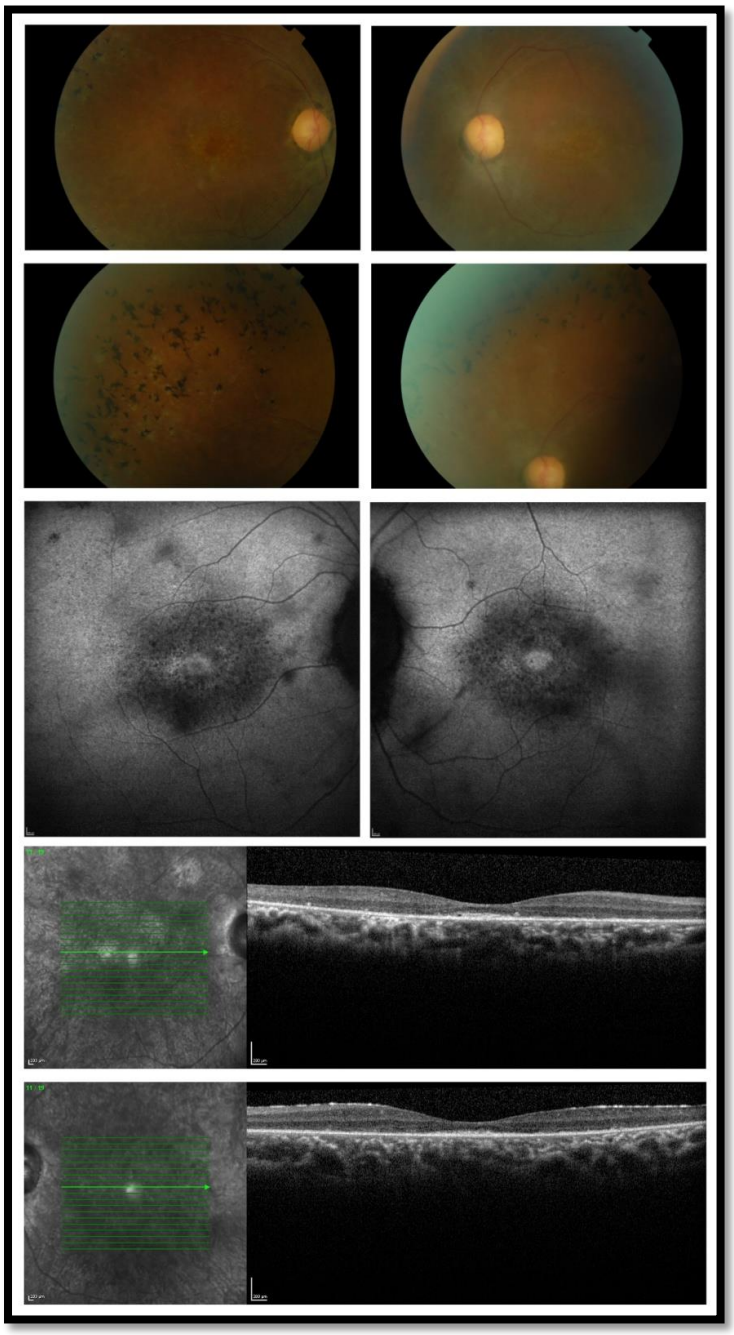

Figure 3-18: GC18899-01 at 34-years-age with novel p.S218L *PRPH2* mutation

Autofluorescence imaging revealed foveal hyper-autofluorescence with surrounding ring of hypo-autofluorescence. There was absence of high density ring around the fovea. OCT evaluation showed patchy demise

of the outer retinal layers and generalised loss of retinal architecture. Electrodiagnostic tests at the age of 31 years showed undetectable pattern ERG and minimal residual photopic and scotopic activity. This implied very severe generalised loss of retinal function involving both rod and cone systems along with loss of macular function.

Various different phenotypes have been associated with *PRPH2* mutations varying from several descriptions of macular dystrophies like pattern dystrophy and central areolar choroidal dystrophy, cone or cone-rod dystrophy and RP (Boon et al., 2008). Combination of the above phenotypes within a single family has also been noted (Leroy et al., 2007). From the phenotypic analysis of the proband in our novel S218L mutation, it is likely that this patient had an RP phenotype with macular involvement. The mutation is located in the D2 loop of the PRPH2 protein, a common locus for mutations for RP phenotype. This missense mutation adds evidence to the assertion that most of the patients with missense *PRPH2* mutations result in the RP phenotype (Boon et al., 2008).

3.1.3.5 Transcription factors – *NRL* and *NR2E3*

We identified a previously known mutation, p.S50T in *NRL* in 2 adRP families (Bessant et al., 1999). 2 different mutations were found in *NR2E3*, p.G56R and p.K57R in 3 separate families (Coppieters et al., 2007). The substitution c.170A>G, p.K57R is a novel mutation not previously associated with adRP. In-silico analysis for the missense change is shown in Table 3-6. This mutation has not been evident in EVS or ExAC mutation databases (EVS, 2015, ExAC, 2015).

Table 3-6: In-silico analysis of the mutation p.K57R in *NR2E3*

Mutation	SIFT	PPH2	MA	FATHMM	CONDEL	Conclusion
c.170A>G, p.K57R	0.02	0.889	1.15		0.57292	Likely deleterious

3.1.3.5.1 Phenotype of the novel NR2E3 mutation

Only one affected individual in the family GC17172 could be phenotyped (Figure 3-19). The affected female noticed difficulty in night vision from early childhood. At 16 years of age, she had visual acuities of 6/6 in both eyes. The visual field was less than 5° with Humphrey's visual field analyser. Ocular examination showed thin retinal vessels and extensive white dots at the level of the retinal pigment epithelium.

Autofluorescence imaging showed hyper-autofluorescent ring surrounding the foveal region. Electrodiagnostic evaluation showed rod-cone dystrophy.

Bi-allelic mutations in *NR2E3* are predominantly associated with Enhanced S-cone syndrome, a recessive retinal dystrophy characterised by nummular intra-retinal pigment and supernormal S-cone ERG (Jacobson et al., 1990, Marmor et al., 1990). Only one allele p.G56R has been causative of adRP so far. These patients have a rod-cone dystrophy with three concentric rings of hyperautofluorescence on FAF imaging (Coppieters et al., 2007). Presence of a mixture of nummular and spicular type of intraretinal pigmentation has also been noted. With the limited phenotypic data that we could acquire from our patient, we could not identify either nummular pigmentation or multiple concentric rings on FAF. However, given the young age of the patient, we could

not exclude subsequent development of a phenotype similar to that noted above.

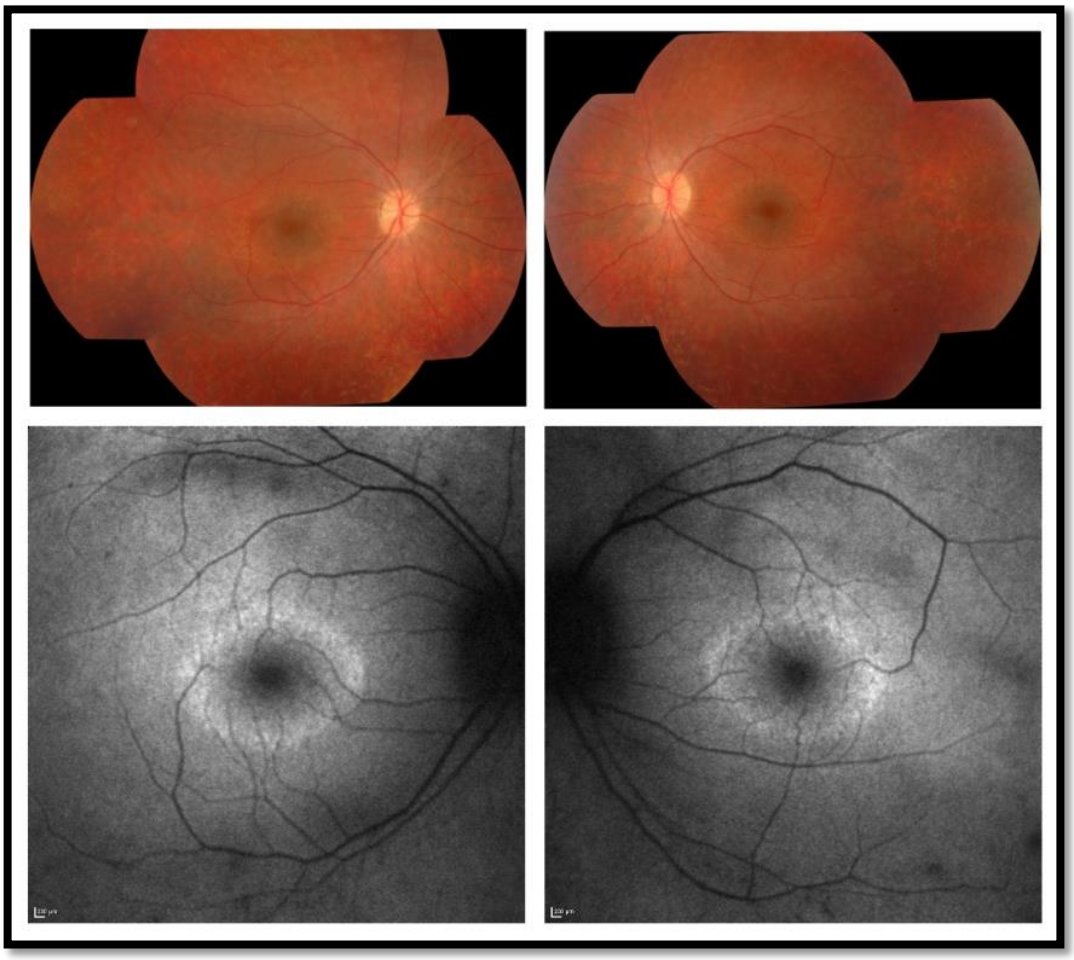

Figure 3-19: Affected female at 16-years of age with *NR2E3* p.K57R mutation

3.1.3.6 *IMPDH1*

We identified 6 different *IMPDH1* mutations, all of which were missense changes. 3/6 (50%) mutations were novel. The following table shows the predicted changes to the function of IMPDH1 protein due to the novel substitutions using in-silico analysis (Table 3-7).

Table 3-7: In-silico analysis of the novel *IMPDH1* mutations

Mutation	SIFT	PPH2	MA	FATHMM	CONDEL	Conclusion
c.928A>C, p.T310P	0	0.944	3.57	-3.32	0.695493	Likely deleterious
c.952T>G, p.Y318D	0	0.812	2.05	-1.31	0.573651	Likely deleterious
c.968A>G, p.K323R	0.02	0.129	2.12	-1.3	0.581156	Likely deleterious

These changes were not found in either EVS or ExAC databases (ExAC, 2015, EVS, 2015).

3.1.3.6.1 Phenotype of the families with novel IMPDH1 mutations

7 affected individuals from three families were examined for this study. The examination findings are shown in the following table (Table 3-8) and the following figures (Figure 3-20, Figure 3-21, Figure 3-22, Figure 3-23).

6/7 (85.7%) affected individuals noted difficulty in seeing in dim light and reduced peripheral vision in early childhood. 2 individuals phenotyped in the third decade of life had visual acuity as poor as legal blindness.

Table 3-8: Phenotypic characteristics of patients affected by novel IMPDH1 mutations. Pt – Patient, CMO – Cystoid macular oedema, PSC – Posterior subcapsular cataract, ERG – Electrodiagnostics

Family (mutation)	**Pt**	**Age of onset**	**Age at exam**	**BCVA in better eye**	**Visual field in better eye**	**Comments**
GC1296 (p.K323R)	01	Early childhood	13 years			CMO
	02	Early childhood	14 years			CMO
GC3776 (p.T310P)	01	Early childhood	9 years	6/9		ERG – rod cone photoreceptor dystrophy
	02	Early childhood	14 years	6/6		ERG – rod cone photoreceptor dystrophy
	03	Early childhood	37 years	PL		PSC
GC5256 (p.Y318D)	01	6 years	35 years	3/60	< 5°	CMO
	02	13 years	16 years	6/36		ERG – rod-cone photoreceptor dystrophy

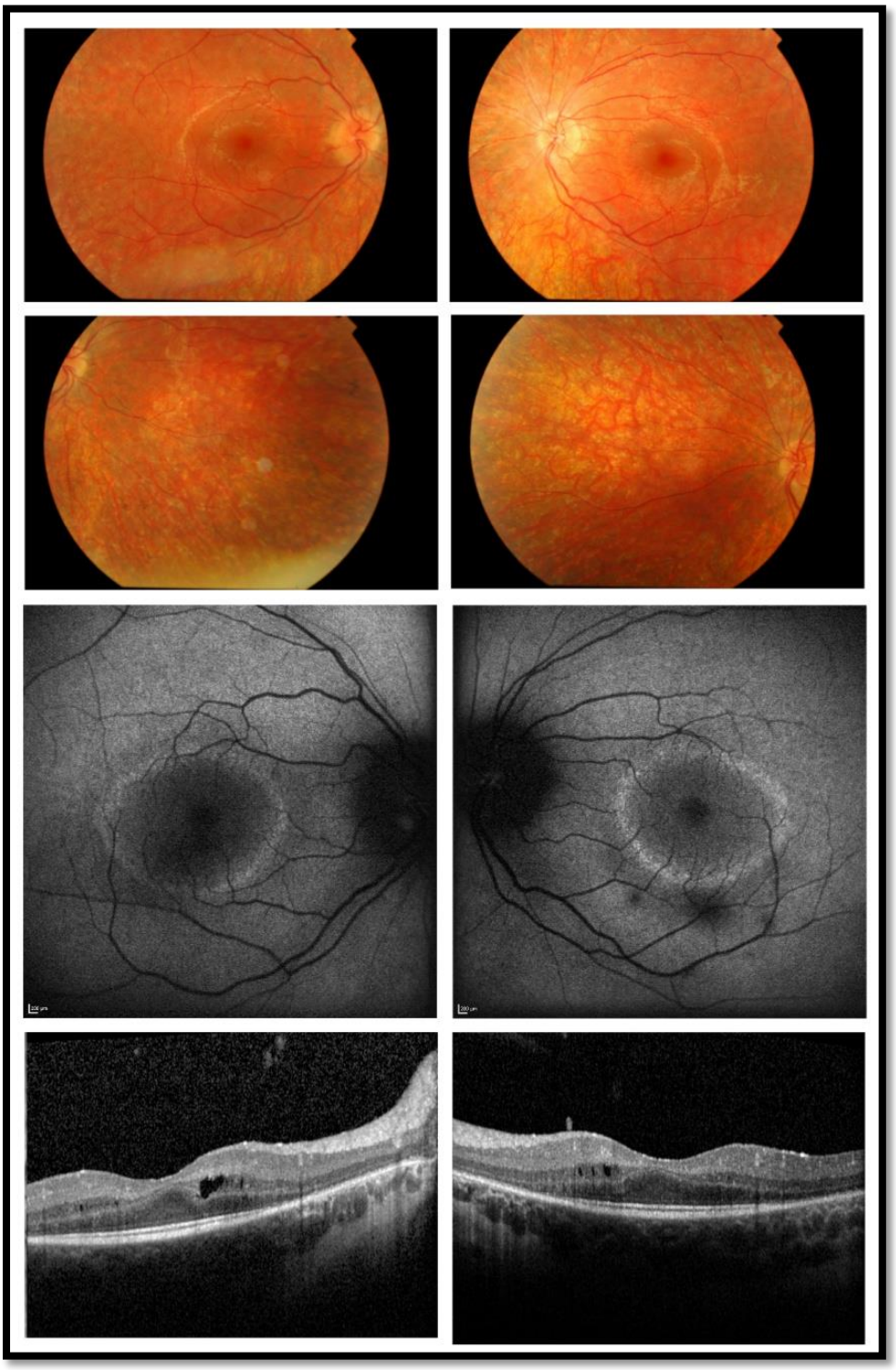

Figure 3-20: GC1296-01 at 13-years-age

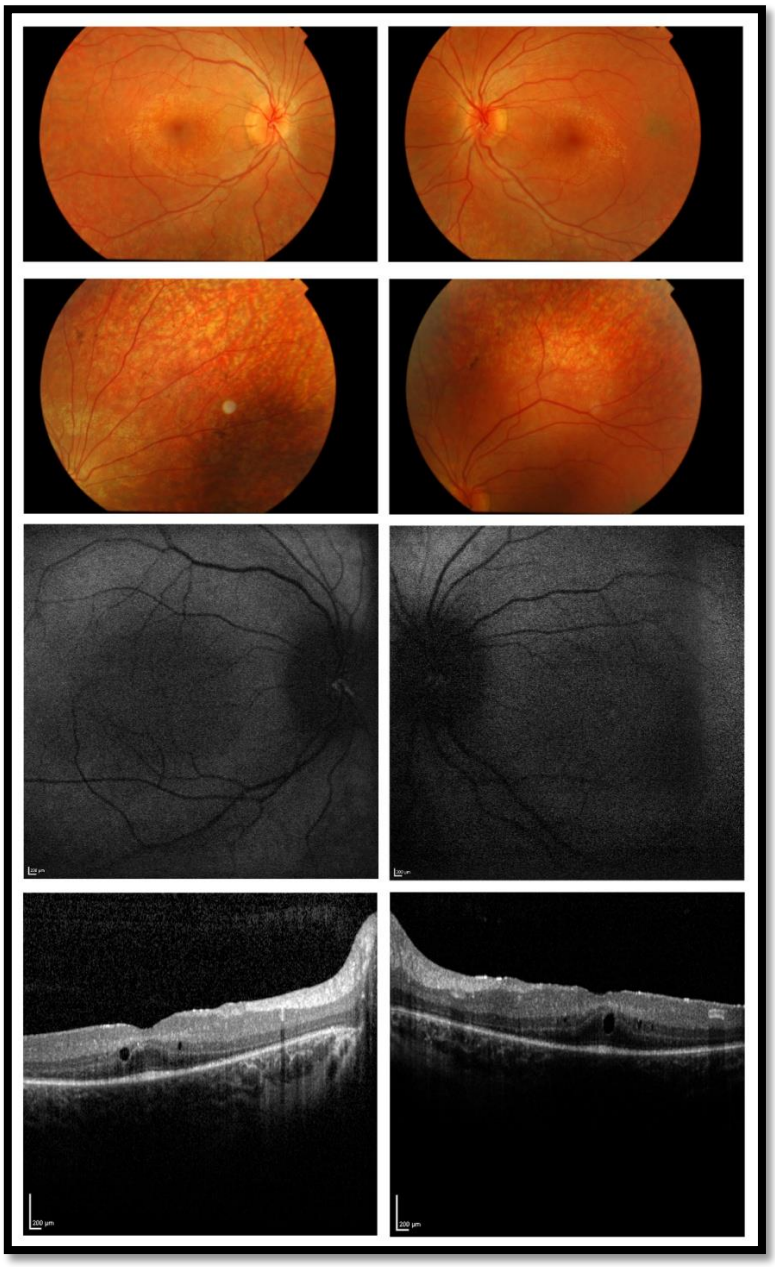

Figure 3-21: GC1296-02 at 14 years of age

Subjects in the paediatric group were examined between 9-16 years of age. There was variability in the signs from normal looking retina (GC5256-02) to optic disc pallor, attenuation of retinal vessels and intra-retinal pigment migration (GC3776-01). Similar variability in the autofluorescence imaging was noted with presence of hyper-autofluorescent peri-foveal ring in GC1296-01 while GC5256-02 had

normal 30° autofluorescence. 3/7 (42.86%) individuals had OCT confirmed cystoid macular oedema.

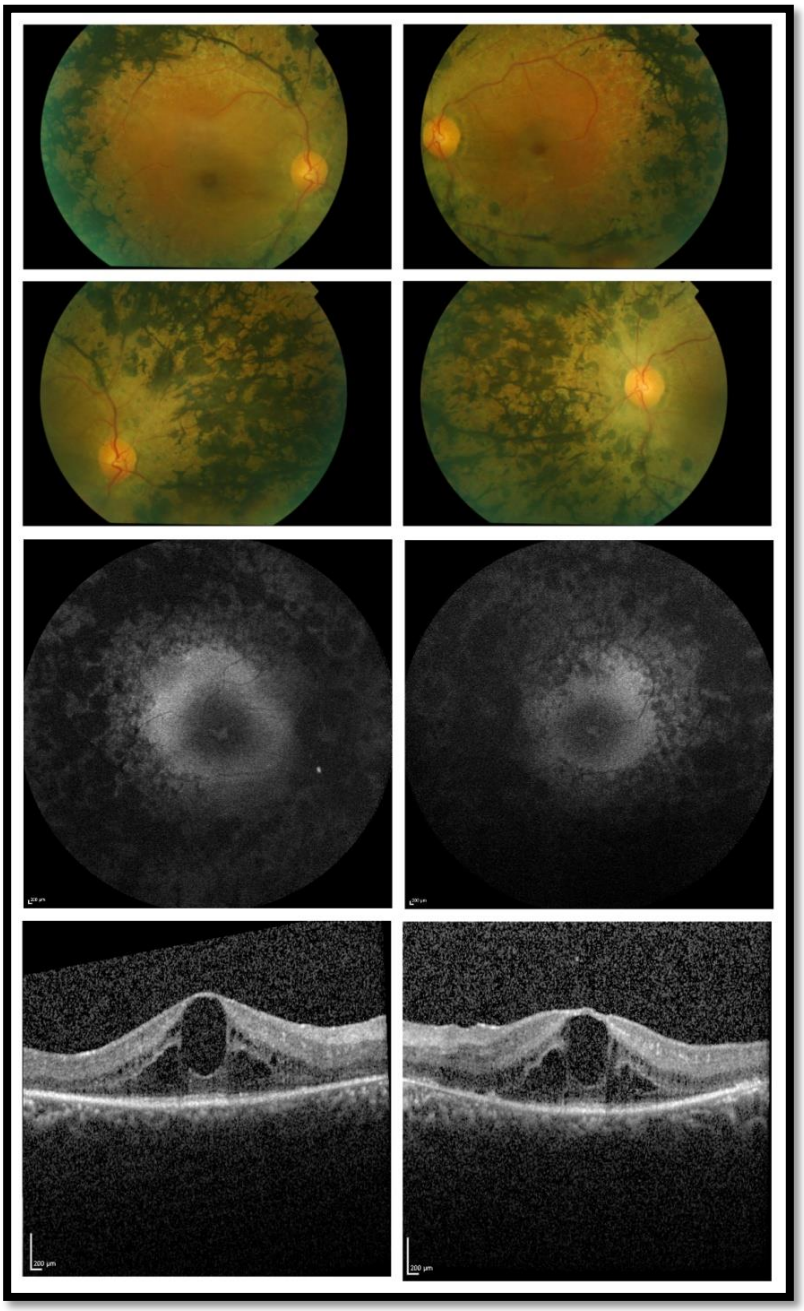

Figure 3-22: GC5256-01 female at 35-years-age

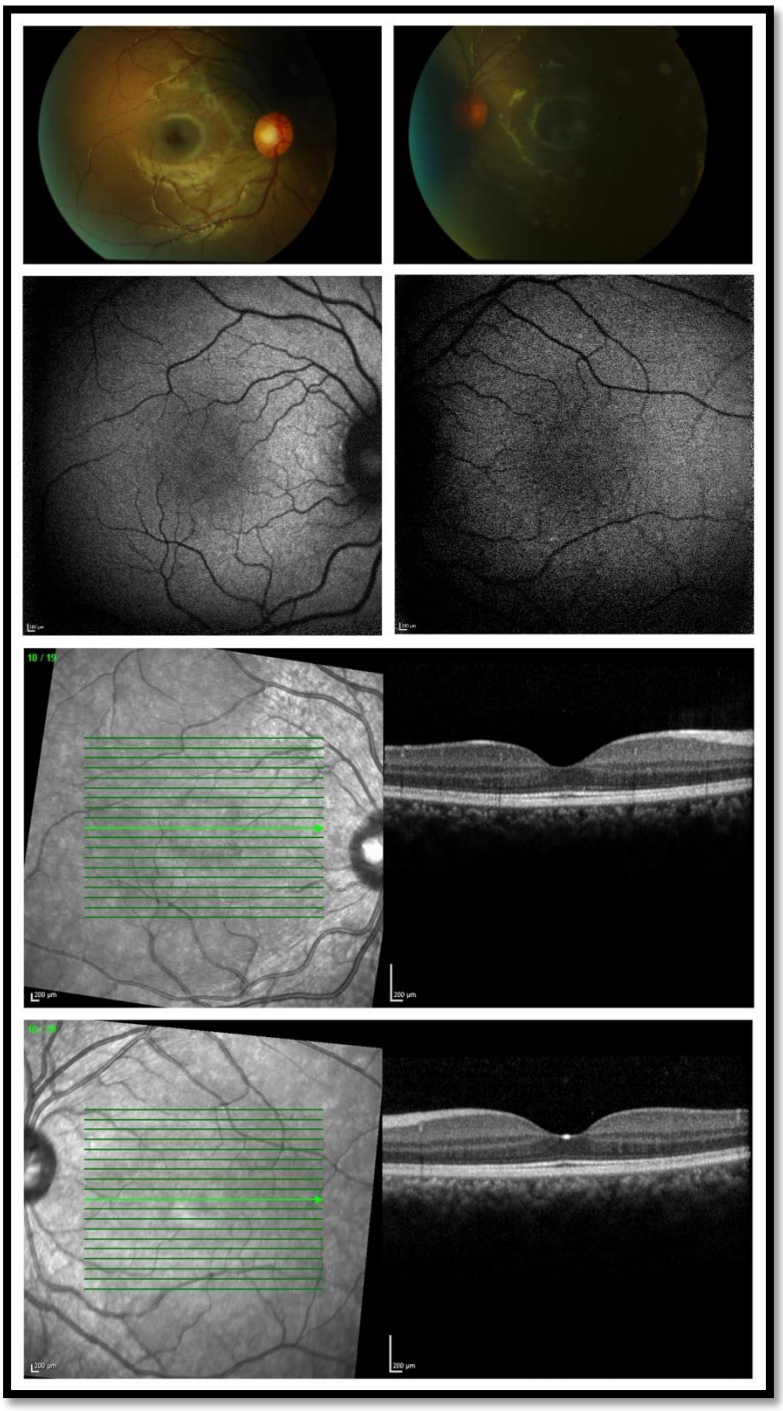

Figure 3-23: GC5256-02 at 16-years-age

Proband of family GC3776, GC3776-03 presented with no history of retinitis pigmentosa in her antecedents of at least 2 generations. The

pedigree structure was amenable to a diagnosis of autosomal recessive retinitis pigmentosa. However, the disease was evident in her 2 sons early in life and the diagnosis was revised to autosomal dominant retinitis pigmentosa.

This high variability in the *IMPDH1* RP phenotype has been described by other groups as well. Patients with T116M and H372P alleles have been noted to present in their thirties with night vision problems while those with R105W and N198K presented at early childhood with severe retinal dystrophy similar to LCA (Bowne et al., 2006b). The commonest mutation D226N usually resulted in a severe RP with onset in early childhood and subsequent decline in visual function with age although intra-familial variability have been noted (Kozma et al., 2005, Schatz et al., 2005). Interestingly in one Pakistani family, this allele produces disease only in homozygous state (Ali et al., 2015). All the alleles in our cohort of novel mutations behaved broadly similar to D226N phenotype although intra-familial variability is clearly evident. *de novo* mutations have not been described in *IMPDH1* before. We could not genotype the parents of the individual GC3776-03 in order to verify the *de novo* nature of her mutation.

In order to determine the probability of X-linked inheritance in the unresolved families, we compared the number of affected females among families with known and unknown molecular diagnosis. Within the families with unknown molecular diagnosis, 61% of the affected individuals were females whereas within a sample of 77 families with known molecular diagnosis, 52% of the affected were females. ($p=0.2$). The difference in the number of females being non-significant

implies that there were few families with X-linked inheritance in the unknown molecular diagnosis group, if any.

3.1.4 DISCUSSION

With 26 genes implicated in the causation of adRP (Table 1-1), identifying the correct molecular diagnosis can be an arduous task, particularly if Sanger sequencing of all the known genes is performed. Most dominant alleles in the genes such as *RP1*, *PRPF3*, *PRPF8*, *RP9*, *IMPDH1*, *NR2E3* and *NRL* are found within single exons (Chakarova et al., 2002, Martinez-Gimeno et al., 2003, Bowne et al., 1999) which allowed us to develop an algorithm for initial screen of the adRP families. The algorithm involved the complete Sanger screening of two genes, *RHO* and *PRPH2*, with targeted screening of key exons in the remaining genes.

Our study identified mutations in 64% of the families with adRP. This is higher than studies previously reported, where the detection rate varied between 28-54% (Ziviello et al., 2005, Hartong et al., 2006, Sullivan et al., 2006a). Our strategy of focussing the sequencing efforts on the mutational hotspots makes the screening procedure more efficient while retaining the probability of detecting novel mutations.

Sequence variants in *RHO*, *RP1* and *PRPF31* were the most common underlying cause of disease in our cohort. As the families were drawn from a database of varied racial background, this result may represent the true genetic distribution of the adRP families in the population. The contribution of *RP1* (23.3%) is significantly higher than the largest previous study of this kind (3.5%) (Sullivan et al., 2006a), which may be a British phenomenon.

The contribution of *RHO* to the genetics of adRP was similar to that found in a previous study (Sullivan et al., 2006a). All but one of the *RHO* mutations in our cohort was amino acid substitutions or in-frame deletions making it likely that the mutant protein is expressed. *RHO* mutations have been classified into different classes depending on the behaviour of the mutant protein (Mendes et al., 2005) (Table 1-2). Two novel mutations identified (p.P171T and p.P171R) affect the same amino acid and would be classified as Class II mutations which cause misfolding of the mutant protein. Functional experiments need to be conducted in order to elucidate the true effect of these alleles. Interestingly, the allele P23H which is one of the commonest causes of adRP (Sullivan et al., 2006a) in North America and has a widely experimented mouse model was not identified in our cohort.

It was evident from the mutations identified in our cohort and that from other databases that there are no mutational hotspots within the *RHO* gene (Stenson et al., 2009). So far, functional experiments have not been conducted to elucidate the pathogenesis of all the mutations identified in *RHO*. Although splice site mutations have been identified, haploinsufficiency has not been put forward as the mechanism of disease. This is supported by the fact that heterozygous rhodopsin knockout mice show little photoreceptor degeneration (Lem et al., 1999).

In spite of limiting the screening of *RP1* to the presumed mutational hotspot in exon 4 (Berson et al., 2001), we identified eight new mutations. All the adRP families harbouring *RP1* mutations were of European descent. It is possible that dominant alleles in this gene is especially prevalent in the European British population as such large incidence has not been noted in patients from South-East Asia, China

or the United States (Sullivan et al., 2006a, Gandra et al., 2008, Zhang et al., 2010). The prevalence of the p.R677X allele in our adRP cohort was 6.7%, making it the commonest adRP allele by far; this suggests that this allele should be screened specifically in the early stages of any screening strategy in the British population.

All the *RP1* mutations identified so far associated with adRP are confined to exon 4 (Audo et al., 2012). In all cases, the mutations result in a truncated protein, which is expressed, at least in cultured lymphocytes (Liu et al., 2003). This makes it likely that the mechanism of disease in these cases is dominant negative or gain-of-function. Furthermore, the presence of null alleles in phenotypically unaffected carriers of autosomal recessive RP (Chen et al., 2010, Aldahmesh et al., 2009) caused by mutations in *RP1* makes haploinsufficiency unlikely. Interestingly, Chinese and Japanese patients with alleles producing stop codons beyond p.D1922 do not have disease (Kawamura et al., 2004, Baum et al., 2001). Thus, the protein domain between p.M500 to p.D1922 performs a hitherto unknown function, alteration in which imparts gain-of-function or a dominant negative property to the mutant RP1 protein.

PRPF31 was the third most common molecular diagnosis in our adRP families. We screened the whole of the gene using Sanger sequencing and/or MLPA in families with demonstrable non-penetrance. Several groups have discovered large deletions involving this gene (Sullivan et al., 2006b, Abu-Safieh et al., 2006, Rose et al., 2011). As these deletions are not easily detected using conventional Sanger sequencing, techniques such as MLPA is essential in screening *PRPF31*.

The predominant mechanism for *PRPF31* related adRP is believed to be haploinsufficiency (Rivolta et al., 2006, Abu-Safieh et al., 2006). This

hypothesis is further supported by the fact that out of 59 mutations reported in this gene so far including those in our cohort (Audo et al., 2010a, Saini et al., 2012, Xu et al., 2012, Rose et al., 2011, Utz et al., 2013), only a few (p.L107V, p.T138K, p.A194E, p.L195P, p.A216P, p.A291P, and p.C299R) are missense mutations. We also identified in-frame duplication (p.E183_M193dup). The p.L107V and p.T138K changes are predicted to create donor splice-sites and frameshift (Rivolta et al., 2006, Waseem et al., 2007). The p.A216P allele has been functionally characterised and it is believed that a dominant negative mechanism may be responsible for disease with this allele (Huranova et al., 2009). Further experimental evidence needs to be obtained to identify the mechanism of disease in other alleles. Thus, although there is overwhelming evidence that haploinsufficiency may be the primary mechanism in *PRPF31* mutations, there may be a dominant negative effect in a minority of alleles. In these cases, however, the disease may not be amenable to gene replacement therapy alone.

Many groups have commented on the propensity of non-penetrance in adRP families associated with *PRPF31* mutations (Moore et al., 1993, Al-Maghtheh et al., 1996, Audo et al., 2010a). One explanation for non-penetrance is differential expression of the wild type allele (Vithana et al., 2003). This expression was determined to be associated with an expression quantitative trait locus (eQTL) on chromosome 14q21-23 (Rio Frio et al., 2008). Recently, it has been demonstrated that high levels of *CNOT3* gene expression on 19q13.4 correlate with low expression of *PRPF31* (Venturini et al., 2012). Hence, multiple influences on the expression of the *PRPF31* wild type allele may determine the phenotypic expression of the disease in mutation carriers.

We investigated other splicing factors in our mutation screening. *PRPF8* was responsible for 2.8% of adRP families in our cohort. This is similar to that observed in other studies (Daiger et al., 2007, Hartong et al., 2006, Martinez-Gimeno et al., 2003, Sullivan et al., 2006a). All the mutations identified in this gene have been in exon 42 of this gene except in one family where it was identified in exon 39 (Towns et al., 2010). In a 43-exon-gene, this region would be the C-terminal end of the protein, which contains the MPN domain whose function may be affected by the observed mutations. Unlike in *PRPF31* mutations, in lymphoblast cell lines, the mutant protein is expressed and probably affects binding to hSnu114 and hBrr2 proteins, which play a role in U4/U6 and U4atac/U6atac snRNA unwinding (Tanackovic et al., 2011b). There is evidence of incomplete penetrance in some of these families as well, although the mechanism remains to be explored (Maubaret et al., 2011).

There have been only three mutations identified in *PRPF3* to date – p.A489D, p.P493S and the commonest, p.T494M (Gamundi et al., 2008, Chakarova et al., 2002). All three mutations are very close to each other in exon 11. As expected, this mutant protein is expressed and these mutations in the C-terminal region of the protein are believed to partially destabilize the assembly of the U4/U6 snRNP complex, which could affect spliceosome assembly (Gonzalez-Santos et al., 2008).

There has been only one mutation identified in the *RP9* gene so far (Keen et al., 2002). We identified this variant in 3 families in our cohort.

Identification of mutations in *PRPH2* causing adRP is dependent on strict phenotypic criteria. We have excluded patients from dominant families with predominant macular involvement in whom *PRPH2* is a significant cause of disease. In our cohort, only 2.4% of the families

harbour mutations in this gene. This is in agreement with the findings of some groups (Hartong et al., 2006) and not with others (Sullivan et al., 2006b). One explanation may be variable phenotypic criteria as several phenotypes have been attributed to this gene (Nichols et al., 1993b, Wells et al., 1993, Weleber et al., 1993). We screened the whole gene to identify mutations in all three exons and identified 1 nonsense mutation, 2 in-frame deletions and 4 missense mutations.

There has previously been only one allele (p.G56R) reported in *NR2E3* associated with adRP (Coppieters et al., 2007). We identified a second dominant allele (p.K57R) in *NR2E3*. This mutation lies next to the previously reported change within the first zinc finger of the DNA-binding domain of the protein (Coppieters et al., 2007). This finding supports the pathogenicity of *NR2E3* in causing adRP.

We identified just one mutation in *NRL* in our adRP cohort. Although this gene has been implicated in cone dysfunction and recessive retinitis pigmentosa (Nishiguchi et al., 2004), mutations in only 4 amino acids – p.S50, p.P51, p.P67 and p.M96 have been associated with adRP (DeAngelis et al., 2002, Ziviello et al., 2005, Hernan et al., 2012). It has been demonstrated that some of these mutations impart a gain-of-function to the mutant protein, which alone and/or together with *CRX*, increased *RHO* transcription by influencing the promoter (Bessant et al., 1999, Hernan et al., 2012).

IMPDH1 analysis in our cohort revealed 6 missense mutations in 7 families, 3 of which were novel. All the mutations identified in this gene are present in or near the CBS domain of the protein. Several hypotheses have been put forward to explain a retina specific phenotype due to mutations in a ubiquitous enzyme. One group identified a unique nucleic acid binding property of *IMPDH1* which is

impaired by the observed mutations (Hedstrom, 2008). Another group identified several retina-specific *IMPDH1* transcripts and suggested that these may have singular properties, which are impaired by the mutations (Bowne et al., 2006a). A third group suggested that some of the mutant proteins have faulty tertiary structures that interferes with folding and thus, the function of wild-type *IMPDH1* (Wang et al., 2011). It is probable that a combination of the above mechanisms play a role in the pathogenesis of this disease.

We failed to identify the underlying genetic cause in a third of families using our algorithm. One explanation may be the presence of mutations in exons which were not included in the screen. There may also be large copy number variations that can be missed by Sanger sequencing. It may also be possible that the mode of inheritance in some of these families is not autosomal dominant. However, the number of affected females in families with unknown molecular diagnosis was not significantly lower than that of confirmed adRP families making X-linked inheritance unlikely.

Finally, it is plausible that some of these families with unknown molecular diagnosis harbour rare or novel mutations in the known genes or mutations in genes that have not yet been identified. The advent of next generation sequencing should allow many of these currently undiagnosed cases to be solved and is likely to lead to the identification of novel genes causing adRP (Daiger et al., 2010).

In conclusion, we describe a strategy concentrating on specific exons and variants where most mutations have been reported, which allowed us to identify the causative mutation in two-thirds of families. Our report provides useful information about the relative contributions made by different genes in adRP within a British cohort.

3.2 A MOLECULAR AND CLINICAL ANALYSIS OF PATIENTS WITH RETINAL DEGENERATION DUE TO DOMINANT ALLELES OF THE *RP1* GENE

3.2.1 INTRODUCTION

RP1 is a four-exon gene located in chromosome 8q12.1 (Pierce et al., 1999). The expressed protein is photoreceptor specific and has been demonstrated in both rods and cones (Sullivan et al., 1999). RP1 is a microtubule-associated protein that forms an integral part of the axoneme of the connecting cilium in the outer segment of the photoreceptors (Liu et al., 2002, Liu et al., 2004).

47 mutations have been described in the *RP1* gene so far. These are associated with both autosomal recessive (ar) and adRP (Audo et al., 2012). All the mutations observed in the *RP1* gene associated with adRP group within a small region in the exon 4 of the gene (Audo et al., 2012). All of these mutations cause premature truncation of the RP1 protein. This is unlike the ones that cause arRP, which include missense mutations and are distributed all along the coding segment of the *RP1* gene including the mutational hotspot (Audo et al., 2012).

In this section, we survey the mutations in *RP1* in families with adRP, determine the detailed phenotype, and assess the degree of variability.

3.2.2 METHODS

All the families with adRP registered to Moorfields Eye Hospital (MEH) Inherited Eye Disease Database were explored to identify families with unknown molecular diagnosis. One affected individual from each family was ascertained for this study. After obtaining informed consent, blood samples were obtained and leukocyte DNA extracted. Polymerase chain reactions (PCR) were set up to amplify the mutational hotspot (c.1847 – c.3245) in exon 4 of the *RP1* gene (MIM *603937, RefSeq NM_006269.1) as two overlapping amplimers. The primers used in the study are illustrated in Table 3-9. The PCR products were sequenced bi-directionally by Sanger sequencing.

Table 3-9: Primer sequences for *RP1* PCR reactions

	Forward primer (5'-3')	**Reverse primer (5'-3')**
First amplimer	AGCAGATGCAACCCATTTTT	GCCCTGGTTGTAGCATGTTGT
Second amplimer	GCACCGCAATCTCAAGCAGAAGT	GTGAAGCATCAGGACTGGTAAG

Affected individuals from the adRP families with a *RP1* mutation were invited for phenotyping. Retrospective evaluation of clinical notes was also made and relevant data were included in the study. The data obtained included colour fundus photography, fundus autofluorescence imaging, perimetry, optical coherence tomography (OCT) and ISCEV standard pattern and full-field electroretinography (PERG/ERG). 20

patients underwent ISCEV standard ERGs while 5 patients had non-Ganzfeld ERGs in the past.

Kinetic perimetry with Goldmann perimeter was performed in the affected patients. The visual field obtained by moving the V4e stimulus from the non-seeing area to the seeing area was plotted. The areas of the Goldmann V4e visual fields were measured in square degrees using custom software called Retinal area analysis tool designed by Dr. Anthony Halfyard and Prof. Fred Fitzke, Institute of Ophthalmology, London, 2002.

3.2.2.1 Statistical Analysis

The Spearman's rank correlation coefficient was used to measure the association between the average visual acuity from both eyes at the last visit and age. Survival analysis was conducted using the visual acuity and the visual field of better-seeing eye. The following failure criteria were applied: Visual acuity 0.3 logMAR (i.e., vision compatible with driving) and visual field area 293 deg^2 (corresponds with visual field of 10° diameter, i.e., criterion for legal blindness). As a control, similar analysis was performed for affected adRP patients with mutations in the *PRPF8* gene using published data (Towns et al., 2010). Statistical analysis was performed using GraphPad Prism 4.00 (GraphPad Software, San Diego, CA).

3.2.2.2 Genotyping

As illustrated in the previous section, 57 out of 287 (19.7%) adRP families showed presence of a mutation in the *RP1* gene. The mutations identified have been listed in Table 3-10.

All the mutations caused premature termination of the protein and resulted in a shortened C-terminal. Depending on the nature of the new C-terminal, the mutations can be -1 frameshifts where the reading frame shifts one base ahead (for example, resulting from deletion of a single base or insertion of two bases), +1 frameshifts where the reading frame shifts one base backwards (by insertion of one base or deletion of two bases) and non-sense (Table 3-11).

Table 3-10: Mutations in *RP1* causing adRP in MEH cohort

Mutation	Number of families	Reference
c. p.Lys673Argfs*9	1	Novel
c.2029C>T, p.Arg677*	19	(Pierce et al., 1999, Sullivan et al., 1999, Guillonneau et al., 1999)
c.2035C>T, p.Gln679*	3	(Berson et al., 2001, Sullivan et al., 1999)
c.2055T>A, p.Tyr685*	1	Novel
c.2098G>T, p.Glu700*	3	(Bowne et al., 1999)

c.2115delA, p.Gly706Valfs*7	1	(Gamundi et al., 2006)
c.2143C>T, p.Gln715*	1	Novel
c.2168_2181delGAGGGATACTTTGT or c.2172_2185delGATACTTTGTGAGG, p.Ile725Argfs*6	11	(Payne et al., 2000)
c.2205_2206insA, p.Thr736Asnfs*4	3	Novel
c.2232C>A, p.Cys744*	1	(Payne et al., 2000)
c.2285_2289delTAAAT, p.Leu762Tyrfs*17	2	(Payne et al., 2000)
c.2596_2597delTT, p.Leu866Lysfs*7	8	Novel
c.2607_2608insA, p.Arg872Thrfs*2	3	(Payne et al., 2000)
Total	57	

Table 3-11: Types of *RP1* mutations identified in MEH cohort

-1 Frameshift mutation	**+1 Frameshift mutation**	**Non-sense mutation**
p.Lys673Argfs*9	p.Ile725Argfs*6	p.Arg677*
p.Gly706Valfs*7	p.Thr736Asnfs*4	p.Gln679*
	p.Leu762Tyrfs*17	p.Tyr685*
	p.Leu866Lysfs*7	p.Glu700*
	p.Arg872Thrfs*2	p.Gln715*
		p.Cys744*
2 families	27 families	28 families

Table 3-12: Variations identified in 98 controls

Missense changes	Frequency	Reference
c.2763G>A	43/196	rs444772
c.2783G>C	1/196	rs753472023
c.3101A>T	69/196	rs2293869

3.2.3 RESULTS

3.2.3.1 Clinical features

The clinical features of all the patients are described in the appendix (Table 5-2).

There were 384 affected individuals in 57 families. 98 mutation-carrier individuals from 54/57 (94.7%) of these families were included in the clinical analysis. 62/98 patients were examined while retrospective evaluation of medical notes was performed for the rest of the patients. 166/384 (43.23%) individuals were females. All 56 families were of white European ancestry. There was no evidence of consanguinity in any of the families. In 6 families, there was evidence of non-penetrance by history (Figure 3-24).

Among the 98 patients phenotyped, 21 individuals were examined only once. Among the rest (77 subjects), the follow up varied from 1 year to 34 years (Median=6 years, Mean=8.65 years, Standard deviation 8.46 years).

The average age at which the patients first noticed symptoms was 34.76 years (Median 32 years, Range 15-72 years). Night blindness was

the most common primary symptom at onset. Only 51% of patients complained about problems in dim light as their sole primary symptom at onset, although no patient reported night blindness in the first decade of life. Flashing lights were reported as the primary symptom by 8% patients, 6% complained of loss of peripheral visual field and 8% had multiple symptoms.

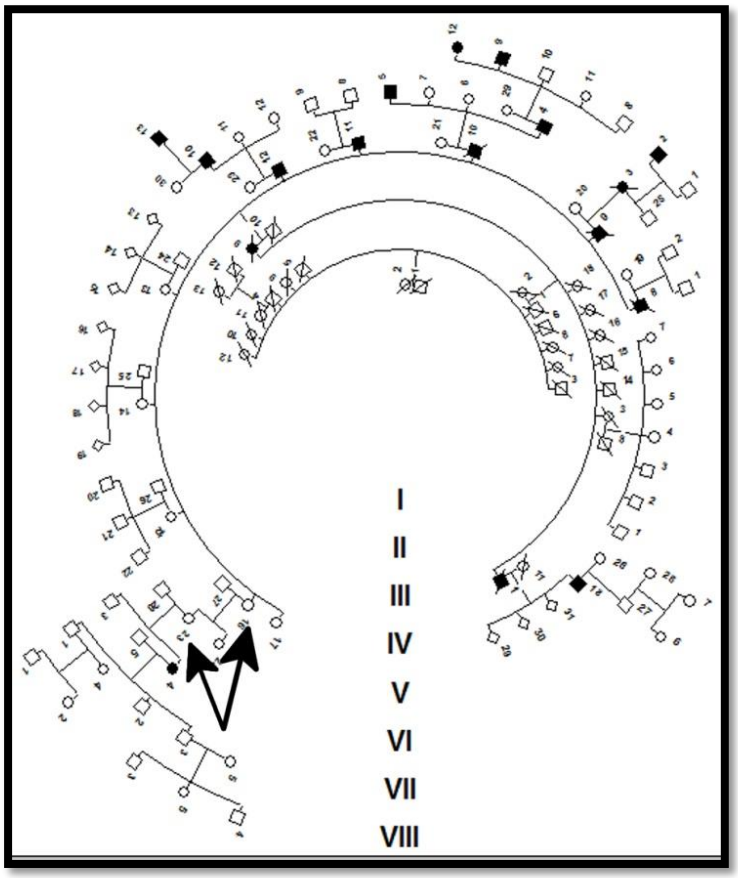

Figure 3-24: GC754 showing 2 generations of non-penetrance – IV:16 and V:23 being obligate carriers

Among the 62 examined patients, 16 (25.8%) were completely asymptomatic and were diagnosed on the basis of genetic test and/or ophthalmic examination. The mean age of these patients was 42.76

years with a median of 40 years. The range varied from 24 years to 63 years of age.

Best Corrected Visual acuity (BCVA) in logMAR correlated with age (Spearman's rank correlation coefficient r = 0.6126, p<0.0001) (Figure 3-25). On performing the survival analysis, the median age at which BCVA deteriorated to worse than 6/9 in *RP1* patients was 77 years which was 20 years later than that observed in *PRPF8* patients (57 years) (Log rank Mantel-Cox test p<0.0001) (Figure 3-26).

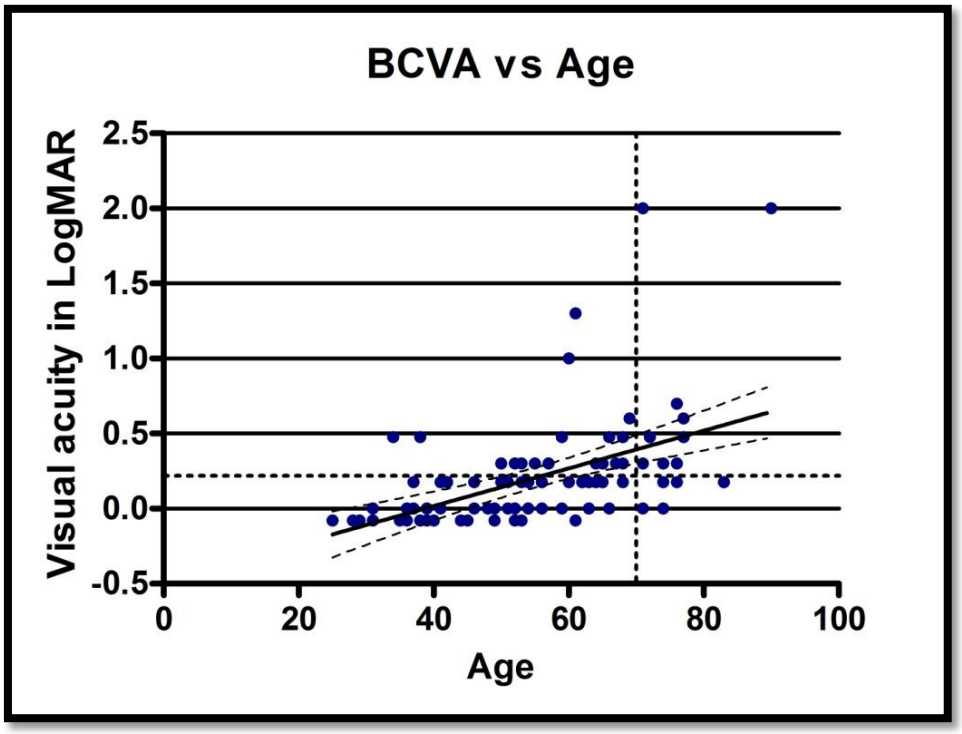

Figure 3-25: Correlation of best-corrected visual acuity with age

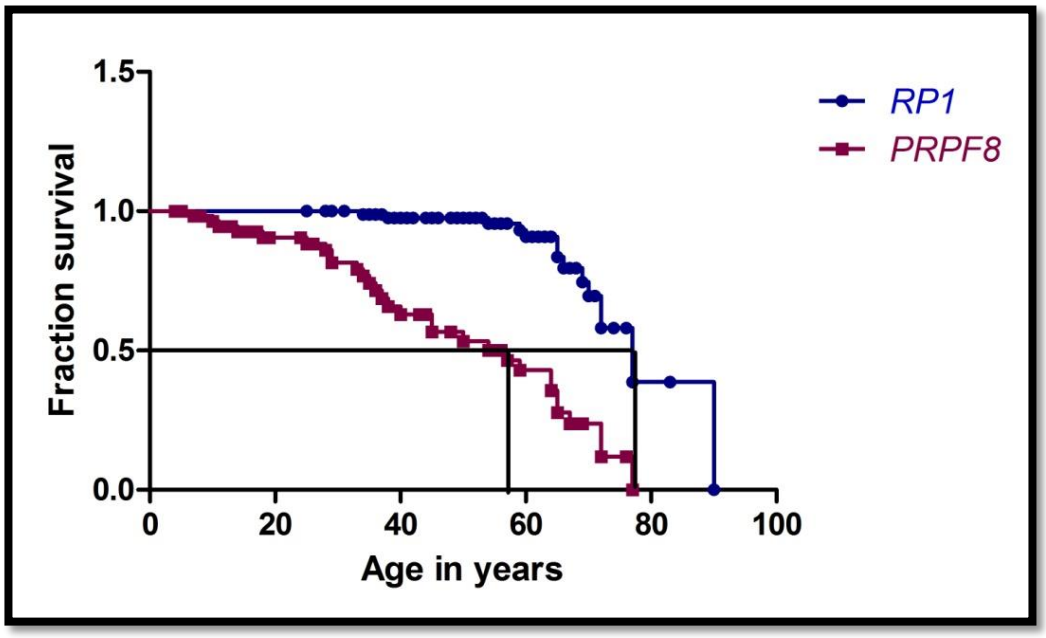

Figure 3-26: Survival analysis of visual acuity of patients with *RP1* mutations and patients with *PRPF8* mutations

Reliable Goldmann visual field data could be obtained from 48 eyes of 24 patients. Some patients had visual fields done multiple times resulting in more data points (57) than eyes (48). The median age at which the visual field in the larger field eye deteriorated to 10° or worse in *RP1* patients was 83 years which was 19 years later than that observed in *PRPF8* patients (64 years) (Log rank Mantel-Cox test $p<0.0001$) (Figure 3-28).

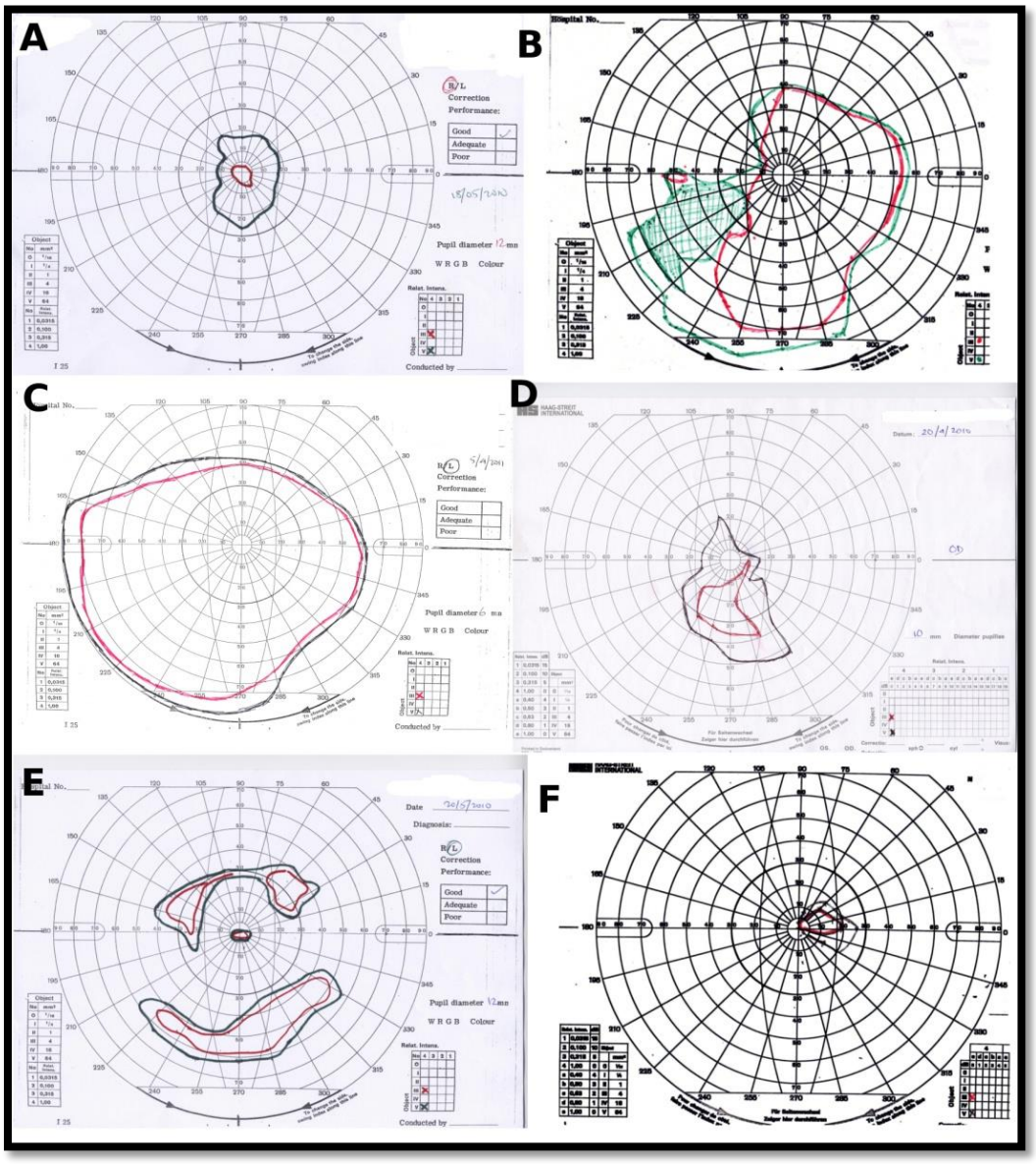

Figure 3-27: Variability of visual fields in *RP1* mutation carriers. A-73-year-old female with p.R677X , B-64-year-old male with p.R677X , C-36-year-old female with p.R677X, D-75-year-old female with p.R677X , E- 52-year-old man with p.L866KfsX7, F- 64-year-old man with p.L866KfsX7.

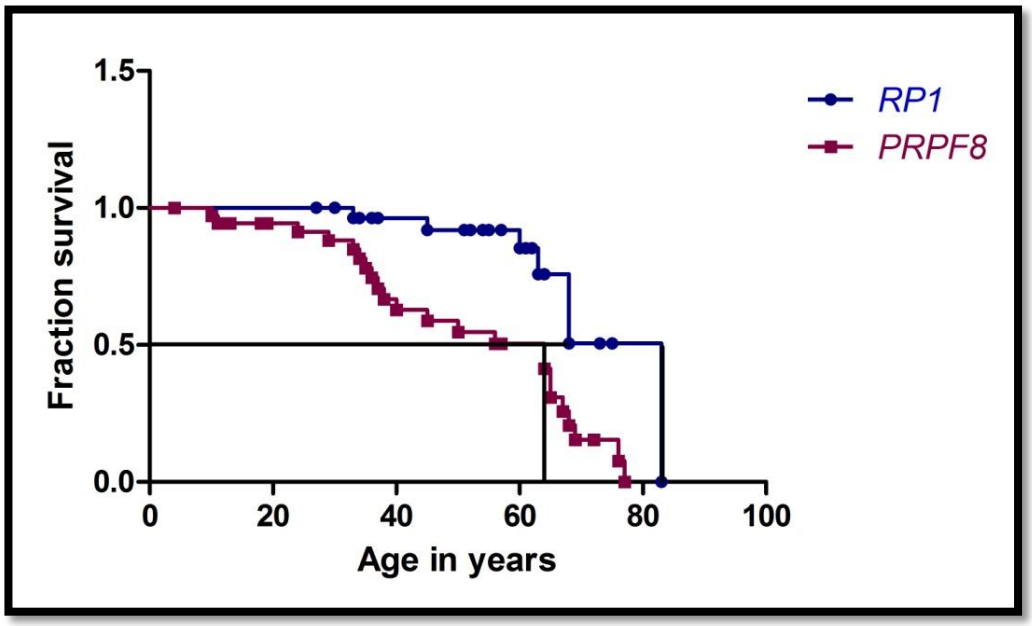

Figure 3-28: Survival analysis of visual field deterioration of patients with *RP1* mutations compared with those with *PRPF8* mutations

56 patients underwent AF imaging while 46 underwent OCT. FAF images in 32/56 (57.14%) cases delineated the area of retinal dystrophy and showed a ring of high autofluorescence around the fovea. Among the rest 18/56 (32.14%) patients had normal 30° autofluorescence. 6/56 (10.71%) patients had widespread hypo-autofluorescence involving the macular region in a patchy distribution.

The spectral domain OCT in patients with *RP1* retinal dystrophy showed preserved photoreceptor-RPE complex at the posterior pole within the hyper-autofluorescent FAF ring in 33/46 (71.7%) patients. Among the rest of the patients (12/46), there were patchy disruptions of the photoreceptor layer which corresponded to the absence of normal autofluorescence pattern. In 1 patient, there was a lamellar macular hole at the fovea.

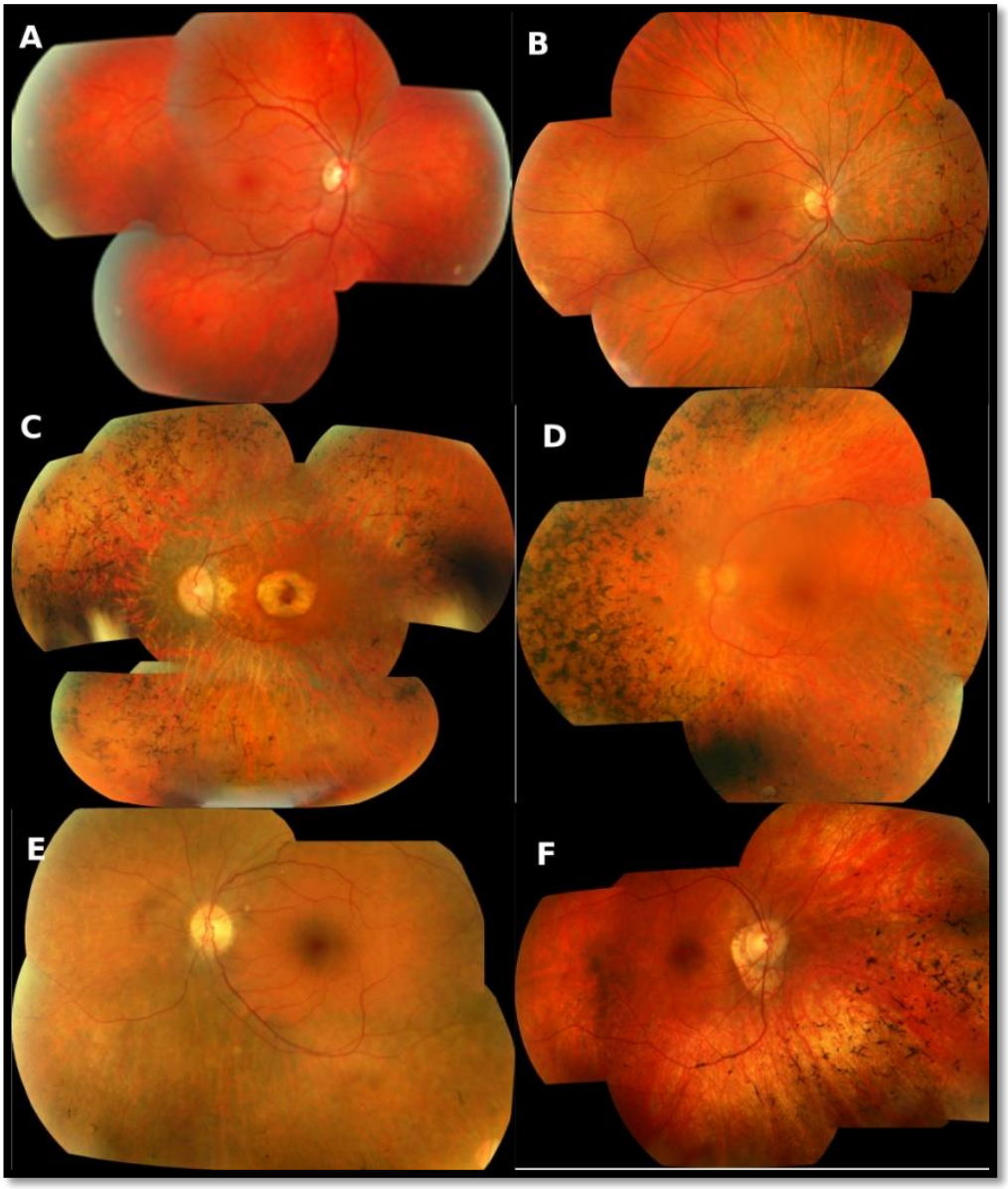

Figure 3-29: Variability of fundus phenotype in *RP1* patients. A - 35-year-old asymptomatic male with p.L866KfsX7 showing absence of pigment, B - 36-year-old female with p.R677X, C – 45-year-old female with perifoveal atrophy having p.I725RfsX6 mutation, D – 64-year-old female with p.K673RfsX9, E - 49-year-old female with p.I725RfsX6 mutation with very little pigment migration, F – 51-year-old female with sectoral pigment distribution.

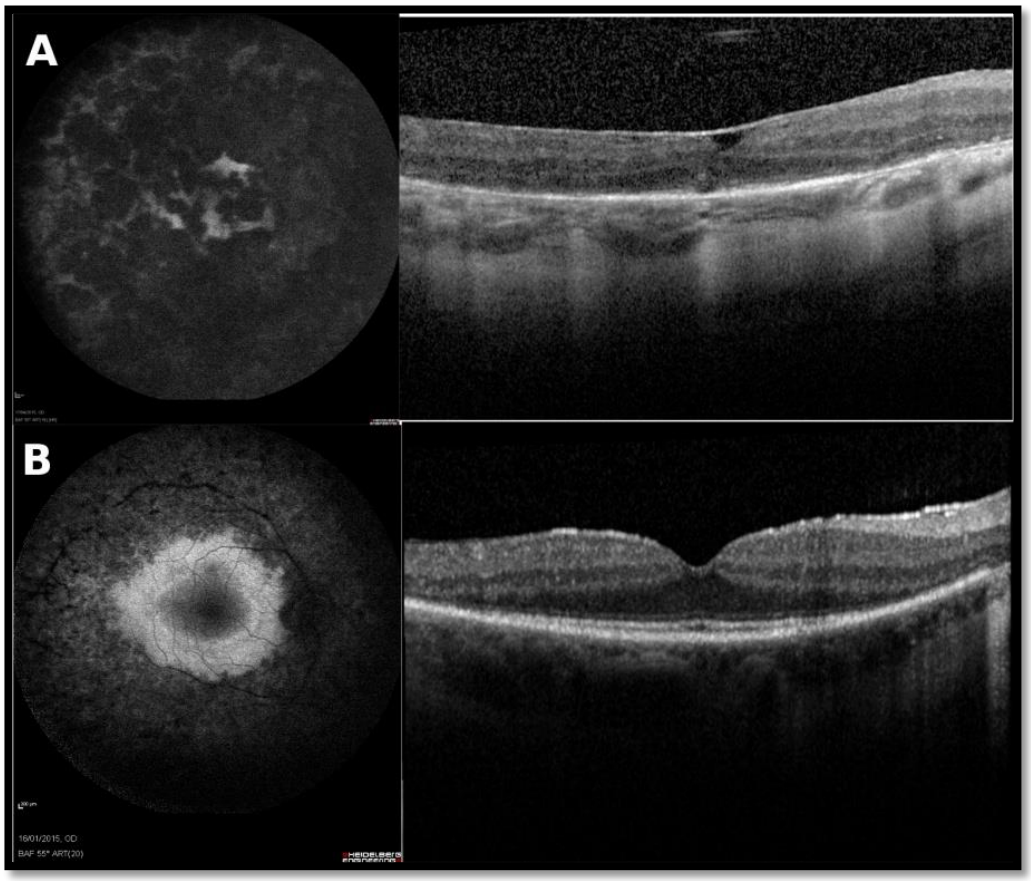

Figure 3-30: Variability of autofluorescence and OCT phenotype in the same family GC903. A and B are images from two sisters carrying the *RP1* mutation p.K673RfsX9; A (72 years) is 3 years older than B (69 years) and has macular involvement while B has perimacular hyperautofluorescent ring and retained macular OCT morphology.

18/98 (18.37%) patients developed macular oedema. The BCVA of eyes with macular oedema varied from 0 (6/6) to 1 (6/60) [Median=0.301 (6/12)]. The ages of the patients who developed macular oedema ranged from 34 years to 72 years.

3.2.3.1.1 Electrophysiology

ERG findings on 33 patients are presented in Figure 3-31. Full-field ERGs of patients with *RP1* mutations were consistent with rod-cone dystrophy. The amplitude of dark-adapted bright flash ERG a-waves varied greatly, consistent with differing degrees of rod photoreceptor involvement. Patients with *RP1* dystrophy showed wide variation in the function of their rods and cones. Retinas with similar rod photoreceptor degeneration demonstrated by dark adapted bright flash a-wave showed wide variation in cone system function (Figure 3-31A).

Transient cone ERG b-wave amplitude showed milder or no reduction in our cohort. 30Hz flicker ERGs were delayed in 16 cases by 1-16ms (median 6ms) indicating variable extent of the degeneration. The major scotopic and photopic ERG amplitude parameters correlated weakly with age (Figure 3-31B).

The macular function as measured by pERG P50 was compared with age (Figure 3-31C). In 3/33 patients (9%) cases the amplitude of p50 was lower than 1μV. Thus, in 91% patients, even those with age more than 60 years, macular function as measured by pERG p50 amplitude were preserved.

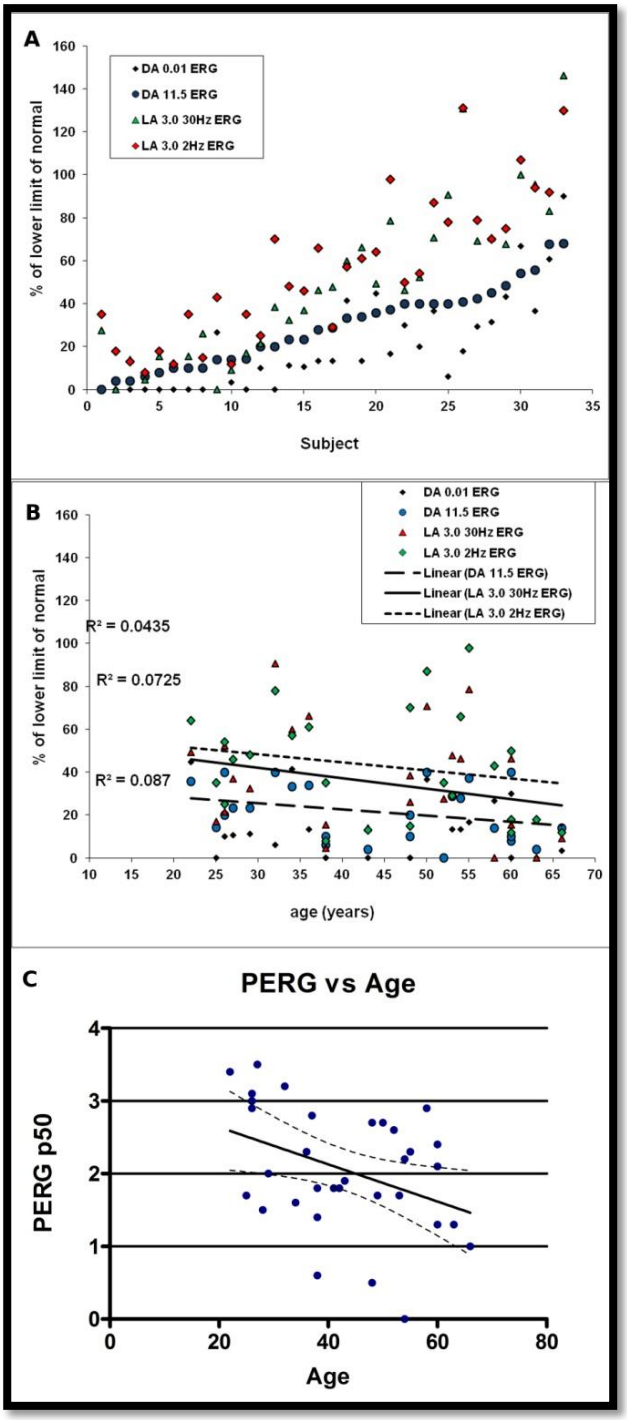

Figure 3-31: A – ERG amplitude as a percentage of lower limit of normal values in ascending order of dark adapted bright flash a-wave in all patients showing the spread of the cone function. B – ERG amplitude as a percentage of lower limits of normal values compared to age. C – pERG p50 amplitudes compared to age

3.2.4 DISCUSSION

This section describes the phenotype of adRP caused by heterozygous mutations in the *RP1* gene and attempts to establish the genotype-phenotype correlations.

About 20% of adRP in MEH is caused by *RP1* mutations. This figure is significantly larger than similar studies conducted previously (3.5%) (Sullivan et al., 2006a). One possible explanation of such a large difference can be racial. Unlike previous studies which were conducted in North America with possible mix of African, Hispanic and Caucasian haplotypes, all families with *RP1* mutations in our cohort belonged to White European population. Thus, *RP1* may be an important cause of adRP in Caucasians in general and White British population in particular.

The screening for mutations in the *RP1* gene was limited to the mutational hotspot (c.617-c.1081). This was based on the available evidence that all the adRP causing mutations are located within this region. Further supporting this hypothesis is the fact that several groups have attempted to screen the whole *RP1* gene including the un-translated regions but have failed to identify a pathogenic change (Jacobson et al., 2000, Audo et al., 2012, Zhang et al., 2010).

All the mutations associated with adRP cause premature truncation of the C-terminal end of the protein due to formation of a stop codon either by frameshift or by alteration of a single base. This study has identified 5 novel mutations all of which cause premature stop codon formation. The main conserved domains in the RP1 protein are the two doublecortin domains near the N-terminal of the protein. However, it is the C-terminal end of the protein, which contains the mutational

hotspot where all the adRP mutations conglomerate. So far the function of this region of the protein is unknown. As the hotspot is in the terminal fourth exon of the gene, it is predicted to survive nonsense-mediated decay. This has been established by Liu et al who demonstrated the presence of truncated protein in human cultured lymphoblasts in a patient with *RP1* p.Arg677* mutation (Liu et al., 2003). Thus, haploinsufficiency is an unlikely mechanism for disease in heterozygous *RP1* mutations while dominant negative effect is more plausible. Interestingly, non-sense mutations near the 3' end of the gene have been shown to be non-pathogenic in Chinese and Japanese populations (Baum et al., 2001, Kawamura et al., 2004). Thus, it can be concluded that a relatively small region near the C-terminus of RP1 performs an unknown important function, alteration of which impairs the working of the normal allele.

Most of the examinations were conducted in patients aged between 20-80 years. This is indicative of the fact that symptoms for *RP1* retinal dystrophy appears rarely in the first two decades of life. Corroborating with this observation is that the median onset of symptoms was 32 years. This agrees with observations from previous studies (Audo et al., 2012, Berson et al., 2001). As expected for an autosomal dominant disease, there was no influence of gender on the onset of the disease.

A quarter of the patients were asymptomatic who were detected by ophthalmic examinations or genetic testing. It can be concluded that similar patients with minimal symptoms can be diagnosed as unaffected or non-penetrant as has been observed in previous studies (Audo et al., 2012, Berson et al., 2001, Jacobson et al., 2000). However, the retinas of all the asymptomatic individuals could be identified as carrying the mutation by fundus photography, autofluorescence or

electrophysiology. Hence, the *RP1* dystrophy can be described as highly variable and with some individuals being non-penetrant for symptoms.

Visual acuity in a patient with retinitis pigmentosa can be influenced by various factors like cataract, macular oedema, keratoconus, amblyopia etc. Overall, when plotted against age, there was a gradual reduction of visual acuity. The Kaplan-Meier survival curve using outcome as the age when visual acuity worsens beyond 6/9, showed that the patients with *RP1* mutations generally retained their visual acuity longer than their counterparts with *PRPF8* mutations. This difference was more marked during early life but tended to persist even in advanced years of life. However, there are limitations to such an analysis like other confounding factors, variability within observations and reliability of subjective testing. The survival analysis also assumed that all patients had better or equal to 6/9 visual acuity at birth and the vision got worse with age and disease. Even with these limitations, the pattern ERG, autofluorescence and OCT data supported the conclusion that patients with *RP1* retinal dystrophy tended to retain their central macular function longer.

Similar survival analysis was performed for visual field with 10° visual field as the outcome. The visual field deteriorated for most patients slowly till the sixth decade following which the rate of decline accelerated. Although this analysis had fewer confounding factors, more data is required to improve the confidence and draw better conclusions.

As observed in previous studies the retinal fundus imaging revealed a variable phenotype (Jacobson et al., 2000, Audo et al., 2012, Berson et al., 2001). Although most patients showed circumferential mid-peripheral disease, several young patients showed evidence of

involvement of nasal and inferior sector only. However, electrophysiology failed to reveal a limited phenotype and these patients had a mild generalised rod-cone dystrophy even though the intra-retinal pigment migration was limited to infero-nasal sectors. In one female, the retinal involvement was completely unilateral (Mukhopadhyay et al., 2011). The complete unilaterality of the disease due to environmental influences or genetic modifiers is difficult to explain. One possible explanation could be a somatic genetic change appearing in the progenitor cells of the unaffected eye ameliorating the effect of pathogenic mutation.

18% patients with *RP1* mutations developed macular oedema which was similar to that observed in other studies (Fishman et al., 1977, Pruett, 1983). However, Hajali et al described a significantly higher incidence of macular oedema (52%) among a genetically heterogeneous group of adRP patients (Hajali et al., 2008). It is probable that *RP1* adRP causes fewer cases of macular oedema. Further studies are required to substantiate or refute the above conclusion.

Electrophysiological analysis was performed in about a quarter of the patients. As observed in other studies, all cases were that of rod-cone dystrophy with rod-system involvement at the photoreceptor level being more pronounced than cone-system involvement (Jacobson et al., 2000). The patients maintained macular function even during their sixth decade of life. This agrees with the previous observations regarding visual acuity, FAF and OCT.

No genotype-phenotype correlations were observed for visual acuity. However, in the case of non-sense mutations, the loss of visual field seemed to progress faster than in case of the frameshift mutations. More data is required to substantiate this observation.

Overall, heterozygosity for the *RP1* mutations generally causes a mild adult onset rod-cone retinal degeneration. Macular function remained normal or relatively preserved until the late stages in most cases. Unilateral disease and sectoral distribution of the pigment have been observed.

3.3 AUTOSOMAL DOMINANT RETINITIS PIGMENTOSA WITH INTRAFAMILIAL VARIABILITY AND INCOMPLETE PENETRANCE IN TWO FAMILIES CARRYING MUTATIONS IN *PRPF8*

3.3.1 INTRODUCTION

Seven genes, *PRPF3, PRPF4, PRPF6, PRPF8, PRFP31, RP9* and *SNRNP200* encode splicing factors which together account for approximately 15% of families with adRP in the United Kingdom (Figure 3-2). There are few detailed descriptions of the clinical phenotype associated with *PRPF8* mutations (Towns et al., 2010). This section describes the detailed clinical phenotype in two British families with adRP associated with mutations in *PRPF8* (Maubaret et al., 2011).

3.3.2 METHODS

3.3.2.1 Clinical Assessment

Two families, a six-generation (GC171) and another three-generation (GC16352), were ascertained from the inherited eye disease clinic of the Moorfields Eye Hospital (Figure 3-32). Eight members of GC171, seven affected and one mildly symptomatic underwent ophthalmic examination. Colour fundus photography was performed in five out of eight patients; three had autofluorescence imaging (FAF) and spectral-domain optical coherence tomography (SD-OCT) and four had Goldmann visual field examination (VF). Four affected members of

GC16352 were examined and underwent colour fundus photography and three had FAF and SD-OCT.

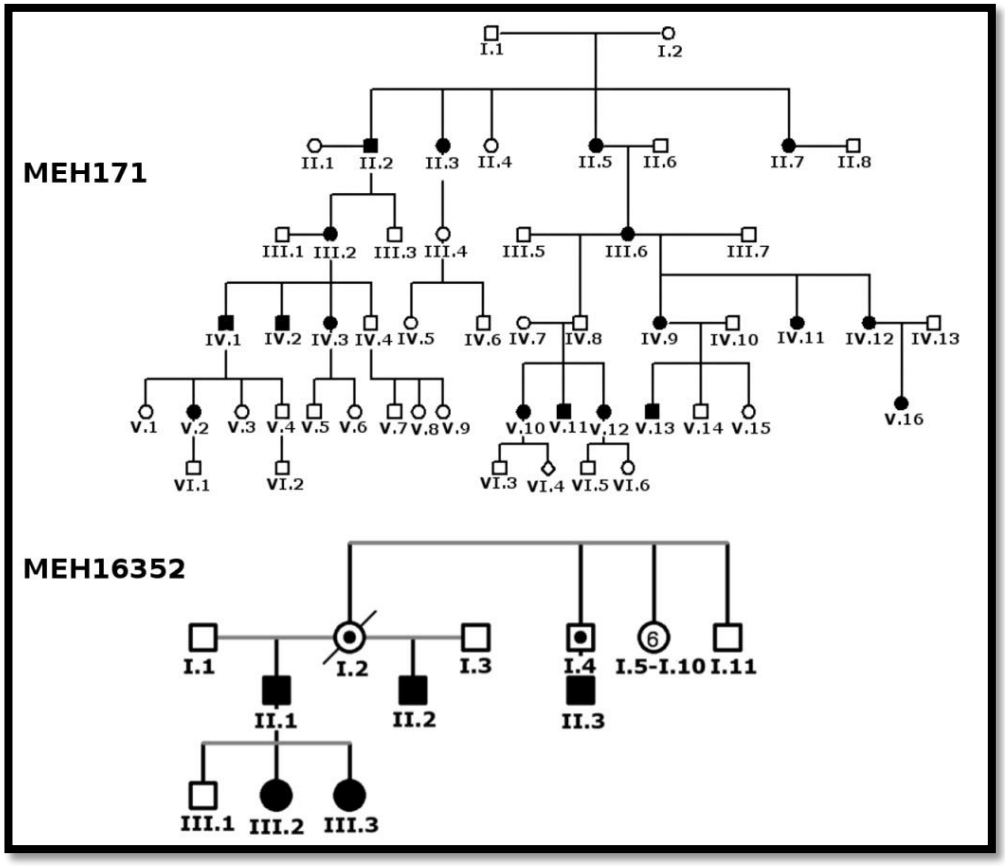

Figure 3-32: Pedigrees of GC171 and GC16352

Full field electroretinography (ERG) was performed using the International Society for Clinical Electrophysiology of Vision (ISCEV) standards (McCulloch et al., 2015) in two of the milder affected members of GC171 (IV.8 and V.12) and a young (6-year-old) affected (III.2) from GC16352 who underwent a modified paediatric ERG protocol (Marmor et al., 2009) (Figure 3-32).

3.3.2.2 Molecular genetic analysis

Molecular genetic analysis and mutation screening was performed by Dr Cecilia Maubaret at UCL Institute of Ophthalmology, London, UK.

After obtaining written consent, blood samples from affected and unaffected family members were collected for DNA and RNA extractions. RNA was isolated from lymphocytes of one affected member from each family (Trizol; Invitrogen, Paisley, UK). Microsatellite markers flanking known genes for adRP were selected from a linkage mapping set (ABI Prism Linkage Mapping Set v 2.5; Applied Biosystems, Foster City, CA) and additional FAM-labeled microsatellite markers were selected from the Ensembl database. 8 PCRs were done (Absolute QPCR; Thermo-Fisher, Epsom, UK) according to manufacturer's instructions. The resultant PCR products were loaded in a DNA sequencer (ABI model 3730; Applied Biosystems) and the genotyping calls and Mendelian error checks were performed with commercial software (GeneMarker, version 1.70; Biogene, Cambridgeshire, UK) for linkage analysis.

3.3.2.2.1 Mutation Screening

cDNA was synthesized from leukocyte RNA (patient IV.2 in GC171 and II.2 in GC16352) using reverse transcriptase (Superscript III Reverse Transcriptase; Invitrogen) according to manufacturer's instructions. Mutation analysis was performed by Sanger sequencing of the cDNA using a terminator sequencing kit (BigDye ver 3.1; Life Technologies, Paisley, UK) on the ABI 3730 machine (Applied Biosystems). cDNA

sequences obtained for patient IV.2 and II.2 were compared with the reference sequence of *PRPF8* from the Ensembl database. 8 Primers used for PCR and sequencing are described in Table 2 of Towns et al (Towns et al., 2010). Exons and nucleotides were numbered according to OMIM (Online Mendelian Inheritance in Man; http://www.ncbi.nlm.nih.gov/Omim/ provided in the public domain by the National Center for Biotechnology Information, Bethesda, MD) ID 607300. For the other members of the families, genomic DNA was sequenced using primers e38F/e39R in GC171 and e42F/e42R in GC16352. DNA from 130 healthy Caucasian controls (Sigma-Aldrich, Dorset, UK) was sequenced for the two identified mutations from GC171 and GC16352.

3.3.3 RESULTS

3.3.3.1 Clinical Assessment

3.3.3.1.1 GC171

Seven clinically affected members aged between 37 and 82 years and one mildly symptomatic, obligate carrier (68 years) were assessed. Six affected subjects complained of night blindness as the first symptom. The age of onset of the night blindness varied within family members from early childhood (patients V.10, V.11, V.12) to mid-thirties (IV.12). Visual field constriction was reported in late teens in patients III.2 and V.11 and after the age of forty in patient IV.12. Patient IV.8, an obligate carrier, reported no problems driving at night or looking at stars in the

night sky although had confessed to mild difficulty in different lighting conditions previously. He did not complain of any visual field constriction. Best corrected visual acuity (BCVA) in the better eye was 6/12 or better in five out of seven symptomatic patients. In the 82-year-old female (III.2), BCVA was 6/18 in the right and 6/36 in the left eye while in a 59-year-old male (IV.2), it was hand movements right and 6/18 left eye. Bilateral sub-capsular cataract was observed in patients III.2 at a young age, IV.2 (age 34 years), and V.11 (age 33 years).

In all patients fundoscopy revealed attenuated retinal vessels, pale optic nerve head and variable degrees of diffuse bone spicule like pigment clumping within the neurosensory retina (Figure 3-33A).

Asteroid hyalosis was observed in the left eye of patient IV.12. Patient V.11 had bilateral optic nerve drusen. Patient IV.2 developed Coats-like retinal telangiectasia in his right retinal periphery resulting in a vitreous haemorrhage when aged 34 years. Patient IV.12 had an episode of angle closure glaucoma at 41 years of age. Cystoid macular oedema of various degrees was observed in four symptomatic patients (IV.2, V.10, V.11, and V.12). Individual IV.8 had a normal retinal appearance (Figure 3-33C).

Extensive peripheral atrophy was present in two affected individuals in FAF images with a small peri-foveal ring of increased autofluorescence (Figure 3-33A). OCT showed preserved outer retinal structure in the area delineated by the ring of hyperautofluorescence (Figure 3-33A). In another patient (IV.2), OCT showed disruption of the outer retinal structure in the fovea (Figure 3-33A). FAF and OCT of the only mildly symptomatic obligate carrier (IV.8) (Figure 3-33C) were normal.

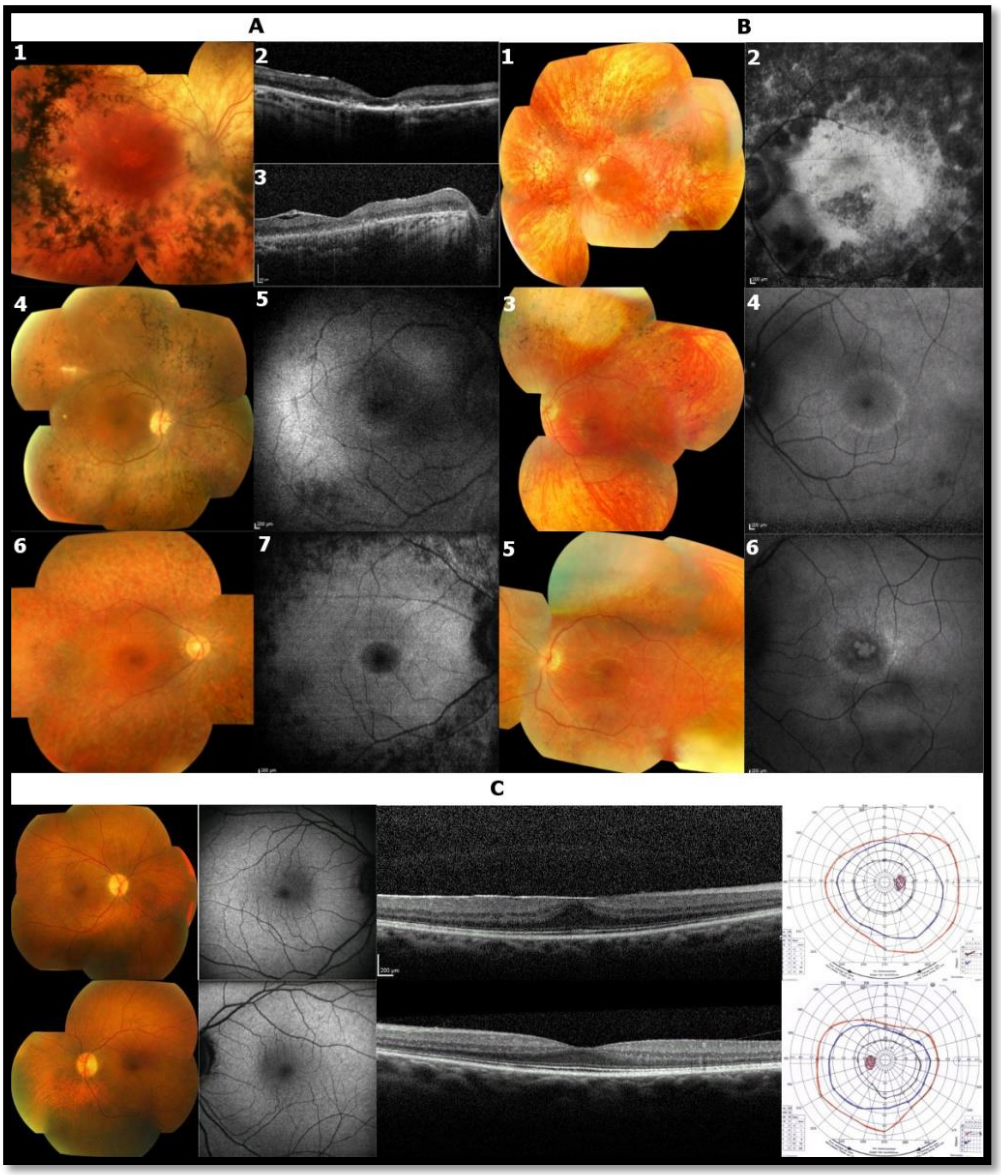

Figure 3-33: Variability of phenotype of *PRPF8* retinitis pigmentosa. (A) GC171 – (A1)-Right fundus of 60-year-old male with OCT of the right (A2) and left eye (A3), (A4, A5)-Right fundus and FAF of a 51-year-old female, (A6, A7) Right fundus of a 38-year-old male with FAF. (B) GC16352 – (B1, B2) show the fundus and AF of a 49-year-old male. Fundus photographs (B3, B5) and FAF (B4, B6) at age 15 and 11 years of age respectively of a female subject (C) Fundus photographs, autofluorescence, spectral-domain OCT, and Goldmann visual fields of asymptomatic individual IV.8 of GC171 showing relative preservation of normal structure and function at 63 years of age.

Goldman perimetry showed a variable degree of visual field loss with patient V.12 retaining approximately 50° of horizontal visual field in the better eye with the biggest and brightest target (V4e) at 34 years of age while V.10 had near normal fields at 37 years of age. Subject IV.2 had a small central field of approximately 15° at 38 years of age with retention of a temporal island of preserved field. Individual IV.8 had normal visual fields at 63 years of age (Figure 3-33C).

Electrophysiological testing of the patient (IV.8) who complained of only mild contrast adjustment showed mildly abnormal rod photoreceptor function (rod specific ERGs were normal but bright flash [DA 11.0] a-wave was mildly reduced). Cone ERGs were normal (Figure 3-34A). Subjects V.10 and V.12 had only residual detectable rod and cone ERGs in keeping with a severe rod-cone dystrophy.

3.3.3.1.2 GC16352:

The proband, a 35-year-old man (Figure 3-32, lower panel, II.2), had night vision problems from early childhood and was diagnosed with RP in his late teens. He later developed deterioration of central vision and when examined aged 35 years, right eye BCVA was 6/24 with hand movements in the left eye. At that time his Esterman supra-threshold bilateral visual fields were reduced to 5°. He developed bilateral subcapsular cataracts in his mid-twenties. His half-brother (II.1), sharing the same mother, was also affected and had early onset of subcapsular cataracts for which he underwent bilateral cataract surgery. His BCVA at 48 years of age was 3/60 right and left. His older daughter (III.2) developed night blindness in early childhood. BCVA at

age 15 years was 6/10 right eye; 6/5 left eye. The youngest daughter (III.3) was noted to be night blind in the first decade and at age 11 years had BCVA of 6/15 in both right and left eyes. According to reports from her sons, the deceased grandmother of the two affected females (I.2) had no visual symptoms when she died at the age of 69 years. All symptomatic family members examined showed severe attenuation of arterioles, pale optic discs, and sparse intraretinal pigment migration (Figure 3-33B).

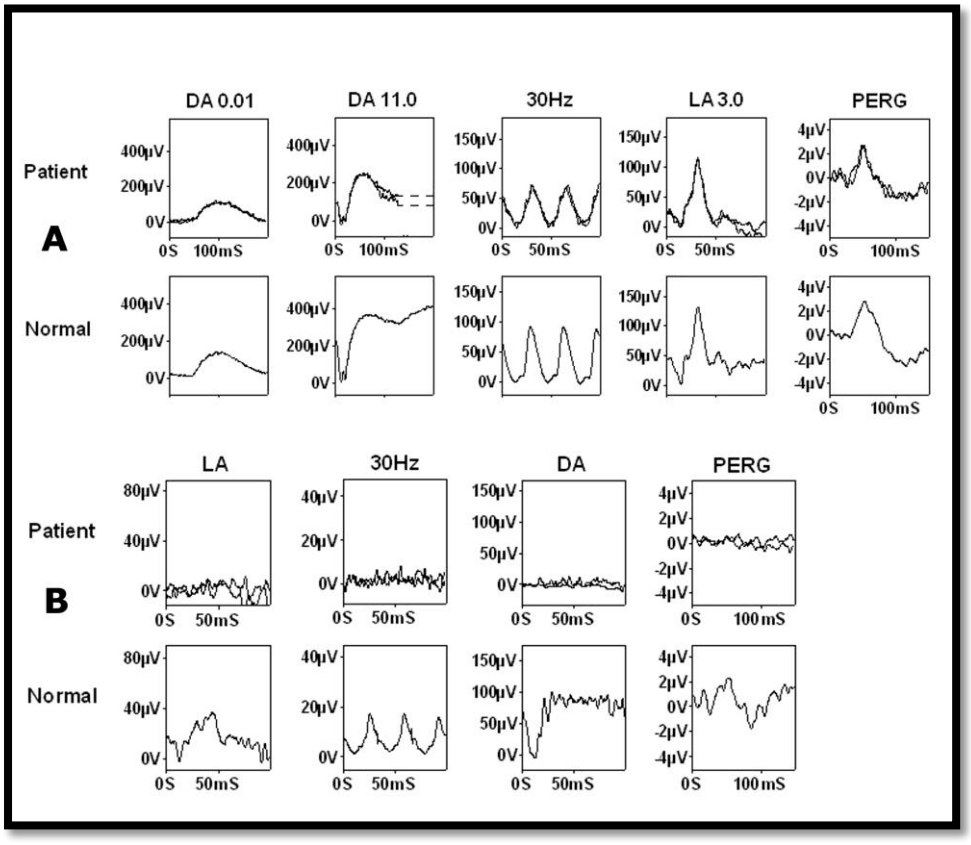

Figure 3-34: Electrophysiology of affected individuals. (A) ISCEV standard ERGs of patient IV.8 of GC171 (see Figure 3-33C 63 years of age, asymptomatic) show subnormal DA 11.0 a-wave amplitude. (B) ERGs of patient III.2 of GC16352 (6 years of age, symptomatic) show severe generalized loss of both rod and cone photoreceptor function

FAF in patient II.1 showed peripheral and central macular atrophy, while there was preservation of central macula with perifoveal hyperautofluorescent ring in the two young females (III.2 and III.3) (Figure 3-33B). FAF and OCT revealed bilateral macular oedema in both III.2 and III.3 with the younger more affected (Figure 3-33B). OCT of II.1 showed central macular atrophy.

Electrophysiological assessment of III.2 at 6 years of age using paediatric protocols revealed severe photoreceptor dysfunction with undetectable waveforms (Figure 3-34B).

3.3.3.2 Mutational Screening:

3.3.3.2.1 GC171:

Linkage analysis with flanking microsatellite markers to all known adRP loci showed strong evidence for linkage at the RP13 locus (markers D17S849, D17S831, D17S1840, D17S1574, and D17S525). Because *PRPF8* is the gene implicated in RP13, it was initially decided to directly sequence exon 42 as all published mutations have been found in this exon. No variant was found by direct sequencing of the proband IV.2. Therefore, RNA from IV.2 was extracted, reverse transcribed, and *PRPF8* cDNA was directly sequenced allowing for a quick investigation of possible splicing defect and/or exonic mutation. The variant c.6353 C>T, was identified in exon 38 in a heterozygous state (Figure 3-35, upper panel). Direct sequencing of the *PRPF8* exon 38 from the genomic DNA of the whole family revealed that all the affected patients, and the one mildly symptomatic carrier harboured this change, which

was not present in unaffected family members. The mutation c.6353 C>T (p.S2118F) was not found in 130 unrelated controls from the same ethnic origin indicating that this change is likely to be causative of the disorder in this family.

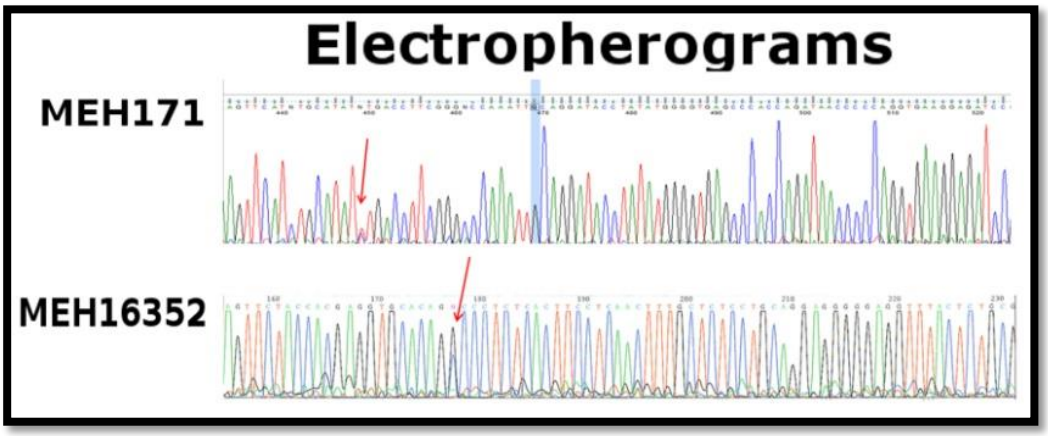

Figure 3-35: Electropherograms of the mutations identified.

3.3.3.2.2 GC16352:

The entire cDNA of affected proband (II.2) was sequenced and the mutation c.6930G>C (Figure 3-35, lower panel) leading to p.R2310S missense change in the protein was identified in exon 42. The same variant was present in all affected family members and was not found in 130 control individuals.

3.3.4 DISCUSSION

This section describes the detailed phenotype of affected members of a large British family carrying the missense *PRPF8* mutation c.6353 C>T (p.S2118F) in exon 38 reported by Towns et al (Towns et al., 2010).

All previous *PRPF8* mutations had been reported to occur in exon 42 of the gene (McKie et al., 2001, Martinez-Gimeno et al., 2003, van Lith-Verhoeven et al., 2002, Tarttelin et al., 1996, Testa et al., 2006). Mutations in *PRPF8* gene are rare, accounting for 2%–3% of patients with adRP in Spanish and American studies,(Daiger et al., 2007, Hartong et al., 2006, Martinez-Gimeno et al., 2003, Sullivan et al., 2006a) and 2.79% in a large United Kingdom cohort (Figure 3-2). These percentages are likely to be underestimates given the current restriction of screening to exon 42 of the gene.

Previous reports have documented a severe form of RP in British, Spanish, Dutch, and African American families, with mutations in exon 42 of *PRPF8* (Martinez-Gimeno et al., 2003, van Lith-Verhoeven et al., 2002, Tarttelin et al., 1996, Testa et al., 2006, Walia et al., 2008). The previous phenotype descriptions were consistent with an infantile onset of night blindness, followed by visual field loss a few years later. All the published adult patients have unrecordable ERG values and the rod function in affected paediatric population is severely abnormal (Martinez-Gimeno et al., 2003, Testa et al., 2006, Walia et al., 2008). The phenotype is relatively uniform and there is no evidence of variability or incomplete penetrance.

The present study reveals a high degree of intrafamilial phenotypic variability. The age of onset of night blindness varied from early childhood to late thirties. One 67-year-old individual heterozygous for the c.6353 C>T (p.S2118F) mutation who was only mildly symptomatic, had a completely normal fundus appearance. Macular oedema was observed in four out of seven patients (IV.2, V.10, V.11, V.12) of GC171 and two out of four patients (III.2 and III.3) in GC16352 and seems to occur with higher frequency in patients with a *PRPF8* mutation than

other forms of adRP (van Lith-Verhoeven et al., 2002, Tarttelin et al., 1996, Testa et al., 2006, Walia et al., 2008). AF imaging in symptomatic patients with relative preservation of visual acuity, when available, revealed a ring of increased autofluorescence surrounding the central macula (Figure 3-33). Hyperfluorescent rings of various types are observed in RP or Leber's congenital amaurosis (usually surrounding healthy macula) and cone or cone-rod dystrophy or X-linked retinoschisis (usually surrounding dystrophic macula)(Robson et al., 2008). However, in primary RPE retinal dystrophies, such as those caused by mutations in *MERTK* or *RPE65*, such rings have not been described (Mackay et al., 2010, Lorenz et al., 2008). Furthermore, SD-OCT images in affected patients demonstrate an intact hyper-reflective layer at the junction of dystrophic retina and choroid which might represent intact RPE-Bruch's membrane complex. However, in the mouse model there is evidence of defective RPE function (Graziotto et al., 2011). It is possible that human *PRPF8* retinopathy may have thus different pathophysiology with relative late demise of RPE.

The ERG in the mildly symptomatic obligate carrier showed a DA 0.01 rod ERG within the normal range but a subnormal DA 11.0 bright flash ERG a-wave. Cone full-field ERGs and pattern ERGs were normal. The consequences of this mutation, which in other family members caused legal blindness, were those of minor rod photoreceptor function. Affected status was not evident from fundus examination or perimetry. This suggests caution in reassuring members of families with *PRPF8*-related disease of their unaffected status and confirms the importance of electroretinography in the detection of subclinical disease.

There is a history of incomplete penetrance in two individuals in the second family, but neither was available for examination. The mutations

p.R2310K (McKie et al., 2001, van Lith-Verhoeven et al., 2002) and p.R2310G (McKie et al., 2001, Martinez-Gimeno et al., 2003) have previously been reported and suggests that c.6930G>C (R2310S) in exon 42 is a hot spot for mutation. *PRPF8, PRPF3*, and *PRPF31* genes are involved in the assembly and function of the spliceosome, which clips introns out of pre-mRNA (Smith et al., 2008). The gene *PRPF8* encodes a large and highly conserved nuclear protein (Grainger and Beggs, 2005) which stimulates a helicase, Brr2, required for activation of the spliceosome (Maeder and Guthrie, 2008). *PRPF8* mutations which cause adRP inhibit this function. More than 15 different mutations, most situated within exon 42 of *PRPF8*, are associated with RP and presumably inhibit the interaction of the PRPF8 protein with Brr2. The only detected mutation in *PRPF8* outside exon 42 is p.S2118F, which was reported occurring in GC16352 (Towns et al., 2010). This non-conservative amino acid change is predicted to cause significant alteration to the structure and function of the PRPF8 protein.

The function of the C-terminal of PRPF8 protein has been investigated using various methods by different laboratories. Grainger and Beggs (Grainger and Beggs, 2005) suggested that the nine RP13 missense mutations reported in exon 42 of *PRPF8* affect seven very highly conserved amino acid residues indicating that those residues have a conserved function which is altered in case of mutation. Those nine amino acids belong to the region of yPrp8p that interacts with Brr2p, one of the spliceosomal RNA helicases, and is close to the *prp8–1* (G2347D) mutation, which ablates the binding of C-terminal yPrp8 peptides by yBrr2p in vitro (van Nues and Beggs, 2001). By yeast two-hybrid, Fan et al. (Fan et al., 2004) have demonstrated that C-terminal 94-amino acid region of hPRPF8 interacts with the multifunctional

plasminogen activator inhibitor type-2 protein (PAI-2). Therefore, it is reasonable to assume that the interaction PRPF8/PAI-2 could also be altered in RP13 patients.

Two different groups have established independently the crystal structure of PRPF8 (Reyes et al., 1999, Pena et al., 2007). Both groups proposed that the C-terminal domain of PRPF8 including the MPN (Mpr-1, Pad-1, N-terminal) domain is an interaction domain. They suggest that the reported residues mutated in RP13 constitute a binding surface between PRPF8 and other partner(s) and the disruption of this interaction provides a plausible molecular mechanism for RP13. It is notable that exon 38 encodes a part of the MPN domain of PRPF8 and S2118 is part of a α1 helix which may be altered by the mutation in the present report.

To conclude, this is the first report of marked intrafamilial variation and nonpenetrance associated with two *PRPF8* mutations: c.6353 C>T (p. S2118F) in exon 38 and c.6930G>C (p.R2310S) in exon 42. The data suggest that all exons of *PRPF8* should be screened in families with adRP and incomplete penetrance. The important role of electrophysiological assessment is noted. The findings extend the range of phenotypes seen in association with *PRPF8* gene mutations and provide important information to assist the management of families in whom this form of adRP is suspected.

3.4 EVALUATION OF THE PHENOTYPES OF RETINAL DYSTROPHIES CAUSED BY *DE NOVO* MUTATIONS

3.4.1 A DETAILED PHENOTYPIC DESCRIPTION OF AUTOSOMAL DOMINANT CONE DYSTROPHY DUE TO A DE NOVO MUTATION IN THE GUCY2D GENE

3.4.1.1 Introduction

The cone dystrophies and cone–rod dystrophies (CORD) are a heterogeneous group of progressive genetically determined retinal disorders, which may be inherited as an autosomal dominant, autosomal recessive, or X-linked trait (RetNet). They are characterised clinically by a loss of visual acuity, abnormal colour vision, photophobia, and visual field loss. Many will develop macular atrophy. Electroretinography demonstrates generalised cone system dysfunction with either no or mild rod system involvement (Michaelides et al., 2006). The gene 'Guanylate cyclase 2D, membrane (retina-specific)' (*GUCY2D*, MIM ID*600179) accounts for up to 35% of patients with autosomal dominant cone dystrophy or CORD (Kitiratschky et al., 2008, Payne et al., 2001, Hunt et al., 2010). It was also the first gene to be implicated in Leber's congenital amaurosis, a major cause of blindness in children (Perrault et al., 1996). The protein translated by *GUCY2D*, retinal guanylate cyclase 1, is expressed in both rod and cone photoreceptors (Yang et al., 1995). Two mutation sites in *GUCY2D*, the codons 575 and 838, have been reported to cause autosomal dominant cone dystrophy or CORD (Hunt et al., 2010, Small et al., 2008). The mutation p.V933A has also been described in *GUCY2D* in association with the phenotype of autosomal dominant central areolar choroidal

dystrophy, a condition similar to CORD (Hughes et al., 2012). The importance of identifying this condition is paramount as, using a gene therapy technique, a partial restoration of visual function has been demonstrated in *GUCY2D* knockout mouse model increasing the likelihood of eventual treatment in humans (Boye et al., 2010). The section describes a family with autosomal dominant cone dystrophy due to a de novo mutation in the codon 838 in the *GUCY2D* gene (Mukherjee et al., 2014).

3.4.1.2 Methods

All affected patients underwent clinical examination and imaging. Electrophysiological assessment was performed in the three affected patients using techniques that incorporated the ISCEV standards (McCulloch et al., 2015). Additional On–Off ERGs were performed using an orange stimulus (560 cd/m2, duration 200 ms) superimposed on a constant green background (150 cd/m2). S-cone ERGs were performed using a blue stimulus (445 nm, duration 5ms, 80 cd/m2) superimposed on a constant orange background (620nm, 560 cd/m2) (Arden et al., 1999).

3.4.1.3 Results

3.4.1.3.1 Molecular genetics

The *GUCY2D* gene was screened for disease-causing mutations using methods described above. The coding region and the intron–exon boundaries of 20 published exons (NM_000180.3) were amplified. Four microsatellite markers (D17S1828, D17S1876, D17S1791, and D17S799) were used to determine the haplotypes of a 9.4-Mb region in chromosome 17p surrounding the *GUCY2D* gene.

3.4.1.3.2 Clinical phenotype

The pedigree of the family is illustrated in Figure 3-37. The clinical data on the subjects are summarised in Table 3-13 and illustrated in Figure 3-36.

The earliest symptom experienced by the affected subjects was reduced central vision. The youngest subject (21-year old) noticed deterioration of her visual acuity at 11 years of age. There was a discordance in onset of symptoms in the monozygotic twins (44-year old) with III:3 noticing problems a decade earlier than III:2. Later in the disorder, photoaversion and a difficulty in colour vision developed. No subject reported nyctalopia.

The best-corrected visual acuity of subject IV:1 was 6/18 while vision was less than 6/60 in subjects III:2 and III:3. The reduction of vision in the right eye of subject II:1 was from an advanced cataract. He had undergone retinal reattachment surgery in his left eye. Visual acuity was normal in subject II:2. Colour vision (Ishihara) was very poor in subjects III:2, III:3, and IV:1.

Fundus examination of IV:1 showed mild pigmentary changes in the macula. The fundi of the monozygotic twins showed symmetrical well-demarcated perifoveal retinal thinning. The retina of the right eye of II:1 was difficult to examine due to dense cataract. The left eye showed peripapillary atrophy and an abnormal foveal reflex. Subject II:2 showed no abnormality on fundus examination.

FAF of IV:1 showed a small area of mild hypo-autofluorescence in the perifoveal region surrounded by a ring of hyperautofluorescence. Subjects III:2 and III:3 both show a larger central area of speckled hypo-autofluorescence, reflecting patchy atrophic changes in the retinal pigment epithelium (RPE), surrounded by a ring of increased autofluorescence. Subject II:2 had normal FAF. FAF could not be performed reliably in II:1 due to cataracts.

OCT was performed in subject IV:1, aged 21 years, and showed abrupt disruption of the inner–outer segment junction layer in the subfoveal photoreceptors. In her mother and aunt (III:2 and III:3), there is thinning of the inner retina with irregular disruption of photoreceptor–RPE complex. The junction between normal and abnormal outer retina corresponded to the hyper-autofluorescent ring referred to above. The OCT was within normal limits in II:2 and was not performed in II:1.

In one of the monozygotic twins III:2, the areas of speckled hypo-autofluorescence were 6.99 and 6.33mm^2 in the right and left eye, respectively, while in case of her twin sister the areas were 6.89 and 6.83mm^2 in the right and left eye, respectively.

Table 3-13: Clinical phenotype of the family with *GUCY2D* mutation. (BCVA – Best-corrected visual acuity, OD – Right eye, OS – Left eye, N/A – not available)

Subject ID	**Age**	**Onset**	**Earliest symptom**	**Current symptoms**	**BCVA**		**Refractive error**	**Colour vision - Ishihara**	**Fundus changes**
					OD	**OS**			
IV:1	21 years	11 years	Reduced central vision	Photoaversion	6/18	6/18	Myopia	0/17	Mild macular mottling
III:2	44 years	23 years	Reduced central vision	Photoaversion	2/60	3/60	None	0/17	Perifoveal retinal thinning
III:3	44 years	12 years	Reduced central vision	Loss of colour and central vision, Photoaversion	3/60	1/60	Myopia	0/17	Perifoveal retinal thinning
II:1	68 years	No symptoms	Never	None	2/60	6/18	Myopia	N/A	Peripapillary atrophy
II:2	65 years	No symptoms	Never	None	6/6	6/6	None	17/17	None

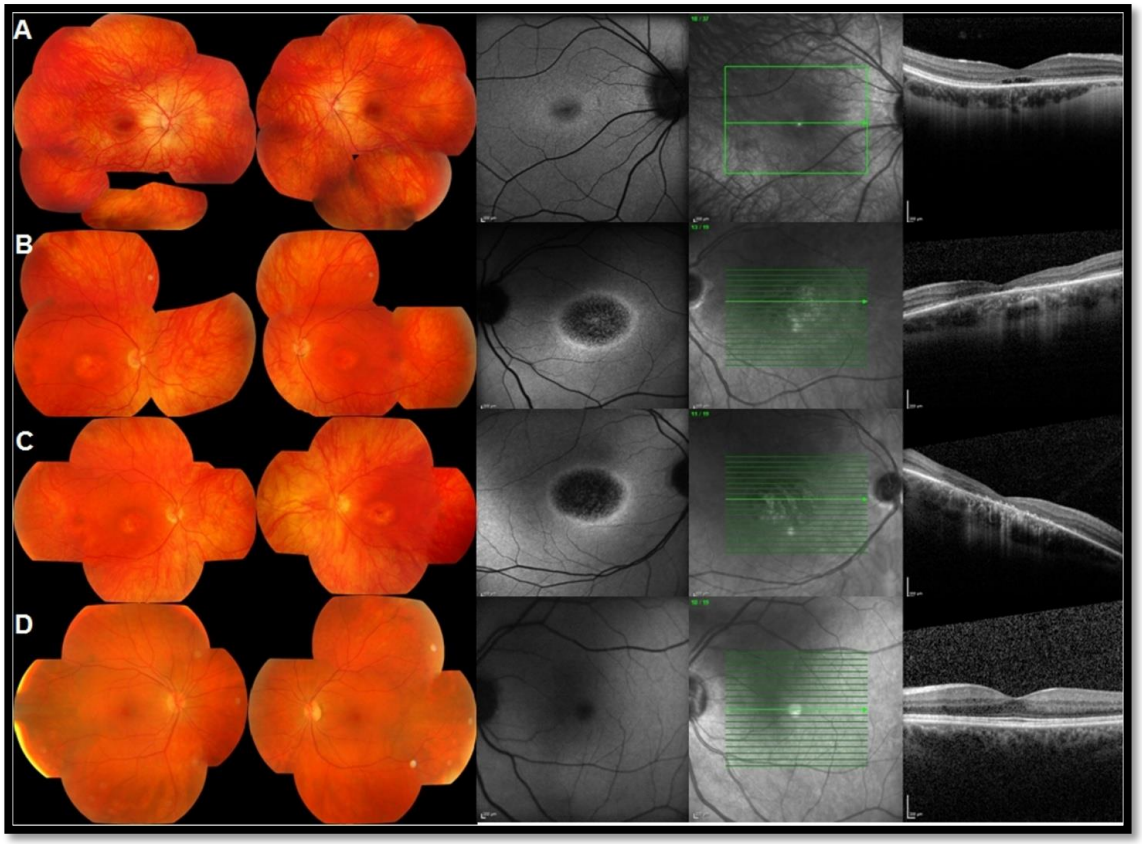

Figure 3-36: Phenotype of affected subjects IV:1 (A), III:2 (B), III:3 (C), and unaffected subject II:2 (D). The fundus photographs show central macular atrophy in III:2 and III:3 (44-year olds) and a normal macula in subjects IV:1 aged 21 years and II:2 (unaffected; 65 years old). FAF shows a hyper-autofluorescent ring surrounding the central macular atrophy in all the affected subjects. The OCT reveals absence of outer retinal layers in the central macula in III:2 and III:3 and absence of outer segments in the young IV:1.

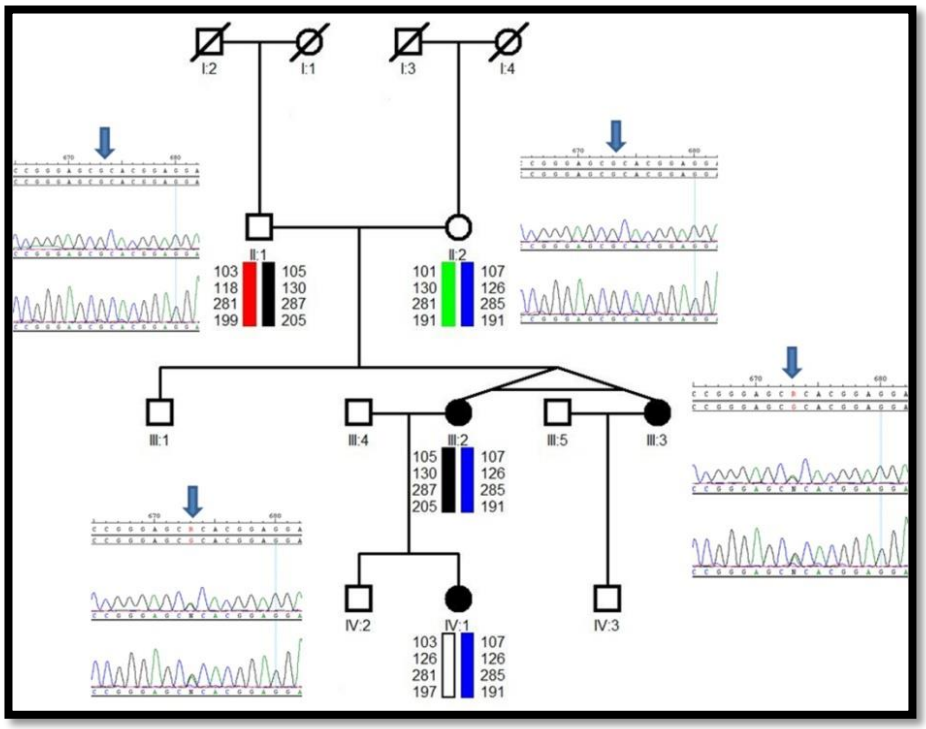

Figure 3-37: Pedigree of the family of cone dystrophy with p.R838H mutation in *GUCY2D*. The electropherograms demonstrating the gene sequence in forward and reverse are demonstrated. The chromosomes of individuals are demonstrated using microsatellite markers and are coded.

The b-wave amplitudes of photopic cone ERG in III:2 was 65% on the right and 75% on the left eye in comparison to the lower limit of normal while the amplitudes were 68 and 72% of the lower limit of normal on the right and left eye, respectively, in her monozygotic twin III:3.

3.4.1.3.3 Functional phenotype

Dark-adapted full-field ERGs (DA 0.01, DA11.0) were normal in III:2, III:3, and IV:1, in keeping with preserved rod system function (Figure 2a). Photopic 30Hz flicker ERGs (LA 3.0 30Hz) showed mild delay (1–4 ms above the upper limit of normal) and amplitude reduction. Single flash

cone ERGs (LA 3.0 2Hz) showed borderline delay with a subnormal b-wave:a-wave ratio in all subjects, suggesting generalised system dysfunction at an inner retinal level. This was confirmed by On–Off ERGs, which showed electronegative On-responses (reduced b-waves); Off-response d-waves were of borderline timing and, although of normal amplitude, showed an abnormal positive 'plateau' following the d-wave. S-cone ERGs were markedly subnormal. Pattern ERGs were undetectable in all the three cases in keeping with severe macular involvement.

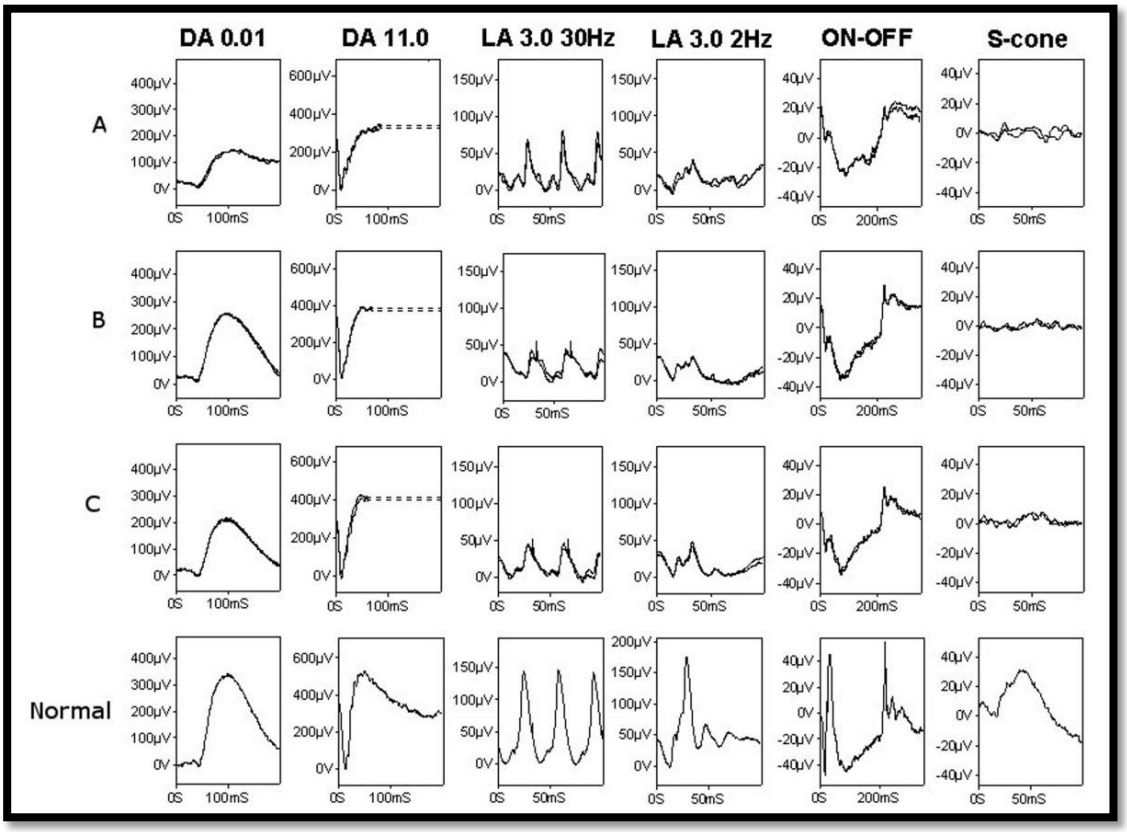

Figure 3-38: Full-field electroretinograms (ERGs) from one eye of subjects IV:1 (A), III:2 (B) and III:3 (C) and representative normal traces (bottom row).

3.4.1.3.4 Molecular genetics

Sanger sequencing of the *GUCY2D* gene was performed in all the five subjects. Three out of the five (IV:1, III:2, and III:3) carried heterozygous mutation c.2513G>A p.R838H. The parents (II:1 and II:2) did not carry the mutation. Microsatellite markers surrounding the *GUCY2D* gene showed that the mutation segregated with the markers derived from the mother (II:2) (Figure 3-37).

3.4.1.4 Discussion

This section describes the detailed phenotype of patients suffering from autosomal dominant cone dystrophy consequent upon a *de novo* mutation in *GUCY2D*, reports the first *de novo* mutation in the gene, compares the phenotype in the monozygotic twins, and expands our knowledge of the clinical, electrophysiological, and psychophysical phenotypes of the disorder. Onset of the disease as evidenced by a decrease in the visual acuity was variable between early teens to early twenties. There was relative concordance among the monozygotic twins when the areas of speckled hypofluorescence and the b-wave amplitudes of the photopic cone ERG were compared. However, there was a discordance of onset between the two monozygotic twins of more than a decade although the final visual acuity was similar at 44 years of age. Similar variability in the age on onset has been described in patients with CORD consequent upon *GUCY2D* mutations (Gregory-Evans et al., 2000, Smith et al., 2007, Downes et al., 2001, Ito et al., 2004). All three affected patients in our family had generalised cone dysfunction with severe macular involvement, but unlike the majority of previous cases, (Ito et al., 2004, Downes et al.,

2001, Smith et al., 2007, Gregory-Evans et al., 2000) there was no ERG evidence of rod system dysfunction. The possibility that rod dysfunction will develop later in life cannot be excluded, but there is no evidence of scotopic ERG reduction with increasing age in this small cohort. An electronegative dark-adapted ERG (b:a ratio < 1.0) has been reported in *GUCY2D* CORD, (Gregory-Evans et al., 2000) but in our family, only the light-adapted ERG had a low b:a ratio. The combination of a flicker ERG delay, an electronegative On- response and the unusual shape of the Off-ERG waveform distinguishes these cases from those with autosomal dominant cone dystrophy due to *GUCA1A* mutation, often associated with a reduced cone ERG of normal timing with subnormal On- and Off- ERG components (Downes et al., 2001). The latter study speculated that these abnormalities could result from impaired transduction kinetics, but there is also evidence of weak RetGC expression in the outer plexiform layer (Liu et al., 1994) and histological evidence of synaptic disruption in cases of CORD (Gregory-Evans et al., 1998). Generalised cone dysfunction was accompanied by perifoveal photoreceptor–RPE disruption in the monozygotic twins. This structural loss of the central cones may result from the high cone density.

In the phototransduction cascade, exposure to a photon results in a decrease in the photoreceptor intracellular Ca^{2+} concentration. This is because light leads to sequential isomerisation of rhodopsin and activation of transducin and phosphodiesterase (PDE). PDE hydrolyses cGMP closing cGMP-gated cation channels ceasing the calcium influx. RetGC-1, the protein translated by *GUCY2D* is involved in the regeneration of cGMP in the photoreceptors. This is achieved in response to lowering of Ca^{2+} concentration under the influence of guanylate cyclase activating proteins (GCAP). The mutation in this report, p.R838H, is believed to cause a gain

of function increasing the affinity of RetGC-1 for GCAP even in high Ca^{2+} concentrations (Wilkie et al., 2000). The cone photoreceptor death in this disorder is believed to be caused by the high cGMP concentration keeping cGMPgated cation channels open, resulting in increased Ca^{2+} concentration in the cell (Tucker et al., 1999). Decreasing the cGMP concentration may be therapeutic for these individuals. This can potentially be achieved by increasing photopic exposure of the photoreceptors resulting in stimulation of PDE (Liu et al., 2009) or can be directly achieved by administration of PDE agonists. Interestingly, PDE6C recessive mutations abrogating the PDE function have been described to cause a phenotype of early-onset cone photoreceptor dystrophy (Thiadens et al., 2009).

Haplotype analysis of our family confirmed a *de novo* mutation in *GUCY2D* transmitted from the unaffected mother. However, *de novo* mutations more commonly derive from the paternal germline (Ellegren, 2007). Ascertainment of a family showing a *de novo* mutation in any inherited disease affects the counselling advice given to a person presenting with the disorder. The diagnosis of the disorder in an individual without a family history would usually suggest a recessive inheritance. The recurrence risk to future siblings in such a pedigree is extremely low but might occur if the *de novo* mutation involved the parent's germ-cells, the so called germline mosaicism. Given the findings in this family, the possibility of *a de novo* mutation causing a dominant allele in *GUCY2D* needs to be considered as this would dramatically change the risks of recurrence in children from a population risk to 50%. The prevalence of families presenting this way is not known but will become clearer with the implementation of high-throughput sequencing. Alternatively, in cone dystrophy, specific tests for dominant alleles in *GUCY2D* and/or *GUCA1A*

should be considered when seeking a molecular diagnosis even in the absence of a family history.

To conclude, this report expands and refines the phenotypic description of patients with the cone dystrophy associated with mutations in *GUCY2D* gene. The existence of a *de novo* germline mutation herein described should alert the physician to its possibility in a family with cone dystrophy and has implications for counselling.

3.4.2 DE NOVO AND GERMLINE MUTATIONS IN CHM CAUSING CHOROIDEREMIA

3.4.2.1 Introduction

Choroideremia, is an X-linked retinal dystrophy predominantly affecting men with early onset night blindness, progressive visual field loss and eventual loss of central vision (Sorsby et al., 1952). Although variable in onset and progression (Renner et al., 2006), this disorder presents with mid-peripheral mottling of retinal pigment epithelium (RPE) which leads to patchy atrophy of RPE and choroid. The atrophy usually progresses both peripherally and centrally until it involves the fovea.

The gene *CHM* (MIM *300390), translates Rab escort protein (REP-1), a protein involved in post-translational modification of Rab GTPases, which are regulators of phagosome function and vesicular trafficking (Preising and Ayuso, 2004, Seabra et al., 2002). Among the mutations reported in *CHM,* all but two (p.L550P (Sergeev et al., 2009) and p.H507R (Esposito et al., 2011)) cause premature truncation of the protein resulting in the

affected hemizygous males to lack REP-1 function (MacDonald et al., 1998). The mutation p.L550P causes destabilisation of the tertiary structure of the REP-1 protein (Sergeev et al., 2009) while p.H507R results in the generation of functionally inactive variant (Esposito et al., 2011) effectively causing a deficiency in REP-1 activity.

In this section, three families are described where choroideremia is caused by a *de novo* germline mutation in *CHM* in females with normal phenotype. This report makes it even more important to confirm the carrier status in a mother of an affected male prior to genetic counselling advice.

3.4.2.2 Methods

Three families were ascertained from the inherited eye disease clinic of Moorfields eye hospital (MEH). All three affected males and their unaffected mothers underwent complete ophthalmic examination and imaging. PCR and Sanger sequencing of the coding region and intron-exon boundaries of the fifteen published exons of *CHM* (NM_000390.2) was performed. Multiplex ligation-dependent probe analysis (MLPA) was performed to detect large deletions or insertions in the *CHM, RP2* and *RPGR* genes on the X-chromosome. Four microsatellite markers (DXS1216, DXS986, DXS1196 and DXS8077) were used to determine the haplotypes spanning approximately 2.7 Mb region on Chromosome Xq surrounding *CHM*.

Splice site prediction tools, Automated splice site analysis (Nalla and Rogan, 2005), Human splicing finder version 2.4.1 (Desmet et al., 2009), NetGene 2 (Brunak et al., 1991) and NNSPLICE 0.9 (Reese et al., 1997) were used to identify the effects of the intronic nucleotide substitutions

3.4.2.3 Results

3.4.2.3.1 Clinical phenotype

The clinical features of the affected individuals are illustrated in Figure 3-39 and described in Table 3-14.

The affected males of the three families presented with an early symptom of night blindness which manifested between 6 to 15 years of age. All the patients complained of visual field loss. None of the patients had significant general medical disorders. Pedigree analysis of all three families showed no other affected relatives (Figure 3-40).

The best-corrected Snellen visual acuities of all patients ranged from 6/6 to 6/9. Slit-lamp examination revealed normal anterior segments with intraocular pressures within normal range. Dilated fundoscopy showed variable amount of atrophy in the mid-peripheral retina with sparing of central macula in both eyes (Figure 3-39). The areas of atrophy became more clearly delineated and increased in size with age. There were variable amounts of intra-retinal pigmentation. In all cases, the optic discs were pink in colour and the retinal blood vessels retained normal calibre.

Autofluorescence imaging delineated the areas of preserved retina in the central macula (Figure 3-39). Optical coherence tomography of both eyes showed preserved retina and choroid in the areas of retained autofluorescence while the areas of atrophy showed complete absence of outer layers of the retina and severe thinning of the choroid (Figure 3-39).

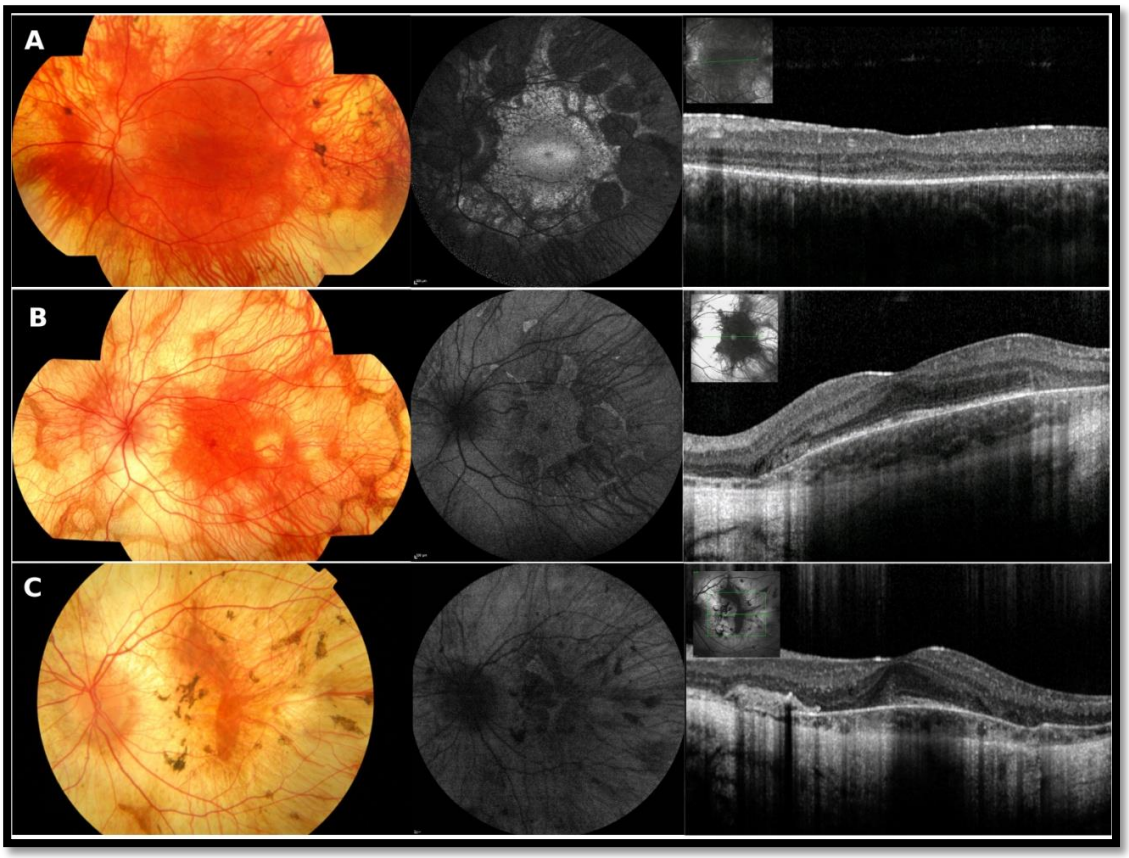

Figure 3-39: Clinical characteristics of the affected males with *de novo CHM* mutations. In all cases, the fundus photographs, FAF images and OCT scans of the left eyes are demonstrated. Panel A: V:1, GC18470; Panel B: IV:5, GC15975; Panel C: IV:2, GC15155. The fundus photographs clearly delineate the areas of extensive chororioretinal atrophy. In the FAF images, the areas of atrophy are shown as dark regions which surround a central area of perimacular sparing. In the areas of normal autofluorescence, OCT shows normal retinal morphology while in other areas there is extensive atrophy and some tubule formation.

Table 3-14: Clinical features of the affected patients with choroideremia.

Subject ID	**Mutation**	**Age**	**Age of onset**	**Earliest symptom**	**Other symptoms**	**BCVA**		**Fundus changes**
						OD	**OS**	
V:1 – GC18470	c.49+3_49+16 delins GCTTCCTGGTG CTTCCTGGAC	21 years	15 years	Night blindness	Peripheral visual field loss	6/9	6/12	Mid-peripheral patchy chorioretinal atrophy. Intra-retinal pigment
IV:5 – GC15975	c.1-?_1413+?del	18 years	6 years	Night blindness	Peripheral visual field loss	6/6	6/6	Mid-peripheral patchy chorioretinal atrophy. Minor intra-retinal pigment
IV:2 – GC15155	c.941-2 A>G	31 years	10 years	Night blindness	Peripheral visual field loss	6/6	6/6	Large areas of chorioretinal atrophy. Minor intra-retinal pigment

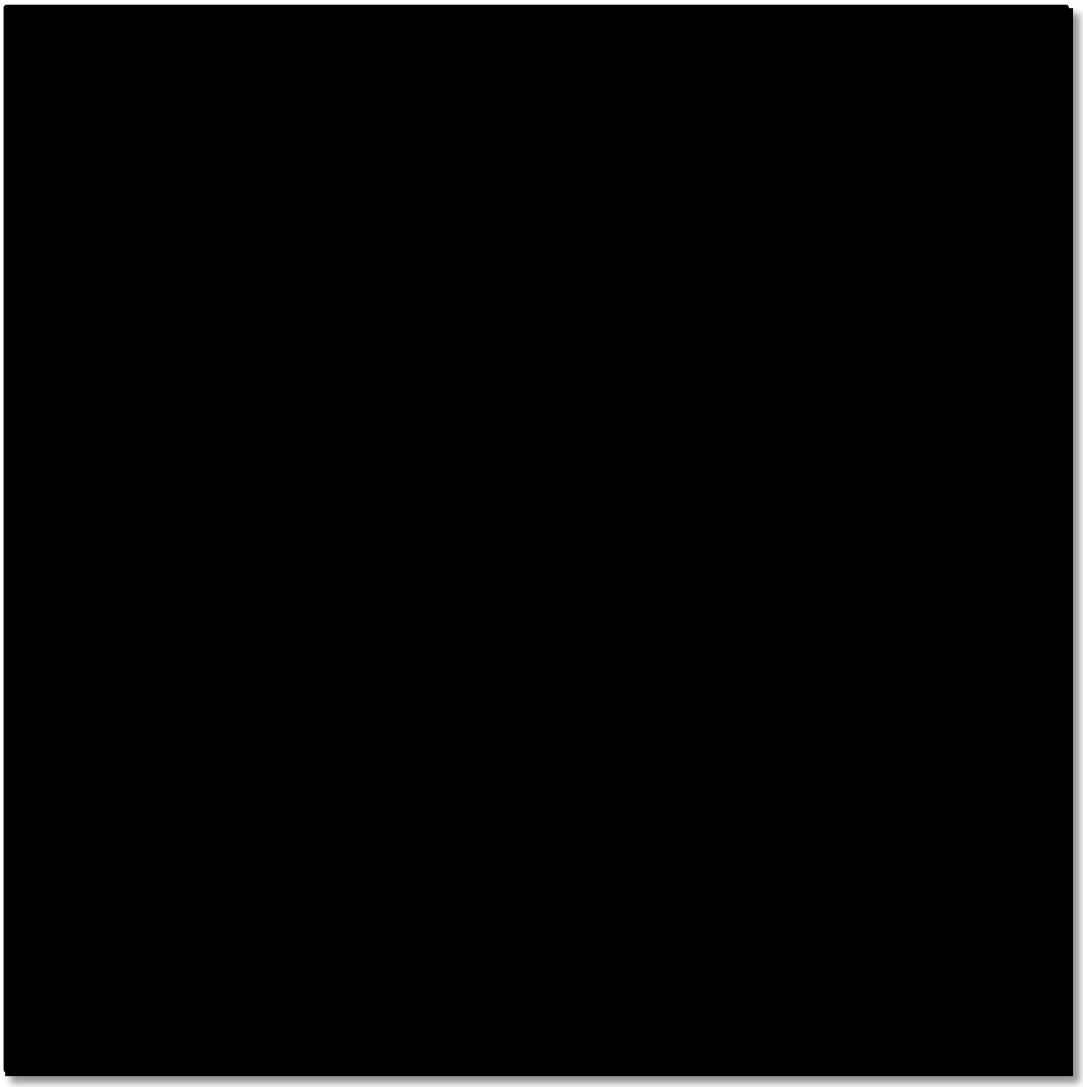

Figure 3-40: The pedigrees of the three *CHM* families. In two families, alleles identified on microsatellite analysis are demonstrated by the bars

Choroideremia was diagnosed in the affected males on the basis of the clinical observations. The asymptomatic mothers of the probands had no significant ocular or medical history. Ophthalmic examination showed normal anterior and posterior segments with no evidence of carrier signs of choroideremia. A detailed family history showed the presence of many ostensibly unaffected male relatives (Figure 3-40) with either a 1 in 2, or 1 in 4 prior risk of being affected.

3.4.2.3.2 Molecular genetics

Bi-directional Sanger sequencing of *CHM* in DNA derived from leukocytes of the proband and the mother showed the mutations shown in Table 3-14. In all three families, the mother was homozygous for the wild-type sequence. In-silico analysis of the intronic mutations predicted disruption of the splice sites.

Haplotype analysis using four microsatellite markers surrounding *CHM* was performed in two families as illustrated in Figure 3-40. In both cases maternity was confirmed. These data strongly suggest the occurrence of the *CHM* mutation *de novo* in the mother, including the cell producing the gamete of the affected son. Analysis of the unaffected brother (IV:1) of the proband of family 15155 showed the wild type *CHM* allele, and inheritance of the other maternal X chromosome to that of his brother.

3.4.2.4 Discussion

In this section, three families showing *de novo* mutations in *CHM* causing choroideremia are presented. This significant incidence of *de novo* mutations in *CHM* makes it important to genetically screen the mother of the affected male. Absence of the mutation in the female significantly alters the risk of having another affected male child from 50% to negligible.

In our cohort of 52 families with genetically confirmed choroideremia, 3 families presented with *de novo* mutations in females with no clinical signs. Our report suggests the incidence of a *de novo* mutation in *CHM* to be 5.77% in the British cohort. The first suggestion of a *de novo* mutation in

CHM was reported in one patient in a screen of 35 patients (2.8%) (van den Hurk et al., 2003). This implies large screens of *CHM* should identify more cases of *de novo* mutations.

Recent studies have suggested a prevalence of between 28-49 *de novo* germline mutations per meiosis in humans (Roach et al., 2010, Durbin et al., 2010). *de novo* germline mutations are more common in paternal germ cells presumably due to the greater number of cell divisions prior to gametogenesis of sperm compared to ova (Ellegren, 2007). In this respect, these families are unusual in there being a maternal origin of the *de novo* mutation.

Deleterious mutations usually decrease the biological fitness of the trait resulting in negative selection. One of the mechanisms of maintenance of the disorder in the population is high frequency of *de novo* mutations. Although rare *de novo* mutations have been described in retinal dystrophies (Gehrig et al., 1999, Schwartz et al., 2003, Chang et al., 2007), these are mainly in the regions of mutational hotspots of the respective genes. In our families, the mutations are novel and are distributed along the whole gene (Table 3-14).

Description of a *de novo* mutation in any inherited disease affects the counselling advice given to families. The diagnosis of the disorder in a male, would usually suggest a 1 in 2 prior risk to brothers, and the same risk of carrier status to sisters. Given the findings in these families, the possibility of a *de novo* mutation has to be considered, particularly if there is no clear maternal history of affected males, and if the mother is unavailable for examination for carrier signs. Moreover, when young, female carrier signs can be subtle and difficult to interpret. This report makes it more important to confirm carrier status in the mother of an affected male prior to genetic counselling advice.

3.5 A PHENOTYPIC DESCRIPTION OF PATIENTS WITH MONO-ALLELIC MUTATIONS IN THE *RPE65* GENE

3.5.1 INTRODUCTION

Retinal dystrophies are a group of inherited disorders characterised by impairment in retinal function. Mutations in the visual cycle genes are responsible for a significant proportion of these disorders. One such gene is *RPE65*, mutations in which are associated with three distinct phenotypes. The phenotype first associated with bi-allelic mutations in *RPE65*, was that of Leber's congenital amaurosis (LCA) (Marlhens et al., 1997, Gu et al., 1997). Since, patients with phenotype similar to LCA have been observed with *RPE65* mutations. These patients presented in infancy, frequently suffered from nystagmus, night blindness and a tendency to fixate on light (Thompson et al., 2000). Fundus examination showed pale retina with retinal pigment epithelium (RPE) atrophy in the periphery. Rod electroretinograms (ERGs) were undetectable and cone ERGs were extinguished late in the first decade. However, unlike classic description by Theodore Leber in 1869 (Leber, 1869), many of these patients retained useful vision until the second decade of their lives (Walia et al., 2010). These patients have been documented variously as juvenile and early-onset retinitis pigmentosa (Foxman et al., 1985, Lorenz et al., 2000), childhood-onset severe retinal dystrophy (Gu et al., 1997), early onset severe retinal dystrophy (Lorenz et al., 2000), and severe early childhood onset retinal dystrophy (Weleber et al., 2011).

The second phenotype described recently was that of fundus albipunctatus (Schatz et al., 2011). The only subject described had compound heterozygous mutations in *RPE65*. She was night blind from birth, had

relatively good visual acuity at 18-years of age and had scattered homogeneous yellow-white dots in the outer retina.

The third distinct phenotype associated with a mono-allelic mutation was identified in an Irish family (Bowne et al., 2011). These patients presented in 2nd to 5th decade with impaired dark adaptation. Although there was variability within the family, the severely affected individuals exhibited extensive diffuse chorioretinal atrophy and variable intra-retinal pigmentation.

In this section, two families with dominant *RPE65* mutation have been described where two distinct phenotypes are expressed, one of which has never been associated with *RPE65*.

3.5.2 METHODS

Patients underwent detailed ophthalmic examination and imaging. Electrophysiological assessments were performed according to ISCEV standards. Sanger sequencing of the coding region and intron-exon boundaries of the published exons of the *RPE65* gene was undertaken.

3.5.3 RESULTS

Two families GC11527 and GC16236 were included in the study. Molecular analysis of the *RPE65* gene in both the families identified the same c.1430A>G, p.Asp477Gly mutation.

3.5.3.1 GC11527:

The pedigree of the family is illustrated in Figure 3-41.

Figure 3-41: Pedigrees of *RPE65* families – A: GC11527, B: GC16236

3/5 affected individuals in the family were phenotyped. The proband, subject III:1 presented at 36-years-age with a distortion of reading vision in the left eye. His best-corrected-visual acuities were 6/5 in the right eye and 6/9 in the left eye. Patchy chorioretinal atrophy and intraretinal pigmentation were observed on fundoscopy. Goldmann kinetic visual fields were full in both eyes. At 50-years-age, he complained of night blindness and significant reduction in visual field. At 71-years-age, the subject's best-corrected visual acuities were hand movements in the right eye and 6/48 in the left eye. Retinal examination revealed extensive chorioretinal atrophy involving large parts of retina in both eyes. Autofluorescence imaging and OCT examination showed extensive atrophy of the retina and the choroid in both eyes. He had retained a small part of his mid-peripheral visual field in his left eye.

His deceased mother, subject II:1 was phenotyped at 87-years-age. Her presenting symptom was decreased reading vision at 45 years of age. She had hand movements vision in the right eye and perception of light vision in the left eye. Ophthalmic examination showed extensive chorioretinal atrophy involving large parts of her retina in both eyes.

Examination of subject III:3 showed a completely different phenotype. He presented with distortion of reading vision at 46-years-age. On dilated fundoscopy, a yellowish-white sub-retinal deposit was observed in his fovea bilaterally. On fundus autofluorescence imaging, the deposit was markedly hyper-autofluorescent. On OCT examination, there was a distinct hyper-reflective dome-shaped sub-retinal lesion in both eyes. Subject II:2 was asymptomatic and could not be phenotyped.

The DNA of the proband, subject III:1 was analysed for mutations in the *C1QTNF5*, the *PRPH2* and the *CHM* gene which failed to detect any pathogenic mutations. Molecular analysis of the *RPE65* gene identified p.Asp477Gly mutation in all the symptomatic individuals as well as asymptomatic subject II:2. The subject III:3 was also screened for mutations in the *PRPH2* gene which did not reveal any pathogenic mutations.

3.5.3.2 GC16236:

The pedigree of the family is illustrated in Figure 3-41. The proband, subject III:1, presented with difficulty in reading at 33-years-age. At the time his best-corrected visual acuities were 6/36 in the right eye and 6/18 in the left eye. Retinal examination showed presence of patchy chorioretinal atrophy in both eyes. He developed night vision difficulties at

38-years-age while his visual acuities worsened with time. At 46 years of age, his best-corrected visual acuities were hand movements in both eyes. Fundoscopy showed extensive chorio-retinal atrophy in both eyes involving the fovea. OCT examination and fluorescein angiography demonstrated the same areas of atrophy. Electrophysiology at 33-years-age showed severely abnormal rod-specific ERG, delayed and subnormal cone function and markedly subnormal pattern ERG. EOG light rise was abolished.

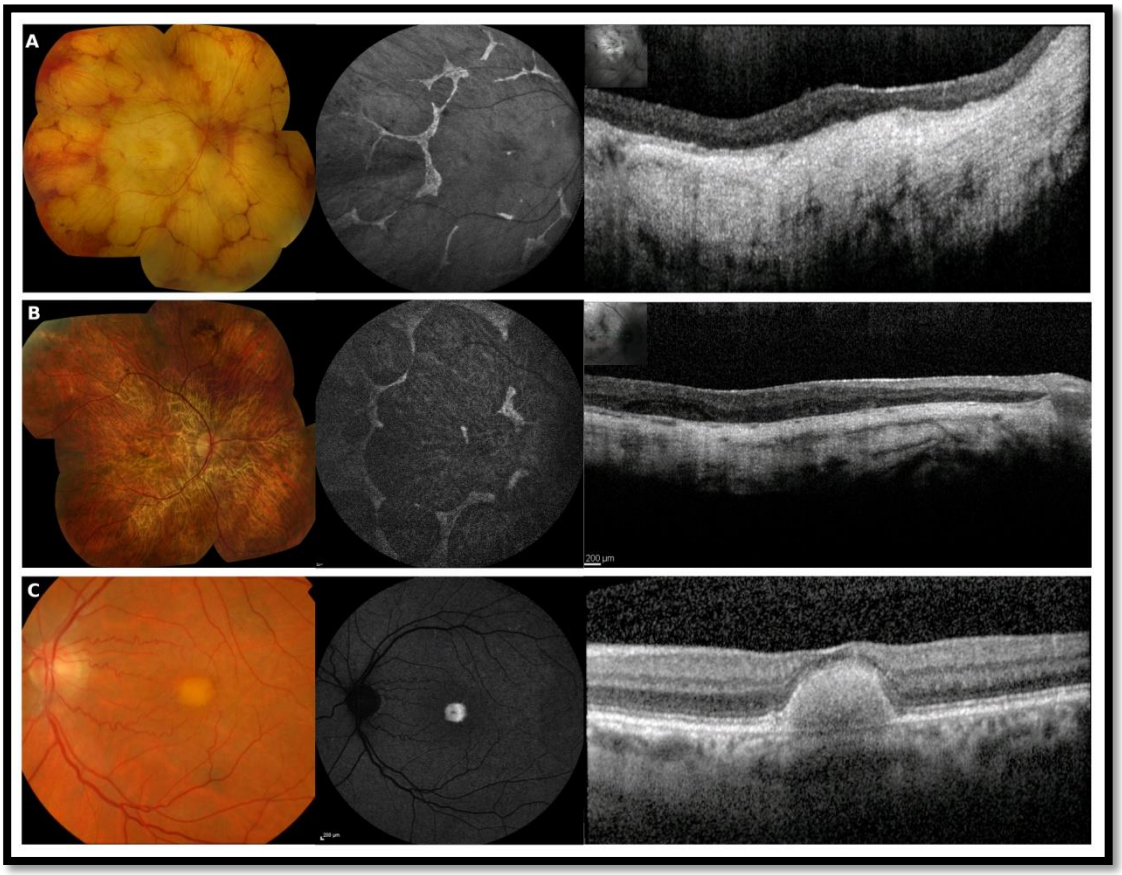

Figure 3-42: Variability in the phenotypes of patients with p.D477G mutation in the *RPE65* gene. A – Patient III:1 of GC11527 and B – Patient III:1 of GC16236 showing similar phenotype of extensive chorioretinal atrophy. C- Patient III:3 of GC11527 showing a much milder phenotype of adult-vitelliform macular dystrophy

Subject II:1 was examined once at 74-years-age before her demise. At the time, her best-corrected visual acuities were 6/60 right eye and 6/24 left eye. She presented with loss of central vision in her thirties although developed night blindness later. Retinal examination showed extensive chorioretinal atrophy and large loss of visual fields with preservation of some mid-peripheral areas.

3.5.4 DISCUSSION

This section explores and further expands the phenotype of dominant-acting p.Asp477Gly mutation in the *RPE65* gene. It associates the phenotype of adult-onset vitelliform macular dystrophy with this mutation for the first time.

The presenting symptom in all of the affected individuals of both families was difficulty in near vision between 33-46 years of age. Although all the individuals eventually became symptomatic of night vision abnormalities, none of them presented with night blindness as the presenting symptom. Subject II:2 of family 11527 carried the mutation and felt asymptomatic from history although he was not available for phenotyping. Similar phenomenon of non-penetrance has been described in the individual #47 of the original Irish family (Bowne et al., 2011).

The individual III:3 of family 11527 carrying a mutation in the *RPE65* gene expressed a phenotype of adult-onset vitelliform macular dystrophy. This has not been observed before. This phenotype is associated with mutations in the *PRPH2* gene in 15-20% of cases (Felbor et al., 1997, Meunier et al., 2011). Recently, mutations in *IMPG1* gene has been observed in some families with adult-onset vitelliform macular dystrophy

(Manes et al., 2013). It is established that genetic heterogeneity underlies this phenotype (Sohocki et al., 1997) and thus, we speculate that *RPE65* mutations could be responsible for at least some of these patients.

4 GENERAL DISCUSSION

Retinal dystrophies are a group of widely-varied retinal pathologies which are linked by the common mechanism of inherited genetic defects. Among the sub-group of retinitis pigmentosa (RP), characterised by rod photoreceptor demise preceding the cone photoreceptor death, Mendelian modes of inheritance are the predominant routes of disease transmission. In general, autosomal dominant (ad) inheritance pattern contributes to about 30-40% of the disease load of RP (Hartong et al., 2006). This study concentrated on studying the inherited retinal dystrophies transmitted by the autosomal dominant route.

Data was collected on phenotypes of retinitis pigmentosa caused by several different genes (Section 3.1) while the phenotypic variability was explored on disease caused by *RP1*, *PRPF8*, *GUCY2D* and *RPE65* genes (Sections 3.2-3.5). Families with novel and *de novo* mutations were identified (Sections 3.1, 3.2 and 3.4) and new phenotype was associated with the *RPE65* gene (Section 3.5). In several families with retinitis pigmentosa, asymptomatic patients were identified (Sections 3.2, 3.3 and 3.5) suggesting the non-penetrance which had implications on the genetic counselling of these families.

The theme underpinning this thesis is the demonstration of extreme phenotypic variability within disorders having the same molecular diagnosis. This has been demonstrated in each sections of the Result chapter with identification of non-penetrance and new phenotypes. At the time of writing of this thesis, no clear explanations have been put forward to explain this phenomenon. Several hypotheses can be examined. From

the geneticist's point of view, there can be several molecular mechanisms which govern the expression of a phenotype. The genes, mutations in which cause the disease do not work in isolation. They function in synergy as well as against genes participant in similar or even the same pathway. This is evident in the splice factors which together form a spliceosome to effect the deletion of introns from the primary transcript. It is conceivable that splice factors influence the expression of each other governing the final phenotype. Similar explanations can be speculated regarding transcription factors and the genes forming the primary cilium. It is also possible that modifier genes are expressed which govern the final protein expression of several genes as a part of their function. Such genes may exist among the several thousand already discovered by Human Genome Project or may exist in the intronic and/or inter-genic regions of the human genome remaining to be identified. It has already been determined that differential expression of the wild-type allele results in an all-or-none disease expression in *PRPF31* retinitis pigmentosa. It is feasible that similar differential expression of the wild-type alleles is one to the factors of the phenotypic variability.

The role of the environment in determining the final disease phenotype has been suggested previously. It is well known that photopic damage of the posterior pole of the retina accelerates the disease process of retinal dystrophies. Lack of anti-oxidants in the diet and smoking show clear link with progression of the disease phenotype. Hence, it is feasible that environment plays a major role in the variability shown in the disease expression. It is likely that a single factor is not responsible for all the variability shown. It is probable that a combination of environmental and genetic influences shape the final disease outcome.

Currently, the molecular diagnosis of about 70% of the families with adRP can be determined in the known genes following a combination of several methods, some of which are expensive and time consuming (Daiger et al., 2014). Section 3.1 showed the usage of one particular algorithm to try and elucidate the genetic causes of a large cohort of families with 63.8% accuracy. This method is considerably quicker and less expensive. This algorithm could be used as a screening tool to eliminate the commonly implicated genes so that resources can be concentrated on the families with no molecular diagnosis. One disadvantage of the method followed in this study is the inability to identify mutations in regions of the gene not considered as hot-spots. This has been shown to be the case in one family with *PRPF8* mutation (Section 3.3).

Detailed phenotyping on patients with *RP1* retinitis pigmentosa helped in characterising the natural history of the disease. Although this was limited by the cross-sectional nature of the study, survival analysis was attempted to increase the plausibility of the conclusions drawn. This had direct impact on patient care as more informed advice could be given to the affected families in the clinic.

Approach to identifying the molecular diagnosis in autosomal dominant disease is limited by the mono-allelic nature of the pathogenesis. The uncertainty on the causality of an amino acid substitution was partially answered in this study using bioinformatic techniques (Section 3.1). The true identification of a mutation can only be achieved using functional studies. One of the limitations of this study is that most of the missense changes identified have not been functionally assessed. This makes it uncertain although plausible to characterise the changes as true mutations.

Identification of the molecular diagnosis in an autosomal dominant family requires usage of linkage strategies even with the prevalence and widespread acceptance of next-generation sequencing. Although whole genome or whole exome sequencing is a significant advance over PCR based strategies, it is vitally important to identify the affected individuals in a pedigree underlying the importance of phenotyping. With the usage and relentless advances in imaging techniques, patients identified as hitherto unaffected may be discovered to carry mutations. As there is expansion of phenotypes associated with a single gene defect (Section 3.5), new mechanisms of disease are being identified and need exploring. It is likely that in future, current phenotype-based nomenclature of the disease would have to be replaced by genotype-based description.

Molecular diagnosis is rapidly becoming important not only into rare monogenetic disorders but also into disorders following non-Mendelian patterns of inheritance. There is a definite expansion of knowledge and interest into susceptibility factors for common disorders like age-related macular degeneration and diabetes. The gap between the laboratory and the clinic has become considerably narrow with increasing knowledge of the influence of genes in most chronic diseases.

As we understand the pathogenesis of the disorders where molecular diagnosis play a major role either by being directly causative or by increasing susceptibility, opportunities for novel therapies like gene supplementation become available. Novel approaches to treating autosomal dominant conditions like repairing mRNA transcript of the defective allele or gene augmentation have been attempted with variable degrees of success (Berger et al., 2015, Lewin et al., 2014, Rossmiller et al., 2012). In this era of exciting new therapies, obtaining a definitive molecular diagnosis has become imperative.

Currently, there is a rapid advancement and consequent explosion in phenotyping, genotyping and functional analytical techniques. Thus, it is inevitable that clinical medicine of the future will be transformed by the influences of genetics and genomics. The holy grail of "genomic medicine" is achievable although there is a need of substantial amount of clinical and basic laboratory research.

5 APPENDIX

Table 5-1: The list of genes screened and the mutations identified in our cohort.

Gene	Mutation	Number of families	Reference	Mutation type
RHO	c.344C>T, p.Thr17Met	2	(Dryja et al., 1991)	Missense
	c.116T>G, p.Met39Arg	5	(Davies et al., 2012)	Missense
	c.119T>G, p.Leu40Arg	1	(al-Maghtheh et al., 1994)	Missense
	c.165C>A, p.Asn55Lys	3	(Ramon et al., 2014)	Missense
	c.173C>G, p.Thr58Arg	6	(Dryja et al., 1990a)	Missense
	c.202_213delCTGCGCACGCCT, p.Leu68_Pro71del	1	(Keen et al., 1991)	In-frame deletion
	c.266G>A, p.Gly89Asp	2	(Sung et al., 1991)	Missense
	c.316G>A, p.Gly106Arg	5	(Inglehearn et al., 1992)	Missense
	c.328T>C, p.Cys110Arg	1	(To et al., 2000)	Missense
	c.403C>T, p.Arg135Trp	2	(Sung et al., 1991)	Missense

	c.511C>A, p.Pro171Thr	1	Novel	Missense
	c.512C>T, p.Pro171Leu	2	(Dryja et al., 1991)	Missense
	c.512C>G, p.Pro171Arg	1	Novel	Missense
	c.533A>G, p.Tyr178Cys	3	(Sung et al., 1991)	Missense
	c.541G>A, p.Glu181Lys	4	(Dryja et al., 1991)	Missense
	c.553T>C, p.Cys185Arg	1	(Liu et al., 2010)	Missense
	c.568G>A, p.Asp190Asn	3	(Dryja et al., 1991)	Missense
	c.632A>C, p.His211Pro	1	(Keen et al., 1991)	Missense
	c.763_765delATC, p.Ile256del	1	(Inglehearn et al., 1991)	In-frame deletion
	c.886A>G, p.Lys296Glu	3	(Keen et al., 1991)	Missense
	c.888G>C, p.Lys296Asn	2	(Sohocki et al., 2001)	Missense
	c.937-1 G>T	2	(Reig et al., 1996)	Splice site mutation
	c.1032G>A, p.Val345Met	2	(Dryja et al., 1991)	Missense
	c.1039C>T, p.Pro347Ser	1	(Dryja et al., 1990a)	Missense
	c.1040C>T, p.Pro347Leu	10	(Dryja et al., 1990b)	Missense
RP1	c.2017delA, p.Lys673Argfs*9	1	Novel	Nonsense

	c.2029C>T, p.Arg677*	19	(Pierce et al., 1999, Sullivan et al., 1999)	Nonsense
	c.2035C>T, p.Gln679*	3	(Berson et al., 2001, Sullivan et al., 1999)	Nonsense
	c.2055T>A, p.Tyr685*	1	Novel	Nonsense
	c.2098G>T, p.Glu700*	3	(Bowne et al., 1999)	Nonsense
	c.2115delA, p.Gly706Valfs*7	1	(Gamundi et al., 2006)	Nonsense
	c.2143C>T, p.Gln715*	1	Novel	Nonsense
	c.2168_2181delGAGGGATACTTTGT or c.2172_2185delGATACTTTGTGAGG, p.Ile725Argfs*6	11	(Payne et al., 2000)	Nonsense
	c.2205_2206insA, p.Thr736Asnfs*4	3	Novel	Nonsense
	c.2232C>A, p.Cys744*	1	(Payne et al., 2000)	Nonsense
	c.2285_2289delTAAAT, p.Leu762Tyrfs*17	2	(Payne et al., 2000)	Nonsense
	c.2596_2597delTT, p.Leu866Lysfs*7	8	Novel	Nonsense
	c.2607_2608insA, p.Arg872Thrfs*2	3	(Payne et al., 2000)	Nonsense
PRPF31	c.79G>T, p.Glu27*	1	(Waseem et al., 2007)	Nonsense
	c.202G>T, p.Glu68*	1	Novel	Nonsense

	c.238+2T>C	1	Novel	Splice site mutation
	c.412C>A, p.Thr138Lys	1	(Martinez-Gimeno et al., 2003)	Missense
	c.528 -3 to -45 del	1	(Vithana et al., 2001)	Splice site mutation
	c.527+1 G>T	1	(Chakarova et al., 2006)	Splice site mutation
	c.528-1 G>A	1	(Waseem et al., 2007)	Splice site mutation
	c.527+3 A>G	7	(Vithana et al., 2001)	Splice site mutation
	c.529C>T, p.Gln177*	1	Novel	Nonsense
	c.580_581 dup 33bp, p.Glu183_Met193dup	1	(Vithana et al., 2001)	In-frame insertion
	c.584T>A, p.Leu195Pro	1	Novel	Missense
	c.646G>A, p.Ala216Pro	1	(Vithana et al., 2001)	Missense
	c.808delC, p.His270Thrfs*51	1	Novel	Nonsense
	c.877delC, p.Arg293Glyfs*28	1	Novel	Nonsense

	c.973G>T, p.Glu325*	1	(Vithana et al., 2001)	Nonsense
	c.1087A>T, p.Lys363*	1	Novel	Nonsense
	c.1115_1125delGGAAGCAGGCC, p.Arg372Glnfs*99	1	(Vithana et al., 2001)	Nonsense
	c.1146+2 T>C	1	Novel	Splice site mutation
	30 kb del	1	(Abu-Safieh et al., 2006)	Nonsense
	112 kb del	1	(Rose et al., 2011)	Nonsense
PRPH2	c.136C>T, p.Arg46*	1	(Meins et al., 1993)	Nonsense
	c.356_358delGCT, p.Cys119del	1	(Farrar et al., 1991)	In-frame deletion
	c.618_626delGGACGGCGT, p.Asp207_V209del	1	(Kalyanasundaram et al., 2009)	In-frame deletion
	c.634A>G, p.Ser212Gly	1	(Farrar et al., 1992)	Missense
	c.646C>T, p.Pro216Ser	1	(Fishman et al., 1994)	Missense
	c.647C>T, p.Pro216Leu	1	(Kajiwara et al., 1991)	Missense
	c.653C>T, p.Ser218Leu	1	Novel	Missense
PRPF3	c.1482C>T, p.Thr494Met	3	(Chakarova et al., 2002)	Missense

PRPF8	c.6353C>T, p.Ser2118Phe	1	(Towns et al., 2010)	Missense
	c.6926A>C, p.His2309Pro	2	(McKie et al., 2001)	Missense
	c.6928A>G, p.Arg2310Gly	1	(McKie et al., 2001)	Missense
	c.6930G>C, p.Arg2310Ser	2	(Towns et al., 2010)	Missense
	c.6942C>A, p.Phe2314Leu	1	(McKie et al., 2001)	Missense
	c.7000T>A, p.Tyr2334Asn	1	(Towns et al., 2010)	Missense
IMPDH1	c.676G>A, p.Asp226Asn	1	(Bowne et al., 2002)	Missense
	c.680T>C, p.Leu227Pro	1	(Wada et al., 2005a)	Missense
	c.713A>G, p.Lys238Arg	2	(Wada et al., 2005b)	Missense
	c.928A>C, p.Thr310Pro	1	Novel	Missense
	c.952T>G, p.Tyr318Asp	1	Novel	Missense
	c.968A>G, p.Lys323Arg	1	Novel	Missense
NR2E3	c.166G>A, p.Gly56Arg	2	(Coppieters et al., 2007)	Missense
	c.170A>G, p.Lys57Arg	1	Novel	Missense
NRL	c.148T>A, p.Ser50Thr	2	(Bessant et al., 1999)	Missense
RP9	c.410A>T, p.His137Leu	3	(Keen et al., 2002)	Missense

Table 5-2: Clinical features of affected adRP patients with *RP1* mutations. Pt- Patient, FAF – Fundus autofluorescence, OCT – Optical Coherence Tomogram, CMO – Cystoid macular oedema, N/A – Not available, A/S - Asymptomatic

Family	Mutation	Pt	Onset	Age at diagnosis (years)	Follow up	Visual acuity	Fundus	FAF	Visual fields degree[2]	OCT	CMO
MCL903	p.Lys673 Argfs*9	1929	34 years	35	33 years	6/18 (OD), 6/12 (OS)	Extensive intra-retinal pigmentation and atrophy	Extensive hypo-autofluorescence involving the macula		Thinning of the retina and absence of photoreceptor layer	Absent
MCL903	p.Lys673 Argfs*9	28375	50 years	50	3 years	6/5 (OD), 6/5 (OS)	Moderate intra-retinal pigmentation mainly nasally	N/A		N/A	Absent
MCL903	p.Lys673 Argfs*9	28271		60	4 years	6/9 (OD), 6/9 (OS)	Moderate intra-retinal pigmentation	Hyper-autofluorescent ring	7434.28, 8465.13	Normal photoreceptor layer within the hyper-autofluorescent ring	Absent
MCL903	p.Lys673Ar gfs*9	28376		61	7 years	6/9 (OD), 6/9 (OS)	Moderate intra-retinal pigmentation	N/A	154.11, 30.52	N/A	Absent
C18881	p.Arg677*	29289	55 years	70	1 year	HM (OD), HM (OS)	Extensive intra-retinal pigmentation and atrophy	Patchy hypo-autofluorescence involving the macula		Disrupted photoreceptor layer	Absent
CG16126	p.Arg677*	22992	23 years	25	Single visit	6/6 (OD),	Little intra-retinal pigmentation	N/A		N/A	Absent

						6/5 (OS)					
CG16126	p.Arg677*	22993		54	Single visit	6/9 (OD), 6/12 (OS)	Very little intra-retinal pigmentation	N/A	13419.52, 13908.62	N/A	N/A
CG16126	p.Arg677*	25967	A/S	50	Single visit	6/9 (OD), 6/9 (OS)	Very little intra-retinal pigmentation	Normal posterior pole		N/A	Absent
DB2879	p.Arg677*	28026	A/S	60	Single visit	6/9 (OD), 6/12 (OS)	Very little intra-retinal pigmentation in the right eye unilaterally	Normal left eye. Hyper-autofluorescent ring in the right eye	12865.28, 16744.83	Normal posterior pole both eyes. Peripheral photoreceptor layer disrupted right eye	Absent
DB2879	p.Arg677*	28029		61	Single visit	6/5 (OD), 6/5 (OS)	Very little intra-retinal pigmentation	Normal posterior pole	11277.82, 10806.15	N/A	Absent
F17215	p.Arg677*	26394	A/S	34	1 year	6/5 (OD), 6/6 (OS)	Intra-retinal pigmentation in the nasal quadrant	N/A		N/A	Absent
F1841	p.Arg677*	1276		72	5 years	6/24 (OD), 6/36 (OS)	Moderate intra-retinal pigmentation	N/A		N/A	Absent
G3315	p.Arg677*	1381		52	7 years	6/6 (OD), 6/6 (OS)	Moderate intra-retinal pigmentation	N/A		N/A	Absent

							and patchy atrophy				
M1048	p.Arg677*	1938	15 years	56	Single visit	6/9 (OD), 6/12 (OS)	Moderate mid-peripheral intra-retinal pigmentation	N/A		N/A	Absent
PE3651	p.Arg677*	2305	42 years	57	17 years	6/9 (OD), 6/9 (OS)	Moderate intra-retinal pigmentation	Small hyper-autofluorescent ring		Normal photoreceptor layer within hyper-autofluorescent ring	Absent
PE3651	p.Arg677*	18792		37	5 years	6/18 (OD), 6/18 (OS)	Little intra-retinal pigmentation	N/A		Normal laminations in posterior pole	Present
R18036	p.Arg677*	27892	15 years	42	Single visit	6/9 (OD), 6/9 (OS)	Very little intra-retinal pigmentation	Normal posterior pole		N/A	Absent
RC14	p.Arg677*	15050		70	6 years	6/12 (OD), 6/60 (OS)	Very little intra-retinal pigmentation. Perifoveal atrophy	Poor		Thin retina	Absent
RC14	p.Arg677*	1	47 years	30	34 years	6/12 (OS)	Moderate mid-peripheral intra-retinal pigmentation	N/A	182.08	N/A	N/A
RC14	p.Arg677*	2		50	11 years			N/A		N/A	N/A

RC14	p.Arg677*	3	25 years	28	32 years	6/9 (OD), 6/12 (OS)	Moderate mid-peripheral intra-retinal pigmentation	N/A	26.39, 21.24	N/A	N/A
RC14	p.Arg677*	4		33	3 years			N/A		N/A	N/A
RC14	p.Arg677*	5		17	25 years			N/A		N/A	N/A
S1348	p.Arg677*	2733	28 years	37	23 years	6/12 (OD), 6/9 (OS)	Very little intra-retinal pigmentation	N/A		N/A	Absent
T19413	p.Arg677*	30119		38	Single visit	6/5 (OD), 6/5 (OS)	Little intra-retinal pigmentation	N/A		N/A	Absent
TW1890	p.Arg677*	2831	35 years	50	3 years	6/12 (OD), 6/12 (OS)	Very little intra-retinal pigmentation	N/A		N/A	Present
TW1890	p.Arg677*	22949	A/S	23	1 year		Normal looking fundus	N/A		N/A	Absent
TW1890	p.Arg677*	28971	31 years	30	1 year	6/6 (OD), 6/6 (OS)	Very little intra-retinal pigmentation in the infero-nasal quadrant	Normal posterior pole	12332.6, 13925.01	Normal posterior pole	Absent
W16317	p.Arg677*	23421		41	8 years	6/5 (OD), 6/5 (OS)	Moderate intra-retinal pigmentation, more nasally	Small hyper-autofluorescent ring		Normal photoreceptor layer within hyper-	Absent

										autofluorescent ring	
W18260	p.Arg677*	28228	23 years	26	12 years	6/6 (OD), 6/6 (OS)	Moderate intra-retinal pigmentation	N/A	262.71, 295.83	N/A	Absent
W18999	p.Arg677*	29473	45 years	46	2 years	6/6 (OD), 6/9 (OS)	Moderate intra-retinal pigmentation, mainly infero-nasally	Small hyper-autofluorescent ring in the posterior pole. Hyper-autofluorescent line outlining infero-nasal dystrophy		Normal photoreceptor layer within hyper-autofluorescent ring	Absent
WB27	p.Arg677*	20911	A/S	55	8 years	6/6 (OD), 6/6 (OS)	Intra-retinal pigmentation limited to nasal quadrants	Normal in posterior pole	9195.79, 10094.73	Normal posterior pole	Absent
WB27	p.Arg677*	3078	39 years	44	28 years	6/18 (OD), 6/18 (OS)	Little intra-retinal pigmentation	N/A		N/A	Absent
WB27	p.Arg677*	28991	A/S	40	Single visit	6/6 (OD), 6/5 (OS)	Very little intra-retinal pigmentation inferiorly	Infero-nasal hyper-autofluorescent line		Normal posterior pole	Absent
WB27	p.Arg677*	23370	A/S	36	Single visit	6/6 (OD), 6/6 (OS)	Moderate intra-retinal pigmentation in the nasal sector	N/A	12524.46, 11308.8, 15055.71, 15084.78	N/A	Absent

B15890	p.Gln679*	22578		33	8 years	6/9 (OD), 6/6 (OS)	Very little intra-retinal pigmentation	Normal posterior pole		Normal posterior pole	Absent
B3001	p.Gln679*	23877		26	3 years	6/5 (OD), 6/6 (OS)	Little intra-retinal pigmentation	Large hyper-autofluorescent ring		N/A	Absent
M18163	p.Gln679*	28084		46	Single visit	6/9 (OD), 6/9 (OS)	Little nummular intra-retinal pigmentation with patchy atrophy	Small hyper-autofluorescent		Normal photoreceptor layer within hyper-autofluorescent ring	Absent
MF15448	p.Tyr685*	21798	26 years	56	9 years	6/12 (OD), 6/12 (OS)	No intra-retinal pigmentation	Hyper-autofluorescent ring which later disappeared		Normal photoreceptor layer within the hyper-autofluorescent ring, Macular oedema	Present
MF15448	p.Tyr685*	23977		35	1 year	6/5 (OD), 6/5 (OS)	No intra-retinal pigmentation	Normal posterior pole	11869.88, 12745.86	Normal posterior pole	Absent
H16907	p.Glu700*	25890	45 years	69	5 years	6/12 (OD), 6/12 (OS)	Moderate intra-retinal pigmentation	Small hyper-autofluorescent ring		Normal photoreceptor layer within the ring	Present
SP45	p.Glu700*	2671	A/S	29	15 years	6/5 (OD), 6/5 (OS)	Very little intra-retinal pigmentation	Small hyper-autofluorescent ring	46.9, 58.32	N/A	Absent

SP45	p.Glu700*	2327	45 years	84	Single visit		Mild intra-retinal pigmentation	N/A		N/A	N/A
TA1154	p.Glu700*	10474		61	10 years	6/12 (OD), 6/12 (OS)	Moderate intra-retinal pigmentation and patchy atrophy	Small hyper-autofluorescent ring	22, 31.66	Normal photoreceptor layer within the hyper-autofluorescent ring	Absent
TA1154	p.Glu700*	14110		64	10 years	6/18 (OD), 6/12 (OS)	Moderate intra-retinal pigmentation and patchy atrophy	Small hyper-autofluorescent ring	1300.68, 1403.21	Disrupted photoreceptor layer within the posterior pole	Present
M18228	p.Gly706Valfs*7	28177	25 years	57	2 years	6/18 (OD), 6/18 (OS)	Extensive intra-retinal pigmentation	Patchy hypo-autofluorescence with small peri-foveal area of retained autofluorescence		Normal photoreceptor layer peri-foveally	Absent
H18297	p.Gln715*	28282	56 years	73	10 years	6/9 (OD), 6/18 (OS)	Moderate intra-retinal pigmentation	N/A	354.14, 57.93, 218.3, 161.2	N/A	Absent
B2481	p.Ile725Argfs*6	21051	15 years	66	10 years	6/30 (OD), 6/38 (OS)	Moderate intra-retinal pigmentation	Normal posterior pole	1742.64, 3237.61	N/A	Present
BO675	p.Ile725Argfs*6	756		70	1 year	6/6 (OD), 6/12 (OS)	Moderate intra-retinal pigmentation	N/A		N/A	Absent

BO675	p.Ile725Argfs*6	29588	51 years	53	Single visit	6/12 (OD), 6/9 (OS)	Moderate intra-retinal pigmentation	Hyper-autofluorescent ring, more prominent in the left eye		Photoreceptor layer preserved within the hyper-autofluorescent ring	Present
C17534	p.Ile725Argfs*6	26917	30 years	45	3 years	6/6 (OD), 6/9 (OS)	Very little intra-retinal pigmentation	Hyper-autofluorescent line in the peripheral macula		N/A	Absent
C932	p.Ile725Argfs*6	8694	26 years	28	33 years	3/60 (OD), HM (OS)	Very little intra-retinal pigmentation	Extensive hypo-autofluorescence involving the macula	3247.52, 1166.52	Disruption of the photoreceptor layer in the posterior pole	Absent
C932	p.Ile725Argfs*6	27438		31	3 years	6/24 (OD), 6/18 (OS)	Little intra-retinal pigmentation	Small hyper-autofluorescent ring		Normal photoreceptor layer within hyper-autofluorescent ring	Present
CS134	p.Ile725Argfs*6	22551	25 years	61	8 years	6/18 (OD), 6/36 (OS)	Moderate mid-peripheral intra-retinal pigmentation	N/A		N/A	Present
CS134	p.Ile725Argfs*6	910	22 years	25	25 years	6/6 (OD), 6/18 (OS)	Moderate mid-peripheral intra-retinal pigmentation	Small hyper-autofluorescent ring		Normal photoreceptor layer within hyper-autofluorescent ring	Present

CS134	p.Ile725Argfs*6	981	20 years	28	18 years	6/7.5 (OD), 3/38 (OS)	Moderate mid-peripheral intra-retinal pigmentation. Left macular atrophy	Small hyper-autofluorescent ring right eye. Macular hypo-autofluorescence left eye		Normal photoreceptor layer within hyper-autofluorescent ring right eye	Absent
CS134	p.Ile725Argfs*6	2569		70	7 years	6/18 (OD), 6/18 (OS)	Moderate mid-peripheral intra-retinal pigmentation	N/A	2067.57, 1275.59	Lamellar hole left eye. Normal photoreceptor layer in peri-foveal region	Absent
H17866	p.Ile725Argfs*6	27628	32 years	33	3 years	6/5 (OD), 6/5 (OS)	Normal central macular	Normal posterior pole		N/A	Absent
PKC3650	p.Ile725Argfs*6	2322	A/S	34	17 years	6/6 (OD), 6/6 (OS)	Moderate intra-retinal pigmentation infero-nasally	N/A	2051.45, 2670.86	N/A	Absent
PKC3650	p.Ile725Argfs*6	27551	35 years	38	18 years	6/7.5 (OD), 1/60 (OS)	Very little intra-retinal pigmentation	Extensive hypo-autofluorescence involving the macula		Disruption of the photoreceptor layer in the posterior pole	Absent
PKC3650	p.Ile725Argfs*6	1	45 years	47	3 years	6/9 (OD), 6/9 (OS)	Moderate intra-retinal pigmentation	N/A		N/A	Absent
PKC3650	p.Ile725Argfs*6	15236	31 years	62	4 years	6/6 (OD),	Little intra-retinal pigmentation	N/A		N/A	Absent

						6/6 (OS)	with marked pigment epithelial atrophy				
S17697	p.Ile725Argfs*6	27228	50 years	51	4 years	6/6 (OD), 6/6 (OS)	No intra-retinal pigmentation	N/A	7912.45, 7458.12	N/A	Absent
S4315	p.Ile725Argfs*6	27512	38 years	52	4 years	6/6 (OD), 6/6 (OS)	Little intra-retinal pigmentation with atrophic patches	Small hyper-autofluorescent ring		Normal photoreceptor layer within the hyper-autofluorescent ring.	Absent
S4315	p.Ile725Argfs*6	28284	29 years	27	4 years	6/9 (OD), 6/6 (OS)	No intra-retinal pigmentation	Hyper-autofluorescent line in the temporal periphery of left eye	4468.21, 3472.22	N/A	Absent
T1560	p.Ile725Argfs*6	2869	34 years	49	8 years	6/18 (OD), 6/12 (OS)	Moderate intra-retinal pigmentation	N/A		N/A	Absent
W139	p.Ile725Argfs*6	2923		66	8 years	6/12 (OD), 1/60 (OS)	Little mid-peripheral intra-retinal pigmentation. Extensive pigment epithelial atrophy	N/A		Disruption of the lamellar structure in the periphery. Interrupted photoreceptor layer in fovea	Present

P18453	p.Thr736Asnfs*4	28513	A/S	26	2 years	6/5 (OD), 6/5 (OS)	Very little intra-retinal pigmentation	Hyper-autofluorescent line outlining infero-nasal dystrophy		Normal posterior pole	Absent
P18591	p.Thr736Asnfs*4	28719	A/S	40	1 year	6/9 (OD), 6/9 (OS)	Little intra-retinal pigmentation limited to infero-nasal quadrant	Normal autofluorescence except infero-nasally		Normal posterior pole	Absent
P128	p.Cys744*	10002	15 years	57	3 years	6/9 (OD), 6/9 (OS)	Extensive intra-retinal pigmentation	N/A		N/A	N/A
P128	p.Cys744*	1	27 years	27	Single visit			N/A		N/A	N/A
D3543	p.Leu762Tyrfs*17	15750	26 years	54	6 years	6/60 (OD), HM (OS)	Moderate intra-retinal pigmentation	Extensive hypo-autofluorescence involving the macula		Disruption of the photoreceptor layer	Present
D3543	p.Leu762Tyrfs*17	1	35 years	35	2 years		No intra-retinal pigmentation	Normal posterior pole	13888.22, 15689.76	N/A	Absent
LP16218	p.Leu762Tyrfs*17	23241	72 years	73	3 years	6/9 (OD), 6/18 (OS)	Moderate mid-peripheral intra-retinal pigmentation	N/A		N/A	Absent
LP16218	p.Leu762Tyrfs*17	23240		47	8 years	6/12 (OD), 6/12 (OS)	Very little intra-retinal pigmentation	Broad hyper-autofluorescent ring	11602.01, 12753.52	Retention of photoreceptor layer within the hyper-	Present

										autofluorescent ring	
GW3902	p.Leu866Lysfs*7	10567	50 years	65	1 year	6/18 (OD), 6/9 (OS)	Extensive intra-retinal pigmentation	Small hyper-autofluorescent ring		N/A	Absent
GW3902	p.Leu866Lysfs*7	23752	30 years	31	6 years	6/9 (OD), 6/9 (OS)	Little intra-retinal pigmentation	Normal posterior pole		N/A	Absent
JC15253	p.Leu866Lysfs*7	21698		47	7 years	6/5 (OD), 6/6 (OS)	Little intra-retinal pigmentation infero-nasally	Normal posterior pole		N/A	Absent
JC15253	p.Leu866Lysfs*7	22067		74	Single visit	6/6 (OD), 6/6 (OS)	Little intra-retinal pigmentation infero-nasally	N/A		N/A	Absent
L5231	p.Leu866Lysfs*7	20978	40 years	81	9 years	HM (OD), HM (OS)	Extensive intra-retinal pigmentation and atrophy	N/A		N/A	Absent
N3837	p.Leu866Lysfs*7	2196		35	16 years	6/36 (OD), 6/12 (OS)	Moderate intra-retinal pigmentation	Centrally preserved autofluorescence		Peripheral disruption of layers	Present
N3837	p.Leu866Lysfs*7	2195	50 years	65	Single visit	6/9 (OD), 6/9 (OS)	Little intra-retinal pigmentation	N/A		N/A	Absent
R15153	p.Leu866Lysfs*7	21538		56	6 years	6/18 (OD),	Moderate intra-retinal pigmentation	Small hyper-autofluorescent ring	1791.18, 1372.1	N/A	Absent

						6/9 (OS)					
RK4589	p.Leu866Lysfs*7	10106		65	4 years	6/36 (OD), 6/24 (OS)	Extensive intra-retinal pigmentation and atrophy	Patchy hypo-autofluorescence in the posterior pole		Disruption of the laminations and photoreceptor layer	Absent
RK4589	p.Leu866Lysfs*7	28733	A/S	36	3 years	6/5 (OD), 6/5 (OS)	Little intra-retinal pigmentation in the nasal quadrant	Hyper-autofluorescent line outlining nasal dystrophy		Normal in posterior pole	Absent
RK4589	p.Leu866Lysfs*7	28849	A/S	28	3 years	6/5 (OD), 6/5 (OS)	Intra-retinal pigmentation in the nasal quadrant	Normal posterior pole		N/A	Absent
RK4589	p.Leu866Lysfs*7	1	A/S	37	Single visit	6/6 (OD), 6/6 (OS)	Intra-retinal pigmentation in the infero-nasal quadrants	Normal posterior pole		Normal posterior pole	Absent
SBM754	p.Leu866Lysfs*7	2677	50 years	50	14 years	6/12 (OD), 6/12 (OS)	Little mid-peripheral intra-retinal pigmentation	Distinct hyper-autofluorescent ring		Normal laminations and IS/OS junction within the ring	Absent
SBM754	p.Leu866Lysfs*7	28378	32 years	63	1 year	6/9 (OD), 6/9 (OS)	Moderate mid-peripheral intra-retinal pigmentation	N/A		Thin and without outer retinal laminations in periphery	Present
SBM754	p.Leu866Lysfs*7	28379	A/S	34	1 year	6/5 (OD),	No pigmentation	N/A		Normal	Absent

						6/5 (OS)					
SBM754	p.Leu866Lysfs*7	1	22 years	51	Single visit	6/9 (OD), 6/12 (OS)	Very little intra-retinal pigmentation. Peripheral atrophy	Small hyper-autofluorescent ring		Normal laminations within the ring, thinning outside	Absent
SBM754	p.Leu866Lysfs*7	2		52	Single visit		No pigmentation	Normal in the posterior pole		Normal in the posterior pole	Absent
SBM754	p.Leu866Lysfs*7	3	A/S	61	Single visit	6/5 (OD), 6/5 (OS)	Very little intra-retinal pigmentation	Hyper-autofluorescent line inferiorly		Normal in the posterior pole	Absent
B1438	p.Arg872Thrfs*2	679		66	1 year	6/12 (OD), 6/12 (OS)	Moderate intra-retinal pigmentation	N/A		N/A	Present
K16588	p.Arg872Thrfs*2	23911	39 years	42	10 years	6/12 (OD), 6/18 (OS)	Very little intra-retinal pigmentation	Broad hyper-autofluorescent ring	4604.58, 4038.3	Normal photoreceptor layer within hyper-autofluorescent ring	Present
R4301	p.Arg872Thrfs*2	24544		58	8 years	6/24 (OD), 6/18 (OS)	Little intra-retinal pigmentation, more in nasal quadrants	Small hyper-autofluorescent more evident in left eye		Disrupted photoreceptor layer in right eye. Normal photoreceptor layer within hyper-autofluorescent ring in left eye	Present

TW3662	p.Arg872Thrfs2	2812	28 years	28	17 years	6/5 (OD), 6/5 (OS)	Moderate intra-retinal pigmentation infero-nasally	Small hyper-autofluorescent ring		Normal photoreceptor layer within hyper-autofluorescent ring	Absent
TW3662	p.Arg872Thrfs*2	2933	A/S	52	Single visit	6/6 (OD), 6/6 (OS)	Intra-retinal pigmentation in infero-nasal sector	N/A	12425.6, 13003.3	N/A	N/A

6 REFERENCES

ABID, A., ISMAIL, M., MEHDI, S. Q. & KHALIQ, S. 2006. Identification of novel mutations in the SEMA4A gene associated with retinal degenerative diseases. *J Med Genet,* 43**,** 378-81.

ABU-SAFIEH, L., VITHANA, E. N., MANTEL, I., HOLDER, G. E., PELOSINI, L., BIRD, A. C. & BHATTACHARYA, S. S. 2006. A large deletion in the adRP gene PRPF31: evidence that haploinsufficiency is the cause of disease. *Mol Vis,* 12**,** 384-8.

ADAMS, N. A., AWADEIN, A. & TOMA, H. S. 2007. The retinal ciliopathies. *Ophthalmic Genet,* 28**,** 113-25.

ADZHUBEI, I. A., SCHMIDT, S., PESHKIN, L., RAMENSKY, V. E., GERASIMOVA, A., BORK, P., KONDRASHOV, A. S. & SUNYAEV, S. R. 2010. A method and server for predicting damaging missense mutations. *Nat Methods,* 7**,** 248-9.

AL-JANDAL, N., FARRAR, G. J., KIANG, A. S., HUMPHRIES, M. M., BANNON, N., FINDLAY, J. B., HUMPHRIES, P. & KENNA, P. F. 1999. A novel mutation within the rhodopsin gene (Thr-94-Ile) causing autosomal dominant congenital stationary night blindness. *Hum Mutat,* 13**,** 75-81.

AL-MAGHTHEH, M., INGLEHEARN, C., LUNT, P., JAY, M., BIRD, A. & BHATTACHARYA, S. 1994. Two new rhodopsin transversion mutations (L40R; M216K) in families with autosomal dominant retinitis pigmentosa. *Hum Mutat,* 3**,** 409-10.

AL-MAGHTHEH, M., VITHANA, E., TARTTELIN, E., JAY, M., EVANS, K., MOORE, T., BHATTACHARYA, S. & INGLEHEARN, C. F. 1996. Evidence for a major retinitis pigmentosa locus on 19q13.4 (RP11) and association with a unique bimodal expressivity phenotype. *Am J Hum Genet,* 59**,** 864-71.

ALDAHMESH, M. A., SAFIEH, L. A., ALKURAYA, H., AL-RAJHI, A., SHAMSELDIN, H., HASHEM, M., ALZAHRANI, F., KHAN, A. O., ALQAHTANI, F., RAHBEENI, Z., ALOWAIN, M., KHALAK, H., AL-HAZZAA, S., MEYER, B. F. & ALKURAYA, F. S. 2009. Molecular characterization of retinitis pigmentosa in Saudi Arabia. *Mol Vis,* 15**,** 2464-9.

ALEMAN, T. S., LAM, B. L., CIDECIYAN, A. V., SUMAROKA, A., WINDSOR, E. A., ROMAN, A. J., SCHWARTZ, S. B., STONE, E. M. & JACOBSON, S. G. 2009. Genetic heterogeneity in autosomal dominant retinitis pigmentosa with low-frequency damped electroretinographic wavelets. *Eye,* 23**,** 230-3.

ALI, S., KHAN, S. Y., NAEEM, M. A., KHAN, S. N., HUSNAIN, T., RIAZUDDIN, S., AYYAGARI, R., HEJTMANCIK, J. F. & RIAZUDDIN, S. A. 2015.

Phenotypic variability associated with the D226N allele of IMPDH1. *Ophthalmology,* 122**,** 429-31.

ALTSCHUL, S. F., MADDEN, T. L., SCHAFFER, A. A., ZHANG, J., ZHANG, Z., MILLER, W. & LIPMAN, D. J. 1997. Gapped BLAST and PSI-BLAST: a new generation of protein database search programs. *Nucleic Acids Res,* 25**,** 3389-402.

ALVAREZ, B. V., VITHANA, E. N., YANG, Z., KOH, A. H., YEUNG, K., YONG, V., SHANDRO, H. J., CHEN, Y., KOLATKAR, P., PALASINGAM, P., ZHANG, K., AUNG, T. & CASEY, J. R. 2007. Identification and characterization of a novel mutation in the carbonic anhydrase IV gene that causes retinitis pigmentosa. *Invest Ophthalmol Vis Sci,* 48**,** 3459-68.

ANTINOLO, G., SANCHEZ, B., BORREGO, S., RUEDA, T., CHAPARRO, P. & CABEZA, J. C. 1994. Identification of a new mutation at codon 171 of rhodopsin gene causing autosomal dominant retinitis pigmentosa. *Hum Mol Genet,* 3**,** 1421.

ARDEN, G., WOLF, J., BERNINGER, T., HOGG, C. R., TZEKOV, R. & HOLDER, G. E. 1999. S-cone ERGs elicited by a simple technique in normals and in tritanopes. *Vision Res,* 39**,** 641-50.

ARSHAVSKY, V. Y., LAMB, T. D. & PUGH, E. N., JR. 2002. G proteins and phototransduction. *Annu Rev Physiol,* 64**,** 153-87.

AUDO, I., BUJAKOWSKA, K., MOHAND-SAID, S., LANCELOT, M. E., MOSKOVA-DOUMANOVA, V., WASEEM, N. H., ANTONIO, A., SAHEL, J. A., BHATTACHARYA, S. S. & ZEITZ, C. 2010a. Prevalence and novelty of PRPF31 mutations in French autosomal dominant rod-cone dystrophy patients and a review of published reports. *BMC Med Genet,* 11**,** 145.

AUDO, I., FRIEDRICH, A., MOHAND-SAID, S., LANCELOT, M. E., ANTONIO, A., MOSKOVA-DOUMANOVA, V., POCH, O., BHATTACHARYA, S., SAHEL, J. A. & ZEITZ, C. 2010b. An Unusual Retinal Phenotype Associated With a Novel Mutation in RHO. *Arch Ophthalmol,* 128**,** 1036-45.

AUDO, I., MOHAND-SAID, S., DHAENENS, C. M., GERMAIN, A., ORHAN, E., ANTONIO, A., HAMEL, C., SAHEL, J. A., BHATTACHARYA, S. S. & ZEITZ, C. 2012. RP1 and autosomal dominant rod-cone dystrophy: Novel mutations, a review of published variants, and genotype-phenotype correlation. *Hum Mutat,* 33**,** 73-80.

AZAM, M., KHAN, M. I., GAL, A., HUSSAIN, A., SHAH, S. T., KHAN, M. S., SADEQUE, A., BOKHARI, H., COLLIN, R. W., ORTH, U., VAN GENDEREN, M. M., DEN HOLLANDER, A. I., CREMERS, F. P. & QAMAR, R. 2009. A homozygous p.Glu150Lys mutation in the opsin gene of two Pakistani families with autosomal recessive retinitis pigmentosa. *Mol Vis,* 15**,** 2526-34.

BACH, M., BRIGELL, M. G., HAWLINA, M., HOLDER, G. E., JOHNSON, M. A., MCCULLOCH, D. L., MEIGEN, T. & VISWANATHAN, S. 2013. ISCEV standard for clinical pattern electroretinography (PERG): 2012 update. *Documenta ophthalmologica. Advances in ophthalmology,* 126**,** 1-7.

BAINBRIDGE, J. W., SMITH, A. J., BARKER, S. S., ROBBIE, S., HENDERSON, R., BALAGGAN, K., VISWANATHAN, A., HOLDER, G. E., STOCKMAN, A., TYLER, N., PETERSEN-JONES, S., BHATTACHARYA, S. S., THRASHER, A. J., FITZKE, F. W., CARTER, B. J., RUBIN, G. S., MOORE, A. T. & ALI, R. R. 2008. Effect of gene therapy on visual function in Leber's congenital amaurosis. *New England Journal of Medicine,* 358**,** 2231-9.

BAIRATI, A. & ORZALESI, N. 1963. Ultrastructure of Pigment Epithelium and of Photoreceptor-Pigment Epithelium Junction in Human Retina. *Journal of Ultrastructure Research,* 9**,** 484-&.

BARALLE, F. 1977. Complete nucleotide sequence of the 5' noncoding region of human alpha-and beta-globin mRNA. *Cell,* 12**,** 1085-95.

BATESON, W. 1909. *Mendel's principles of heredity,* Cambridge, Cambridge University Press.

BAUM, L., CHAN, W. M., YEUNG, K. Y., LAM, D. S., KWOK, A. K. & PANG, C. P. 2001. RP1 in Chinese: Eight novel variants and evidence that truncation of the extreme C-terminal does not cause retinitis pigmentosa. *Hum Mutat,* 17**,** 436.

BENAGLIO, P., MCGEE, T. L., CAPELLI, L. P., HARPER, S., BERSON, E. L. & RIVOLTA, C. 2011. Next generation sequencing of pooled samples reveals new SNRNP200 mutations associated with retinitis pigmentosa. *Hum Mutat,* 32**,** E2246-58.

BERGER, A., LORAIN, S., JOSEPHINE, C., DESROSIERS, M., PECCATE, C., VOIT, T., GARCIA, L., SAHEL, J. A. & BEMELMANS, A. P. 2015. Repair of rhodopsin mRNA by spliceosome-mediated RNA trans-splicing: a new approach for autosomal dominant retinitis pigmentosa. *Molecular therapy : the journal of the American Society of Gene Therapy,* 23**,** 918-30.

BERSON, E. L., GRIMSBY, J. L., ADAMS, S. M., MCGEE, T. L., SWEKLO, E., PIERCE, E. A., SANDBERG, M. A. & DRYJA, T. P. 2001. Clinical features and mutations in patients with dominant retinitis pigmentosa-1 (RP1). *Invest Ophthalmol Vis Sci,* 42**,** 2217-24.

BESSANT, D. A., HOLDER, G. E., FITZKE, F. W., PAYNE, A. M., BHATTACHARYA, S. S. & BIRD, A. C. 2003. Phenotype of retinitis pigmentosa associated with the Ser50Thr mutation in the NRL gene. *Arch Ophthalmol,* 121**,** 793-802.

BESSANT, D. A., PAYNE, A. M., MITTON, K. P., WANG, Q. L., SWAIN, P. K., PLANT, C., BIRD, A. C., ZACK, D. J., SWAROOP, A. & BHATTACHARYA, S. S. 1999. A mutation in NRL is associated with autosomal dominant retinitis pigmentosa. *Nat Genet,* 21**,** 355-6.

BIANCHI, M., CRINELLI, R., SERAFINI, G., GIAMMARINI, C. & MAGNANI, M. 1997. Molecular bases of hexokinase deficiency. *Biochim Biophys Acta,* 1360**,** 211-21.

BLACQUE, O. E. & LEROUX, M. R. 2006. Bardet-Biedl syndrome: an emerging pathomechanism of intracellular transport. *Cell Mol Life Sci,* 63**,** 2145-61.

BONE, R. A., LANDRUM, J. T., FRIEDES, L. M., GOMEZ, C. M., KILBURN, M. D., MENENDEZ, E., VIDAL, I. & WANG, W. 1997. Distribution of lutein and zeaxanthin stereoisomers in the human retina. *Experimental eye research,* 64**,** 211-8.

BOON, C. J., DEN HOLLANDER, A. I., HOYNG, C. B., CREMERS, F. P., KLEVERING, B. J. & KEUNEN, J. E. 2008. The spectrum of retinal dystrophies caused by mutations in the peripherin/RDS gene. *Prog Retin Eye Res,* 27**,** 213-35.

BOWMAKER, J. K. & HUNT, D. M. 2006. Evolution of vertebrate visual pigments. *Curr Biol,* 16**,** R484-9.

BOWNE, S. J., DAIGER, S. P., HIMS, M. M., SOHOCKI, M. M., MALONE, K. A., MCKIE, A. B., HECKENLIVELY, J. R., BIRCH, D. G., INGLEHEARN, C. F., BHATTACHARYA, S. S., BIRD, A. & SULLIVAN, L. S. 1999. Mutations in the RP1 gene causing autosomal dominant retinitis pigmentosa. *Hum Mol Genet,* 8**,** 2121-8.

BOWNE, S. J., HUMPHRIES, M. M., SULLIVAN, L. S., KENNA, P. F., TAM, L. C., KIANG, A. S., CAMPBELL, M., WEINSTOCK, G. M., KOBOLDT, D. C., DING, L., FULTON, R. S., SODERGREN, E. J., ALLMAN, D., MILLINGTON-WARD, S., PALFI, A., MCKEE, A., BLANTON, S. H., SLIFER, S., KONIDARI, I., FARRAR, G. J., DAIGER, S. P. & HUMPHRIES, P. 2011. A dominant mutation in RPE65 identified by whole-exome sequencing causes retinitis pigmentosa with choroidal involvement. *European journal of human genetics : EJHG*.

BOWNE, S. J., LIU, Q., SULLIVAN, L. S., ZHU, J., SPELLICY, C. J., RICKMAN, C. B., PIERCE, E. A. & DAIGER, S. P. 2006a. Why do mutations in the ubiquitously expressed housekeeping gene IMPDH1 cause retina-specific photoreceptor degeneration? *Invest Ophthalmol Vis Sci,* 47**,** 3754-65.

BOWNE, S. J., SULLIVAN, L. S., BLANTON, S. H., CEPKO, C. L., BLACKSHAW, S., BIRCH, D. G., HUGHBANKS-WHEATON, D., HECKENLIVELY, J. R. & DAIGER, S. P. 2002. Mutations in the inosine monophosphate dehydrogenase 1 gene (IMPDH1) cause the RP10 form of autosomal dominant retinitis pigmentosa. *Hum Mol Genet,* 11**,** 559-68.

BOWNE, S. J., SULLIVAN, L. S., GIRE, A. I., BIRCH, D. G., HUGHBANKS-WHEATON, D., HECKENLIVELY, J. R. & DAIGER, S. P. 2008. Mutations in the TOPORS gene cause 1% of autosomal dominant retinitis pigmentosa. *Mol Vis,* 14**,** 922-7.

BOWNE, S. J., SULLIVAN, L. S., MORTIMER, S. E., HEDSTROM, L., ZHU, J., SPELLICY, C. J., GIRE, A. I., HUGHBANKS-WHEATON, D., BIRCH, D. G., LEWIS, R. A., HECKENLIVELY, J. R. & DAIGER, S. P. 2006b. Spectrum and frequency of mutations in IMPDH1 associated with autosomal dominant retinitis pigmentosa and leber congenital amaurosis. *Invest Ophthalmol Vis Sci,* 47**,** 34-42.

BOYE, S. E., BOYE, S. L., PANG, J., RYALS, R., EVERHART, D., UMINO, Y., NEELEY, A. W., BESHARSE, J., BARLOW, R. & HAUSWIRTH, W. W.

2010. Functional and behavioral restoration of vision by gene therapy in the guanylate cyclase-1 (GC1) knockout mouse. *PLoS One,* 5**,** e11306.

BREDHOLT, G., STORSTEIN, A., HAUGEN, M., KROSSNES, B. K., HUSEBYE, E., KNAPPSKOG, P. & VEDELER, C. A. 2006. Detection of autoantibodies to the BTB-kelch protein KLHL7 in cancer sera. *Scand J Immunol,* 64**,** 325-35.

BROMAN, K. W., MURRAY, J. C., SHEFFIELD, V. C., WHITE, R. L. & WEBER, J. L. 1998. Comprehensive human genetic maps: individual and sex-specific variation in recombination. *Am J Hum Genet,* 63**,** 861-9.

BRUNAK, S., ENGELBRECHT, J. & KNUDSEN, S. 1991. Prediction of human mRNA donor and acceptor sites from the DNA sequence. *J Mol Biol,* 220**,** 49-65.

BUNKER, C. H., BERSON, E. L., BROMLEY, W. C., HAYES, R. P. & RODERICK, T. H. 1984. Prevalence of retinitis pigmentosa in Maine. *Am J Ophthalmol,* 97**,** 357-65.

BURGESS, R., MILLAR, I. D., LEROY, B. P., URQUHART, J. E., FEARON, I. M., DE BAERE, E., BROWN, P. D., ROBSON, A. G., WRIGHT, G. A., KESTELYN, P., HOLDER, G. E., WEBSTER, A. R., MANSON, F. D. & BLACK, G. C. 2008. Biallelic mutation of BEST1 causes a distinct retinopathy in humans. *Am J Hum Genet,* 82**,** 19-31.

CARROLL, J., DUBRA, A., GARDNER, J. C., MIZRAHI-MEISSONNIER, L., COOPER, R. F., DUBIS, A. M., NORDGREN, R., GENEAD, M., CONNOR, T. B., JR., STEPIEN, K. E., SHARON, D., HUNT, D. M., BANIN, E., HARDCASTLE, A. J., MOORE, A. T., WILLIAMS, D. R., FISHMAN, G., NEITZ, J., NEITZ, M. & MICHAELIDES, M. 2012. The effect of cone opsin mutations on retinal structure and the integrity of the photoreceptor mosaic. *Investigative ophthalmology & visual science,* 53**,** 8006-15.

CHAKAROVA, C. F., CHERNINKOVA, S., TOURNEV, I., WASEEM, N., KANEVA, R., JORDANOVA, A., VERAITCH, B. K., GILL, B., COLCLOUGH, T., NAKOVA, A., OSCAR, A., MIHAYLOVA, V., NIKOLOVA-HILL, A., WRIGHT, A. F., BLACK, G. C., RAMSDEN, S., KREMENSKY, I. & BHATTACHARYA, S. S. 2006. Molecular genetics of retinitis pigmentosa in two Romani (Gypsy) families. *Mol Vis,* 12**,** 909-14.

CHAKAROVA, C. F., HIMS, M. M., BOLZ, H., ABU-SAFIEH, L., PATEL, R. J., PAPAIOANNOU, M. G., INGLEHEARN, C. F., KEEN, T. J., WILLIS, C., MOORE, A. T., ROSENBERG, T., WEBSTER, A. R., BIRD, A. C., GAL, A., HUNT, D., VITHANA, E. N. & BHATTACHARYA, S. S. 2002. Mutations in HPRP3, a third member of pre-mRNA splicing factor genes, implicated in autosomal dominant retinitis pigmentosa. *Hum Mol Genet,* 11**,** 87-92.

CHAKAROVA, C. F., KHANNA, H., SHAH, A. Z., PATIL, S. B., SEDMAK, T., MURGA-ZAMALLOA, C. A., PAPAIOANNOU, M. G., NAGEL-WOLFRUM, K., LOPEZ, I., MUNRO, P., CHEETHAM, M., KOENEKOOP, R. K., RIOS, R. M., MATTER, K., WOLFRUM, U., SWAROOP, A. & BHATTACHARYA,

S. S. 2011. TOPORS, implicated in retinal degeneration, is a cilia-centrosomal protein. *Hum Mol Genet,* 20**,** 975-87.

CHAKAROVA, C. F., PAPAIOANNOU, M. G., KHANNA, H., LOPEZ, I., WASEEM, N., SHAH, A., THEIS, T., FRIEDMAN, J., MAUBARET, C., BUJAKOWSKA, K., VERAITCH, B., ABD EL-AZIZ, M. M., PRESCOTT DE, Q., PARAPURAM, S. K., BICKMORE, W. A., MUNRO, P. M., GAL, A., HAMEL, C. P., MARIGO, V., PONTING, C. P., WISSINGER, B., ZRENNER, E., MATTER, K., SWAROOP, A., KOENEKOOP, R. K. & BHATTACHARYA, S. S. 2007. Mutations in TOPORS cause autosomal dominant retinitis pigmentosa with perivascular retinal pigment epithelium atrophy. *Am J Hum Genet,* 81**,** 1098-103.

CHANG, W., DING, Q., TANG, Z., LIU, P., JIANG, F., KE, T., REN, X., WANG, Z., LIU, J., WANG, Q. K. & LIU, M. 2007. A novel de novo frameshift mutation of RPGR ORF15 is associated with X-linked retinitis pigmentosa in a Chinese family. *Mol Vis,* 13**,** 1548-54.

CHEN, L. J., LAI, T. Y., TAM, P. O., CHIANG, S. W., ZHANG, X., LAM, S., LAI, R. Y., LAM, D. S. & PANG, C. P. 2010. Compound heterozygosity of two novel truncation mutations in RP1 causing autosomal recessive retinitis pigmentosa. *Invest Ophthalmol Vis Sci,* 51**,** 2236-42.

CHEN, X., LIU, Y., SHENG, X., TAM, P. O., ZHAO, K., RONG, W., LIU, X., PAN, X., CHEN, L. J., ZHAO, Q., VOLLRATH, D., PANG, C. P. & ZHAO, C. 2014. PRPF4 mutations cause autosomal dominant retinitis pigmentosa. *Hum Mol Genet,* 23**,** 2926-39.

CHENG, H., KHANNA, H., OH, E. C., HICKS, D., MITTON, K. P. & SWAROOP, A. 2004. Photoreceptor-specific nuclear receptor NR2E3 functions as a transcriptional activator in rod photoreceptors. *Hum Mol Genet,* 13**,** 1563-75.

CHU, D., KAKAZU, N., GORRIN-RIVAS, M. J., LU, H. P., KAWATA, M., ABE, T., UEDA, K. & ADACHI, Y. 2001. Cloning and characterization of LUN, a novel ring finger protein that is highly expressed in lung and specifically binds to a palindromic sequence. *J Biol Chem,* 276**,** 14004-13.

CIDECIYAN, A. V., ALEMAN, T. S., BOYE, S. L., SCHWARTZ, S. B., KAUSHAL, S., ROMAN, A. J., PANG, J. J., SUMAROKA, A., WINDSOR, E. A., WILSON, J. M., FLOTTE, T. R., FISHMAN, G. A., HEON, E., STONE, E. M., BYRNE, B. J., JACOBSON, S. G. & HAUSWIRTH, W. W. 2008. Human gene therapy for RPE65 isomerase deficiency activates the retinoid cycle of vision but with slow rod kinetics. *Proc Natl Acad Sci U S A,* 105**,** 15112-7.

CIDECIYAN, A. V., HOOD, D. C., HUANG, Y., BANIN, E., LI, Z. Y., STONE, E. M., MILAM, A. H. & JACOBSON, S. G. 1998. Disease sequence from mutant rhodopsin allele to rod and cone photoreceptor degeneration in man. *Proc Natl Acad Sci U S A,* 95**,** 7103-8.

CLANCY, S. 2008. RNA splicing: introns, exons and spliceosome. *Nature Education,* 1.

COLLART, F. R. & HUBERMAN, E. 1988. Cloning and sequence analysis of the human and Chinese hamster inosine-5'-monophosphate dehydrogenase cDNAs. *J Biol Chem,* 263**,** 15769-72.

CONNELL, G., BASCOM, R., MOLDAY, L., REID, D., MCINNES, R. R. & MOLDAY, R. S. 1991. Photoreceptor peripherin is the normal product of the gene responsible for retinal degeneration in the rds mouse. *Proc Natl Acad Sci U S A,* 88**,** 723-6.

COOLEN, M., SII-FELICE, K., BRONCHAIN, O., MAZABRAUD, A., BOURRAT, F., RETAUX, S., FELDER-SCHMITTBUHL, M. P., MAZAN, S. & PLOUHINEC, J. L. 2005. Phylogenomic analysis and expression patterns of large Maf genes in Xenopus tropicalis provide new insights into the functional evolution of the gene family in osteichthyans. *Development genes and evolution,* 215**,** 327-39.

COPPIETERS, F., LEROY, B. P., BEYSEN, D., HELLEMANS, J., DE BOSSCHER, K., HAEGEMAN, G., ROBBERECHT, K., WUYTS, W., COUCKE, P. J. & DE BAERE, E. 2007. Recurrent mutation in the first zinc finger of the orphan nuclear receptor NR2E3 causes autosomal dominant retinitis pigmentosa. *Am J Hum Genet,* 81**,** 147-57.

CORRENS, G. C. 1900. Regel über das Verhalten der Nachkommenschaft der Rassenbastarde. *Berichte der Deutschen Botanischen Gesellschaft,* 18.

CRICK, F. 1970. Central dogma of molecular biology. *Nature,* 227**,** 561-3.

CRICK, F. H. 1958. On protein synthesis. *Symposia of the Society for Experimental Biology,* 12**,** 138-63.

DAIGER, S. P., BOWNE, S. J. & SULLIVAN, L. S. 2007. Perspective on genes and mutations causing retinitis pigmentosa. *Arch Ophthalmol,* 125**,** 151-8.

DAIGER, S. P., BOWNE, S. J., SULLIVAN, L. S., BLANTON, S. H., WEINSTOCK, G. M., KOBOLDT, D. C., FULTON, R. S., LARSEN, D., HUMPHRIES, P., HUMPHRIES, M. M., PIERCE, E. A., CHEN, R. & LI, Y. 2014. Application of next-generation sequencing to identify genes and mutations causing autosomal dominant retinitis pigmentosa (adRP). *Adv Exp Med Biol,* 801**,** 123-9.

DAIGER, S. P., ROSSITER, B. J. F., GREENBERG, J., CHRISTOFFELS, A. & HIDE, W. 1998. Data services and software for identifying genes and mutations causing retinal degeneration. *Invest. Ophthalmol. Vis. Sci.,* 39**,** S295.

DAIGER, S. P., SULLIVAN, L. S., BOWNE, S. J., BIRCH, D. G., HECKENLIVELY, J. R., PIERCE, E. A. & WEINSTOCK, G. M. 2010. Targeted high-throughput DNA sequencing for gene discovery in retinitis pigmentosa. *Adv Exp Med Biol,* 664**,** 325-31.

DAVIDSON, A. E., MILLAR, I. D., URQUHART, J. E., BURGESS-MULLAN, R., SHWEIKH, Y., PARRY, N., O'SULLIVAN, J., MAHER, G. J., MCKIBBIN, M., DOWNES, S. M., LOTERY, A. J., JACOBSON, S. G., BROWN, P. D., BLACK, G. C. & MANSON, F. D. 2009. Missense mutations in a retinal pigment epithelium protein, bestrophin-1, cause retinitis pigmentosa. *Am J Hum Genet,* 85**,** 581-92.

DAVIES, W. I., DOWNES, S. M., FU, J. K., SHANKS, M. E., COPLEY, R. R., LISE, S., RAMSDEN, S. C., BLACK, G. C., GIBSON, K., FOSTER, R. G., HANKINS, M. W. & NEMETH, A. H. 2012. Next-generation sequencing in health-care delivery: lessons from the functional analysis of rhodopsin. *Genet Med,* 14**,** 891-9.

DE VRIES, H. 1900. Sur la loi de disjonction des hybrids. *Comptes Rendus de l'Acade'mie des sciences de paris,* 130**,** 845-847.

DEANGELIS, M. M., GRIMSBY, J. L., SANDBERG, M. A., BERSON, E. L. & DRYJA, T. P. 2002. Novel mutations in the NRL gene and associated clinical findings in patients with dominant retinitis pigmentosa. *Arch Ophthalmol,* 120**,** 369-75.

DEN HOLLANDER, A. I., MCGEE, T. L., ZIVIELLO, C., BANFI, S., DRYJA, T. P., GONZALEZ-FERNANDEZ, F., GHOSH, D. & BERSON, E. L. 2009. A homozygous missense mutation in the IRBP gene (RBP3) associated with autosomal recessive retinitis pigmentosa. *Invest Ophthalmol Vis Sci,* 50**,** 1864-72.

DESMET, F. O., HAMROUN, D., LALANDE, M., COLLOD-BEROUD, G., CLAUSTRES, M. & BEROUD, C. 2009. Human Splicing Finder: an online bioinformatics tool to predict splicing signals. *Nucleic Acids Res,* 37**,** e67.

DONDERS, F. 1857. Beitra¨ge zur pathologischen Anatomie des Auges. 2. Pigmentbildung in der Netzhaut. *Archives of Ophthalmology***,** 139-165.

DOWLING, J. E. & BOYCOTT, B. B. 1966. Organization of the primate retina: electron microscopy. *Proc R Soc Lond B Biol Sci,* 166**,** 80-111.

DOWNES, S. M., PAYNE, A. M., KELSELL, R. E., FITZKE, F. W., HOLDER, G. E., HUNT, D. M., MOORE, A. T. & BIRD, A. C. 2001. Autosomal dominant cone-rod dystrophy with mutations in the guanylate cyclase 2D gene encoding retinal guanylate cyclase-1. *Arch Ophthalmol,* 119**,** 1667-73.

DRYJA, T. P., BERSON, E. L., RAO, V. R. & OPRIAN, D. D. 1993. Heterozygous missense mutation in the rhodopsin gene as a cause of congenital stationary night blindness. *Nat Genet,* 4**,** 280-3.

DRYJA, T. P., HAHN, L. B., COWLEY, G. S., MCGEE, T. L. & BERSON, E. L. 1991. Mutation spectrum of the rhodopsin gene among patients with autosomal dominant retinitis pigmentosa. *Proc Natl Acad Sci U S A,* 88**,** 9370-4.

DRYJA, T. P., MCGEE, T. L., HAHN, L. B., COWLEY, G. S., OLSSON, J. E., REICHEL, E., SANDBERG, M. A. & BERSON, E. L. 1990a. Mutations within the rhodopsin gene in patients with autosomal dominant retinitis pigmentosa. *N Engl J Med,* 323**,** 1302-7.

DRYJA, T. P., MCGEE, T. L., REICHEL, E., HAHN, L. B., COWLEY, G. S., YANDELL, D. W., SANDBERG, M. A. & BERSON, E. L. 1990b. A point mutation of the rhodopsin gene in one form of retinitis pigmentosa. *Nature,* 343**,** 364-6.

DUNWELL, J. M. 2007. 100 years on: a century of genetics. *Nat Rev Genet,* 8**,** 231-5.

DURBIN, R. M., ABECASIS, G. R., ALTSHULER, D. L., AUTON, A., BROOKS, L. D., GIBBS, R. A., HURLES, M. E. & MCVEAN, G. A. 2010. A map of human genome variation from population-scale sequencing. *Nature,* 467**,** 1061-73.

EL SHAMIEH, S., BOULANGER-SCEMAMA, E., LANCELOT, M. E., ANTONIO, A., DEMONTANT, V., CONDROYER, C., LETEXIER, M., SARAIVA, J. P., MOHAND-SAID, S., SAHEL, J. A., AUDO, I. & ZEITZ, C. 2015. Targeted next generation sequencing identifies novel mutations in RP1 as a relatively common cause of autosomal recessive rod-cone dystrophy. *BioMed research international,* 2015**,** 485624.

ELLEGREN, H. 2007. Characteristics, causes and evolutionary consequences of male-biased mutation. *Proc Biol Sci,* 274**,** 1-10.

ESPOSITO, G., DE FALCO, F., TINTO, N., TESTA, F., VITAGLIANO, L., TANDURELLA, I. C., IANNONE, L., ROSSI, S., RINALDI, E., SIMONELLI, F., ZAGARI, A. & SALVATORE, F. 2011. Comprehensive mutation analysis (20 families) of the choroideremia gene reveals a missense variant that prevents the binding of REP1 with Rab geranylgeranyl transferase. *Human mutation,* 32**,** 1460-9.

EVS 2015. Exome Variant Server (EVS).

EXAC. 2015. *Exome Aggregation Consortium (ExAC) browser* [Online]. Available: http://exac.broadinstitute.org.

FAN, J., ZHANG, Y. Q., LI, P., TONG, C., TAN, L. & ZHU, Y. S. 2004. Interaction between plasminogen activator inhibitor type-2 and pre-mRNA processing factor 8. *Acta Biochim Biophys Sin (Shanghai),* 36**,** 623-8.

FARRAR, G. J., FINDLAY, J. B., KUMAR-SINGH, R., KENNA, P., HUMPHRIES, M. M., SHARPE, E. & HUMPHRIES, P. 1992. Autosomal dominant retinitis pigmentosa: a novel mutation in the rhodopsin gene in the original 3q linked family. *Hum Mol Genet,* 1**,** 769-71.

FARRAR, G. J., KENNA, P., JORDAN, S. A., KUMAR-SINGH, R., HUMPHRIES, M. M., SHARP, E. M., SHEILS, D. & HUMPHRIES, P. 1993. Autosomal dominant retinitis pigmentosa: a novel mutation at the peripherin/RDS locus in the original 6p-linked pedigree. *Genomics,* 15**,** 466.

FARRAR, G. J., KENNA, P., JORDAN, S. A., KUMAR-SINGH, R., HUMPHRIES, M. M., SHARP, E. M., SHEILS, D. M. & HUMPHRIES, P. 1991. A three-base-pair deletion in the peripherin-RDS gene in one form of retinitis pigmentosa. *Nature,* 354**,** 478-80.

FAUSTINO, N. A. & COOPER, T. A. 2003. Pre-mRNA splicing and human disease. *Genes & development,* 17**,** 419-37.

FELBOR, U., SCHILLING, H. & WEBER, B. H. 1997. Adult vitelliform macular dystrophy is frequently associated with mutations in the peripherin/RDS gene. *Hum Mutat,* 10**,** 301-9.

FINGERT, J. H., OH, K., CHUNG, M., SCHEETZ, T. E., ANDORF, J. L., JOHNSON, R. M., SHEFFIELD, V. C. & STONE, E. M. 2008. Association of a novel mutation in the retinol dehydrogenase 12 (RDH12) gene with autosomal dominant retinitis pigmentosa. *Arch Ophthalmol,* 126**,** 1301-7.

FISHMAN, G. A., FISHMAN, M. & MAGGIANO, J. 1977. Macular lesions associated with retinitis pigmentosa. *Arch Ophthalmol,* 95**,** 798-803.

FISHMAN, G. A., STONE, E., GILBERT, L. D., VANDENBURGH, K., SHEFFIELD, V. C. & HECKENLIVELY, J. R. 1994. Clinical features of a previously undescribed codon 216 (proline to serine) mutation in the peripherin/retinal degeneration slow gene in autosomal dominant retinitis pigmentosa. *Ophthalmology,* 101**,** 1409-21.

FLICEK, P., AKEN, B. L., BALLESTER, B., BEAL, K., BRAGIN, E., BRENT, S., CHEN, Y., CLAPHAM, P., COATES, G., FAIRLEY, S., FITZGERALD, S., FERNANDEZ-BANET, J., GORDON, L., GRAF, S., HAIDER, S., HAMMOND, M., HOWE, K., JENKINSON, A., JOHNSON, N., KAHARI, A., KEEFE, D., KEENAN, S., KINSELLA, R., KOKOCINSKI, F., KOSCIELNY, G., KULESHA, E., LAWSON, D., LONGDEN, I., MASSINGHAM, T., MCLAREN, W., MEGY, K., OVERDUIN, B., PRITCHARD, B., RIOS, D., RUFFIER, M., SCHUSTER, M., SLATER, G., SMEDLEY, D., SPUDICH, G., TANG, Y. A., TREVANION, S., VILELLA, A., VOGEL, J., WHITE, S., WILDER, S. P., ZADISSA, A., BIRNEY, E., CUNNINGHAM, F., DUNHAM, I., DURBIN, R., FERNANDEZ-SUAREZ, X. M., HERRERO, J., HUBBARD, T. J., PARKER, A., PROCTOR, G., SMITH, J. & SEARLE, S. M. 2010. Ensembl's 10th year. *Nucleic Acids Res,* 38**,** D557-62.

FLINT, D. H. & HARRINGTON, R. E. 1972. Gel electrophoresis of deoxyribonucleic acid. *Biochemistry,* 11**,** 4858-64.

FOXMAN, S. G., HECKENLIVELY, J. R., BATEMAN, J. B. & WIRTSCHAFTER, J. D. 1985. Classification of congenital and early onset retinitis pigmentosa. *Arch Ophthalmol,* 103**,** 1502-6.

FREUND, C. L., GREGORY-EVANS, C. Y., FURUKAWA, T., PAPAIOANNOU, M., LOOSER, J., PLODER, L., BELLINGHAM, J., NG, D., HERBRICK, J. A., DUNCAN, A., SCHERER, S. W., TSUI, L. C., LOUTRADIS-ANAGNOSTOU, A., JACOBSON, S. G., CEPKO, C. L., BHATTACHARYA, S. S. & MCINNES, R. R. 1997. Cone-rod dystrophy due to mutations in a novel photoreceptor-specific homeobox gene (CRX) essential for maintenance of the photoreceptor. *Cell,* 91**,** 543-53.

FRIEDMAN, J. S., KHANNA, H., SWAIN, P. K., DENICOLA, R., CHENG, H., MITTON, K. P., WEBER, C. H., HICKS, D. & SWAROOP, A. 2004. The minimal transactivation domain of the basic motif-leucine zipper transcription factor NRL interacts with TATA-binding protein. *J Biol Chem,* 279**,** 47233-41.

FRIEDMAN, J. S., RAY, J. W., WASEEM, N., JOHNSON, K., BROOKS, M. J., HUGOSSON, T., BREUER, D., BRANHAM, K. E., KRAUTH, D. S., BOWNE, S. J., SULLIVAN, L. S., PONJAVIC, V., GRANSE, L., KHANNA, R., TRAGER, E. H., GIESER, L. M., HUGHBANKS-WHEATON, D., COJOCARU, R. I., GHIASVAND, N. M., CHAKAROVA, C. F., ABRAHAMSON, M., GORING, H. H., WEBSTER, A. R., BIRCH, D. G., ABECASIS, G. R., FANN, Y., BHATTACHARYA, S. S., DAIGER, S. P., HECKENLIVELY, J. R., ANDREASSON, S. & SWAROOP, A. 2009.

Mutations in a BTB-Kelch protein, KLHL7, cause autosomal-dominant retinitis pigmentosa. *Am J Hum Genet,* 84**,** 792-800.

FURUKAWA, T., MORROW, E. M., LI, T., DAVIS, F. C. & CEPKO, C. L. 1999. Retinopathy and attenuated circadian entrainment in Crx-deficient mice. *Nat Genet,* 23**,** 466-70.

FUTTER, C. E. 2006. The molecular regulation of organelle transport in mammalian retinal pigment epithelial cells. *Pigment Cell Research,* 19**,** 104-111.

GALLI-RESTA, L., LEONE, P., BOTTARI, D., ENSINI, M., RIGOSI, E. & NOVELLI, E. 2008. The genesis of retinal architecture: an emerging role for mechanical interactions? *Prog Retin Eye Res,* 27**,** 260-83.

GAMUNDI, M. J., HERNAN, I., MARTINEZ-GIMENO, M., MASERAS, M., GARCIA-SANDOVAL, B., AYUSO, C., ANTINOLO, G., BAIGET, M. & CARBALLO, M. 2006. Three novel and the common Arg677Ter RP1 protein truncating mutations causing autosomal dominant retinitis pigmentosa in a Spanish population. *BMC medical genetics,* 7**,** 35.

GAMUNDI, M. J., HERNAN, I., MASERAS, M., BAIGET, M., AYUSO, C., BORREGO, S., ANTINOLO, G., MILLAN, J. M., VALVERDE, D. & CARBALLO, M. 2005. Sequence variations in the retinal fascin FSCN2 gene in a Spanish population with autosomal dominant retinitis pigmentosa or macular degeneration. *Mol Vis,* 11**,** 922-8.

GAMUNDI, M. J., HERNAN, I., MUNTANYOLA, M., MASERAS, M., LOPEZ-ROMERO, P., ALVAREZ, R., DOPAZO, A., BORREGO, S. & CARBALLO, M. 2008. Transcriptional expression of cis-acting and trans-acting splicing mutations cause autosomal dominant retinitis pigmentosa. *Hum Mutat,* 29**,** 869-78.

GANDRA, M., ANANDULA, V., AUTHIAPPAN, V., SUNDARAMURTHY, S., RAMAN, R., BHATTACHARYA, S. & GOVINDASAMY, K. 2008. Retinitis pigmentosa: mutation analysis of RHO, PRPF31, RP1, and IMPDH1 genes in patients from India. *Mol Vis,* 14**,** 1105-13.

GAO, J., CHEON, K., NUSINOWITZ, S., LIU, Q., BEI, D., ATKINS, K., AZIMI, A., DAIGER, S. P., FARBER, D. B., HECKENLIVELY, J. R., PIERCE, E. A., SULLIVAN, L. S. & ZUO, J. 2002. Progressive photoreceptor degeneration, outer segment dysplasia, and rhodopsin mislocalization in mice with targeted disruption of the retinitis pigmentosa-1 (Rp1) gene. *Proc Natl Acad Sci U S A,* 99**,** 5698-703.

GARROD, A. E. 2002. The incidence of alkaptonuria: a study in chemical individuality. 1902 [classical article]. *Yale J Biol Med,* 75**,** 221-31.

GEHRIG, A., WEBER, B. H., LORENZ, B. & ANDRASSI, M. 1999. First molecular evidence for a de novo mutation in RS1 (XLRS1) associated with X linked juvenile retinoschisis. *J Med Genet,* 36**,** 932-4.

GHERMAN, A., DAVIS, E. E. & KATSANIS, N. 2006. The ciliary proteome database: an integrated community resource for the genetic and functional dissection of cilia. *Nat Genet,* 38**,** 961-2.

GLOESMANN, M., HERMANN, B., SCHUBERT, C., SATTMANN, H., AHNELT, P. K. & DREXLER, W. 2003. Histologic correlation of pig retina radial stratification with ultrahigh-resolution optical coherence tomography. *Investigative ophthalmology & visual science,* 44**,** 1696-703.

GONZALEZ-PEREZ, A. & LOPEZ-BIGAS, N. 2011. Improving the assessment of the outcome of nonsynonymous SNVs with a consensus deleteriousness score, Condel. *Am J Hum Genet,* 88**,** 440-9.

GONZALEZ-SANTOS, J. M., CAO, H., DUAN, R. C. & HU, J. 2008. Mutation in the splicing factor Hprp3p linked to retinitis pigmentosa impairs interactions within the U4/U6 snRNP complex. *Hum Mol Genet,* 17**,** 225-39.

GRAINGER, R. J. & BEGGS, J. D. 2005. Prp8 protein: at the heart of the spliceosome. *Rna,* 11**,** 533-57.

GRAZIOTTO, J. J., FARKAS, M. H., BUJAKOWSKA, K., DERAMAUDT, B. M., ZHANG, Q., NANDROT, E. F., INGLEHEARN, C. F., BHATTACHARYA, S. S. & PIERCE, E. A. 2011. Three gene-targeted mouse models of RNA splicing factor RP show late-onset RPE and retinal degeneration. *Invest Ophthalmol Vis Sci,* 52**,** 190-8.

GREGORY-EVANS, K., FARISS, R. N., POSSIN, D. E., GREGORY-EVANS, C. Y. & MILAM, A. H. 1998. Abnormal cone synapses in human cone-rod dystrophy. *Ophthalmology,* 105**,** 2306-12.

GREGORY-EVANS, K., KELSELL, R. E., GREGORY-EVANS, C. Y., DOWNES, S. M., FITZKE, F. W., HOLDER, G. E., SIMUNOVIC, M., MOLLON, J. D., TAYLOR, R., HUNT, D. M., BIRD, A. C. & MOORE, A. T. 2000. Autosomal dominant cone-rod retinal dystrophy (CORD6) from heterozygous mutation of GUCY2D, which encodes retinal guanylate cyclase. *Ophthalmology,* 107**,** 55-61.

GRONDAHL, J. 1987. Estimation of prognosis and prevalence of retinitis pigmentosa and Usher syndrome in Norway. *Clin Genet,* 31**,** 255-64.

GU, S. M., THOMPSON, D. A., SRIKUMARI, C. R., LORENZ, B., FINCKH, U., NICOLETTI, A., MURTHY, K. R., RATHMANN, M., KUMARAMANICKAVEL, G., DENTON, M. J. & GAL, A. 1997. Mutations in RPE65 cause autosomal recessive childhood-onset severe retinal dystrophy. *Nat Genet,* 17**,** 194-7.

GUILLONNEAU, X., PIRIEV, N. I., DANCIGER, M., KOZAK, C. A., CIDECIYAN, A. V., JACOBSON, S. G. & FARBER, D. B. 1999. A nonsense mutation in a novel gene is associated with retinitis pigmentosa in a family linked to the RP1 locus. *Hum Mol Genet,* 8**,** 1541-6.

HAESELEER, F., JANG, G. F., IMANISHI, Y., DRIESSEN, C. A., MATSUMURA, M., NELSON, P. S. & PALCZEWSKI, K. 2002. Dual-substrate specificity short chain retinol dehydrogenases from the vertebrate retina. *J Biol Chem,* 277**,** 45537-46.

HAIDER, N. B., JACOBSON, S. G., CIDECIYAN, A. V., SWIDERSKI, R., STREB, L. M., SEARBY, C., BECK, G., HOCKEY, R., HANNA, D. B., GORMAN, S., DUHL, D., CARMI, R., BENNETT, J., WELEBER, R. G., FISHMAN, G.

A., WRIGHT, A. F., STONE, E. M. & SHEFFIELD, V. C. 2000. Mutation of a nuclear receptor gene, NR2E3, causes enhanced S cone syndrome, a disorder of retinal cell fate. *Nat Genet,* 24**,** 127-31.

HAJALI, M., FISHMAN, G. A. & ANDERSON, R. J. 2008. The prevalence of cystoid macular oedema in retinitis pigmentosa patients determined by optical coherence tomography. *Br J Ophthalmol,* 92**,** 1065-8.

HAMEL, C. P., TSILOU, E., PFEFFER, B. A., HOOKS, J. J., DETRICK, B. & REDMOND, T. M. 1993. Molecular cloning and expression of RPE65, a novel retinal pigment epithelium-specific microsomal protein that is post-transcriptionally regulated in vitro. *J Biol Chem,* 268**,** 15751-7.

HAMMARLUND, E. R. & RISING, L. W. 1953. The electrophoretic analysis and antibacterial determination of madronin in agar gel. *J Am Pharm Assoc Am Pharm Assoc (Baltim),* 42**,** 431-3.

HARPER, P. S. 2005. William Bateson, human genetics and medicine. *Hum Genet,* 118**,** 141-51.

HARTONG, D. T., BERSON, E. L. & DRYJA, T. P. 2006. Retinitis pigmentosa. *Lancet,* 368**,** 1795-809.

HECKENLIVELY, J. R. & ARDEN, G. B. (eds.) 2006. *Principles and Practice of Clinical Electrophysiology of Vision,* Cambridge, Massachusetts: The MIT Press.

HEDSTROM, L. 1999. IMP dehydrogenase: mechanism of action and inhibition. *Curr Med Chem,* 6**,** 545-60.

HEDSTROM, L. 2008. IMP dehydrogenase-linked retinitis pigmentosa. *Nucleosides Nucleotides Nucleic Acids,* 27**,** 839-49.

HERNAN, I., GAMUNDI, M. J., BORRAS, E., MASERAS, M., GARCIA-SANDOVAL, B., BLANCO-KELLY, F., AYUSO, C. & CARBALLO, M. 2012. Novel p.M96T variant of NRL and shRNA-based suppression and replacement of NRL mutants associated with autosomal dominant retinitis pigmentosa. *Clin Genet,* 82**,** 446-52.

HOLBROOK, J. A., NEU-YILIK, G., HENTZE, M. W. & KULOZIK, A. E. 2004. Nonsense-mediated decay approaches the clinic. *Nat Genet,* 36**,** 801-8.

HOON, M., OKAWA, H., DELLA SANTINA, L. & WONG, R. O. 2014. Functional architecture of the retina: development and disease. *Prog Retin Eye Res,* 42**,** 44-84.

HOROWITZ, D. S., KOBAYASHI, R. & KRAINER, A. R. 1997. A new cyclophilin and the human homologues of yeast Prp3 and Prp4 form a complex associated with U4/U6 snRNPs. *Rna,* 3**,** 1374-87.

HUANG, J. C., VOADEN, M. J., ZARBIN, M. A. & MARSHALL, J. 2000. Morphologic preservation and variability of human donor retina. *Curr Eye Res,* 20**,** 231-41.

HUGHES, A. E., MENG, W., LOTERY, A. J. & BRADLEY, D. T. 2012. A novel GUCY2D mutation, V933A, causes central areolar choroidal dystrophy. *Invest Ophthalmol Vis Sci,* 53**,** 4748-53.

HUGOSSON, T., FRIEDMAN, J. S., PONJAVIC, V., ABRAHAMSON, M., SWAROOP, A. & ANDREASSON, S. 2010. Phenotype associated with

mutation in the recently identified autosomal dominant retinitis pigmentosa KLHL7 gene. *Arch Ophthalmol,* 128**,** 772-8.

HUMPHRIES, M. M., RANCOURT, D., FARRAR, G. J., KENNA, P., HAZEL, M., BUSH, R. A., SIEVING, P. A., SHEILS, D. M., MCNALLY, N., CREIGHTON, P., ERVEN, A., BOROS, A., GULYA, K., CAPECCHI, M. R. & HUMPHRIES, P. 1997. Retinopathy induced in mice by targeted disruption of the rhodopsin gene. *Nat Genet,* 15**,** 216-9.

HUNT, D. M., BUCH, P. & MICHAELIDES, M. 2010. Guanylate cyclases and associated activator proteins in retinal disease. *Mol Cell Biochem,* 334**,** 157-68.

HURANOVA, M., HNILICOVA, J., FLEISCHER, B., CVACKOVA, Z. & STANEK, D. 2009. A mutation linked to retinitis pigmentosa in HPRP31 causes protein instability and impairs its interactions with spliceosomal snRNPs. *Hum Mol Genet,* 18**,** 2014-23.

INGLEHEARN, C. F., BASHIR, R., LESTER, D. H., JAY, M., BIRD, A. C. & BHATTACHARYA, S. S. 1991. A 3-bp deletion in the rhodopsin gene in a family with autosomal dominant retinitis pigmentosa. *Am J Hum Genet,* 48**,** 26-30.

INGLEHEARN, C. F., KEEN, T. J., BASHIR, R., JAY, M., FITZKE, F., BIRD, A. C., CROMBIE, A. & BHATTACHARYA, S. 1992. A completed screen for mutations of the rhodopsin gene in a panel of patients with autosomal dominant retinitis pigmentosa. *Hum Mol Genet,* 1**,** 41-5.

INGLEHEARN, C. F., TARTTELIN, E. E., KEEN, T. J., BHATTACHARYA, S. S., MOORE, A. T., TAYLOR, R. & BIRD, A. C. 1998. A new dominant retinitis pigmentosa family mapping to the RP18 locus on chromosome 1q11-21. *J Med Genet,* 35**,** 788-9.

ITO, S., NAKAMURA, M., NUNO, Y., OHNISHI, Y., NISHIDA, T. & MIYAKE, Y. 2004. Novel complex GUCY2D mutation in Japanese family with cone-rod dystrophy. *Invest Ophthalmol Vis Sci,* 45**,** 1480-5.

JACOBSON, S. G., CIDECIYAN, A. V., IANNACCONE, A., WELEBER, R. G., FISHMAN, G. A., MAGUIRE, A. M., AFFATIGATO, L. M., BENNETT, J., PIERCE, E. A., DANCIGER, M., FARBER, D. B. & STONE, E. M. 2000. Disease expression of RP1 mutations causing autosomal dominant retinitis pigmentosa. *Invest Ophthalmol Vis Sci,* 41**,** 1898-908.

JACOBSON, S. G., KEMP, C. M., SUNG, C. H. & NATHANS, J. 1991. Retinal function and rhodopsin levels in autosomal dominant retinitis pigmentosa with rhodopsin mutations. *Am J Ophthalmol,* 112**,** 256-71.

JACOBSON, S. G., MARMOR, M. F., KEMP, C. M. & KNIGHTON, R. W. 1990. SWS (blue) cone hypersensitivity in a newly identified retinal degeneration. *Investigative ophthalmology & visual science,* 31**,** 827-38.

JAIN, J., ALMQUIST, S. J., FORD, P. J., SHLYAKHTER, D., WANG, Y., NIMMESGERN, E. & GERMANN, U. A. 2004. Regulation of inosine monophosphate dehydrogenase type I and type II isoforms in human lymphocytes. *Biochem Pharmacol,* 67**,** 767-76.

JANECKE, A. R., THOMPSON, D. A., UTERMANN, G., BECKER, C., HUBNER, C. A., SCHMID, E., MCHENRY, C. L., NAIR, A. R., RUSCHENDORF, F., HECKENLIVELY, J., WISSINGER, B., NURNBERG, P. & GAL, A. 2004. Mutations in RDH12 encoding a photoreceptor cell retinol dehydrogenase cause childhood-onset severe retinal dystrophy. *Nat Genet,* 36**,** 850-4.

JAY, M. & PHIL, M. 1983. Nettleship's two pedigrees of retinitis pigmentosa: a historical postscript. *Surv Ophthalmol,* 27**,** 264-8.

JIN, M., LI, S., NUSINOWITZ, S., LLOYD, M., HU, J., RADU, R. A., BOK, D. & TRAVIS, G. H. 2009. The role of interphotoreceptor retinoid-binding protein on the translocation of visual retinoids and function of cone photoreceptors. *Journal of Neuroscience,* 29**,** 1486-95.

KAJIWARA, K., BERSON, E. L. & DRYJA, T. P. 1994. Digenic retinitis pigmentosa due to mutations at the unlinked peripherin/RDS and ROM1 loci. *Science,* 264**,** 1604-8.

KAJIWARA, K., HAHN, L. B., MUKAI, S., TRAVIS, G. H., BERSON, E. L. & DRYJA, T. P. 1991. Mutations in the human retinal degeneration slow gene in autosomal dominant retinitis pigmentosa. *Nature,* 354**,** 480-3.

KALYANASUNDARAM, T. S., BLACK, G. C., O'SULLIVAN, J. & BISHOP, P. N. 2009. A novel peripherin/RDS mutation resulting in a retinal dystrophy with phenotypic variation. *Eye (Lond),* 23**,** 237-9.

KANDA, A., FRIEDMAN, J. S., NISHIGUCHI, K. M. & SWAROOP, A. 2007. Retinopathy mutations in the bZIP protein NRL alter phosphorylation and transcriptional activity. *Hum Mutat,* 28**,** 589-98.

KARTASASMITA, A., FUJIKI, K., ISKANDAR, E., SOVANI, I., FUJIMAKI, T. & MURAKAMI, A. 2011. A novel nonsense mutation in rhodopsin gene in two Indonesian families with autosomal recessive retinitis pigmentosa. *Ophthalmic genetics,* 32**,** 57-63.

KAWAMURA, M., WADA, Y., NODA, Y., ITABASHI, T., OGAWA, S., SATO, H., TANAKA, K., ISHIBASHI, T. & TAMAI, M. 2004. Novel 2336-2337delCT mutation in RP1 gene in a Japanese family with autosomal dominant retinitis pigmentosa. *Am J Ophthalmol,* 137**,** 1137-9.

KEELER, C. R. 1997. 150 years since Babbage's ophthalmoscope. *Archives of ophthalmology,* 115**,** 1456-7.

KEEN, T. J., HIMS, M. M., MCKIE, A. B., MOORE, A. T., DORAN, R. M., MACKEY, D. A., MANSFIELD, D. C., MUELLER, R. F., BHATTACHARYA, S. S., BIRD, A. C., MARKHAM, A. F. & INGLEHEARN, C. F. 2002. Mutations in a protein target of the Pim-1 kinase associated with the RP9 form of autosomal dominant retinitis pigmentosa. *Eur J Hum Genet,* 10**,** 245-9.

KEEN, T. J., INGLEHEARN, C. F., LESTER, D. H., BASHIR, R., JAY, M., BIRD, A. C., JAY, B. & BHATTACHARYA, S. S. 1991. Autosomal dominant retinitis pigmentosa: four new mutations in rhodopsin, one of them in the retinal attachment site. *Genomics,* 11**,** 199-205.

KENNAN, A., AHERNE, A., PALFI, A., HUMPHRIES, M., MCKEE, A., STITT, A., SIMPSON, D. A., DEMTRODER, K., ORNTOFT, T., AYUSO, C., KENNA,

P. F., FARRAR, G. J. & HUMPHRIES, P. 2002. Identification of an IMPDH1 mutation in autosomal dominant retinitis pigmentosa (RP10) revealed following comparative microarray analysis of transcripts derived from retinas of wild-type and Rho(-/-) mice. *Hum Mol Genet,* 11**,** 547-57.

KEREM, B., ROMMENS, J. M., BUCHANAN, J. A., MARKIEWICZ, D., COX, T. K., CHAKRAVARTI, A., BUCHWALD, M. & TSUI, L. C. 1989. Identification of the cystic fibrosis gene: genetic analysis. *Science,* 245**,** 1073-80.

KEVANY, B. M. & PALCZEWSKI, K. 2010. Phagocytosis of retinal rod and cone photoreceptors. *Physiology,* 25**,** 8-15.

KHALIQ, S., ABID, A., ISMAIL, M., HAMEED, A., MOHYUDDIN, A., LALL, P., AZIZ, A., ANWAR, K. & MEHDI, S. Q. 2005. Novel association of RP1 gene mutations with autosomal recessive retinitis pigmentosa. *J Med Genet,* 42**,** 436-8.

KIBBE, W. A. 2007. OligoCalc: an online oligonucleotide properties calculator. *Nucleic Acids Res,* 35**,** W43-6.

KIM, R. Y., FITZKE, F. W., MOORE, A. T., JAY, M., INGLEHEARN, C., ARDEN, G. B., BHATTACHARYA, S. S. & BIRD, A. C. 1995. Autosomal dominant retinitis pigmentosa mapping to chromosome 7p exhibits variable expression. *Br J Ophthalmol,* 79**,** 23-7.

KITIRATSCHKY, V. B., GLOCKNER, C. J. & KOHL, S. 2011. Mutation screening of the GUCA1B gene in patients with autosomal dominant cone and cone rod dystrophy. *Ophthalmic genetics,* 32**,** 151-5.

KITIRATSCHKY, V. B., NAGY, D., ZABEL, T., ZRENNER, E., WISSINGER, B., KOHL, S. & JAGLE, H. 2008. Cone and cone-rod dystrophy segregating in the same pedigree due to the same novel CRX gene mutation. *Br J Ophthalmol,* 92**,** 1086-91.

KLEPPE, K., OHTSUKA, E., KLEPPE, R., MOLINEUX, I. & KHORANA, H. G. 1971. Studies on polynucleotides. XCVI. Repair replications of short synthetic DNA's as catalyzed by DNA polymerases. *J Mol Biol,* 56**,** 341-61.

KOBAYASHI, M., TAKEZAWA, S., HARA, K., YU, R. T., UMESONO, Y., AGATA, K., TANIWAKI, M., YASUDA, K. & UMESONO, K. 1999. Identification of a photoreceptor cell-specific nuclear receptor. *Proc Natl Acad Sci U S A,* 96**,** 4814-9.

KOHN, L., BURSTEDT, M. S., JONSSON, F., KADZHAEV, K., HAAMER, E., SANDGREN, O. & GOLOVLEVA, I. 2008. Carrier of R14W in carbonic anhydrase IV presents Bothnia dystrophy phenotype caused by two allelic mutations in RLBP1. *Invest Ophthalmol Vis Sci,* 49**,** 3172-7.

KONARSKA, M. M., GRABOWSKI, P. J., PADGETT, R. A. & SHARP, P. A. 1985. Characterization of the branch site in lariat RNAs produced by splicing of mRNA precursors. *Nature,* 313**,** 552-7.

KOZMA, P., HUGHBANKS-WHEATON, D. K., LOCKE, K. G., FISH, G. E., GIRE, A. I., SPELLICY, C. J., SULLIVAN, L. S., BOWNE, S. J., DAIGER, S. P. & BIRCH, D. G. 2005. Phenotypic characterization of a large family with

RP10 autosomal-dominant retinitis pigmentosa: an Asp226Asn mutation in the IMPDH1 gene. *Am J Ophthalmol,* 140**,** 858-867.

KRAMER, F., WHITE, K., PAULEIKHOFF, D., GEHRIG, A., PASSMORE, L., RIVERA, A., RUDOLPH, G., KELLNER, U., ANDRASSI, M., LORENZ, B., ROHRSCHNEIDER, K., BLANKENAGEL, A., JURKLIES, B., SCHILLING, H., SCHUTT, F., HOLZ, F. G. & WEBER, B. H. 2000. Mutations in the VMD2 gene are associated with juvenile-onset vitelliform macular dystrophy (Best disease) and adult vitelliform macular dystrophy but not age-related macular degeneration. *European journal of human genetics : EJHG,* 8**,** 286-92.

KUMAR, P., HENIKOFF, S. & NG, P. C. 2009. Predicting the effects of coding non-synonymous variants on protein function using the SIFT algorithm. *Nat Protoc,* 4**,** 1073-81.

KUMARAMANICKAVEL, G., MAW, M., DENTON, M. J., JOHN, S., SRIKUMARI, C. R., ORTH, U., OEHLMANN, R. & GAL, A. 1994. Missense rhodopsin mutation in a family with recessive RP. *Nat Genet,* 8**,** 10-1.

LAATIKAINEN, L. & LARINKARI, J. 1977. Capillary-free area of the fovea with advancing age. *Invest Ophthalmol Vis Sci,* 16**,** 1154-7.

LATCHMAN, D. S. 1997. Transcription factors: an overview. *The international journal of biochemistry & cell biology,* 29**,** 1305-12.

LAUBER, J., FABRIZIO, P., TEIGELKAMP, S., LANE, W. S., HARTMANN, E. & LUHRMANN, R. 1996. The HeLa 200 kDa U5 snRNP-specific protein and its homologue in Saccharomyces cerevisiae are members of the DEXH-box protein family of putative RNA helicases. *Embo J,* 15**,** 4001-15.

LAUBER, J., PLESSEL, G., PREHN, S., WILL, C. L., FABRIZIO, P., GRONING, K., LANE, W. S. & LUHRMANN, R. 1997. The human U4/U6 snRNP contains 60 and 90kD proteins that are structurally homologous to the yeast splicing factors Prp4p and Prp3p. *Rna,* 3**,** 926-41.

LEBER, T. 1869. Ueber Retinitis pigmentosa und angeborene Amaurose. *Albert von Graefes Arch Ophthal,* 15**,** 1-25.

LEM, J., KRASNOPEROVA, N. V., CALVERT, P. D., KOSARAS, B., CAMERON, D. A., NICOLO, M., MAKINO, C. L. & SIDMAN, R. L. 1999. Morphological, physiological, and biochemical changes in rhodopsin knockout mice. *Proc Natl Acad Sci U S A,* 96**,** 736-41.

LEROUX, M. R. 2007. Taking vesicular transport to the cilium. *Cell,* 129**,** 1041-3.

LEROY, B. P., KAILASANATHAN, A., DE LAEY, J. J., BLACK, G. C. & MANSON, F. D. 2007. Intrafamilial phenotypic variability in families with RDS mutations: exclusion of ROM1 as a genetic modifier for those with retinitis pigmentosa. *Br J Ophthalmol,* 91**,** 89-93.

LEVINE, M. & TJIAN, R. 2003. Transcription regulation and animal diversity. *Nature,* 424**,** 147-51.

LEWIN, A. S., ROSSMILLER, B. & MAO, H. 2014. Gene augmentation for adRP mutations in RHO. *Cold Spring Harbor perspectives in medicine,* 4**,** a017400.

LI, N., MEI, H., MACDONALD, I. M., JIAO, X. & HEJTMANCIK, J. F. 2010. Mutations in ASCC3L1 on 2q11.2 are associated with autosomal dominant retinitis pigmentosa in a Chinese family. *Invest Ophthalmol Vis Sci,* 51**,** 1036-43.

LIM, K. H., FERRARIS, L., FILLOUX, M. E., RAPHAEL, B. J. & FAIRBROTHER, W. G. 2011. Using positional distribution to identify splicing elements and predict pre-mRNA processing defects in human genes. *Proc Natl Acad Sci U S A,* 108**,** 11093-8.

LINDER, B., HIRMER, A., GAL, A., RUTHER, K., BOLZ, H. J., WINKLER, C., LAGGERBAUER, B. & FISCHER, U. 2014. Identification of a PRPF4 loss-of-function variant that abrogates U4/U6.U5 tri-snRNP integration and is associated with retinitis pigmentosa. *PLoS One,* 9**,** e111754.

LITT, M. & LUTY, J. A. 1989. A hypervariable microsatellite revealed by in vitro amplification of a dinucleotide repeat within the cardiac muscle actin gene. *Am J Hum Genet,* 44**,** 397-401.

LIU, H., WANG, M., XIA, C. H., DU, X., FLANNERY, J. G., RIDGE, K. D., BEUTLER, B. & GONG, X. 2010. Severe retinal degeneration caused by a novel rhodopsin mutation. *Invest Ophthalmol Vis Sci,* 51**,** 1059-65.

LIU, Q., LYUBARSKY, A., SKALET, J. H., PUGH, E. N., JR. & PIERCE, E. A. 2003. RP1 is required for the correct stacking of outer segment discs. *Invest Ophthalmol Vis Sci,* 44**,** 4171-83.

LIU, Q., ZHOU, J., DAIGER, S. P., FARBER, D. B., HECKENLIVELY, J. R., SMITH, J. E., SULLIVAN, L. S., ZUO, J., MILAM, A. H. & PIERCE, E. A. 2002. Identification and subcellular localization of the RP1 protein in human and mouse photoreceptors. *Invest Ophthalmol Vis Sci,* 43**,** 22-32.

LIU, Q., ZUO, J. & PIERCE, E. A. 2004. The retinitis pigmentosa 1 protein is a photoreceptor microtubule-associated protein. *The Journal of neuroscience : the official journal of the Society for Neuroscience,* 24**,** 6427-36.

LIU, T., JIN, X., ZHANG, X., YUAN, H., CHENG, J., LEE, J., ZHANG, B., ZHANG, M., WU, J., WANG, L., TIAN, G. & WANG, W. 2012. A novel missense SNRNP200 mutation associated with autosomal dominant retinitis pigmentosa in a Chinese family. *PLoS One,* 7**,** e45464.

LIU, X., PAWLYK, B. S., ADAMIAN, M., OLSHEVSKAYA, E. V., DIZHOOR, A. M., MAKINO, C. L. & LI, T. 2009. Increased light exposure alleviates one form of photoreceptor degeneration marked by elevated calcium in the dark. *PLoS One,* 4**,** e8438.

LIU, X., SENO, K., NISHIZAWA, Y., HAYASHI, F., YAMAZAKI, A., MATSUMOTO, H., WAKABAYASHI, T. & USUKURA, J. 1994. Ultrastructural localization of retinal guanylate cyclase in human and monkey retinas. *Experimental eye research,* 59**,** 761-8.

LIU, X., UDOVICHENKO, I. P., BROWN, S. D., STEEL, K. P. & WILLIAMS, D. S. 1999. Myosin VIIa participates in opsin transport through the photoreceptor cilium. *J Neurosci,* 19**,** 6267-74.

LORENZ, B., GYURUS, P., PREISING, M., BREMSER, D., GU, S., ANDRASSI, M., GERTH, C. & GAL, A. 2000. Early-onset severe rod-cone dystrophy in young children with RPE65 mutations. *Invest Ophthalmol Vis Sci,* 41**,** 2735-42.

LORENZ, B., POLIAKOV, E., SCHAMBECK, M., FRIEDBURG, C., PREISING, M. N. & REDMOND, T. M. 2008. A comprehensive clinical and biochemical functional study of a novel RPE65 hypomorphic mutation. *Invest Ophthalmol Vis Sci,* 49**,** 5235-42.

LUO, H. R., MOREAU, G. A., LEVIN, N. & MOORE, M. J. 1999. The human Prp8 protein is a component of both U2- and U12-dependent spliceosomes. *Rna,* 5**,** 893-908.

MA, X., GUAN, L., WU, W., ZHANG, Y., ZHENG, W., GAO, Y. T., LONG, J., WU, N., WU, L., XIANG, Y., XU, B., SHEN, M., CHEN, Y., WANG, Y., YIN, Y., LI, Y., XU, H. & XU, X. 2015. Whole-exome sequencing identifies OR2W3 mutation as a cause of autosomal dominant retinitis pigmentosa. *Scientific reports,* 5**,** 9236.

MACDONALD, I. M., MAH, D. Y., HO, Y. K., LEWIS, R. A. & SEABRA, M. C. 1998. A practical diagnostic test for choroideremia. *Ophthalmology,* 105**,** 1637-40.

MACKAY, D. S., HENDERSON, R. H., SERGOUNIOTIS, P. I., LI, Z., MORADI, P., HOLDER, G. E., WASEEM, N., BHATTACHARYA, S. S., ALDAHMESH, M. A., ALKURAYA, F. S., MEYER, B., WEBSTER, A. R. & MOORE, A. T. 2010. Novel mutations in MERTK associated with childhood onset rod-cone dystrophy. *Mol Vis,* 16**,** 369-77.

MAEDA, T., IMANISHI, Y. & PALCZEWSKI, K. 2003. Rhodopsin phosphorylation: 30 years later. *Prog Retin Eye Res,* 22**,** 417-34.

MAEDER, C. & GUTHRIE, C. 2008. Modifications target spliceosome dynamics. *Nat Struct Mol Biol,* 15**,** 426-8.

MAGUIRE, A. M., SIMONELLI, F., PIERCE, E. A., PUGH, E. N., JR., MINGOZZI, F., BENNICELLI, J., BANFI, S., MARSHALL, K. A., TESTA, F., SURACE, E. M., ROSSI, S., LYUBARSKY, A., ARRUDA, V. R., KONKLE, B., STONE, E., SUN, J., JACOBS, J., DELL'OSSO, L., HERTLE, R., MA, J. X., REDMOND, T. M., ZHU, X., HAUCK, B., ZELENAIA, O., SHINDLER, K. S., MAGUIRE, M. G., WRIGHT, J. F., VOLPE, N. J., MCDONNELL, J. W., AURICCHIO, A., HIGH, K. A. & BENNETT, J. 2008. Safety and efficacy of gene transfer for Leber's congenital amaurosis. *New England Journal of Medicine,* 358**,** 2240-8.

MAITA, H., HARADA, Y., NAGAKUBO, D., KITAURA, H., IKEDA, M., TAMAI, K., TAKAHASHI, K., ARIGA, H. & IGUCHI-ARIGA, S. M. 2000. PAP-1, a novel target protein of phosphorylation by pim-1 kinase. *Eur J Biochem,* 267**,** 5168-78.

MAITA, H., KITAURA, H., ARIGA, H. & IGUCHI-ARIGA, S. M. 2005. Association of PAP-1 and Prp3p, the products of causative genes of dominant retinitis pigmentosa, in the tri-snRNP complex. *Exp Cell Res,* 302**,** 61-8.

MAITA, H., KITAURA, H., KEEN, T. J., INGLEHEARN, C. F., ARIGA, H. & IGUCHI-ARIGA, S. M. 2004. PAP-1, the mutated gene underlying the RP9 form of dominant retinitis pigmentosa, is a splicing factor. *Exp Cell Res,* 300**,** 283-96.

MAKAROV, E. M., MAKAROVA, O. V., ACHSEL, T. & LUHRMANN, R. 2000. The human homologue of the yeast splicing factor prp6p contains multiple TPR elements and is stably associated with the U5 snRNP via protein-protein interactions. *Journal of molecular biology,* 298**,** 567-75.

MANES, G., MEUNIER, I., AVILA-FERNANDEZ, A., BANFI, S., LE MEUR, G., ZANLONGHI, X., CORTON, M., SIMONELLI, F., BRABET, P., LABESSE, G., AUDO, I., MOHAND-SAID, S., ZEITZ, C., SAHEL, J. A., WEBER, M., DOLLFUS, H., DHAENENS, C. M., ALLORGE, D., DE BAERE, E., KOENEKOOP, R. K., KOHL, S., CREMERS, F. P., HOLLYFIELD, J. G., SENECHAL, A., HEBRARD, M., BOCQUET, B., GARCIA, C. A. & HAMEL, C. P. 2013. Mutations in IMPG1 Cause Vitelliform Macular Dystrophies. *Am J Hum Genet,* 93**,** 571-8.

MANSERGH, F. C., MILLINGTON-WARD, S., KENNAN, A., KIANG, A. S., HUMPHRIES, M., FARRAR, G. J., HUMPHRIES, P. & KENNA, P. F. 1999. Retinitis pigmentosa and progressive sensorineural hearing loss caused by a C12258A mutation in the mitochondrial MTTS2 gene. *Am J Hum Genet,* 64**,** 971-85.

MARCHETTE, L. D., THOMPSON, D. A., KRAVTSOVA, M., NGANSOP, T. N., MANDAL, M. N. & KASUS-JACOBI, A. 2010. Retinol dehydrogenase 12 detoxifies 4-hydroxynonenal in photoreceptor cells. *Free Radic Biol Med,* 48**,** 16-25.

MARLHENS, F., BAREIL, C., GRIFFOIN, J. M., ZRENNER, E., AMALRIC, P., ELIAOU, C., LIU, S. Y., HARRIS, E., REDMOND, T. M., ARNAUD, B., CLAUSTRES, M. & HAMEL, C. P. 1997. Mutations in RPE65 cause Leber's congenital amaurosis. *Nat Genet,* 17**,** 139-41.

MARLHENS, F., GRIFFOIN, J. M., BAREIL, C., ARNAUD, B., CLAUSTRES, M. & HAMEL, C. P. 1998. Autosomal recessive retinal dystrophy associated with two novel mutations in the RPE65 gene. *Eur J Hum Genet,* 6**,** 527-31.

MARMOR, M. F., FULTON, A. B., HOLDER, G. E., MIYAKE, Y., BRIGELL, M. & BACH, M. 2009. ISCEV Standard for full-field clinical electroretinography (2008 update). *Doc Ophthalmol,* 118**,** 69-77.

MARMOR, M. F., JACOBSON, S. G., FOERSTER, M. H., KELLNER, U. & WELEBER, R. G. 1990. Diagnostic clinical findings of a new syndrome with night blindness, maculopathy, and enhanced S cone sensitivity. *American journal of ophthalmology,* 110**,** 124-34.

MARTINEZ-GIMENO, M., GAMUNDI, M. J., HERNAN, I., MASERAS, M., MILLA, E., AYUSO, C., GARCIA-SANDOVAL, B., BENEYTO, M., VILELA, C., BAIGET, M., ANTINOLO, G. & CARBALLO, M. 2003. Mutations in the pre-mRNA splicing-factor genes PRPF3, PRPF8, and PRPF31 in Spanish

families with autosomal dominant retinitis pigmentosa. *Invest Ophthalmol Vis Sci,* 44**,** 2171-7.

MASLAND, R. H. 2001a. The fundamental plan of the retina. *Nat Neurosci,* 4**,** 877-86.

MASLAND, R. H. 2001b. Neuronal diversity in the retina. *Curr Opin Neurobiol,* 11**,** 431-6.

MATTICK, J. S. 2003. Challenging the dogma: the hidden layer of non-protein-coding RNAs in complex organisms. *BioEssays : news and reviews in molecular, cellular and developmental biology,* 25**,** 930-9.

MAUBARET, C. G., VACLAVIK, V., MUKHOPADHYAY, R., WASEEM, N. H., CHURCHILL, A., HOLDER, G. E., MOORE, A. T., BHATTACHARYA, S. S. & WEBSTER, A. R. 2011. Autosomal dominant retinitis pigmentosa with intrafamilial variability and incomplete penetrance in two families carrying mutations in PRPF8. *Invest Ophthalmol Vis Sci,* 52**,** 9304-9.

MCCULLOCH, D. L., MARMOR, M. F., BRIGELL, M. G., HAMILTON, R., HOLDER, G. E., TZEKOV, R. & BACH, M. 2015. ISCEV Standard for full-field clinical electroretinography (2015 update). *Documenta ophthalmologica. Advances in ophthalmology,* 130**,** 1-12.

MCGEE, T. L., DEVOTO, M., OTT, J., BERSON, E. L. & DRYJA, T. P. 1997. Evidence that the penetrance of mutations at the RP11 locus causing dominant retinitis pigmentosa is influenced by a gene linked to the homologous RP11 allele. *Am J Hum Genet,* 61**,** 1059-66.

MCKIE, A. B., MCHALE, J. C., KEEN, T. J., TARTTELIN, E. E., GOLIATH, R., VAN LITH-VERHOEVEN, J. J., GREENBERG, J., RAMESAR, R. S., HOYNG, C. B., CREMERS, F. P., MACKEY, D. A., BHATTACHARYA, S. S., BIRD, A. C., MARKHAM, A. F. & INGLEHEARN, C. F. 2001. Mutations in the pre-mRNA splicing factor gene PRPC8 in autosomal dominant retinitis pigmentosa (RP13). *Hum Mol Genet,* 10**,** 1555-62.

MEARS, A. J., KONDO, M., SWAIN, P. K., TAKADA, Y., BUSH, R. A., SAUNDERS, T. L., SIEVING, P. A. & SWAROOP, A. 2001. Nrl is required for rod photoreceptor development. *Nat Genet,* 29**,** 447-52.

MEINS, M., GRUNING, G., BLANKENAGEL, A., KRASTEL, H., RECK, B., FUCHS, S., SCHWINGER, E. & GAL, A. 1993. Heterozygous 'null allele' mutation in the human peripherin/RDS gene. *Hum Mol Genet,* 2**,** 2181-2.

MENDEL, G. 1866. Versuche über Plflanzenhybriden. Verhandlungen des naturforschenden Vereines in Brünn, Bd. IV für das Jahr 1865. *Abhandlungen***,** 3–47.

MENDES, H. F., VAN DER SPUY, J., CHAPPLE, J. P. & CHEETHAM, M. E. 2005. Mechanisms of cell death in rhodopsin retinitis pigmentosa: implications for therapy. *Trends Mol Med,* 11**,** 177-85.

MEUNIER, I., SENECHAL, A., DHAENENS, C. M., ARNDT, C., PUECH, B., DEFOORT-DHELLEMMES, S., MANES, G., CHAZALETTE, D., MAZOIR, E., BOCQUET, B. & HAMEL, C. P. 2011. Systematic screening of BEST1 and PRPH2 in juvenile and adult vitelliform macular dystrophies: a rationale for molecular analysis. *Ophthalmology,* 118**,** 1130-6.

MICHAELIDES, M., HARDCASTLE, A. J., HUNT, D. M. & MOORE, A. T. 2006. Progressive cone and cone-rod dystrophies: phenotypes and underlying molecular genetic basis. *Surv Ophthalmol,* 51**,** 232-58.

MIN JOU, W., HAEGEMAN, G., YSEBAERT, M. & FIERS, W. 1972. Nucleotide sequence of the gene coding for the bacteriophage MS2 coat protein. *Nature,* 237**,** 82-8.

MOORE, A., ESCUDIER, E., ROGER, G., TAMALET, A., PELOSSE, B., MARLIN, S., CLEMENT, A., GEREMEK, M., DELAISI, B., BRIDOUX, A. M., COSTE, A., WITT, M., DURIEZ, B. & AMSELEM, S. 2006. RPGR is mutated in patients with a complex X linked phenotype combining primary ciliary dyskinesia and retinitis pigmentosa. *J Med Genet,* 43**,** 326-33.

MOORE, A. T., FITZKE, F., JAY, M., ARDEN, G. B., INGLEHEARN, C. F., KEEN, T. J., BHATTACHARYA, S. S. & BIRD, A. C. 1993. Autosomal dominant retinitis pigmentosa with apparent incomplete penetrance: a clinical, electrophysiological, psychophysical, and molecular genetic study. *Br J Ophthalmol,* 77**,** 473-9.

MOORE, M. J. & PROUDFOOT, N. J. 2009. Pre-mRNA processing reaches back to transcription and ahead to translation. *Cell,* 136**,** 688-700.

MORGAN, T. H. 1910. Sex Limited Inheritance in Drosophila. *Science,* 32**,** 120-2.

MORIMURA, H., SAINDELLE-RIBEAUDEAU, F., BERSON, E. L. & DRYJA, T. P. 1999. Mutations in RGR, encoding a light-sensitive opsin homologue, in patients with retinitis pigmentosa. *Nat Genet,* 23**,** 393-4.

MUKHERJEE, R., ROBSON, A. G., HOLDER, G. E., STOCKMAN, A., EGAN, C. A., MOORE, A. T. & WEBSTER, A. R. 2014. A detailed phenotypic description of autosomal dominant cone dystrophy due to a de novo mutation in the GUCY2D gene. *Eye,* 28**,** 481-7.

MUKHOPADHYAY, R., HOLDER, G. E., MOORE, A. T. & WEBSTER, A. R. 2011. Unilateral Retinitis Pigmentosa Occurring in an Individual With a Germline Mutation in the RP1 Gene. *Arch Ophthalmol,* 129**,** 954-6.

MULLIS, K. B. 1990a. Target amplification for DNA analysis by the polymerase chain reaction. *Ann Biol Clin (Paris),* 48**,** 579-82.

MULLIS, K. B. 1990b. The unusual origin of the polymerase chain reaction. *Sci Am,* 262**,** 56-61, 64-5.

NACHURY, M. V., LOKTEV, A. V., ZHANG, Q., WESTLAKE, C. J., PERANEN, J., MERDES, A., SLUSARSKI, D. C., SCHELLER, R. H., BAZAN, J. F., SHEFFIELD, V. C. & JACKSON, P. K. 2007. A core complex of BBS proteins cooperates with the GTPase Rab8 to promote ciliary membrane biogenesis. *Cell,* 129**,** 1201-13.

NAKAZAWA, M., NAOI, N., WADA, Y., NAKAZAKI, S., MARUIWA, F., SAWADA, A. & TAMAI, M. 1996. Autosomal dominant cone-rod dystrophy associated with a Val200Glu mutation of the peripherin/RDS gene. *Retina,* 16**,** 405-10.

NALLA, V. K. & ROGAN, P. K. 2005. Automated splicing mutation analysis by information theory. *Hum Mutat,* 25**,** 334-42.

NATHANS, J. & HOGNESS, D. S. 1984. Isolation and nucleotide sequence of the gene encoding human rhodopsin. *Proc Natl Acad Sci U S A,* 81**,** 4851-5.

NETTLESHIP, E. 1907. On retinitis pigmentosa and allied diseases. *Royal London Ophthalmol Hosp Rev,* 17**,** 1-56.

NICHOLS, B. E., DRACK, A. V., VANDENBURGH, K., KIMURA, A. E., SHEFFIELD, V. C. & STONE, E. M. 1993a. A 2 base pair deletion in the RDS gene associated with butterfly-shaped pigment dystrophy of the fovea. *Hum Mol Genet,* 2**,** 1347.

NICHOLS, B. E., SHEFFIELD, V. C., VANDENBURGH, K., DRACK, A. V., KIMURA, A. E. & STONE, E. M. 1993b. Butterfly-shaped pigment dystrophy of the fovea caused by a point mutation in codon 167 of the RDS gene. *Nat Genet,* 3**,** 202-7.

NICOLETTI, A., WONG, D. J., KAWASE, K., GIBSON, L. H., YANG-FENG, T. L., RICHARDS, J. E. & THOMPSON, D. A. 1995. Molecular characterization of the human gene encoding an abundant 61 kDa protein specific to the retinal pigment epithelium. *Hum Mol Genet,* 4**,** 641-9.

NILSSON, S. E. 1985. The retinal photoreceptors and the pigment epithelium. Structure and function. Transduction. A brief review. *Acta Ophthalmol Suppl,* 173**,** 4-8.

NISHIGUCHI, K. M., FRIEDMAN, J. S., SANDBERG, M. A., SWAROOP, A., BERSON, E. L. & DRYJA, T. P. 2004. Recessive NRL mutations in patients with clumped pigmentary retinal degeneration and relative preservation of blue cone function. *Proc Natl Acad Sci U S A,* 101**,** 17819-24.

NOJIMA, S., TOYOFUKU, T., KAMAO, H., ISHIGAMI, C., KANEKO, J., OKUNO, T., TAKAMATSU, H., ITO, D., KANG, S., KIMURA, T., YOSHIDA, Y., MORIMOTO, K., MAEDA, Y., OGATA, A., IKAWA, M., MORII, E., AOZASA, K., TAKAGI, J., TAKAHASHI, M. & KUMANOGOH, A. 2013. A point mutation in Semaphorin 4A associates with defective endosomal sorting and causes retinal degeneration. *Nature communications,* 4**,** 1406.

NORDENSON, J. W. 1962. Allvar GULLSTRAND (1862-1930). *Documenta ophthalmologica. Advances in ophthalmology,* 16**,** 283-337.

PALCZEWSKI, K., KUMASAKA, T., HORI, T., BEHNKE, C. A., MOTOSHIMA, H., FOX, B. A., LE TRONG, I., TELLER, D. C., OKADA, T., STENKAMP, R. E., YAMAMOTO, M. & MIYANO, M. 2000. Crystal structure of rhodopsin: A G protein-coupled receptor. *Science,* 289**,** 739-45.

PALCZEWSKI, K. & SAARI, J. C. 1997. Activation and inactivation steps in the visual transduction pathway. *Current Opinion in Neurobiology,* 7**,** 500-504.

PAN, X., CHEN, X., LIU, X., GAO, X., KANG, X., XU, Q., ZHAO, K., ZHANG, X., CHU, Q., WANG, X. & ZHAO, C. 2014. Mutation analysis of pre-mRNA splicing genes in Chinese families with retinitis pigmentosa. *Molecular vision,* 20**,** 770-9.

PAYNE, A., VITHANA, E., KHALIQ, S., HAMEED, A., DELLER, J., ABU-SAFIEH, L., KERMANI, S., LEROY, B. P., MEHDI, S. Q., MOORE, A. T., BIRD, A.

C. & BHATTACHARYA, S. S. 2000. RP1 protein truncating mutations predominate at the RP1 adRP locus. *Invest Ophthalmol Vis Sci,* 41**,** 4069-73.

PAYNE, A. M., DOWNES, S. M., BESSANT, D. A., PLANT, C., MOORE, T., BIRD, A. C. & BHATTACHARYA, S. S. 1999. Genetic analysis of the guanylate cyclase activator 1B (GUCA1B) gene in patients with autosomal dominant retinal dystrophies. *J Med Genet,* 36**,** 691-3.

PAYNE, A. M., MORRIS, A. G., DOWNES, S. M., JOHNSON, S., BIRD, A. C., MOORE, A. T., BHATTACHARYA, S. S. & HUNT, D. M. 2001. Clustering and frequency of mutations in the retinal guanylate cyclase (GUCY2D) gene in patients with dominant cone-rod dystrophies. *J Med Genet,* 38**,** 611-4.

PEARSON, H. 2006. Genetics: what is a gene? *Nature,* 441**,** 398-401.

PENA, V., LIU, S., BUJNICKI, J. M., LUHRMANN, R. & WAHL, M. C. 2007. Structure of a multipartite protein-protein interaction domain in splicing factor prp8 and its link to retinitis pigmentosa. *Mol Cell,* 25**,** 615-24.

PEREZ-TORRADO, R., YAMADA, D. & DEFOSSEZ, P. A. 2006. Born to bind: the BTB protein-protein interaction domain. *Bioessays,* 28**,** 1194-202.

PERRAULT, I., ROZET, J. M., CALVAS, P., GERBER, S., CAMUZAT, A., DOLLFUS, H., CHATELIN, S., SOUIED, E., GHAZI, I., LEOWSKI, C., BONNEMAISON, M., LE PASLIER, D., FREZAL, J., DUFIER, J. L., PITTLER, S., MUNNICH, A. & KAPLAN, J. 1996. Retinal-specific guanylate cyclase gene mutations in Leber's congenital amaurosis. *Nat Genet,* 14**,** 461-4.

PETRUKHIN, K., KOISTI, M. J., BAKALL, B., LI, W., XIE, G., MARKNELL, T., SANDGREN, O., FORSMAN, K., HOLMGREN, G., ANDREASSON, S., VUJIC, M., BERGEN, A. A., MCGARTY-DUGAN, V., FIGUEROA, D., AUSTIN, C. P., METZKER, M. L., CASKEY, C. T. & WADELIUS, C. 1998. Identification of the gene responsible for Best macular dystrophy. *Nat Genet,* 19**,** 241-7.

PHILLIPS, T. & HOOPES, L. 2008. Transcription Factors and Transcriptional Control in Eukaryotic Cells. *Nature Education,* 1.

PIERCE, E. A., QUINN, T., MEEHAN, T., MCGEE, T. L., BERSON, E. L. & DRYJA, T. P. 1999. Mutations in a gene encoding a new oxygen-regulated photoreceptor protein cause dominant retinitis pigmentosa. *Nat Genet,* 22**,** 248-54.

PRASAD, C. & GALBRAITH, P. A. 2005. Sir Archibald Garrod and alkaptonuria -'story of metabolic genetics'. *Clin Genet,* 68**,** 199-203.

PREISING, M. & AYUSO, C. 2004. Rab escort protein 1 (REP1) in intracellular traffic: a functional and pathophysiological overview. *Ophthalmic Genet,* 25**,** 101-10.

PROVIS, J. M., PENFOLD, P. L., CORNISH, E. E., SANDERCOE, T. M. & MADIGAN, M. C. 2005. Anatomy and development of the macula: specialisation and the vulnerability to macular degeneration. *Clin Exp Optom,* 88**,** 269-81.

PRUETT, R. C. 1983. Retinitis pigmentosa: clinical observations and correlations. *Trans Am Ophthalmol Soc,* 81**,** 693-735.

RAJENDRA, R., MALEGAONKAR, D., PUNGALIYA, P., MARSHALL, H., RASHEED, Z., BROWNELL, J., LIU, L. F., LUTZKER, S., SALEEM, A. & RUBIN, E. H. 2004. Topors functions as an E3 ubiquitin ligase with specific E2 enzymes and ubiquitinates p53. *J Biol Chem,* 279**,** 36440-4.

RAMAMURTHY, V. & CAYOUETTE, M. 2009. Development and disease of the photoreceptor cilium. *Clin Genet,* 76**,** 137-45.

RAMON, E., CORDOMI, A., AGUILA, M., SRINIVASAN, S., DONG, X., MOORE, A. T., WEBSTER, A. R., CHEETHAM, M. E. & GARRIGA, P. 2014. Differential Light-induced Responses in Sectorial Inherited Retinal Degeneration. *J Biol Chem,* 289**,** 35918-28.

RAO, V. R., COHEN, G. B. & OPRIAN, D. D. 1994. Rhodopsin mutation G90D and a molecular mechanism for congenital night blindness. *Nature,* 367**,** 639-42.

REBELLO, G., RAMESAR, R., VORSTER, A., ROBERTS, L., EHRENREICH, L., OPPON, E., GAMA, D., BARDIEN, S., GREENBERG, J., BONAPACE, G., WAHEED, A., SHAH, G. N. & SLY, W. S. 2004. Apoptosis-inducing signal sequence mutation in carbonic anhydrase IV identified in patients with the RP17 form of retinitis pigmentosa. *Proc Natl Acad Sci U S A,* 101**,** 6617-22.

REESE, M. G., EECKMAN, F. H., KULP, D. & HAUSSLER, D. 1997. Improved splice site detection in Genie. *J Comput Biol,* 4**,** 311-23.

REIG, C., ALVAREZ, A. I., TEJADA, I., MOLINA, M., AROSTEGUI, E., MARTIN, R., ANTICH, J. & CARBALLO, M. 1996. New mutation in the 3'-acceptor splice site of intron 4 in the rhodopsin gene associated with autosomal dominant retinitis pigmentosa in a Basque family. *Hum Mutat,* 8**,** 93-4.

REINERS, J., NAGEL-WOLFRUM, K., JURGENS, K., MARKER, T. & WOLFRUM, U. 2006. Molecular basis of human Usher syndrome: deciphering the meshes of the Usher protein network provides insights into the pathomechanisms of the Usher disease. *Exp Eye Res,* 83**,** 97-119.

RENNER, A. B., KELLNER, U., CROPP, E., PREISING, M. N., MACDONALD, I. M., VAN DEN HURK, J. A., CREMERS, F. P. & FOERSTER, M. H. 2006. Choroideremia: variability of clinical and electrophysiological characteristics and first report of a negative electroretinogram. *Ophthalmology,* 113**,** 2066 e1-10.

RETNET. *http://www.sph.uth.tmc.edu/RetNet/* [Online]. Available: http://www.sph.uth.tmc.edu/RetNet/.

REVA, B., ANTIPIN, Y. & SANDER, C. 2011. Predicting the functional impact of protein mutations: application to cancer genomics. *Nucleic Acids Res,* 39**,** e118.

REYES, J. L., GUSTAFSON, E. H., LUO, H. R., MOORE, M. J. & KONARSKA, M. M. 1999. The C-terminal region of hPrp8 interacts with the conserved GU dinucleotide at the 5' splice site. *Rna,* 5**,** 167-79.

RIAZUDDIN, S. A., ZULFIQAR, F., ZHANG, Q., SERGEEV, Y. V., QAZI, Z. A., HUSNAIN, T., CARUSO, R., RIAZUDDIN, S., SIEVING, P. A. & HEJTMANCIK, J. F. 2005. Autosomal recessive retinitis pigmentosa is associated with mutations in RP1 in three consanguineous Pakistani families. *Invest Ophthalmol Vis Sci,* 46**,** 2264-70.

RIO FRIO, T., CIVIC, N., RANSIJN, A., BECKMANN, J. S. & RIVOLTA, C. 2008. Two trans-acting eQTLs modulate the penetrance of PRPF31 mutations. *Hum Mol Genet,* 17**,** 3154-65.

RIVOLTA, C., BERSON, E. L. & DRYJA, T. P. 2001. Dominant Leber congenital amaurosis, cone-rod degeneration, and retinitis pigmentosa caused by mutant versions of the transcription factor CRX. *Hum Mutat,* 18**,** 488-98.

RIVOLTA, C., MCGEE, T. L., RIO FRIO, T., JENSEN, R. V., BERSON, E. L. & DRYJA, T. P. 2006. Variation in retinitis pigmentosa-11 (PRPF31 or RP11) gene expression between symptomatic and asymptomatic patients with dominant RP11 mutations. *Hum Mutat,* 27**,** 644-53.

ROACH, J. C., GLUSMAN, G., SMIT, A. F., HUFF, C. D., HUBLEY, R., SHANNON, P. T., ROWEN, L., PANT, K. P., GOODMAN, N., BAMSHAD, M., SHENDURE, J., DRMANAC, R., JORDE, L. B., HOOD, L. & GALAS, D. J. 2010. Analysis of genetic inheritance in a family quartet by whole-genome sequencing. *Science,* 328**,** 636-9.

ROBSON, A. G., EGAN, C. A., LUONG, V. A., BIRD, A. C., HOLDER, G. E. & FITZKE, F. W. 2004. Comparison of fundus autofluorescence with photopic and scotopic fine-matrix mapping in patients with retinitis pigmentosa and normal visual acuity. *Investigative ophthalmology & visual science,* 45**,** 4119-25.

ROBSON, A. G., MICHAELIDES, M., SAIHAN, Z., BIRD, A. C., WEBSTER, A. R., MOORE, A. T., FITZKE, F. W. & HOLDER, G. E. 2008. Functional characteristics of patients with retinal dystrophy that manifest abnormal parafoveal annuli of high density fundus autofluorescence; a review and update. *Documenta ophthalmologica. Advances in ophthalmology,* 116**,** 79-89.

ROBSON, A. G., SAIHAN, Z., JENKINS, S. A., FITZKE, F. W., BIRD, A. C., WEBSTER, A. R. & HOLDER, G. E. 2006. Functional characterisation and serial imaging of abnormal fundus autofluorescence in patients with retinitis pigmentosa and normal visual acuity. *Br J Ophthalmol,* 90**,** 472-9.

ROBSON, A. G., WEBSTER, A. R., MICHAELIDES, M., DOWNES, S. M., COWING, J. A., HUNT, D. M., MOORE, A. T. & HOLDER, G. E. 2010. "Cone dystrophy with supernormal rod electroretinogram": a comprehensive genotype/phenotype study including fundus autofluorescence and extensive electrophysiology. *Retina,* 30**,** 51-62.

RODIECK, R. W. 1998. *The first steps in seeing*, Sinauer Associate, Sunderland, Massachusetts.

ROSE, A. M., MUKHOPADHYAY, R., WEBSTER, A. R., BHATTACHARYA, S. S. & WASEEM, N. H. 2011. A 112kb deletion in chromosome 19q13.42 leads to retinitis pigmentosa. *Invest Ophthalmol Vis Sci*.

ROSENFELD, P. J., COWLEY, G. S., MCGEE, T. L., SANDBERG, M. A., BERSON, E. L. & DRYJA, T. P. 1992. A null mutation in the rhodopsin gene causes rod photoreceptor dysfunction and autosomal recessive retinitis pigmentosa. *Nat Genet,* 1**,** 209-13.

ROSSMILLER, B., MAO, H. & LEWIN, A. S. 2012. Gene therapy in animal models of autosomal dominant retinitis pigmentosa. *Molecular vision,* 18**,** 2479-96.

ROZET, J. M., PERRAULT, I., GIGAREL, N., SOUIED, E., GHAZI, I., GERBER, S., DUFIER, J. L., MUNNICH, A. & KAPLAN, J. 2002. Dominant X linked retinitis pigmentosa is frequently accounted for by truncating mutations in exon ORF15 of the RPGR gene. *J Med Genet,* 39**,** 284-5.

RUSHTON, A. R. 2000. Nettleship, Pearson and Bateson: the biometric-Mendelian debate in a medical context. *J Hist Med Allied Sci,* 55**,** 134-57.

SAINI, S., ROBINSON, P. N., SINGH, J. R. & VANITA, V. 2012. A novel 7 bp deletion in PRPF31 associated with autosomal dominant retinitis pigmentosa with incomplete penetrance in an Indian family. *Exp Eye Res,* 104**,** 82-8.

SANGER, F., AIR, G. M., BARRELL, B. G., BROWN, N. L., COULSON, A. R., FIDDES, C. A., HUTCHISON, C. A., SLOCOMBE, P. M. & SMITH, M. 1977a. Nucleotide sequence of bacteriophage phi X174 DNA. *Nature,* 265**,** 687-95.

SANGER, F., NICKLEN, S. & COULSON, A. R. 1977b. DNA sequencing with chain-terminating inhibitors. *Proc Natl Acad Sci U S A,* 74**,** 5463-7.

SATO, H., WADA, Y., ITABASHI, T., NAKAMURA, M., KAWAMURA, M. & TAMAI, M. 2005a. Mutations in the pre-mRNA splicing gene, PRPF31, in Japanese families with autosomal dominant retinitis pigmentosa. *Am J Ophthalmol,* 140**,** 537-40.

SATO, M., NAKAZAWA, M., USUI, T., TANIMOTO, N., ABE, H. & OHGURO, H. 2005b. Mutations in the gene coding for guanylate cyclase-activating protein 2 (GUCA1B gene) in patients with autosomal dominant retinal dystrophies. *Graefes Arch Clin Exp Ophthalmol,* 243**,** 235-42.

SCHATZ, P., PONJAVIC, V., ANDREASSON, S., MCGEE, T. L., DRYJA, T. P. & ABRAHAMSON, M. 2005. Clinical phenotype in a Swedish family with a mutation in the IMPDH1 gene. *Ophthalmic Genet,* 26**,** 119-24.

SCHATZ, P., PREISING, M., LORENZ, B., SANDER, B., LARSEN, M. & ROSENBERG, T. 2011. Fundus albipunctatus associated with compound heterozygous mutations in RPE65. *Ophthalmology,* 118**,** 888-94.

SCHOUTEN, J. P., MCELGUNN, C. J., WAAIJER, R., ZWIJNENBURG, D., DIEPVENS, F. & PALS, G. 2002. Relative quantification of 40 nucleic acid sequences by multiplex ligation-dependent probe amplification. *Nucleic Acids Res,* 30**,** e57.

SCHWARTZ, S. B., ALEMAN, T. S., CIDECIYAN, A. V., SWAROOP, A., JACOBSON, S. G. & STONE, E. M. 2003. De novo mutation in the RP1 gene (Arg677ter) associated with retinitis pigmentosa. *Invest Ophthalmol Vis Sci,* 44**,** 3593-7.

SEABRA, M. C., MULES, E. H. & HUME, A. N. 2002. Rab GTPases, intracellular traffic and disease. *Trends Mol Med,* 8**,** 23-30.

SELMER, K. K., GRONDAHL, J., RIISE, R., BRANDAL, K., BRAATEN, O., BRAGADOTTIR, R. & UNDLIEN, D. E. 2009. Autosomal dominant pericentral retinal dystrophy caused by a novel missense mutation in the TOPORS gene. *Acta Ophthalmol*.

SERGEEV, Y. V., SMAOUI, N., SUI, R., STILES, D., GORDIYENKO, N., STRUNNIKOVA, N. & MACDONALD, I. M. 2009. The functional effect of pathogenic mutations in Rab escort protein 1. *Mutat Res,* 665**,** 44-50.

SERGOUNIOTIS, P. 2012. *Genetic and phenotypic heterogeneity in autosomal recessive retinal disease.* Doctor of Philosophy, University College London.

SHIHAB, H. A., ROGERS, M. F., GOUGH, J., MORT, M., COOPER, D. N., DAY, I. N., GAUNT, T. R. & CAMPBELL, C. 2015. An integrative approach to predicting the functional effects of non-coding and coding sequence variation. *Bioinformatics*.

SIMONSZ, H. J. 2004. Christian Theodor Georg Ruete: the first strabismologist, coauthor of listing's law, maker of the first ophthalmotrope and inventor of indirect fundoscopy. *Strabismus,* 12**,** 53-7.

SMALL, K. W., SILVA-GARCIA, R., UDAR, N., NGUYEN, E. V. & HECKENLIVELY, J. R. 2008. New mutation, P575L, in the GUCY2D gene in a family with autosomal dominant progressive cone degeneration. *Arch Ophthalmol,* 126**,** 397-403.

SMITH, D. J., QUERY, C. C. & KONARSKA, M. M. 2008. "Nought may endure but mutability": spliceosome dynamics and the regulation of splicing. *Mol Cell,* 30**,** 657-66.

SMITH, M., WHITTOCK, N., SEARLE, A., CROFT, M., BREWER, C. & COLE, M. 2007. Phenotype of autosomal dominant cone-rod dystrophy due to the R838C mutation of the GUCY2D gene encoding retinal guanylate cyclase-1. *Eye,* 21**,** 1220-5.

SNODDERLY, D. M., AURAN, J. D. & DELORI, F. C. 1984. The macular pigment. II. Spatial distribution in primate retinas. *Investigative ophthalmology & visual science,* 25**,** 674-85.

SOHOCKI, M. M., DAIGER, S. P., BOWNE, S. J., RODRIQUEZ, J. A., NORTHRUP, H., HECKENLIVELY, J. R., BIRCH, D. G., MINTZ-HITTNER, H., RUIZ, R. S., LEWIS, R. A., SAPERSTEIN, D. A. & SULLIVAN, L. S. 2001. Prevalence of mutations causing retinitis pigmentosa and other inherited retinopathies. *Hum Mutat,* 17**,** 42-51.

SOHOCKI, M. M., SULLIVAN, L. S., MINTZ-HITTNER, H. A., BIRCH, D., HECKENLIVELY, J. R., FREUND, C. L., MCINNES, R. R. & DAIGER, S. P. 1998. A range of clinical phenotypes associated with mutations in CRX, a photoreceptor transcription-factor gene. *Am J Hum Genet,* 63**,** 1307-15.

SOHOCKI, M. M., SULLIVAN, L. S., MINTZ-HITTNER, H. A., SMALL, K., FERRELL, R. E. & DAIGER, S. P. 1997. Exclusion of atypical vitelliform

macular dystrophy from 8q24.3 and from other known macular degenerative loci. *Am J Hum Genet,* 61**,** 239-41.

SORSBY, A., FRANCESCHETTI, A., JOSEPH, R. & DAVEY, J. B. 1952. Choroideremia; clinical and genetic aspects. *Br J Ophthalmol,* 36**,** 547-81.

SPRITZ, R. A., DERIEL, J. K., FORGET, B. G. & WEISSMAN, S. M. 1980. Complete nucleotide sequence of the human delta-globin gene. *Cell,* 21**,** 639-46.

SRINIVASAN, V. J., MONSON, B. K., WOJTKOWSKI, M., BILONICK, R. A., GORCZYNSKA, I., CHEN, R., DUKER, J. S., SCHUMAN, J. S. & FUJIMOTO, J. G. 2008. Characterization of outer retinal morphology with high-speed, ultrahigh-resolution optical coherence tomography. *Investigative ophthalmology & visual science,* 49**,** 1571-9.

STENSON, P. D., MORT, M., BALL, E. V., HOWELLS, K., PHILLIPS, A. D., THOMAS, N. S. & COOPER, D. N. 2009. The Human Gene Mutation Database: 2008 update. *Genome Med,* 1**,** 13.

STOCKMAN, A., SHARPE, L. T. & FACH, C. 1999. The spectral sensitivity of the human short-wavelength sensitive cones derived from thresholds and color matches. *Vision Res,* 39**,** 2901-27.

STRACHAN, T. & READ, A. P. 2004. *Human Molecular Genetics*, Garland Science, Taylor and Francis group.

SUBCZYNSKI, W. K., WISNIEWSKA, A. & WIDOMSKA, J. 2010. Location of macular xanthophylls in the most vulnerable regions of photoreceptor outer-segment membranes. *Arch Biochem Biophys,* 504**,** 61-6.

SULLIVAN, L. S., BOWNE, S. J., BIRCH, D. G., HUGHBANKS-WHEATON, D., HECKENLIVELY, J. R., LEWIS, R. A., GARCIA, C. A., RUIZ, R. S., BLANTON, S. H., NORTHRUP, H., GIRE, A. I., SEAMAN, R., DUZKALE, H., SPELLICY, C. J., ZHU, J., SHANKAR, S. P. & DAIGER, S. P. 2006a. Prevalence of disease-causing mutations in families with autosomal dominant retinitis pigmentosa: a screen of known genes in 200 families. *Invest Ophthalmol Vis Sci,* 47**,** 3052-64.

SULLIVAN, L. S., BOWNE, S. J., SEAMAN, C. R., BLANTON, S. H., LEWIS, R. A., HECKENLIVELY, J. R., BIRCH, D. G., HUGHBANKS-WHEATON, D. & DAIGER, S. P. 2006b. Genomic rearrangements of the PRPF31 gene account for 2.5% of autosomal dominant retinitis pigmentosa. *Invest Ophthalmol Vis Sci,* 47**,** 4579-88.

SULLIVAN, L. S., HECKENLIVELY, J. R., BOWNE, S. J., ZUO, J., HIDE, W. A., GAL, A., DENTON, M., INGLEHEARN, C. F., BLANTON, S. H. & DAIGER, S. P. 1999. Mutations in a novel retina-specific gene cause autosomal dominant retinitis pigmentosa. *Nat Genet,* 22**,** 255-9.

SULLIVAN, L. S., KOBOLDT, D. C., BOWNE, S. J., LANG, S., BLANTON, S. H., CADENA, E., AVERY, C. E., LEWIS, R. A., WEBB-JONES, K., WHEATON, D. H., BIRCH, D. G., COUSSA, R., REN, H., LOPEZ, I., CHAKAROVA, C., KOENEKOOP, R. K., GARCIA, C. A., FULTON, R. S., WILSON, R. K., WEINSTOCK, G. M. & DAIGER, S. P. 2014. A dominant

mutation in hexokinase 1 (HK1) causes retinitis pigmentosa. *Investigative ophthalmology & visual science,* 55**,** 7147-58.

SUNG, C. H., DAVENPORT, C. M., HENNESSEY, J. C., MAUMENEE, I. H., JACOBSON, S. G., HECKENLIVELY, J. R., NOWAKOWSKI, R., FISHMAN, G., GOURAS, P. & NATHANS, J. 1991. Rhodopsin mutations in autosomal dominant retinitis pigmentosa. *Proc Natl Acad Sci U S A,* 88**,** 6481-5.

SWANSON, E. A., IZATT, J. A., HEE, M. R., HUANG, D., LIN, C. P., SCHUMAN, J. S., PULIAFITO, C. A. & FUJIMOTO, J. G. 1993. In vivo retinal imaging by optical coherence tomography. *Optics letters,* 18**,** 1864-6.

SWAROOP, A., XU, J. Z., PAWAR, H., JACKSON, A., SKOLNICK, C. & AGARWAL, N. 1992. A conserved retina-specific gene encodes a basic motif/leucine zipper domain. *Proc Natl Acad Sci U S A,* 89**,** 266-70.

TAM, B. M. & MORITZ, O. L. 2009. The role of rhodopsin glycosylation in protein folding, trafficking, and light-sensitive retinal degeneration. *J Neurosci,* 29**,** 15145-54.

TANACKOVIC, G., RANSIJN, A., AYUSO, C., HARPER, S., BERSON, E. L. & RIVOLTA, C. 2011a. A Missense Mutation in PRPF6 Causes Impairment of pre-mRNA Splicing and Autosomal-Dominant Retinitis Pigmentosa. *Am J Hum Genet*.

TANACKOVIC, G., RANSIJN, A., THIBAULT, P., ABOU ELELA, S., KLINCK, R., BERSON, E. L., CHABOT, B. & RIVOLTA, C. 2011b. PRPF mutations are associated with generalized defects in spliceosome formation and pre-mRNA splicing in patients with retinitis pigmentosa. *Hum Mol Genet,* 20**,** 2116-30.

TARTTELIN, E. E., PLANT, C., WEISSENBACH, J., BIRD, A. C., BHATTACHARYA, S. S. & INGLEHEARN, C. F. 1996. A new family linked to the RP13 locus for autosomal dominant retinitis pigmentosa on distal 17p. *J Med Genet,* 33**,** 518-20.

TESTA, F., ZIVIELLO, C., RINALDI, M., ROSSI, S., DI IORIO, V., INTERLANDI, E., CICCODICOLA, A., BANFI, S. & SIMONELLI, F. 2006. Clinical phenotype of an Italian family with a new mutation in the PRPF8 gene. *Eur J Ophthalmol,* 16**,** 779-81.

THAU, W. 1942. Purkyně - a pioneer in ophthalmoscopy. *Archives of Ophthalmology,* 27**,** 299-316.

THIADENS, A. A., DEN HOLLANDER, A. I., ROOSING, S., NABUURS, S. B., ZEKVELD-VROON, R. C., COLLIN, R. W., DE BAERE, E., KOENEKOOP, R. K., VAN SCHOONEVELD, M. J., STROM, T. M., VAN LITH-VERHOEVEN, J. J., LOTERY, A. J., VAN MOLL-RAMIREZ, N., LEROY, B. P., VAN DEN BORN, L. I., HOYNG, C. B., CREMERS, F. P. & KLAVER, C. C. 2009. Homozygosity mapping reveals PDE6C mutations in patients with early-onset cone photoreceptor disorders. *Am J Hum Genet,* 85**,** 240-7.

THOMPSON, D. A., GYURUS, P., FLEISCHER, L. L., BINGHAM, E. L., MCHENRY, C. L., APFELSTEDT-SYLLA, E., ZRENNER, E., LORENZ, B.,

RICHARDS, J. E., JACOBSON, S. G., SIEVING, P. A. & GAL, A. 2000. Genetics and phenotypes of RPE65 mutations in inherited retinal degeneration. *Invest Ophthalmol Vis Sci,* 41**,** 4293-9.

THOMPSON, D. A., LI, Y., MCHENRY, C. L., CARLSON, T. J., DING, X., SIEVING, P. A., APFELSTEDT-SYLLA, E., ZRENNER, E. & GAL, A. 2001. Mutations in lecithin retinol acyltransferase (LRAT) cause early-onset severe retinal dystrophy. *Invest Ophthalmol Vis Sci,* 42**,** S647-S647.

THORNE, H. V. 1966. Electrophoretic separation of polyoma virus DNA from host cell DNA. *Virology,* 29**,** 234-9.

TIAN, Y., TANG, L., CUI, J. & ZHU, X. 2010. Screening for the carbonic anhydrase IV gene mutations in Chinese retinitis pigmentosa patients. *Curr Eye Res,* 35**,** 440-4.

TO, K., ADAMIAN, M., DRYJA, T. P. & BERSON, E. L. 2000. Retinal histopathology of an autopsy eye with advanced retinitis pigmentosa in a family with rhodopsin Glu181Lys. *Am J Ophthalmol,* 130**,** 790-2.

TOBIN, J. L. & BEALES, P. L. 2007. Bardet-Biedl syndrome: beyond the cilium. *Pediatr Nephrol,* 22**,** 926-36.

TOWNS, K. V., KIPIOTI, A., LONG, V., MCKIBBIN, M., MAUBARET, C., VACLAVIK, V., EHSANI, P., SPRINGELL, K., KAMAL, M., RAMESAR, R. S., MACKEY, D. A., MOORE, A. T., MUKHOPADHYAY, R., WEBSTER, A. R., BLACK, G. C., O'SULLIVAN, J., BHATTACHARYA, S. S., PIERCE, E. A., BEGGS, J. D. & INGLEHEARN, C. F. 2010. Prognosis for splicing factor PRPF8 retinitis pigmentosa, novel mutations and correlation between human and yeast phenotypes. *Hum Mutat,* 31**,** E1361-76.

TRAVIS, G. H., CHRISTERSON, L., DANIELSON, P. E., KLISAK, I., SPARKES, R. S., HAHN, L. B., DRYJA, T. P. & SUTCLIFFE, J. G. 1991a. The human retinal degeneration slow (RDS) gene: chromosome assignment and structure of the mRNA. *Genomics,* 10**,** 733-9.

TRAVIS, G. H. & HEPLER, J. E. 1993. A medley of retinal dystrophies. *Nat Genet,* 3**,** 191-2.

TRAVIS, G. H., SUTCLIFFE, J. G. & BOK, D. 1991b. The retinal degeneration slow (rds) gene product is a photoreceptor disc membrane-associated glycoprotein. *Neuron,* 6**,** 61-70.

TRIOLO, G., PIERRO, L., PARODI, M. B., DE BENEDETTO, U., GAGLIARDI, M., MANITTO, M. P. & BANDELLO, F. 2013. Spectral domain optical coherence tomography findings in patients with retinitis pigmentosa. *Ophthalmic research,* 50**,** 160-4.

TSCHERMAK, E. V. 1900. Ueber künstliche Kreuzung bei Pisum sativum. *Ber. Dt. Bot. Ges.,* 18**,** 232-239.

TUCKER, C. L., WOODCOCK, S. C., KELSELL, R. E., RAMAMURTHY, V., HUNT, D. M. & HURLEY, J. B. 1999. Biochemical analysis of a dimerization domain mutation in RetGC-1 associated with dominant cone-rod dystrophy. *Proc Natl Acad Sci U S A,* 96**,** 9039-44.

UTZ, V. M., BEIGHT, C. D., MARINO, M. J., HAGSTROM, S. A. & TRABOULSI, E. I. 2013. Autosomal Dominant Retinitis Pigmentosa Secondary to Pre-

mRNA Splicing-Factor Gene PRPF31 (RP11): Review of Disease Mechanism and Report of a Family with a Novel 3-Base Pair Insertion. *Ophthalmic Genet*.

VACLAVIK, V., GAILLARD, M. C., TIAB, L., SCHORDERET, D. F. & MUNIER, F. L. 2010. Variable phenotypic expressivity in a Swiss family with autosomal dominant retinitis pigmentosa due to a T494M mutation in the PRPF3 gene. *Mol Vis,* 16**,** 467-75.

VAITHINATHAN, R., BERSON, E. L. & DRYJA, T. P. 1994. Further screening of the rhodopsin gene in patients with autosomal dominant retinitis pigmentosa. *Genomics,* 21**,** 461-3.

VAN DEN HURK, J. A., VAN DE POL, D. J., WISSINGER, B., VAN DRIEL, M. A., HOEFSLOOT, L. H., DE WIJS, I. J., VAN DEN BORN, L. I., HECKENLIVELY, J. R., BRUNNER, H. G., ZRENNER, E., ROPERS, H. H. & CREMERS, F. P. 2003. Novel types of mutation in the choroideremia (CHM) gene: a full-length L1 insertion and an intronic mutation activating a cryptic exon. *Hum Genet,* 113**,** 268-75.

VAN LITH-VERHOEVEN, J. J., VAN DER VELDE-VISSER, S. D., SOHOCKI, M. M., DEUTMAN, A. F., BRINK, H. M., CREMERS, F. P. & HOYNG, C. B. 2002. Clinical characterization, linkage analysis, and PRPC8 mutation analysis of a family with autosomal dominant retinitis pigmentosa type 13 (RP13). *Ophthalmic Genet,* 23**,** 1-12.

VAN NUES, R. W. & BEGGS, J. D. 2001. Functional contacts with a range of splicing proteins suggest a central role for Brr2p in the dynamic control of the order of events in spliceosomes of Saccharomyces cerevisiae. *Genetics,* 157**,** 1451-67.

VENTURINI, G., ROSE, A. M., SHAH, A. Z., BHATTACHARYA, S. S. & RIVOLTA, C. 2012. CNOT3 is a modifier of PRPF31 mutations in retinitis pigmentosa with incomplete penetrance. *PLoS Genet,* 8**,** e1003040.

VITHANA, E. N., ABU-SAFIEH, L., ALLEN, M. J., CAREY, A., PAPAIOANNOU, M., CHAKAROVA, C., AL-MAGHTHEH, M., EBENEZER, N. D., WILLIS, C., MOORE, A. T., BIRD, A. C., HUNT, D. M. & BHATTACHARYA, S. S. 2001. A human homolog of yeast pre-mRNA splicing gene, PRP31, underlies autosomal dominant retinitis pigmentosa on chromosome 19q13.4 (RP11). *Mol Cell,* 8**,** 375-81.

VITHANA, E. N., ABU-SAFIEH, L., PELOSINI, L., WINCHESTER, E., HORNAN, D., BIRD, A. C., HUNT, D. M., BUSTIN, S. A. & BHATTACHARYA, S. S. 2003. Expression of PRPF31 mRNA in patients with autosomal dominant retinitis pigmentosa: a molecular clue for incomplete penetrance? *Invest Ophthalmol Vis Sci,* 44**,** 4204-9.

VON RUCKMANN, A., FITZKE, F. W. & BIRD, A. C. 1995a. Distribution of fundus autofluorescence with a scanning laser ophthalmoscope. *The British journal of ophthalmology,* 79**,** 407-12.

VON RUCKMANN, A., FITZKE, F. W. & BIRD, A. C. 1995b. Distribution of fundus autofluorescence with a scanning laser ophthalmoscope. *Br J Ophthalmol,* 79**,** 407-12.

WADA, Y., ABE, T., TAKESHITA, T., SATO, H., YANASHIMA, K. & TAMAI, M. 2001. Mutation of human retinal fascin gene (FSCN2) causes autosomal dominant retinitis pigmentosa. *Invest Ophthalmol Vis Sci,* 42**,** 2395-400.

WADA, Y., ITABASHI, T., SATO, H. & TAMAI, M. 2004. Clinical features of a Japanese family with autosomal dominant retinitis pigmentosa associated with a Thr494Met mutation in the HPRP3 gene. *Graefes Arch Clin Exp Ophthalmol,* 242**,** 956-61.

WADA, Y., SANDBERG, M. A., MCGEE, T. L., STILLBERGER, M. A., BERSON, E. L. & DRYJA, T. P. 2005a. Screen of the IMPDH1 gene among patients with dominant retinitis pigmentosa and clinical features associated with the most common mutation, Asp226Asn. *Invest Ophthalmol Vis Sci,* 46**,** 1735-41.

WADA, Y., TADA, A., ITABASHI, T., KAWAMURA, M., SATO, H. & TAMAI, M. 2005b. Screening for mutations in the IMPDH1 gene in Japanese patients with autosomal dominant retinitis pigmentosa. *Am J Ophthalmol,* 140**,** 163-5.

WADE, N. J. 2007. Image, eye, and retina (invited review). *Journal of the Optical Society of America. A, Optics, image science, and vision,* 24**,** 1229-49.

WALIA, S., FISHMAN, G. A., JACOBSON, S. G., ALEMAN, T. S., KOENEKOOP, R. K., TRABOULSI, E. I., WELEBER, R. G., PENNESI, M. E., HEON, E., DRACK, A., LAM, B. L., ALLIKMETS, R. & STONE, E. M. 2010. Visual acuity in patients with Leber's congenital amaurosis and early childhood-onset retinitis pigmentosa. *Ophthalmology,* 117**,** 1190-8.

WALIA, S., FISHMAN, G. A., ZERNANT-RAJANG, J., RAIME, K. & ALLIKMETS, R. 2008. Phenotypic expression of a PRPF8 gene mutation in a Large African American family. *Arch Ophthalmol,* 126**,** 1127-32.

WANG, A., FORMAN-KAY, J., LUO, Y., LUO, M., CHOW, Y. H., PLUMB, J., FRIESEN, J. D., TSUI, L. C., HENG, H. H., WOOLFORD, J. L., JR. & HU, J. 1997. Identification and characterization of human genes encoding Hprp3p and Hprp4p, interacting components of the spliceosome. *Hum Mol Genet,* 6**,** 2117-26.

WANG, F., WANG, Y., ZHANG, B., ZHAO, L., LYUBASYUK, V., WANG, K., XU, M., LI, Y., WU, F., WEN, C., BERNSTEIN, P. S., LIN, D., ZHU, S., WANG, H., ZHANG, K. & CHEN, R. 2014. A missense mutation in HK1 leads to autosomal dominant retinitis pigmentosa. *Investigative ophthalmology & visual science,* 55**,** 7159-64.

WANG, X. T., MION, B., AHERNE, A. & ENGEL, P. C. 2011. Molecular recruitment as a basis for negative dominant inheritance? Propagation of misfolding in oligomers of IMPDH1, the mutated enzyme in the RP10 form of retinitis pigmentosa. *Biochim Biophys Acta*.

WASEEM, N. H., VACLAVIK, V., WEBSTER, A., JENKINS, S. A., BIRD, A. C. & BHATTACHARYA, S. S. 2007. Mutations in the gene coding for the pre-mRNA splicing factor, PRPF31, in patients with autosomal dominant retinitis pigmentosa. *Invest Ophthalmol Vis Sci,* 48**,** 1330-4.

WATSON, J. D. & CRICK, F. H. 1953. Molecular structure of nucleic acids; a structure for deoxyribose nucleic acid. *Nature,* 171**,** 737-8.

WEIDENHAMMER, E. M., SINGH, M., RUIZ-NORIEGA, M. & WOOLFORD, J. L., JR. 1996. The PRP31 gene encodes a novel protein required for pre-mRNA splicing in Saccharomyces cerevisiae. *Nucleic Acids Res,* 24**,** 1164-70.

WEIL, D., BLANCHARD, S., KAPLAN, J., GUILFORD, P., GIBSON, F., WALSH, J., MBURU, P., VARELA, A., LEVILLIERS, J., WESTON, M. D. & ET AL. 1995. Defective myosin VIIA gene responsible for Usher syndrome type 1B. *Nature,* 374**,** 60-1.

WELEBER, R. G., CARR, R. E., MURPHEY, W. H., SHEFFIELD, V. C. & STONE, E. M. 1993. Phenotypic variation including retinitis pigmentosa, pattern dystrophy, and fundus flavimaculatus in a single family with a deletion of codon 153 or 154 of the peripherin/RDS gene. *Arch Ophthalmol,* 111**,** 1531-42.

WELEBER, R. G., MICHAELIDES, M., TRZUPEK, K. M., STOVER, N. B. & STONE, E. M. 2011. The phenotype of Severe Early Childhood Onset Retinal Dystrophy (SECORD) from mutation of RPE65 and differentiation from Leber congenital amaurosis. *Invest Ophthalmol Vis Sci,* 52**,** 292-302.

WELLS, J., WROBLEWSKI, J., KEEN, J., INGLEHEARN, C., JUBB, C., ECKSTEIN, A., JAY, M., ARDEN, G., BHATTACHARYA, S., FITZKE, F. & ET AL. 1993. Mutations in the human retinal degeneration slow (RDS) gene can cause either retinitis pigmentosa or macular dystrophy. *Nat Genet,* 3**,** 213-8.

WILKIE, S. E., NEWBOLD, R. J., DEERY, E., WALKER, C. E., STINTON, I., RAMAMURTHY, V., HURLEY, J. B., BHATTACHARYA, S. S., WARREN, M. J. & HUNT, D. M. 2000. Functional characterization of missense mutations at codon 838 in retinal guanylate cyclase correlates with disease severity in patients with autosomal dominant cone-rod dystrophy. *Hum Mol Genet,* 9**,** 3065-73.

WILLIAMS, D. S. 2008. Usher syndrome: animal models, retinal function of Usher proteins, and prospects for gene therapy. *Vision Res,* 48**,** 433-41.

WILSON, E. B. 1911. The sex chromosomes. *Archiv fu¨ r Mikroskopische Anatomie. II Abteilung, fu¨ r Zeugungs- und Vererbungslehre,* 77**,** 249-271.

WOLF, G. 2003. Lipofuscin and macular degeneration. *Nutr Rev,* 61**,** 342-6.

XU, F., SUI, R., LIANG, X., LI, H., JIANG, R. & DONG, F. 2012. Novel PRPF31 mutations associated with Chinese autosomal dominant retinitis pigmentosa patients. *Mol Vis,* 18**,** 3021-xxx.

XU, S. Y., SCHWARTZ, M., ROSENBERG, T. & GAL, A. 1996. A ninth locus (RP18) for autosomal dominant retinitis pigmentosa maps in the pericentromeric region of chromosome 1. *Hum Mol Genet,* 5**,** 1193-7.

XUE, L., GOLLAPALLI, D. R., MAITI, P., JAHNG, W. J. & RANDO, R. R. 2004. A palmitoylation switch mechanism in the regulation of the visual cycle. *Cell,* 117**,** 761-71.

YAMAMOTO, H., SIMON, A., ERIKSSON, U., HARRIS, E., BERSON, E. L. & DRYJA, T. P. 1999. Mutations in the gene encoding 11-cis retinol dehydrogenase cause delayed dark adaptation and fundus albipunctatus. *Nat Genet,* 22**,** 188-91.

YAMASHITA, T., LIU, J., GAO, J., LENOUE, S., WANG, C., KAMINOH, J., BOWNE, S. J., SULLIVAN, L. S., DAIGER, S. P., ZHANG, K., FITZGERALD, M. E., KEFALOV, V. J. & ZUO, J. 2009. Essential and synergistic roles of RP1 and RP1L1 in rod photoreceptor axoneme and retinitis pigmentosa. *J Neurosci,* 29**,** 9748-60.

YANG, R. B., FOSTER, D. C., GARBERS, D. L. & FULLE, H. J. 1995. Two membrane forms of guanylyl cyclase found in the eye. *Proc Natl Acad Sci U S A,* 92**,** 602-6.

YOUNG, R. W. 1976. Visual cells and the concept of renewal. *Invest Ophthalmol Vis Sci,* 15**,** 700-25.

ZEITZ, C., GROSS, A. K., LEIFERT, D., KLOECKENER-GRUISSEM, B., MCALEAR, S. D., LEMKE, J., NEIDHARDT, J. & BERGER, W. 2008. Identification and functional characterization of a novel rhodopsin mutation associated with autosomal dominant CSNB. *Invest Ophthalmol Vis Sci,* 49**,** 4105-14.

ZEITZ, C., ROBSON, A. G. & AUDO, I. 2015. Congenital stationary night blindness: an analysis and update of genotype-phenotype correlations and pathogenic mechanisms. *Prog Retin Eye Res,* 45**,** 58-110.

ZHANG, L., XU, T., MAEDER, C., BUD, L. O., SHANKS, J., NIX, J., GUTHRIE, C., PLEISS, J. A. & ZHAO, R. 2009. Structural evidence for consecutive Hel308-like modules in the spliceosomal ATPase Brr2. *Nat Struct Mol Biol,* 16**,** 731-9.

ZHANG, Q., LI, S., XIAO, X., JIA, X. & GUO, X. 2007. The 208delG mutation in FSCN2 does not associate with retinal degeneration in Chinese individuals. *Invest Ophthalmol Vis Sci,* 48**,** 530-3.

ZHANG, X., CHEN, L. J., LAW, J. P., LAI, T. Y., CHIANG, S. W., TAM, P. O., CHU, K. Y., WANG, N., ZHANG, M. & PANG, C. P. 2010. Differential pattern of RP1 mutations in retinitis pigmentosa. *Mol Vis,* 16**,** 1353-60.

ZHANG, X., LAI, T. Y., CHIANG, S. W., TAM, P. O., LIU, D. T., CHAN, C. K., PANG, C. P., ZHAO, C. & CHEN, L. J. 2013. Contribution of SNRNP200 sequence variations to retinitis pigmentosa. *Eye,* 27**,** 1204-13.

ZHAO, C., BELLUR, D. L., LU, S., ZHAO, F., GRASSI, M. A., BOWNE, S. J., SULLIVAN, L. S., DAIGER, S. P., CHEN, L. J., PANG, C. P., ZHAO, K., STALEY, J. P. & LARSSON, C. 2009. Autosomal-dominant retinitis pigmentosa caused by a mutation in SNRNP200, a gene required for unwinding of U4/U6 snRNAs. *Am J Hum Genet,* 85**,** 617-27.

ZHOU, R., WEN, H. & AO, S. Z. 1999. Identification of a novel gene encoding a p53-associated protein. *Gene,* 235**,** 93-101.

ZIMMERMAN, A. L. 1995. Cyclic nucleotide gated channels. *Curr Opin Neurobiol,* 5**,** 296-303.

ZIVIELLO, C., SIMONELLI, F., TESTA, F., ANASTASI, M., MARZOLI, S. B., FALSINI, B., GHIGLIONE, D., MACALUSO, C., MANITTO, M. P., GARRE, C., CICCODICOLA, A., RINALDI, E. & BANFI, S. 2005. Molecular genetics of autosomal dominant retinitis pigmentosa (ADRP): a comprehensive study of 43 Italian families. *J Med Genet,* 42**,** e47.

6.1 LIST OF PUBLICATIONS GENERATED FROM THIS THESIS:

1. **MUKHERJEE, R**., ROBSON, A. G., HOLDER, G. E., STOCKMAN, A., EGAN, C. A., MOORE, A. T. & WEBSTER, A. R. 2014. A detailed phenotypic description of autosomal dominant cone dystrophy due to a de novo mutation in the GUCY2D gene. *Eye,* 28**,** 481-7.
2. MAUBARET, C. G., VACLAVIK, V., **MUKHOPADHYAY, R**., WASEEM, N. H., CHURCHILL, A., HOLDER, G. E., MOORE, A. T., BHATTACHARYA, S. S. & WEBSTER, A. R. 2011. Autosomal dominant retinitis pigmentosa with intrafamilial variability and incomplete penetrance in two families carrying mutations in PRPF8. *Invest Ophthalmol Vis Sci,* 52**,** 9304-9
3. ROSE, A. M., **MUKHOPADHYAY, R**., WEBSTER, A. R., BHATTACHARYA, S. S. & WASEEM, N. H. 2011. A 112kb deletion in chromosome 19q13.42 leads to retinitis pigmentosa. *Invest Ophthalmol Vis Sci*.
4. **MUKHOPADHYAY, R**., HOLDER, G. E., MOORE, A. T. & WEBSTER, A. R. 2011. Unilateral Retinitis Pigmentosa Occurring in an Individual With a Germline Mutation in the RP1 Gene. *Arch Ophthalmol,* 129**,** 954-6.
5. TOWNS, K. V., KIPIOTI, A., LONG, V., MCKIBBIN, M., MAUBARET, C., VACLAVIK, V., EHSANI, P., SPRINGELL, K., KAMAL, M., RAMESAR, R. S., MACKEY, D. A., MOORE, A. T., **MUKHOPADHYAY, R**., WEBSTER, A. R., BLACK, G. C., O'SULLIVAN, J., BHATTACHARYA, S. S., PIERCE, E. A., BEGGS, J. D. & INGLEHEARN, C. F. 2010. Prognosis for splicing factor PRPF8 retinitis pigmentosa, novel mutations and correlation between human and yeast phenotypes. *Hum Mutat,* 31**,** E1361-76.